Université de Montréal

# The Role of MicroRNA Regulation of Cardiac Ion Channel in Arrhythmia

par

**Xiaobin Luo**

Département de Médecine

Faculté de Médecine

Thèse présentée à la Faculté des études supérieures

en vue de l'obtention du grade de

**Philosophiae Doctor (Ph.D.)**

en Sciences Biomédicales

Août 2012

© Xiaobin Luo, 2012

Université de Montréal
Faculté des études supérieures et postdoctorales

Cette thèse intitulée:

# The Role of MicroRNA Regulation of Cardiac Ion Channel in Arrhythmia

Présentée par :
Xiaobin Luo

a été évaluée par un jury composé des personnes suivantes :

| | |
|---|---|
| Dr Eric Thorin | Président-rapporteur |
| Dr Stanley Nattel | Directeur de recherche |
| Dr Lucie Parent | Membre du jury |
| Dr Alvin Shrier | Examinateur externe |
| Dr Jacques Turgeon | Représentant du doyen de la FES |

# RÉSUMÉ

La fibrillation auriculaire (FA) est le trouble du rythme le plus fréquemment observé en pratique clinique. Elle constitue un risque important de morbi-mortalité. Le traitement de la FA reste un défi majeur en lien avec les nombreux effets secondaires associés aux approches thérapeutiques actuelles. Dans ce contexte, une meilleure compréhension des mécanismes sous-jacents à la FA est essentielle pour le développement de nouvelles thérapies offrant un meilleur rapport bénéfice/risque pour les patients. La FA est caractérisée par *i)* un remodelage électrique délétère associé le plus souvent *ii)* à un remodelage structurel du myocarde favorisant la récurrence et le maintien de l'arythmie. La diminution de la période réfractaire effective au sein du tissu auriculaire est un élément clef du remodelage électrique. Le remodelage structurel, quant à lui, se manifeste principalement par une fibrose tissulaire qui altère la propagation de l'influx électrique dans les oreillettes. Les mécanismes moléculaires impliqués dans la mise en place de ces deux substrats restent mal connus. Récemment, le rôle des microARNs (miARNs) a été pointé du doigt dans de nombreuses pathologies notamment cardiaques. Dans ce contexte les objectifs principaux de ce travail ont été i) d'acquérir une compréhension approfondie du rôle des miARNs dans la régulation de l'expression des canaux ioniques et ii) de mieux comprendre le rôle de ces molécules dans l'installation d'un substrat favorable a la FA.

Nous avons, dans un premier temps, effectué une analyse bio-informatique combinée à des approches expérimentales spécifiques afin d'identifier clairement les miARNs démontrant un fort potentiel de régulation des gènes codant pour l'expression des canaux ioniques cardiaques humains. Nous avons identifié un nombre limité de miARNs cardiaques qui possédaient ces propriétés. Sur la base de ces résultats, nous avons démontré que l'altération de l'expression des canaux ioniques, observée dans diverse maladies cardiaques (par exemple, les cardiomyopathies, l'ischémie myocardique, et la fibrillation auriculaire), peut être soumise à ces miARNs suggérant leur implication dans l'arythmogénèse.

La régulation du courant potassique $I_{K1}$ est un facteur déterminant du remodelage électrique auriculaire associée à la FA. Les mécanismes moléculaires sous-jacents sont peu connus. Nous avons émis l'hypothèse que l'altération de l'expression des miARNs soit

corrélée à l'augmentation de l'expression d'$I_{K1}$ dans la FA. Nous avons constaté que l'expression de miR-26 est réduite dans la FA et qu'elle régule $I_{K1}$ en modulant l'expression de sa sous-unité Kir2.1. Nous avons démontré que miR-26 est sous la répression transcriptionnelle du facteur nucléaire des lymphocytes T activés (NFAT) et que l'activité accrue de NFATc3/c4, aboutit à une expression réduite de miR-26. En conséquence $I_{K1}$ augmente lors de la FA. Nous avons enfin démontré que l'interférence *in vivo* de miR-26 influence la susceptibilité à la FA en régulant $I_{K1}$, confirmant le rôle prépondérant de miR-26 dans le remodelage auriculaire électrique.

La fibrose auriculaire est un constituant majeur du remodelage structurel associé à la FA, impliquant l'activation des fibroblastes et l'influx cellulaire du $Ca^{2+}$. Nous avons cherché à déterminer *i)* si le canal perméable au $Ca^{2+}$, TRPC3, jouait un rôle dans la fibrose auriculaire en favorisant l'activation des fibroblastes et *ii)* étudié le rôle potentiel des miARNs dans ce contexte. Nous avons démontré que les canaux TRPC3 favorisent l'influx du $Ca^{2+}$, activant la signalisation $Ca^{2+}$-dépendante ERK et en conséquence activent la prolifération des fibroblastes. Nous avons également démontré que l'expression du TRPC3 est augmentée dans la FA et que le blocage *in vivo* de TRPC3 empêche le développement de substrats reliés à la FA. Nous avons par ailleurs validé que miR-26 régule les canaux TRPC3 en diminuant leur expression dans les fibroblastes. Enfin, nous avons montré que l'expression réduite du miR-26 est également due à l'activité augmentée de NFATc3/c4 dans les fibroblastes, expliquant ainsi l'augmentation de TRPC3 lors de la FA, confirmant la contribution de miR-26 dans le processus de remodelage structurel lié à la FA.

En conclusion, nos résultats mettent en évidence l'importance des miARNs dans la régulation des canaux ioniques cardiaques. Notamment, miR-26 joue un rôle important dans le remodelage électrique et structurel associé à la FA et ce, en régulant $I_{K1}$ et l'expression du canal TRPC3. Notre étude démasque ainsi un mécanisme moléculaire de contrôle de la FA innovateur associant des miARNs. miR-26 en particulier représente apres ces travaux une nouvelle cible thérapeutique prometteuse pour traiter la FA.

**Mots clés** : Arythmie, fibrillation auriculaire, microARN, miR-26, $I_{K1}$ et TRPC3

# ABSTRACT

Atrial fibrillation (AF) is the most frequently-encountered arrhythmia in clinical practice and constitutes a major cause of cardiac morbidity and mortality. The management of AF remains a major challenge as current therapeutic approaches are limited by potential adverse effects and high rate of AF recurrence/persistence. A better understanding of the mechanisms underlying AF is of great importance to improve AF therapy. AF is characterized by impaired electrical and structural remodeling, both of which favors the recurrence and maintenance of the arrhythmia. A key feature in electrical remodeling is the reduced atrial effective refractory period, due to ion channel alteration. Structural remodeling, on the other hand, mainly results from atrial fibrosis. However, the precise molecular mechanisms underlying these remodeling processes are still incompletely understood. The importance of microRNAs (miRNAs) in various pathophysiological conditions of the heart has been well established, but little is known with regard to cardiac arrhythmias. Emerging evidence suggests that dysregulation of miRNAs may underlie heart rhythm disturbances. The aim of the present work was to acquire a comprehensive understanding of miRNA-mediated regulation of ion channels in cardiac arrhythmias. Notably, we will focus on the mechanistic insights of miRNAs related to the control of AF.

Currently available experimental approaches do not permit thorough characterization of miRNA targeting. For this purpose, we performed bioinformatic analyses in conjunction with experimental approaches to identify miRNAs from the database that potentially regulate human cardiac ion channel genes. We found that only a subset of miRNAs target cardiac ion channel genes. Based on these results, we further demonstrated that the dysregulation of ion channel gene expression observed in various cardiac disorders (e.g. cardiomyopathy, myocardial ischemia, and atrial fibrillation) can be explained by the dysregulation of miRNAs. These findings further support the potential implication of miRNAs in arrhythmogenesis under these cardiac conditions.

The upregulation of the cardiac inward rectifying potassium current, $I_{K1}$, is a key determinant of adverse atrial electrical remodeling associated with AF. The molecular mechanisms underlying this ionic remodeling are poorly understood. We hypothesized that altered miRNA expression is responsible for $I_{K1}$ upregulation in AF. We found that miR-26

is significantly downregulated in AF and regulates $I_{K1}$ by controlling the expression of its underlying subunit Kir2.1. Moreover, we demonstrated that miR-26 is under the transcriptional repression of the nuclear factor of activated T cells (NFAT) and enhanced activities of members of the NFAT family, NFATc3/c4, results in miR-26 downregulation, which accounts for $I_{K1}$ enhancement in AF. Furthermore, we observed that *in vivo* interference of miR-26 affects AF susceptibility via the regulation of $I_{K1}$, suggesting an important role of miR-26 in atrial electrical remodeling.

Atrial fibrosis is a major constituent in AF-associated adverse atrial structural remodeling, involving the activation of fibroblasts and cellular $Ca^{2+}$ entry. Here, we sought to determine whether the $Ca^{2+}$ permeable channel, TRPC3, plays a role in AF-induced fibrosis by promoting fibroblast activation. Furthermore, we investigated the potential role of miRNAs in this context. We found that TRPC3 channels promote $Ca^{2+}$-entry, which results in activation of $Ca^{2+}$-dependent ERK-signaling and consequently fibroblast activation. We also demonstrated that TRPC3 is upregulated in AF and in vivo TRPC3 blockade suppresses the development of AF-promoting substrate. Furthermore, we observed that miR-26 regulates TRPC3 channels via controlling the expression of the underlying channel subunit and is downregulated in AF-fibroblasts. Finally, we showed that the reduced expression of miR-26 is also due to the enhanced NFATc3/c4 activities in AF-fibroblasts and accounts for AF-induced upregulation of TRPC3, suggesting the potential contribution of miR-26 in AF-related adverse structural remodeling process.

In conclusion, our findings emphasize the importance of miRNAs in the regulation of cardiac ion channels. Notably, miR-26 plays a crucial role in AF-associated electrical and structural remodeling via the regulation of $I_{K1}$ and TRPC3 channel genes. Thus, our study unravels a novel molecular control mechanism of AF at the miRNA level, suggesting miR-26 as a new and promising therapeutic target for AF.

**Keywords** : Arrhythmia, atrial fibrillation, microRNA, miR-26, $I_{K1}$ and TRPC3

# TABLE OF CONTENTS

# LIST OF FIGURES AND TABLES

## CHAPTER 1



## CHAPTER 2

## CHAPTER 3

## CHAPTER 4

# LIST OF ABBREVIATIONS

| | |
|---|---|
| 2’-OMe | 2’-O-methyl |
| 3’-UTR | 3’-untranslated region |
| AAVs | Adeno-associated viruses |
| AAV9 | Adeno-associated viruses serotype 9 |
| ACC | American College of Cardiology |
| ACE | Angiotensin converting enzyme |
| AF | Atrial fibrillation |
| AFFIRM | Atrial Fibrillation Follow-up Investigation of Rhythm Management |
| AHA | American Heart Association |
| AngII | Angiotensin II |
| AP | Action potential |
| APD | Action potential duration |
| Arl2 | ADP-ribosylation factor-like 2 |
| ATP | Atrial tachypacing |
| ATR | Atrial tachycardia remodeling |
| AT1R | Angiotensin II type 1 receptor |
| $Ba^{2+}$ | Barium ion |
| Bcl2 | B-cell lymphoma 2 |
| Bim | BH3-only protein |
| $Ca^{2+}$ | Calcium ion |
| $[Ca^{2+}]_i$ | Intracellular calcium concentration |
| CaMKII | $Ca^{2+}$/calmodulin-dependent protein kinase II |
| CAMKIIδ | $Ca^{2+}$/calmodulin-dependent protein kinase II delta |
| *C elegans* | *Caenorhabditis elegans* |
| CH | Cardiac hypertrophy |

| | |
|---|---|
| CHF | Congestive heart failure |
| CMs | Cardiomyocytes |
| Col1A1 | Collagen 1A1 |
| $Cs^+$ | Cesium ion |
| CTGF | Connective tissue growth factor |
| CV | Conduction velocity |
| Cx40 | Connexin 40 |
| Cx43 | Connexin 43 |
| DAD | Delayed afterdepolarization |
| DAG | Diacylglycerol |
| Dyrk1a | Dual-specificity tyrosine-(Y)-phosphorylation regulated kinase 1a |
| EAD | Early-afterdepolarization |
| EADs | Early-afterdepolarizations |
| ECM | Extracellular matrix |
| ECs | Endothelial cells |
| ESC | European Society of Cardiology |
| ERK1/2 | Extracellular signal-regulated kinase 1/2 |
| ERP | Effective refractory period |
| FasL | Fas ligand |
| $Gd^{3+}$ | Gadolinium ion |
| GPCR | G protein-coupled receptor |
| HEK293 | Human embryonic kidney cell line |
| HF | Heart failure |
| Hif-1α | Hypoxia-inducible factor 1 alpha |
| $I_{CaL}$ | Inward L-type calcium current |

| | |
|---|---|
| IGF-1 | Insulin-like growth factor-1 |
| $I_{K1}$ | Inward rectifier potassium current |
| $I_{KACh}$ | Acetylcholine-activated inward potassium current |
| $I_{Kr}$ | Rapidly activated delayed rectifier potassium current |
| $I_{Ks}$ | Slowly activated delayed rectifier potassium current |
| $I_{Kur}$ | Ultra-rapidly activating delayed-rectifier $K^+$-current |
| $I_{Na}$ | Inward sodium current |
| $IP_3$ | Inositol 1,4,5-triphosphate |
| IR | Ischemia reperfusion |
| ITGA5 | alpha-5 integrin |
| $I_{to}$ | Transient outward potassium current |
| $La^{3+}$ | Lanthanum ion |
| LNA | Locked nucleic acid |
| $Mg^{2+}$ | Magnesium |
| MEF2A | Myocytes enhancer factor 2A |
| MFs | Myofibroblasts |
| miRNAs | microRNAs |
| MMP-2 | Metalloproteinase-2 |
| MuRF1 | Muscle specific ring finger protein 1 |
| $Na^+$ | Sodium ion |
| NCX | $Na^+$/ $Ca^{2+}$ exchanger |
| NFAT | Nuclear factor of activated T cells |
| PAK4 | p21-activated kinase-4 |
| PDCD4 | Programmed cell death 4 |
| PDGF | Platelet-derived growth factor |

| | |
|---|---|
| PIP2 | Phosphatidylinosital-4, 5-bisphosphate |
| PKA | Protein kinase A |
| PKC | protein kinase C |
| PLC | Phospholipase C |
| Ppp2r5a | Protein phosphatase 2A |
| PTEN | Phosphatase and tensin homolog |
| Pyr3 | Pyrazole |
| RISC | RNA-induced silencing complex |
| ROCE | Receptor-operated $Ca^{2+}$ entry |
| ROCK1 | Rho-associated coiled-coil containing protein kinase-1 |
| RP | Refractory period |
| RT | Reverse transcription |
| RyR2 | Ryanodine receptor 2 |
| SA | Sinoatrial |
| SERCA | SR $Ca^{2+}$-ATPase |
| siRNAs | Short interfering RNAs |
| SMCs | Smooth muscle cells |
| SOCE | Store-operated $Ca^{2+}$ entry |
| Spred-1 | Sprouty-related EVH1 domain-containing protein 1 |
| Spry1 | Sprouty homolog 1 |
| SR | Sarcoplasmic reticulum |
| SRF | Serum response factor |
| TAC | Transverse aortic constriction |
| TFIIB | Transcription factor II B |
| TFs | Transcription factors |

| | |
|---|---|
| TGF-$\beta_1$ | Transforming growth factor $\beta_1$ |
| TGF-βRII | TGF-β receptor type II |
| THRAP1 | Thyroid hormone receptor associated protein 1 |
| TM | Transmembrane domains |
| TRP | Transient receptor potential |
| TRPA | Transient receptor potential ankyrin |
| TRPC | Transient receptor potential canonical |
| TRPM | Transient receptor potential melastatin |
| TRPML | Transient receptor potential mucolipin |
| TRPP | Transient receptor potential polycystin |
| TRPV | Transient receptor potential vanilloid |
| US | United States |
| VSMCs | Vascular smooth muscle cells |
| WL | Wavelength |

# DEDICATION

*This thesis is dedicated to:*

*My parents, for their unconditional love and support, endless patience and understanding. Were it not for their sacrifice, this thesis may have never been completed.*

# ACKNOWLEDGEMENTS

First of all, I would like to express my deepest appreciation to my supervisor, Dr. Stanley Nattel, for providing me the opportunity to be part of the lab. Were it not for his invaluable support, persistent encouragement, and pertinent guidance, my graduate studies and this thesis would have never been completed. I also want to extend my sincere gratitude to him for inspiring me not only with his rich scientific thoughts but with his philosophy of life.

This work could never have been done without the help and the continued excellence of my wonderful colleagues and friends; Drs. Zhenwei Pan, Hongli Shan, Ling Xiao, Masahedi Harada, Jiening Xiao, Huixian Lin, Ange Maguy, Xiaoyan Qi, and Balazs Ordog. I am also deeply indebted to them for their warmhearted help along the way of my graduate study. I am truly thankful for Kristin Dawson, Mona Aflaky, Artavazd Tadevosyan, and Dr. Ange Maguy for reading the thesis and providing helpful suggestions, as well as the encouragement.

Many thanks go to Jennifer Bacchi, Chantal St-Cyr, Nathalie L'Heureux, and Audrey Bernard, for providing the excellent support and help and making the better working environment for the lab. I would also like to thank the other people in the lab; Patrice Naud, Yu Chen, Takeshi Kato, Jin Li, Sirirat Surinkaew, Patrick Vigneault, Feng Xiong, Hai Huang, and Chia-Tung Wu. The joyfulness they have brought in, was always appreciated.

Finally, I would like to extend my sincere gratitude to Dr. Eric Thorin, Dr. Alvin Shrier, and Dr. Lucie Parent for evaluating this thesis and providing insightful suggestions and constructive comments.

Xiaobin Luo, August 2012

# STATEMENT OF AUTHORSHIP

Here is a statement regarding the contribution of coauthors and myself to the three papers included in this thesis.

**Chapter 2:**

**Luo X**, Zhang H, Xiao j, Wang Z. Regulation of Human Cardiac Ion Channel Genes by MicroRNAs: Theoretical Perspective and Pathophysiological Implications. ***Cell. Physiol. Biochem.*** 2010;25(6):571-86.

*I designed the experiments, performed the miRNA microarray and real-time RT-PCR experiments, partially contributed to bioinformatic works, and analyzed the data. Haijun Zhang took part into the analysis of the bioinformatic results and helped in generating the figures. Dr. Jiening Xiao participated in the miRNA microarray and real-time RT-PCR experiments. Dr. Zhiguo Wang generated the original idea, supervised the work, wrote the manuscript, and finalized the manuscript for publication. More specifically, I generated the Fig. 1A, which is based on the re-analysis of the experimental results of a previous paper (Liang et al, BMC Genomics, 2007), showing the relative expression of all miRNAs in different organs in humans by Realtime RT-PCR. In addition, in collaboration with Dr. Jiening Xiao, we performed Realtime RT-PCR to verify the relative abundance of the cardiac-enriched miRNA reported in Liang's paper in the healthy human ventricular sample. These data are presented as supplementary figure 1. I also prepared Fig. 1B, which summarizes the total number of ion-channel target genes each cardiac-enriched miRNAs shown in Fig. 1A. Moreover, together with Haijun Zhang, we prepared Fig. 2, which is the cartoon illustration of the cardiac-enriched miRNAs and their corresponding predicted ion-channel target genes. For Fig. 3, I was responsible for the summary and the comparison of all the previously-reported deregulated miRNAs under cardiac hypertrophy and congestive heart failure. For Fig. 4, I compared and summarized the miRNAs changes in ischemic hearts which were reported by three previous publications as well as the miRNA microarray analysis we performed in the hearts of MI rat (the cardiac tissuses of the rat MI model were kindly provided by Dr. Baofeng Yang) and these data are presented in supplementary figure 2. Furthermore, together with Dr. Jiening Xiao, we conducted the*

*microarray analysis of miRNAs expression profile in the left atrium of a canine AF model (The AF dog atrial samples were also kindly provided by Dr. Baofeng Yang) and I performed Realtime RT-PCR to verify the deregulated miRNAs and prepared Fig. 5. Finally, I summarized the list of ion channel genes selected in the study with their detailed descriptions and prepared Table 1.*

**Chapter 3:**

**Luo X***, Pan Z*, Shan H*, Xiao J, Sun X, Wang N, Lin H, Xiao L, Maguy A, Qi X-Y, Li Y, Gao X, Dong D, Zhang Y, Bai Y, Ai J, Sun L, Lu H, Luo X, Wang Z, Lu Y, Yang B, Nattel S. MicroRNA-26 governs profibrillatory inward-rectifier potassium current changes in atrial fibrillation. ***J. Clin. Invest.*** (accepted for publication, in press).

*Along with Dr. Zhenwei Pan, I designed all the experiments, conducted majority of the luciferase, western blot, real-time RT-PCR, EMSA, and a portion of in vivo experiments, and analyzed the data. During the subsequent revision work of this paper Dr. Hongli Shan has made significant contribution to the in vivo NFAT-overexpression study as well as AF time-course study. Therefore, Dr. Zhenwei Pan, Dr. Hongli Shan and I were considered to have an equal contribution to the present study. Xiao-Yan Luo and Drs. Xuelin Sun, Jiening Xiao, Huixian Lin, Ling Xiao, Deli Dong, Jing Ai, Ange Maguy, Xiaoyan Qi, and Ning Wang performed parts of the luciferase, real-time RT-PCR, CHIP and Western blot analyses. Drs. Hongli Shan, Xuelin Sun, Lihua Sun, and Yunlong Bai conducted patch-clamp recordings. Dr Hang Lu provided the human samples. Drs. Yanjie Lu, Xu Gao and Y.Z. conducted parts of the animal studies. Dr. Zhiguo Wang helped in the conceptualization and design of the studies. Dr. Stanley Nattel and Dr. Baofeng Yang supervised the project and wrote the manuscript. More specifically, I proposed and designed the experiments presented in Fig.1A-F. I designed and performed the Western blot and Realtime RT-PCR experiments as shown in Fig.2A, 2B, 2C and 2F. Together with Dr. Jiening Xiao, we designed and generated the wild-type and mutant luciferase report constructs containing the sequences correspond to the miR-26 binding sites in 3'UTR of KCNJ2 mRNA (Fig. 2E). In addition, I conceived and designed the experiments related to the in vivo assessment of miR-26 overexpression or knockdown on AF vulnerability and worked collaboratively with Dr. Zhenwei Pan on the AF induction experiments in mice*

*subjected to in-vivo miRNA-26 interference as shown in Fig. 3A. Moreover, I designed the miR-mimics and miR-masks constructs and worked collaboratively with Dr. Pan for the measurement of AF induction rate as well as duration in mice received these constructs (Fig 4A and 4C). Furthermore, I proposed, designed and performed the majority of the experiments related to molecular mechanism underlying the transcriptional control of miR-26 in AF (Fig. 6A, 6C and 6D and Fig. 7A and 7C). I also partially contributed to the works in Fig. 6B and Fig. 7B together with Drs. Jiening Xiao and Huixian Lin. Finally, I carried out bioinformatic analysis or western blot experiments and prepared Suppl. Fig. 1, 2, 3, 4, 9, 11, 12, and 13.*

**Chapter 4:**

Harada M, **Luo X**, Qi X, Tadevosyan A, Maguy A, Ordog B, Ledoux J, Kato T, Naud P, Voigt N, Shi Y, Kamiya K, Murohara T, Kodama I, Tardif J, Schotten U, Van Wagoner D, Dobrev D, Nattel S. TRPC3-dependent Fibroblast Regulation in Atrial Fibrillation. ***Circulation.*** 2012 Oct 23; 126(17):2051-64.

*In this work, I proposed, designed, performed, and analyzed all the experiments related to miRNAs (Figure 6 and Suppl. Figure 12). Dr. Masahide Harada was the primary investigator of this study, performed most of the in vivo and in vitro experiments, and wrote the manuscript. Dr. Xiao-Yan Qi performed the patch clamp experiments. Artavazd Tadevosyan conducted the NFAT immuno-staining study. Dr. Ange Maguy was involved in experiments of western blotting. Dr. Balazs Ordog helped in producing TRPC3 knockdown viruses. Dr. Jonathan Ledoux participated in recording of $Ca^{2+}$ transient. Dr. Takeshi Kato helped in electrophysiological study of the animal model. Dr. Patrice Naud participated in real-time RT-PCR experiments. Drs. Niels Voigt, Ulrich Schotten, David R. Van Wagoner, and Dobromir Dobrev provided atrial samples from human, goats, and CHF dogs. Drs. Yanfen Shi and Jean-Claude Tardif were involved in echocardiographic measurements. Drs. Kaichiro Kamiya, Toyoaki Murohara, and Itsuo Kodama consulted on the manuscript. Dr. Stanley Nattel generated the original idea, supervised all the aspect of the work, and finalized the manuscript for publication. As the second author of this paper, my major contribution to this paper is to unveil the role of miR-26 in regulation of TRPC3 in AF, for which I proposed the original idea. My findings are important for the understanding of how*

*TRPC3 is dysregulated in AF and help importantly to the final acceptance of the paper in Circulation. More specifically, I proposed, designed, and performed the experiments (Real-time RT-PCR and bioinformatic analysis) related to the identification of miR-26 as the candidate to regulate TRPC3 in AF, as shown in Figure 6A; I designed and helped Dr. Harada with the cloning of the luciferase constructs of 3'UTR of TRPC3 mRNA bearing the wild-type or mutated miR-26 binding sites. In addition, I designed the miR-26 mimic duplex and miR-26 knockdown oligos and helped in the luciferase experiments, together with Dr. Harada, we measured the luciferase activities of the wild-type and mutated constructs in response to miR-26 overexpression and knockdown in HEK293 cells, the results of which generate Figure 6B. Moreover, I designed, proposed, and, partially contributed to the cell proliferation as well as the Western blot experiments in freshly-isolated fibroblasts subjected to miR-26 over-expression or knockdown and these results are shown in Fig. 6C, 6D and 6E. Furthermore, I proposed and helped in the design of study related to the NFAT-regulation of miR-26 in AF, for which, I partially performed the Realtime RT-PCR and Western blot experiments as shown in Fig 7D and 7E, respectively. Finally, I performed experiments looking at the relative expression of miR-26 in both cardiomyocytes and freshly-isolated fibroblasts and generated the Suppl. Fig. 12.*

# CHAPTER 1. INTRODUCTION

## 1.1 Overview of Atrial Fibrillation

Atrial fibrillation (AF) represents the most clinically-encountered sustained cardiac arrhythmia and contributes significantly to cardiac morbidity and mortality. AF increases the risk of developing congestive heart failure (CHF) and stroke, leading to an increased demand on healthcare, and thereby posing a significant socioeconomic burden [1, 2].

### 1.1.1 Epidemiology of AF

Approximately 0.5% to 1% of the general population is affected by AF [3, 4]. According to a retrospective study in the United States (US), it is estimated that 3.03 million Americans were suffering from AF in 2005 and this number will reach 7.56 million by 2050 [5]. Several epidemiological studies have suggested that the prevalence and incidence of AF increases dramatically in aging population [6-9]. The prevalence of AF increases from 1% in people under 60 to 8% in the population aged 80 or older [4]. It is predicted that the number of AF patients will likely increase by two or three fold within the next two or three decades [10]. The incidence of AF also displays a gender-specific disparity. Based on the Framingham Heart Study, the likelihood of developing AF in men is 1.5 fold greater than that in women with the corrections for age and other predisposing conditions [6]. However, the total number of female AF patients is actually equal to or greater than that of male AF patients because women have longer lifespan [11]. The racial discrepancy of AF has also been reported in several studies, showing that AF is more prevalent in whites than in blacks among the populations either with or without cardiac complications [12-14]. However, the reason for this discrepancy is complex and remains unclear [12, 13, 15].

### 1.1.2 Classification of AF

The classification of AF was well defined in the 2006 guideline laid out by the joint effort of ACC (American College of Cardiology), AHA (America Heart Association) and ESC (European Society of Cardiology) [16-18]. According to this guideline, AF is classified based on the duration and responses to treatments, which generally falls into three main

categories: paroxysmal, persistent and permanent [16-18]. Paroxysmal AF occurs periodically and is able to self-terminate within a short period (as short as a few seconds or as long as a few hours or days). Persistent AF does not terminate spontaneously but it can be ceased upon proper treatments (either pharmacologic or direct-current electrical cardioversion). Permanent AF, which is irreversible, shows no response to either medication or electrical cardioversion, and hence lasts indefinitely. Permanent AF can arise from paroxysmal and persistent AF [19]. Paroxysmal AF is believed to represent the natural origin of AF. It can gradually develop into persistent or permanent forms through a process termed "atrial remodeling", in which, the changes in the electrical and structural properties of the atria is caused by AF itself and/or the underlying cardiac conditions [19, 20]. In addition to the above classification, AF can also be classified by the features of the patients: lone AF (AF patients aged under 60 in the absence of underlying cardio-pulmonary disease), valvular AF (AF in these patients is caused by structural changes in the mitral valve or congenital heart diseases), non-valvular AF (AF patients with no sign of rheumatic mitral valve disease, prosthetic heart valve, or mitral valve repair), and secondary AF (AF occurs as a secondary event under pre-existing cardiac disorders) [16-18].

### 1.1.3 Signs, Symptoms and Predisposing Factors of AF

#### 1.1.3.1 Signs and Symptoms of AF

AF patients can be symptomatic or asymptomatic depending on their awareness of the rapid and irregular heart rate. Clinical presentations of symptomatic AF patients include palpitation (the most common symptom in AF), dizziness, fainting, weakness, fatigue, breath shortness, or angina (chest pain caused by lack of blood supply) [16-18].

#### 1.1.3.2 Predisposing Factors for AF

Substantial evidence has indicated that age is one of the most important risk factors for AF [4-11, 21-23]. Meanwhile, at any given age, gender is also considered as a predisposing factor for AF [8, 9, 21-25]. Other important risk factors predisposing to AF include hypertension [8, 9, 26-29], coronary artery disease [8, 30-32], congestive heart failure [8, 9,

33, 34], valvular heart disease [8, 9, 35, 36], cardiomyopathies [37, 38], myocardial infarction [9, 39-41], diabetes mellitus [8, 9, 42, 43], pulmonary disease [8, 44], postoperative state [45, 46] and hyperthyroidism [47, 48]. AF-promoting phenomenon as seen under the above cardiac conditions is likely due to the accompanied augmentation of atrial pressure and/or atrial dilation [49]. Nonetheless, detailed mechanisms remain largely unknown and merit further investigations.

### 1.1.4 Current Management and Challenges in Treatment of AF

The goals of AF treatment and management are to correct chaotic and irregular atrial contraction and to prevent thromboembolism and stroke [16-18]. In clinical practice, two main strategies (rhythm control and rate control) are commonly applied to restore normal atrial activities [16-18, 50]. Rhythm control aims to restore and maintain sinus rhythm, whereas rate control focuses on maintenance of normal ventricular response (or the effective heart rate). Furthermore, anticoagulation therapy serves as an important strategy to prevent thromboembolism and stroke during AF treatment and is recommended as a mandatory procedure for both rhythm and rate control treatments [16-18, 50]. Approaches adopted in AF treatment generally fall into two main categories: pharmacological and non-pharmacological. Pharmacological approaches primarily involve using anti-arrhythmic drugs that preferentially control rhythm (Class I and III) or ventricular rate (Class II and IV) or, in some cases, control both rhythm and rate depending on the principle actions of the drug. Non-pharmacological approaches, on the other hand, refer to interventions with attempts to terminate arrhythmia without using pharmacological agents; these include direct current cardioversion (electrical cardioversion), catheter ablation, and other surgical therapies (maze procedure and left atrial appendage obliteration). In general, pharmacological approaches (except amiodarone) are considered as the first-line treatments of AF because of their non-invasive properties, whereas most of the non-pharmacological approaches involve invasive intervention, and thus are considered as the second-line treatment for AF.

In spite of the availability of various approaches for rhythm and rate control strategies, there has been a long debate for clinicians in the choice of intervention. From the

theoretical point of view, rhythm control seems to be a better option. This is based on a notion that reduced ventricle function manifested during AF is able to be reversed once the regular cardiac rhythm is restored, and consequently, the normal heart rate would be retained and thromboembolism would be prevented [51]. However, data from several comparative studies [52-56] and meta-analysis [57] have suggested that rhythm control is suboptimal in terms of mortality due to adverse cardiovascular events [52-56]. In fact, none of these studies showed the expected outcomes from rhythm control [52-56]. Instead, in Atrial Fibrillation Follow-Up Investigation of Rhythm Management (AFFIRM) study, lack of anticoagulants appeared to be the strongest risk factor for stroke, with increased incident of stroke in patients for whom the oral anticoagulation treatment was discontinued while their sinus rhythm was restored [56]. The suboptimal outcome of rhythm control in AF treatment is, probably, in part due to the poor tolerability, limited efficacy, and the potential pro-arrhythmic effect of presently available anti-arrhythmic drugs. Moreover, re-analysis of the cause-specific mortality in AFFIRM study further revealed that several of the anti-arrhythmic drugs used for rhythm control were also correlated with significant increase in mortality due to non-cardiovascular causes [58]. Collectively, it seems that rate control is more preferable than rhythm control in AF treatment. Nevertheless, this conclusion might be oversimplified, given the fact that the currently available population study is limited and that none of these studies shows clear advantages between the two strategies [59]. Taken together, it appears that neither of rate-control, rhythm-control, or anticoagulation strategies is mutually exclusive of each other.

## 1.2 Mechanisms of AF

### 1.2.1 Physiological Basis of Cardiac Action Potential

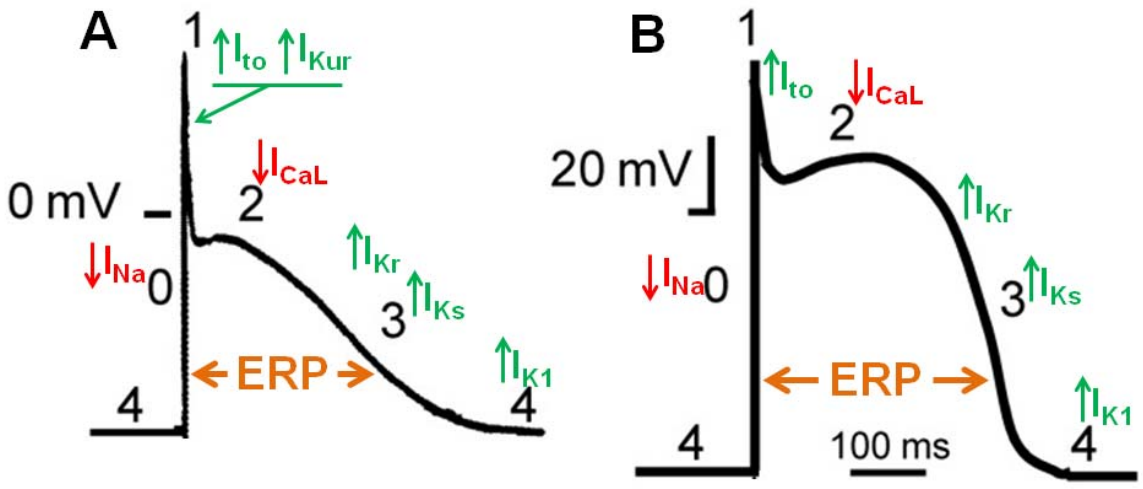


Figure 1. Schematic representation of atrial (A) and ventricular (B) action potentials with underlying principle ionic currents. Inward currents (with downward arrows): $I_{Na}$-sodium current; $I_{CaL}$-L-type calcium current; Outward currents (with upward arrows): $I_{to}$-transient outward current; $I_{Kur}$-ultra rapidly activating delayed rectifier current; $I_{Kr}$ and $I_{Ks}$-rapidly and slowly activating delayed rectifier current; $I_{K1}$-inward rectifier current; Note that $I_{Kur}$ is presented only in the atria. Numbers in black indicate the different phases of action potential. ERP: effective refractory period. (Adapted from Ravens U. et al. [60] with modifications).

The normal electrophysiological behavior of the heart is determined by the orderly propagation of electrical impulses resulting in rapid depolarization and slow repolarization, thereby generating action potentials in individual cardiac cells. In order to better understand AF mechanisms, it is essential to review the basic physiology of the cardiac action potential (AP). As the key determinant of the rhythmical contraction of cardiac cells, cardiac AP reflects the alterations of transmembrane potentials which are determined by inward (depolarizing) and outward (repolarizing) currents (Figure 1). Both atrial (Figure 1A) and ventricular (Figure 1B) APs last several hundred milliseconds and consist of five phases: Phase 0, Phase 1, Phase 2, Phase 3, and Phase 4. A rapid depolarization occurs during the phase 0 of AP, which is the result of a large inward current carried by voltage-gated sodium channels ($I_{Na}$) (Figure 1). This rapid depolarization is followed by a phase 1 early repolarization, which is primarily due to the inactivation of $I_{Na}$ as well as the activation of the transient outward potassium current ($I_{to}$) and the ultra-rapidly activating delayed

rectifier potassium current ($I_{Kur}$) (in atria) (Figure 1A). Repolarization continues in phase 2 of AP, where inward L-type calcium current ($I_{CaL}$) counteracts with a gradually-increasing outward repolarizing potassium currents that are mainly composed of the rapid delayed rectifier potassium current ($I_{Kr}$) (Figure 1A&B). This results in a long lasting repolarization, constituting a morphological "plateau" shape in cardiac AP (Figure 1A&B). It is noteworthy that the shape of atrial AP (Figure 1A) is normally triangular because of the relatively short plateau phase compared with ventricular action potential (Figure 1B). Phase 3 is the final repolarization step in AP. Both $I_{Kr}$ and slow delayed rectifier potassium current ($I_{Ks}$) contribute to terminate the repolarization during this phase. Once repolarization is complete, cardiac cells return to resting membrane potential during phase 4 of AP. The maintenance of the resting membrane potential in phase 4 is determined by the inward rectifier potassium current ($I_{K1}$). Collectively, increase in inward currents will tend to prolong the action potential duration (APD), whereas increased outward currents abbreviate it. It is important to note that cardiac cells are refractory to the initiation of new APs during phases 0, 1, 2, and part of phase 3 (Figure 1A&B). This is termed the effective refractory period (ERP). During this period, no stimulus regardless of its strength is able to initiate a propagated AP until cells return to phase 4. The ERP acts as a protective mechanism to keep the heart rate in check and coordinate the cardiac muscle contraction, thereby preventing arrhythmia. It is directly correlated with APD. For example, the shorter ERP is often associated with shorter APD.

### 1.2.2 Overview of AF Pathophysiology

AF is defined as a supraventricular tachyarrhythmia with characteristic chaotic and uncoordinated contraction of atrium, which results in a mechanical dysfunction of the atria. The first modern notions about the mechanism of AF was introduced in the early twentieth century [49]. Over the past century, researches have greatly increased our knowledge in understanding of AF mechanisms; it is now believed that focal ectopic activity (or triggered activity) and reentry (single-circuit reentry or multiple-circuit reentry) are the underlying pathophysiological mechanisms for AF initiation and maintenance [49, 61, 62], as shown in Figure 2.

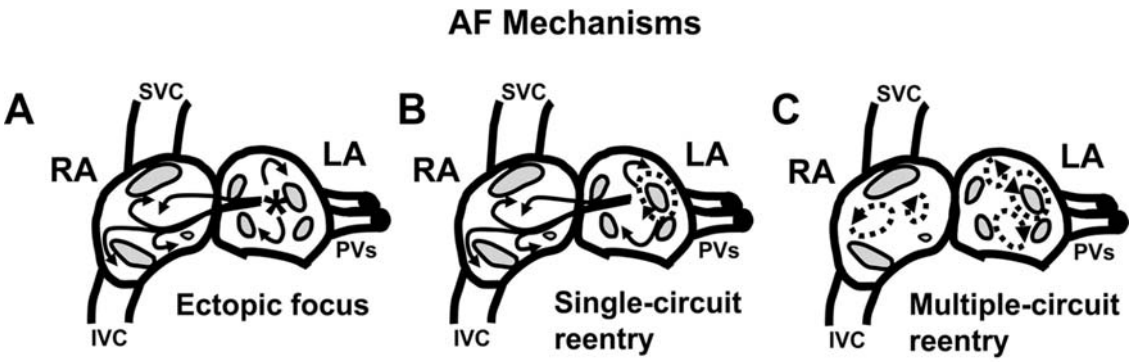


Figure 2. Arrhythmogenic mechanisms underlying AF. A. Ectopic focus. B. Single-circuit reentry. C. Multiple-circuit reentry. (Adapted from Iwasaki Y. et al. [61]).

### 1.2.2.1 Ectopic Mechanism

Up until Haissaguerre et al. [63] discovered that ectopic beats originating in the pulmonary veins played a pivotal role in AF initiation, the multiple-circuit reentry remained the sole dominant theory for AF mechanism. Abnormal automaticity, delayed afterdepolarization (DAD), and early afterdepolarization (EAD) constitute the principle mechanisms underlying focal ectopic activity as demonstrated in Figure 3 [62].

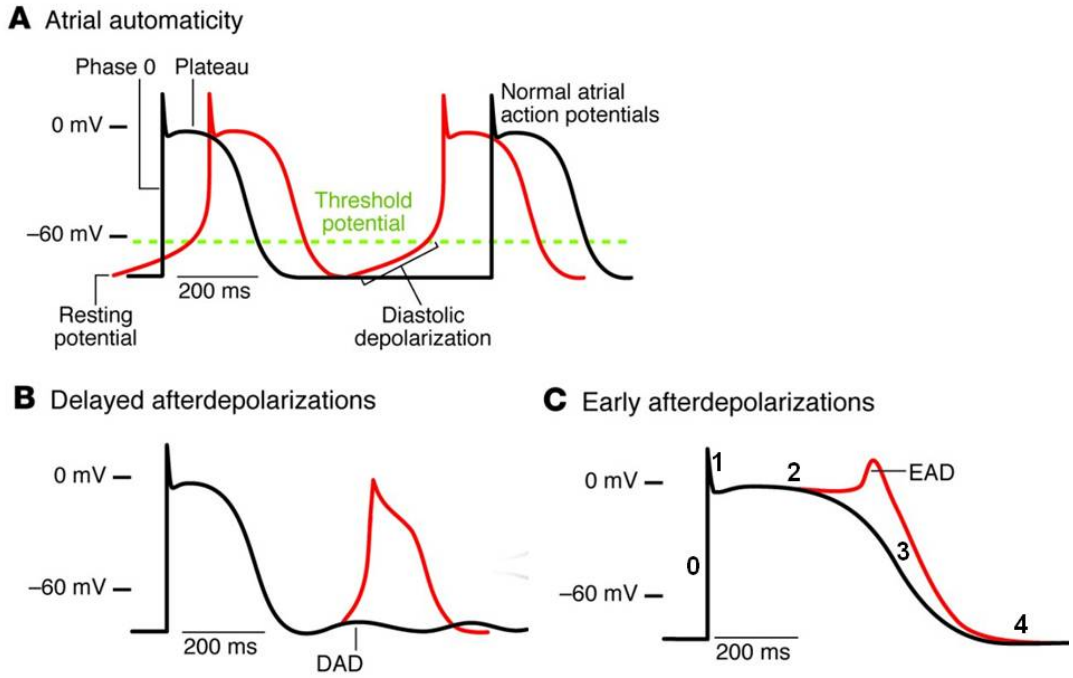


Figure 3. Cellular mechanisms underlying focal ectopic activity. A. Abnormal automaticity. B. Delayed afterdepolarization. C. Earlier afterdepolarization. Numbers in panel C indicate

the different phases of action potential. (Adapted from Wakili R. et al. [62] with modifications).

#### 1.2.2.1.1 Abnormal Automaticity

Normal atrial cells are fired through the sinoatrial (SA) node pacemaking system, and then return to negative potential (resting potential, ~ -80mV) until the next firing from SA node (Figure 3A, black line). However, when the cell membrane reaches critical potential (or threshold potential, ~ -60mV) before the next normal impulse from SA node, an abnormal spontaneous depolarization may occur, resulting in abnormal automaticity (Figure 3A, red line). It is worth noting that the role of abnormal automaticity as a proarrhythmic mechanism during AF remains unclear [62].

#### 1.2.2.1.2 Delayed Afterdepolarization

Delayed afterdepolarizations (DADs) occur after the complete repolarization of the triggering action potential and account for the most important mechanism underlying focal ectopic activity in AF (Figure 3B) [62]. DADs are caused by excessive diastolic $Ca^{2+}$ released from sarcoplasmic reticulum (SR, the main cardiac $Ca^{2+}$ storage organelle). The excessive diastolic $Ca^{2+}$ are handled by transmembrane $Na^{+}$/ $Ca^{2+}$ exchanger (NCX) in an electrogenic manner, extruding one $Ca^{2+}$ ion while pumping 3 $Na^{+}$ into the cell. This creates a net inward current, which can depolarize the cell, resulting in an afterdepolarization. Therefore, both increased diastolic $Ca^{2+}$ and enhanced NCX activity may contribute to DADs. The DAD-related AF is associated with congestive heart failure [64] and genetic defect [65].

#### 1.2.2.1.3 Early Afterdepolarization

Early afterdepolarizations (EADs) occur during phase 2 or 3 of the action potential (Figure 3C). This type of afterdepolarization is primarily caused by recovering of L-type $Ca^{2+}$

channels from inactivation during the plateau phase due to the excessively-prolonged APD. EAD-related AF has been seen in patients with congenital long-QT syndrome [66].

### 1.2.2.2 Re-entrant Mechanisms

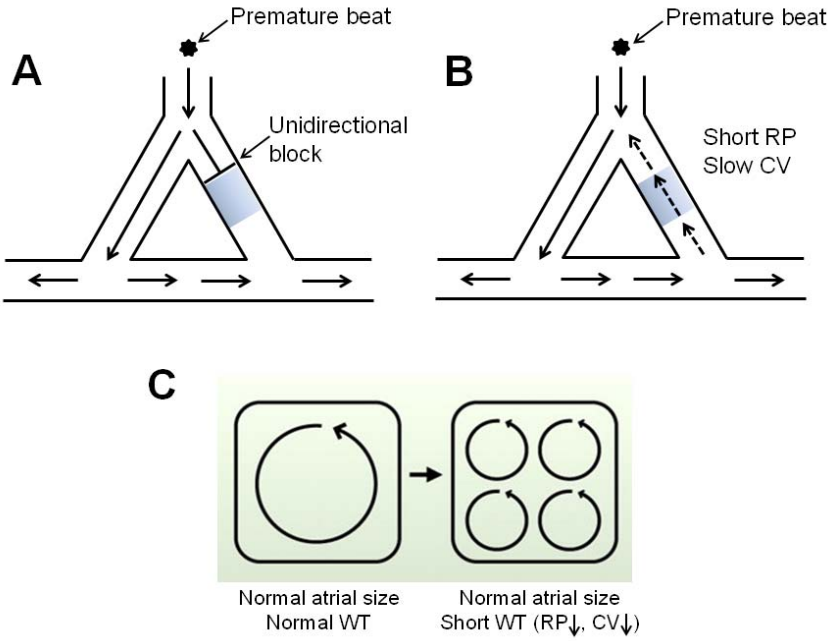


Figure 4. Mechanisms for reentry. A. An unidirectional block occurs when an ectopic impulse dies out in a still-refractory region. B. Conditions for maintenance of reentry. C. Conditions favoring multiple-circuit reentry. RP: refractory period; CV: conduction velocity. Blue-shadow area represents still-refractory region. (Panel C adapted from Nattel S et al. [67] with modifications).

Reentry is conventionally initiated by a premature ectopic beat (Figure 4A). This ectopic beat fails to conduct through a still-refractory region in one direction ("unidirectional block") (Figure 4A), while conducting in the other direction through a region that is no longer refractory (Figure 4A). However, if enough time has elapsed for the recovery of excitability in the refractory region, the impulse can re-enter this region, resulting in reentry (Figure 4B). Accordingly, shorter refractory period (allowing faster recovery of excitability) and/or slower conduction velocity (gaining more time for the non-refractory region to regain excitability) may favor the maintenance of reentry (Figure 4B). Reentry can sustain either as a single circuit form (Figure 1B) or a multiple-circuit form (Figure 1C). For single circuit reentry, the irregular activity is maintained by rapid regular firing

(Figure 1B), whereas for multiple-circuit reentry, the irregularity is determined by the co-existence of multiple dyssynchronous reentry circuits (Figure 1C). There are two leading theoretical models that conceptualize the mechanism of reentry: leading circuit [68] and spiral wave [69]. While both models predict the presence of vulnerable substrates as the key determinant in reentry sustainability, the leading circle theory fails to explain the clinical observation that blocking of $Na^+$ channel effectively terminates AF [70]. Nevertheless, leading circle theory still remains the widely-accepted notion to explain reentry mechanism. An important concept of leading circle theory is the "wavelength of reentry" [49, 68]. The wavelength (WL) of a reentry circuit refers to the shortest pathlength by which a reentry can be established. It is given as the distance that an electrical impulse travels in one refractory period and is critically determined by refractory period (RP) and conduction velocity (CV), as shown in the equation: WL=RP × CV [70, 71]. Accordingly, a shorter wavelength (as the result of abbreviated RP and/or reduced CV) may allow more available reentry circuits to be accommodated in a given atria, favoring multiple-circuit reentry that sustains AF (Figure 4C).

#### 1.2.2.3 Relation of basic AF mechanisms to different forms of clinically-encountered AFs

The natural course of AF is believed to begin as the paroxysmal form, which is triggered by the ectopic foci originated from pulmonary vein sleeves [63].With time, AF tends to become persistent if ectopic firing is sustained or reversible reentry substrates are developed [62]. If the reentry substrates further become irreversible or fixed, AF becomes permanent [62].

## 1.3 Atrial Remodeling in AF

The introduction of the concept "atrial remodeling" over the past two decades has greatly advanced our understanding of AF mechanisms. Atrial remodeling refers to the process by which AF, once initiated, alters atrial electrophysiological (in a short term) and/or structural (over a long term) properties in ways that sustain itself [72].

### 1.3.1 Electrical Remodeling in AF

AF-induced electrical remodeling, which results in trigger activity and functional reentry substrates by altering ion channel/transporter expression and/or function, occurs normally within a short time after AF initiation [73]. Both focal ectopic activity and functional reentry are primarily caused by increased $Ca^{2+}$ loading due to the very rapid atrial rate (tachycardia) during AF [73]. Therefore, more recently, AF-induced electrical remodeling has been termed as atrial tachycardia remodeling (ATR) [67]. Evidence from animal models and clinical studies has highlighted the importance of ATR in pathogenesis of AF and in the transition from paroxysmal AF to persistent AF [72, 74-81]. A prominent finding in ATR is the abbreviation of refractoriness as the result of APD shortening. Consistently, a shorter atrial APD is found in AF patients compared to patients with sinus rhythm [78-81]. Similar observations have also been seen in animal models of AF [72, 74-76].

The ionic mechanisms underlying APD shortening primarily involve downregulation and/or inactivation of L-type calcium current ($I_{CaL}$) and enhancement of inward rectifier potassium currents ($I_{K1}$ and/or $I_{KACh}$). The functional implication of the deregulation of other ion channels in APD shortening remains obscure. Details regarding the pathophysiological significance of these changes will be described below.

#### 1.3.1.1 Upregulation of $I_{K1}$

One of the most important electrophysiological changes in AF-related ATR is the upregulation of inward-rectifier potassium channel, particularly, $I_{K1}$. Increased $I_{K1}$ has been consistently observed in isolated atrial cardiomyocytes from AF patients [82-89] and experimental AF animal models [90-92]. Interestingly, the functional change of $I_{K1}$ in AF is in parallel with increased expression of its underlying subunits Kir2.1 at both mRNA and protein levels [83, 85]. The pathophysiological significance of $I_{K1}$ upregulation in AF is believed to enhance AF sustainability by substantiating reentrant substrates [20, 73]. This is likely attributable to the crucial roles of $I_{K1}$ in maintenance of resting potential and termination of action potential [67, 73]. Increased $I_{K1}$ hyperpolarizes the atrial cells, which, on one hand, inhibits the abnormal automaticity, whereas on the other hand, shortens APD and ERP, thereby favoring the reentrant substrates for AF [67, 73, 93, 94]. Recently,

genetic evidence from familial AF as the result of a Kir2.1 gain-of-function mutation further indicates the pivotal role of $I_{K1}$ upregulation in AF pathogenesis [95]. Nevertheless, the underlying molecular mechanism responsible for enhanced $I_{K1}$ in AF is largely unknown. Interestingly, a new class of recently-discovered small non-coding RNA, namely microRNAs (miRNAs), has been suggested to be responsible for the upregulation of $I_{K1}$ in AF [96].

#### 1.3.1.2 Downregulation of $I_{CaL}$

Another key finding in AF-related ATR is the downregulation of $I_{CaL}$. $I_{CaL}$ has been consistently found to be downregulated in both clinical and experimental AF paradigms [76, 82, 87, 97-100], accompanied by corresponding decreases of its α-subunit Cav1.2 at mRNA level [101-107]. However, discrepant changes for Cav1.2 protein have been reported [99, 101, 103, 104, 107, 108], implying the complicated underlying mechanisms as well as uncontrollable variables in clinical studies [67]. The observed $I_{CaL}$ reduction in AF is believed to be an adaptive response of atrial cardiomyocytes to calcium overload as a consequence of rapid atrial rate during AF [49]. This adaptive response, in a short term, tends to reduce channels activity, but over a longer term, tends to decrease the expression of the channels at the gene level [49]. As a result, reduced $I_{CaL}$ decreases APD and wavelength, creating reentry substrate for AF perpetuation [49]. Although the molecular mechanism underlying ATR-induced $I_{CaL}$ downregulation has been extensively investigated by many research groups, it is still not completely understood. While some studies indicated that the transcriptional downregulation of Cav1.2 α-subunit is likely due to the activation of $Ca^{2+}$/calmodulin/calcineurin/NFAT signaling pathway caused by $Ca^{2+}$ overload [107, 109], others suggested the possible involvements of the downregulation of accessory $\beta_1$-, $\beta_{2a}$-, $\beta_{2b}$-, $\beta_3$- and $\alpha_2\delta_2$-subunits, impairment of Cav1.2 protein trafficking, and dephosphorylation of the channels due to enhanced PP1 and PP2A activities [85, 99, 102, 110-112]. Furthermore, a recent study demonstrated that miRNAs may potentially contribute to the downregulation of $I_{CaL}$ in AF through a post-transcriptional regulatory mechanism [113]. Taken together, the underlying molecular mechanism for AF-induced $I_{CaL}$ downregulation appears to be a very complex process, involving both transcriptional and post-transcriptional regulations.

#### 1.3.1.3 Abnormal $Ca^{2+}$ Handling

In addition to the reduction of $I_{CaL}$, AF-induced electrical remodeling also causes abnormal intracellular $Ca^{2+}$ handling, which primarily promotes spontaneous diastolic SR $Ca^{2+}$ release that enhances NCX-mediated $Ca^{2+}$ extrusion. The NCX-mediated $Ca^{2+}$ extrusion is an electrogenic process, which produces a net inward (depolarizing) current, causing DADs [62, 73]. Several studies have suggested that the spontaneous diastolic SR $Ca^{2+}$ release is attributed to the dysfunction of ryanodine receptor 2 (RyR2, cardiac $Ca^{2+}$ release channel on SR) [114-117], which is likely due to hyperphosphorylation caused either by increased activities of protein kinase A (PKA) and $Ca^{2+}$/calmodulin-dependent kinase II (CaMKII) [115-118] or by decreased activities of phosphatases [119]. Additionally, abnormal RyR2 release can also be a result of excess SR $Ca^{2+}$ loading due to abnormal enhancement of SR $Ca^{2+}$ uptake mediated through SR $Ca^{2+}$ ATPase (SERCA, $Ca^{2+}$ uptake pump on SR), which is activated by hyperphophorylated phospholamban [119].

#### 1.3.1.4 Alterations of other $K^+$ currents

$I_{KACh}$, another important inward rectifier potassium current, is activated upon the stimulation of acetylcholine released from vagal nerve and is responsible for cardiac vagal effects. Activation of the channels hyperpolarizes the cell membrane and shortens APD, contributing to AF pathogenesis. Several studies have shown that the agonist-dependent $I_{KACh}$ is reduced, whereas constitutively-active $I_{KACh}$ (agonist-independent) is significantly enhanced during AF-induced ATR [83, 91, 120, 121]. However, mRNA and protein levels of its underlying subunit Kir3.1 and Kir3.4 are found unaltered in experimental AF animal models [120, 121] but decreased in AF patients [122]. The enhanced constitutively-active $I_{KACh}$ is attributable to increased single channel open probability, which is controlled by the balance between different protein kinase C (PKC) isoforms [123, 124].

Consistent reduction of $I_{to}$ along with the mRNA and protein of its underlying α-subunit Kv4.3 is found in both AF patients and experimental AF animal models [76, 86, 101, 104]. However, the functional implication of $I_{to}$ reduction in AF remains to be unclear [67, 73].

Inconsistent changes of $I_{Kur}$ have been reported in both experimental AF animal models and AF patients [67], indicating the lack of pathological relevance of this channel in AF. However, given the atrial specific property of $I_{Kur}$, it still remains as a very attractive therapeutic target for the treatment of AF [49].

No changes of delayed rectifier currents $I_{Ks}$ and $I_{Kr}$ were observed in a canine model of AF [76] and there is lack of information regarding the changes of these currents in humans due to the technical difficulty in acquiring human samples and cell isolation [125].

## 1.3.2 Structural Remodeling in AF

Atrial structural remodeling (ASR) is another major aspect of atrial remodeling in AF. It is a relatively slower remodeling process compared to electrical remodeling, primarily comprising morphological changes to atrial myocardial structure and atrial architecture [20, 126]. ASR has been observed in AF from both clinical settings and experimental models, and significantly contributes to form the reentry substrates for AF. Consequences of ASR include increased atrial fibrosis, altered connexin expression, myocyte hypertrophy, myocyte apoptosis, and atrial dilation, among which, the first three aspects have been extensively studied.

### 1.3.2.1 Atrial Fibrosis

Atrial fibrosis, although not exclusively related to AF but appears as a common feature of clinical AF. It is one of the most important arrhythmogenic contributors to AF [73]. Atrial fibrosis has been commonly observed in lone AF [127, 128] and AF-associated pathophysiological conditions, including congestive heart failure (CHF) [129, 130], valvular diseases [131], rheumatic heart disease [132, 133], dilated and hypertrophic cardiomyopathy [134, 135], and senescence [136, 137]. Moreover, a reduced AF stability and delayed atrial structural remodeling process have been observed in some experimental and clinical studies using compounds with known anti-fibrotic effect, such as statins (HMG-CoA reductase inhibitors) [138, 139], angiotensin II type 1 receptor (AT1R) blocker

[140], and fish oil [141]. However, the observed beneficial outcome of these compounds may be a result of the improvements in hemodynamic [73]. Together, these findings suggest an important association between atrial fibrosis and AF but fail to establish a causal significance of atrial fibrosis in AF occurrence and perpetuation. It is also important to note that AF may itself promote atrial fibrosis, which in turn sustains AF [142, 143]. Evidence supporting this notion came from the observations that the quantity of fibrosis positively correlates with the persistence of AF in patients [144], and that atrial tachypacing alone causes atrial fibrosis in a canine ATP model with well-controlled ventricular rate [145].

Cardiac fibrosis is either a reparative or reactive process, which primarily involves excessive accumulation of extracellular matrix (ECM) proteins secreted by myofibroblasts (cells derived from fibroblasts in the presence of various stimuli) [142, 143]. Reparative fibrosis maintains tissue structural integrity by replacing dead cardiomyocytes, whereas reactive fibrosis occurs in response to various cardiac insults and causes interstitial expansion, separating muscle bundles [142, 143]. The resultant fibrotic tissue creates an obstacle to interfere with normal impulse propagation and thus causes conduction abnormalities [129]. In addition, recent studies have suggested that cardiac fibroblasts can electrically influence adjacent cardiomyocytes and thus alter cardiac electrical function [143]. Taken together, the fibrotic remodeling manifested during AF may cause conduction abnormalities and increase fibroblast-cardiomyocyte electrical interaction, favoring AF occurrence and maintenance.

#### 1.3.2.1.1 Profibrotic Factors and Atrial Fibrosis

The precise molecular mechanisms underlying ECM formation during atrial fibrosis remain incompletely understood. Emerging evidence has suggested that several cardiomyocyte and/or fibroblast secreted factors with known profibrotic effects are critically involved [142]. Among these factors, angiotensin II (AngII) and its downstream mediator transforming growth factor $\beta_1$ (TGF-$\beta_{1)}$ have been well characterized to contribute to fibroblast differentiation and proliferation, whereas platelet-derived growth factor (PDGF) and connective tissue growth factor (CTGF) have just emerged as potential fibrosis mediators [20, 142].

It has been shown that increased production of AngII as a consequence of cardiac-specific overexpression of angiotensin converting enzyme (ACE) may cause severe atrial dilation accompanied by atrial fibrosis and AF in mice [146]. AngII promotes cardiac fibrosis via signaling cascades coupled to AT1R and AT2R, which have distinct and sometimes opposite effects (eg. AT1R facilitates fibrosis while AT2R counteracts the effect of AT1R); the net outcome of these opposite effects is an activation of mitogen-activated protein kinase (MAPK) that is considered as an important mediator for fibrotic remodeling [142, 147]. In addition, stimulation of AT1R can also activate protein kinase C (PKC) and increase intracellular $Ca^{2+}$ release, together contributing to AngII-mediated fibrotic remodeling [147].

TGF-$\beta_1$ has been suggested to play a central role in signaling cascades involved in cardiac fibrosis [142, 148]. TGF-$\beta_1$ is a primary downstream mediator upon AngII stimulation and is secreted by both fibroblasts and cardiomyocytes [149]. Cardiac-specific overexpression of constitutively-active TGF-$\beta_1$ in mice causes atrial fibrosis and atrial conduction heterogeneity and increases AF vulnerability [150]. TGF-$\beta_1$ primarily acts through the SMAD signaling pathway, stimulating fibroblast activation and collagen production [151].

More recently, a study showing the presence of cardiac fibrosis in mice with cardiac-specific PDGF overexpression has indicated the potentially-important role of PDGF in the genesis of cardiac fibrosis [152, 153]; however, the link between PDGF and fibrosis-related AF susceptibility was missing, given that AF vulnerability was not assessed in these animals [142, 152]. CTGF is also found to be an important mediator in cardiac fibroblast activation upon AngII stimulation [154]. Moreover, pathway analysis in a genomic study of CHF-related AF substrate has suggested a possible involvement of CTGF in this process [155].

#### 1.3.2.1.2 Potential role of TRP Channels in Atrial Fibrosis

There is a growing body of evidence suggesting that fibrotic susceptibility is more profound in atria than in ventricle [129, 146, 150, 156, 157]. Atrial fibroblasts show greater proliferative response and faster myofibroblast differentiation upon growth stimuli, as

compared to ventricular fibroblasts [149]. Fibroblast proliferation and differentiation into myofibroblasts are the characteristics of fibrogenesis and numerous studies have suggested that $Ca^{2+}$ entry is essential for fibroblast proliferation and fibroblast function [158-162]. Interestingly, however, the absence of voltage-gated $Ca^{2+}$ channels in cardiac fibroblasts suggests the existence of other $Ca^{2+}$-permeable ion channels that are responsible for $Ca^{2+}$ entry in these cells [163]. The presence of transient receptor potential (TRP) channels in cardiac fibroblasts has shed light on this matter. TRP channels are well-known to be responsible for $Ca^{2+}$ entry in a variety of cell types and are activated upon mechanical stretch, oxidative stress, and metabolic disturbance, conditions commonly observed in AF [164-166]. Hence, it is very likely that TRP channels may participate in atrial fibrogenesis in AF, particularly via stimulation of fibroblast proliferation and differentiation. To date, 28 mammalian TRP channel genes have been identified [164]. Based on sequence homology, they are categorized into six subfamilies: TRPC subfamily (canonical, TRPC1-7), TRPM subfamily (melastatin, TRPM1-8), TRPV subfamily (vanilloid, TRPV1-6), TRPA subfamily (ankyrin, TRPA1), TRPP subfamily (polycystin, TRPP1-3), and TRPML subfamily (mucolipin, TRPML1-3). However, only subsets of these families are detectable in cardiac fibroblasts. For instance, TRPC1-3, TRPC5-7, TRPM7 and TRPV4 are expressed in rat and human cardiac fibroblast as measured by RT-PCR [167, 168]. Of note, a recent study has highlighted the potentially important role of TRP channels in AF fibrogenesis [168]. This study showed that atrial fibroblasts from AF patients are more prone to myofibroblast differentiation with concomitant increases of TRPM7 expression and $Ca^{2+}$ influx. Moreover, in vitro knockdown of TRPM7 largely attenuates AF fibroblast differentiation, suggesting an essential role of TRPM7 in AF fibrogenesis [168].

#### 1.3.2.2 Dysregulation of Gap junction protein

The conduction abnormality in AF can also result from altered and/or heterogeneous expression of the gap junction proteins, namely connexins, which are responsible for cell-to-cell conduction [67, 73]. Connexin40 (Cx40) and connexin43 (Cx43) are two main subunits in atria, whereas, in ventricular tissue, Cx43 appears to be the sole underlying subunit [169, 170]. Several studies have reported inconsistent changes of Cx40 and Cx43 in

AF, as some found increased while others found unaltered or decreased expression [67, 73]. Nevertheless, heterogeneous expression of Cx40 and Cx43 has been consistently documented in both experimental and clinical AF [171-174]. The increased connexin heterogeneity may contribute to abnormal conduction, thereby favoring reentry substrates for AF.

## 1.4 Inward Rectifier Potassium Channel ($I_{K1}$)

### 1.4.1 Biophysical Properties and Cellular Functions of $I_{K1}$

$I_{K1}$ is the main component of inward rectifier basal currents in human atrial myocytes [175, 176]. It plays two key roles in cardiac electrophysiology: 1) to maintain the cellular resting membrane potential; and 2) to terminate repolarization of cardiac AP [93, 177]. These are largely due to its "inwardly rectifying" property, which allows the channels selectively support the flow of positively-charged $K^+$ into the cells (inward current), when membrane potential is negative to potassium equilibrium potential (or reversal potential) [93, 177]. A simpler way to understand this is that the channels pass inward current more easily than outward current. Because the inward rectification of $I_{K1}$ is strong, this allows the channels to carry substantial inward current at negative potentials (even more negative than the $K^+$ reversal potential), thereby stabilizing the membrane resting potential [177, 178]. On the other hand, when cell membrane depolarizes or is positive to $K^+$ reversal potential, the large conductance for inward current is progressively shut down as a result of "rectification", eliciting a relatively small but significant outward current, which helps to terminate the cardiac AP [177, 178]. The phenomenon of inward rectification of $I_{K1}$ is the result of the block of the channel pore by intracellular $Mg^{2+}$ and polyamines at positive potentials, resulting in a decrease of outward current [179, 180]. $I_{K1}$ is constitutively active and extracellular $Ba^{2+}$ and $Cs^+$ selectively block the channels in a voltage-dependent manner. This selective blockade by $Ba^{2+}$ and $Cs^+$ is often used to distinguish $I_{K1}$ from other currents in voltage clamp experiments [181].

### 1.4.2 Molecular Basis of $I_{K1}$

Substantial evidence has indicated that native cardiac $I_{K1}$ is carried by channels that appear as heterotetramers consisting of Kir2 subunits (Kir2.1, Kir2.2, and Kir2.3) [182, 183]. Each of these subunits consists of two transmembrane domains (TM1 and TM2) [184]. As defined by human genome organization, genes encoding Kir2 subunits are given name *KCNJ*, i.e., *KCNJ2* (encoding Kir2.1), *KCNJ12* (encoding Kir2.2), and *KCNJ4* (encoding Kir2.3) [185]. In human, Kir2.1 is the most abundantly-expressed subunit underlying $I_{K1}$ [186, 187]. The predominant role of Kir2.1 as the main molecular identity underlying $I_{K1}$ was elucidated by using Kir2.1 and Kir2.2 knockout mice [188, 189]. No detectable $I_{K1}$ was recorded in the isolated cardiomyocytes from Kir2.1 knockout mice, whereas, ~ 50% reduction of $I_{K1}$ was observed in the myocytes from Kir2.2 knockout littermates, suggesting a crucial role of Kir2.1 in genesis of $I_{K1}$ and functional $I_{K1}$ channels are likely heteromeric [188, 189]. Indeed, this is supported by subsequent biochemical studies, confirming the co-assembly of different Kir2 subunits in cardiomyocytes [190, 191].

### 1.4.3 Regulation of $I_{K1}$

In addition to the direct regulation of the channel pore by intracellular $Mg^{2+}$ and polyamines, native $I_{K1}$ can also be regulated by many other factors including phosphatidylinositol-4, 5-bisphosphate (PIP2), adrenergic stimulation, protein kinases (PKA and PKC), and pH [192]. While circumstantial evidence has suggested that $I_{K1}$ can be activated by PIP2 through its direct interaction with a group of positively charged residues located in the transmembrane domain 2 (TM2) region of Kir2.1 [193-195], other studies have suggested that residues harbored in cytoplasmic $NH_2$ and COOH termini also contribute to PIP2 activation of Kir2.1 [196]. Adrenergic stimulation is also reported to regulate the native $I_{K1}$ [197, 198]. In isolated human cardiomyocytes, stimulations of both α1- and β-adrenergic receptors strongly inhibite native $I_{K1}$ [197, 198]. This inhibitory effect upon stimulation of α1- adrenergic receptors is attributable to PKC activation [197], whereas β-adrenergic inhibition of the channel primarily is mediated by a PKA-dependent pathway [198]. Furthermore, modulation of $I_{K1}$ can be achieved via phosphorylation of the channel subunits by protein kinases such as PKA and PKC [192]. PKC activators were

shown to repress $I_{K1}$ associated with Kir2.2 and Kir2.3 but not that with Kir2.1 [123, 199]. Activation of PKA, however, increases currents carried by Kir2.1 or Kir2.2 [200, 201]. The native $I_{K1}$ is also affected by intracellular pH. Decreased intracellular pH was shown to cause significant reduction of $I_{K1}$ [202]; this is likely due to the abolishment of channel-PIP2 interaction [203]. Interestingly, a recent study has clearly demonstrated an involvement of microRNA in the regulation of $I_{K1}$. In this study, the authors showed that microRNA-1 (a type of cardiac-enriched muscle-specific non-coding small RNA) is able to repress native $I_{K1}$ current through a post-transcriptional repression of the channel subunit Kir2.1, suggesting a potentially-important novel regulatory mechanism for $I_{K1}$ [204].

### 1.4.4 Dysregulation of $I_{K1}$ and its pathophysiological implication in AF

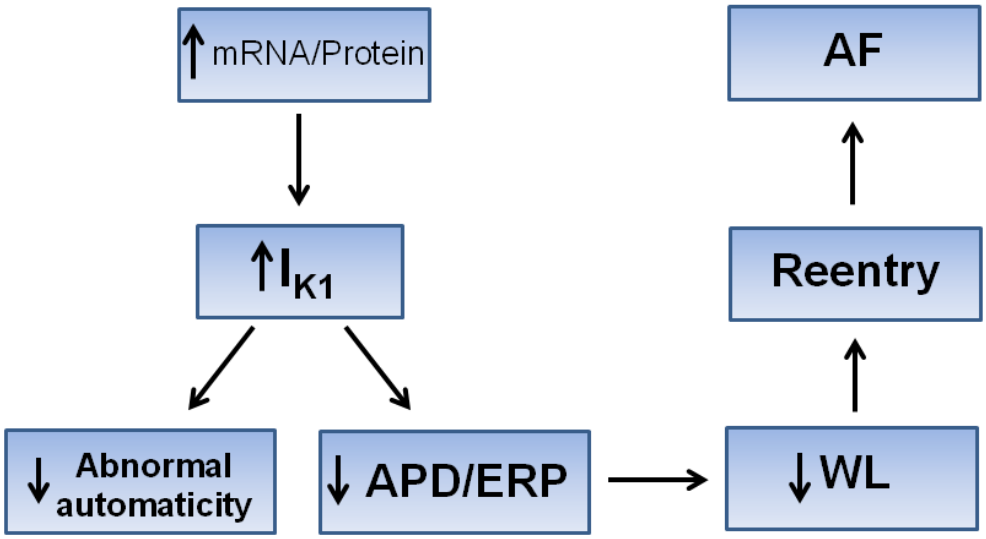


Figure 5. Schematic representation of pathophysiological significance of $I_{K1}$ upregulation in AF. APD: action potential duration; ERP: effective refractory period; WL: wavelength; AF: atrial fibrillation.

A schematic illustration of the pathophysiological significance of $I_{K1}$ upregulation in AF is shown in Figure 5. As discussed in Section 3.1.1, upregulated $I_{K1}$ has been consistently observed during AF [82-89], and this upregulation was accompanied with the increased expression of its underlying subunit Kir2.1 at both mRNA and protein levels [83, 85]. Given the crucial role of $I_{K1}$ in setting the cellular membrane resting potential and terminating cardiac AP, the upregulation of $I_{K1}$ in AF, may have two pathophysiological

consequences: 1) the increased $I_{K1}$ may favor the maintenance of cellular membrane resting potential, thereby preventing the abnormal automaticity (Figure 5); 2) the enhanced $I_{K1}$ may contribute to the shortening of APD and ERP, favoring the maintenance of reentrant substrates for AF (Figure 5). However, little is known about the molecular mechanism underlying AF-induced upregulation of $I_{K1}$. Recently, a study provided a novel insight into this matter. In this study, the authors evaluated the correlation between the changes of miR-1 and the alterations of $I_{K1}$ as well as Kir2.1 expression in the left atrium of the valvular heart disease patients with persistent AF [96]. $I_{K1}$ was found to be significantly upregulated with a corresponding increase in Kir2.1 protein expression in the atrial samples from these AF patients [96]. Conversely, miR-1 levels were found to be significantly reduced [96]. The authors proposed that AF-induced upregulation of $I_{K1}$ and its underlying subunit (Kir2.1) expression is likely attributable to the reduction of miR-1 [96], because miR-1 was previously reported to post-transcriptionally repress *KCNJ2* (gene encoding Kir2.1) [204]. The findings of this study are valuable in the sense that they suggest a potentially-important novel regulatory mechanism for AF-induced $I_{K1}$ upregulation. However, the evidence provided in this study to support the role of miR-1 downregulation in AF-induced $I_{K1}$ upregulation is only suggestive. Further studies are required to establish a direct role of miR-1 in AF. Moreover, it is important to determine whether there are other miRNAs involved in this AF-induced ionic remodeling process.

## 1.5 Transient Receptor Potential Canonical Channel Type 3 (TRPC3)

TRPC3 belongs to a group of TRPC channels, a classical or canonical subclass in TRP channels superfamily. The human TRPC family consists of six isoforms (TRPC1, 3-7), which can be grouped into two subfamilies: TRPC1/4/5 and TRPC3/6/7, based on sequence homology and functional similarities [205-207]. For example, TRPC3 shares ~75% sequence identity with TRPC6 and TRPC7 [208].

### 1.5.1 Biophysical Properties and Cellular Functions of TRPC3

Owing to the high degree of similarities among all TRPC isoforms and the lack of specific pharmacological blockers, it is technically difficult to record the currents carried by TRPC3 channels in a native environment; thus, the biophysical properties of TRPC3 channels are mainly characterized in either homologous or heterologous expression systems [205, 209, 210]. TRPC3 as well as its homologues TRPC6 and TRPC7 typically assemble as homo- or heterotetramer to form functional channels permeable to cations ($Ca^{2+}$ and $Na^{+}$) [205, 209, 210]. The resultant currents show voltage independence and dual rectifications in both inward and outward directions [208, 211]. Moreover, TRPC3 channels are constitutively active and are effectively blocked by $La^{3+}$ and $Gd^{3+}$ ions, which also block the other TRPC channels. Interestingly, a recent study found a pyrazole compound (Pyr3) to be a selective blocker for TRPC3 channels [212]. This compound may serve as a powerful tool for the in vivo functional study of TRPC3 channels [212].

TRPC3 channels broadly exist in a variety of cell types including excitable and non-excitable cells and are predominantly located on the plasma membrane [205, 206, 209]. Their primary cellular function is thought to be non-voltage-gated $Ca^{2+}$ entry [205-207, 213]. There are two types of $Ca^{2+}$ entry mechanisms: store-operated $Ca^{2+}$ entry (SOCE) and receptor-operated $Ca^{2+}$ entry (ROCE). However, the participation of TRPC channels in these mechanisms is controversial [205-207, 213].

### 1.5.2 Molecular Basis of TRPC3

Functional TRPC3 channels are comprised of four TRPC subunits [209]; however, it is unclear whether the native TRPC3 channels exist as homotetramers or heterotetramers [209]. Typical structure of TRPC3 subunit includes six transmembrane domains (TM1-TM6), a putative pore region constituted by TM5 and TM6 together with their connecting loop, and intracellular N and C termini that are functionally important for channel trafficking, anchoring, localization, and gating [214, 215]. Of note, the lack of voltage sensing in TM4 makes the channels non voltage-dependent [206, 209, 215]. The *TRPC3* gene was originally cloned from human embryonic kidney cell line (HEK293) and consists of 11 exons that locate on chromosome 4 in the human genome [215]. The regional

expression profile of *TRPC3* in the heart is incompletely known, although evidence has indicated its broad expression in a variety of cardiac cells such as cardiac endothelial cells, cardiac smooth muscle cells, and cardiomyocytes [206, 216].

### 1.5.3 Regulation of TRPC3

The activity of TRPC3 channels can be regulated by mechanical stretch and various ligands and plasma membrane receptors [206, 209]. Substantial evidence suggests that mechanical stress may enhance TRPC3 channel activation and/or expression [217, 218]. It has been shown that TRPC3 channels are constitutively active and this basal activity of TRPC3 channel is attributable to the glycosylation status, which is increased upon stimulation of G protein-coupled receptor (GPCR) or receptor tyrosine kinase [211, 219-221]. Consequently, ligands such as AngII and ET-1, which can stimulate GPCR, were found to increase TRPC3 channel activity [222, 223]. Increased phospholipase C (PLC) activity as a result of activated GPCR-dependent signaling also enhances TRPC3 channel activity [224, 225]. This is primarily due to a direct activation of TRPC3 channels by diacylglycerol (DAG), a lipid mediator that is generated by the GPCR-PLC signaling pathway [224-226]. In addition to GPCR, several other studies have suggested that activation of inositol 1,4,5-trisphosphate ($IP_3$) receptor may indirectly activate TRPC3 channels through a displacement of inhibitory calmodulin from a common binding domain on the channel [227, 228]. Despite the regulation by plasma membrane receptors, TRPC3 channel activity as well as its expression can also be regulated by a redox-dependent alteration in membrane lipids, more specially, cholesterol [229-232]. Mechanistically, the agonist effect of cholesterol on TRPC3 channels is attributable to the association between TRPC3 and scaffolding protein, caveolin-1 [233]. Additionally, an interaction between immunophilin and TRPC3 protein has been suggested to be essential for channel activation, as there is a direct binding domain for immunophilin in the C-terminal proline-rich region of TRPC3 protein [234]. Finally, protein kinases have also been suggested to regulate TRPC3 channel activity [235, 236]. Indeed, PKC was found to negatively regulate TRPC3 through direct phosphorylation of serine at position 712 [236], whereas enhanced PKA activity was able to increase TRPC3 expression [235].

### 1.5.4 Dysregulation of TRPC3 and its potential pathophysiological implication in AF

As discussed in Section 3.2.1.2, TRP channels may likely contribute to $Ca^{2+}$-mediated atrial fibrogenesis in AF. Indeed, a recent study has highlighted an important role of TRPM7 channels in AF-associated fibrotic remodeling [168]. However, it is important to determine whether other TRP channels also participate in this remodeling process, given that several TRP channels including TRPM7 are abundantly expressed in cardiac fibroblasts and many of them are functionally and structurally similar [164, 168]. Interestingly, it has been shown in a recent study that, unlike other TRP members, TRPC3 is mainly enriched in freshly-isolated atrial fibroblasts and this enrichment diminishes upon fibroblast differentiation to myofibroblasts [237]. These findings suggest a potentially-important role of TRPC3 in mediating fibroblast function, which contributes importantly to fibrogenesis. In this regard, any deregulation of TRPC3 occurring during AF may potentially contribute to the AF-associated atrial fibrosis. Further studies are required to determine the changes of TRPC3 in AF as well as the underlying mechanisms responsible for this deregulation.

## 1.6 MicroRNA Biology

### 1.6.1 Historical View of MicroRNAs

MicroRNAs (miRNAs) belong to a new class of non-coding RNAs. The discovery of the first microRNA (miRNA), lin-4 occurred almost twenty years ago [238, 239]. However, this discovery was initially considered an anomaly. These small non-coding RNAs were not brought into attention until the identification of a second miRNA, let-7, which was found to be crucially involved in the development of *Caenorhabditis elegans* (*C elegans*) [240]. Subsequent studies soon revealed that let-7, as well as many other newly-identified miRNAs, broadly exist in various vertebrate species including humans, suggesting that these miRNAs are not only evolutionarily conserved but also ubiquitously expressed across different species [241-244]. Since then, miRNAs have increasingly attracted interest, leading to the discovery of many more mammalian miRNAs. A pioneer study showing the correlation between miRNAs and human disease appeared in 2002 [245]. 3 years later, in

2005, the first cardiac miRNA study was conducted, revealing that miRNA is essential during cardiogenesis [246]. During the past 6 years, the roles of miRNAs have been increasingly appreciated in the cardiovascular system by researchers, as these tiny molecules appear to be essential in controlling a wide range of biological processes. Recent studies in the field have clearly demonstrated that aberrant expression of miRNA is tightly correlated with the onset and progression of cardiovascular diseases [247, 248]; and in some cases, correcting an aberrantly-expressed miRNA is able to prevent or attenuate the progression of certain cardiac diseases [247, 248]. Together, these findings have greatly advanced our current understanding of the potential pathophysiological implications of miRNAs in various cardiac conditions [247, 248]. Hence, miRNAs may potentially serve as new diagnostic tools and therapeutic targets for cardiovascular diseases.

### 1.6.2 MiRNA Biogenesis

MiRNA biogenesis is a multi-step process that requires synergistic participation of a variety of enzymes and regulatory proteins [249, 250]. Similar to protein-coding genes, the primary transcripts of miRNAs, namely pri-miRNAs, are initially transcribed from genomic sequences by RNA polymerase II in the nucleus [251, 252], as shown in Figure 6. Of note, depending on the locations of original miRNA-coding genes, miRNAs can be classified into three different categories: intergenic miRNAs (miRNA coding genes not belonging to any annotated transcripts), intronic miRNAs (miRNA coding genes falling within an intron of a host protein coding gene), and exonic miRNAs (miRNA coding genes overlapping with an exon of a known protein coding gene) [247, 253] (Figure 6). For intronic and exonic miRNAs, an extra step of trimming by spliceosome is required to release the pri-miRNAs from their host gene transcripts [253] (Figure 6). In addition, pri-miRNAs can give rise to either a single or multiple miRNAs, so-called “polycistronic miRNAs”, a cluster of miRNAs with similar sequences [247, 253]. Unlike protein-coding genes, the primary transcripts of miRNAs (or pri-miRNAs), with length ranging from hundreds to thousands of nucleotides (nt), subsequently fold into imperfectly base-paired stem-loop structures that are further excised by RNase III endonuclease Drosha and the double-stranded RNA binding protein DGCR8, resulting in ~70- to 100-nt hairpin-shaped

precursor miRNA (pre-miRNA) [254-256] (Figure 6). It is noteworthy that the processing of intronic miRNAs from their pri-miRNAs to pre-miRNAs escapes the Drosha pathway, but uses an alternative splicing-mediated mechanism and the resultant hairpin pre-miRNAs are named "mirtron" [257, 258] (Figure 6). Through incorporating with the nuclear export factor exportin 5 [259-261], the pre-miRNAs are then translocated from the nucleus to the cytoplasm, where they are further cleaved by another RNase III endonuclease Dicer to generate ~19- to 25-nt mature miRNA duplex [252, 262] (Figure 6).

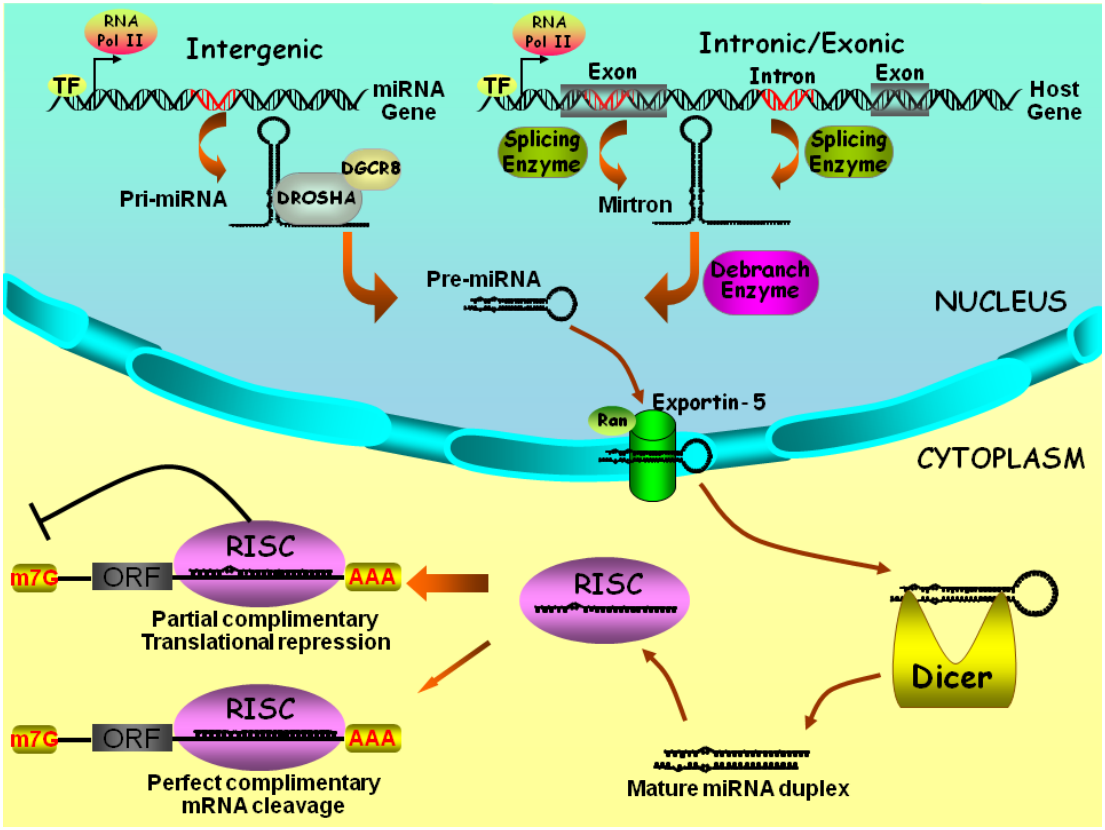


Figure 6. Biogenesis and actions of miRNA. TF: transcription factor; Pri-miRNA: primary transcript of miRNA; Pre-miRNA: precursor miRNA; RISC: RNA-induced silencing complex; ORF: open reading frame. Adapted from Wang Z et al. [263] with modification.

## 1.6.3 Action and Biological Functions of MiRNAs

### 1.6.3.1 Action of MiRNAs

The primary action of miRNAs is to repress the translation output from the target mRNAs [252]. As the first step leading to this action, the mature miRNA duplex is incorporated into

the protein complex known as RNA-induced silencing complex (RISC) [264, 265] (In Figure 6). Only one strand of the mature miRNA (guide strand) remains in RISC, whereas the other strand (passenger strand) is often degraded [264, 265] (Figure 6). This single-stranded miRNAs-RISC primarily binds to the 3'-untranslated region (3'UTR) of their target mRNAs according to Watson and Crick base-paring rule [266, 267]. Unlike short interfering RNAs (siRNAs), the majority of miRNAs **:** mRNAs bindings are partially complementary [266-269]. However, a perfect complementary between the first 2- to 8- nt 5' sequence of a miRNA (also known as the "seed site" region of a miRNA) and the target mRNA is essential for the miRNA action [266-269]. Finally, depending on the degree of complementarity between miRNAs and their target mRNAs, miRNAs either inhibit the translation of the encoded proteins (by partial complementarity, Figure 6) or lead to mRNA degradation (by perfect complementarity, Figure 6) [269, 270].

#### 1.6.3.2 Biological Functions of MiRNAs

Since the discovery of the first functional miRNA, research over the past twenty years has generated substantial evidence showing the essential roles of miRNAs in various fundamental biological processes such as development, apoptosis, cell differentiation and proliferation, cell growth and cell death, and aging [249, 250]. Another major advancement in our understanding of the biological functions of miRNAs is that miRNAs have emerged not only as indicative but also causative factors in numerous diseases, including cancer, heart diseases, diabetes, and neurological diseases [248-250, 271-273].

### 1.6.4 MiRNA Nomenclature

Table 1. MiRNA nomenclature.

| miRNA | Nomenclature | Example |
|---|---|---|
| **Mature form of miRNA** | **The prefix "miR" is followed by a dash and a number, which is designated sequentially** | **miR-1 was likely discovered before miR-26** |
| **miRNAs with nearly identical sequences** | **Denoted with an additional lowercase letter** | **miR-26a/miR-26b; miR-29a/miR-29b** |
| **miRNA originated from different species** | **The three-letter prefix representing the species of origin is followed by "miR"** | **has-miR-26 (*Homo sapiens*)**<br>**mmu-miR-26 (*Mus musculus*)** |

According to the guideline of miRNA registry [274], the designation of mature miRNAs is given as number that follows a chronological order based on the time of their discoveries (Table 1). Exceptions are seen for some of the earliest discovered miRNAs, such as lin-4 and let-7, whose name are defined according to their target genes. Similar miRNAs that differ only in one or two oligonucleotides in 3' region of their sequences are classified as a family and are denoted with an extra letter for their designations (Table 1). Since the majority of miRNAs are highly conserved across different species, a three-letter prefix representing their species of origin is adopted in miRNA nomenclature (Table 1).

### 1.6.5 Determination of MiRNA Targets

To date, over 900 human miRNAs have been identified [248]; it has been predicted that the human genome may encode more than 1000 miRNAs, which may regulate two thirds of all human protein coding genes [250, 253, 275, 276]. Given that a single miRNA could theoretically target hundreds or thousands of potential targets, and conversely, one mRNA could be simultaneously targeted by multiple miRNAs, identification and validation of authentic miRNAs targets inevitably represents the major challenges in miRNA research

[250, 275]. Current practice to overcome these problems involves a two-step procedure, including an initial computational target prediction followed by an experimental validation.

#### 1.6.5.1 Computational Prediction of MiRNA Targets

There is an array of tools that are currently available for miRNA target prediction, which are presented as website-based interfaces for an easy-access purpose. Of note, most of these tools are developed by using seemingly distinct but actually similar algorithms that follow a series of important standards in regards to the identification and ranking of potential targets [247, 250]. For example, most of the programs primarily rely on sequence complementarity between the 5' seed region (2-8 nt of the 5' sequence) of a miRNA and the 3'UTRs of target mRNAs to determine the likelihood of miRNA targets [247, 250, 275]. The ranking of these predicted targets is based on the degree of overall complementarity as well as the conservation of both miRNA and 3'UTR target sequences across species [247, 250, 275]. Currently, three most commonly and widely used programs are TargetScan [267], PicTar [277], and miRanda [278], which differ in prediction sensitivity and specificity [250]. A practice to combine the results generated from different programs could theoretically enhance the sensitivity and/or specificity and, hence, becomes increasingly favorable for miRNA researchers [247]. There are two advantages of using in silico approach for miRNA target prediction prior to the experimental identification. First, the inherent high throughput feature allows researchers to easily portray a more thorough picture of the miRNA candidates for a given gene or the genes targeted by a given miRNA. Second, it serves as a powerful mean to predict a potential cellular function of a miRNA or a cluster of miRNAs.

#### 1.6.5.2 Experimental Validation of MiRNA Targets

A common scheme to experimentally validate miRNA targets includes two parts [247, 279]: 1) to verify the binding ability of a miRNA to its predicted 3'UTR binding site by using luciferase reporter assay; i.e., insert the partial or full length of 3'UTR of a target gene containing the predicted binding site for a given miRNA into the luciferase reporter vector; by this way, any physical interaction between the miRNA and the 3'UTR can affect

the production of the luciferase protein; therefore, the effectiveness of the binding can be determined by measuring of the fluorescent signal generated by the luciferase [247, 279]. 2) to observe whether an endogenous protein encoded by a given miRNA target gene, is indeed affected by the miRNA in a native cellular environment [247, 279].

Two strategies are commonly used in the luciferase study to validate the miRNA targets [247, 279]. The first strategy involves the construction of a luciferase report vector that contains either the wild-type 3'UTR (bearing the intact putative binding for a specific miRNA) or the mutant 3'UTR (bearing the mutated binding site for the same miRNA); these constructs are then separately transfected into a cell line that abundantly expresses the miRNA of interest; if the luciferase activity from cells transfected with wild-type 3'UTR is reduced and indeed this reduction is absent in cells transfected with mutant construct, the binding site is likely to be authentic for the miRNA [247, 279]. Of note, an additional experiment to inhibit the endogenously expressed miRNA by anti-miRNA oligos (miRNA inhibitor) in the same settings can further prove the specificity [247]. The second strategy relies on a cell line, in which the miRNA of interest is modestly or poorly expressed [247, 279]. Instead of knocking down the endogenous miRNA, a specific miRNA is overexpressed in the cells by using the synthetic "miRNA mimic" or the miRNA overexpression vector [279]. Consequently, if cells transfected with wild-type 3'UTR show a dose-dependent reduction of the luciferase activity in response to the miRNA overexpression while this effect is absent in cells transfected with the mutant 3'UTR, the tested binding site is considered to be responsive to the given miRNA [247, 279].

Unlike luciferase reporter assay, western blotting allows a direct measurement of the effect of a miRNA on the level of its target protein. Similar to luciferase study, transfection of the synthetic miRNA mimic or the miRNA overexpression vector can be used as an overexpression approach, whereas inhibition can be achieved by using anti-miRNA oligos [279, 280]. It should be noted that choosing a proper cell type with relatively-high expression levels of the target protein and the corresponding miRNA is important for a successful western blotting verification [279, 280]. Ideally, the selected cell type should modestly express the miRNA of interest because the changes of the protein expression in response to either miRNA knockdown or overexpression can be more accurately reflected when the background level of the studied miRNA in the cells is modest.

## 1.6.6 MiRNA Expression in the Heart

### 1.6.6.1 Cardiac Selectivity of MiRNA Expression

Under the normal conditions, expression of miRNAs in heart displays a distinct pattern comparing to the other organs [281]. Of ~ 900 miRNAs identified in human, only a subset of these miRNAs is abundantly expressed in heart. Based on a recent study, the top 20 most abundant miRNAs in human heart are miR-1, miR-133a/b, miR-26a/b, miR-125a/b, let-7a/b/c/f/g, miR-16, miR-100, miR-126, miR-145, miR-195, miR-199, miR-20, miR-21, miR-23, miR-24, miR-29a/b, miR-27a/b, miR-30a/b/c, miR-92a/b, and miR-99 [281]. Interestingly, the majority of these cardiac-enriched miRNAs are ubiquitously expressed in various organs except for miR-1 and miR-133a/b [281], both of which are preferentially expressed in cardiac and skeletal muscle [282]. In addition to miR-1 and miR-133a, some less abundantly-expressed miRNAs, miR-208a/b and miR-499, are also found to be cardiac-specific [283], as they are co-transcribed with the cardiac-specific genes, MYH6 (encoding the α-myosin heavy chain, miR-208a), MYH7 (encoding the β-myosin heavy chain, miR-208b), and MYH7b (encoding isoforms b of the β-myosin heavy chain, miR-499), respectively [283].

### 1.6.6.2 Cell Type Specification of MiRNA Expression in the Heart

Although the majority of cardiac-enriched miRNAs are ubiquitously expressed in various organs, many of them exhibit cell-type preferential expression. For example, miR-1 and miR-133a/b are muscle-specific miRNAs that are preferentially expressed in cardiac and skeletal muscle cells [282]; miR-21 and miR-29a/b are preferentially expressed in fibroblasts [284, 285]; miR-126, miR-24, and miR-92a are largely enriched in endothelial cells [286]; miR-145 is detectable mainly in smooth muscle cells [287].

### 1.6.6.3 MiRNA Detection and Quantification

Current methods for miRNA detection primarily focus on the detection of mature miRNAs. This is due to the fact that the expression level of pri-miRNAs is generally not in linear

relation with the expression level of their corresponding mature miRNAs [247]. To date, a variety of techniques have been employed to determine the abundance and/or presence of miRNAs. Microarray and deep sequencing serve as profiling approaches to determine the global expression of miRNAs, whereas the expression of individual miRNA can be more precisely quantified by real-time RT-PCR and Northern blotting.

#### 1.6.6.3.1 Detection of MiRNAs by Microarray

One of the most significant advantages of using microarray for miRNA detection is that it allows a large number of miRNAs in a given tissue or cell sample to be simultaneously analyzed [288, 289]. Owing to this high through-put feature, microarray analysis is generally considered as the most practical approach for miRNA screening. However, given that the principle for microarray is based on the hybridization between capture probes (synthetic oligonucleotides) and targeted miRNAs, and that the binding affinities towards the capture probes differ among miRNAs, microarray should not be considered as a quantitative method to determine the expression level of miRNAs [290-292]. Instead, it can serve as a comparative approach to show the relative changes of miRNAs expression between 2 states or the presence of miRNAs between different tissues or cell-types [290-292]. For example, it will be ideal to use microarray analysis to compare the miRNA expression profiles between diseased and non-diseased hearts [247, 289]. Currently, there are several commercially available miRNA microarray platforms, which differ in sensitivity and specificity due to the different designs of capture probes [290]. Although microarray represents a practical and easy approach for miRNA screening, there are several inherent limitations: 1) relatively low sensitivity of the capture probes may fail to detect the low abundant miRNAs; 2) owing to the low specificity of the hybridization, a false positive result is unavoidable; and 3) microarray results represent the relative changes between samples and are unable to conduct quantitative analysis. Therefore, the microarray results should be confirmed by other detection methods [288, 289, 293].

#### 1.6.6.3.2 Detection and Quantification of MiRNAs by Deep Sequencing

Similar to microarray analysis, deep sequencing is also a high through-put approach for profiling a large number of miRNAs [292]; however, unlike microarray that is solely based on hybridization, deep sequencing relies on the PCR-based parallel sequencing, which can capture miRNAs with low copy numbers (few molecules per cell) that are normally undetectable by microarray [292, 294]. In addition to the superior sensitivity, deep sequencing can measure the absolute abundance of the miRNAs, and thus the result is quantitative [294]. Despite the advantages over microarray as a miRNA profiling method, deep sequencing can also serve as a powerful tool for new miRNA discovery [294, 295]. This is due to the fact that this sequencing based-technique can theoretically capture any known and unknown miRNAs or even structurally-similar RNA fragments during the robust PCR reactions [294, 296]. However, a proper interpretation of the massive information generated by deep sequencing poses a great challenge for subsequent bioinformatic analysis and experimental verification, which are normally costly and time-consuming [292, 294]. Therefore, deep sequencing still remains as a second option for miRNA profiling in comparison to microarray.

#### 1.6.6.3.3 Quantification of MiRNAs by Real-time RT-PCR

Although the overview of global miRNA expression provided by microarray or deep sequencing is useful and informative, the accuracy of the results needs to be further validated by more specific approaches that allow individual quantification of the miRNA expression [297, 298]. To date, real-time RT-PCR is the most commonly used quantitative method for the assessment of individual miRNA expression [299-301]. Unlike detection of protein-coding RNA, detection of miRNA by real-time RT-PCR is bound with difficulties, particularly for the synthesis of first strand cDNA (reverse transcription). These are largely due to the unique features of miRNAs, i.e., the lack of poly (A) tail, short length (~22nt), and the presence of mature miRNA sequence in its precursor and primary transcript [300-302]. Therefore, over the past several years, researchers in the field have developed two different methods for reverse transcription (RT) of miRNAs, namely miRNA-specific RT or universal RT [300]. During miRNA-specific reverse transcription, miRNAs are reversely

transcribed individually by using miRNA-specific primers, which are designed to form a "stem loop" structure, as shown in Figure 7A [300, 302]. Each stem loop primer is composed of three parts: 1) a short single-stranded part of the stem containing sequence that is complementary to the 3' end of a target miRNA; 2) double-stranded part of the stem; and 3) a loop region that contains the sequence for binding of the universal primer during real-time PCR [300, 302]. The purpose of this stem-loop design is to reduce the annealing of the primers to pre- or pri-miRNAs, thereby enhancing the specificity of the primers [300, 302]. Of note, as each stem-loop RT primer is specifically designed for its targeted miRNA, the RT reactions should be performed individually for the corresponding miRNAs [300, 302]. For universal reverse transcription, all miRNAs are first tailed with a common sequence (normally a ploy (A) tail) and then are reversely transcribed with a universal primer (Figure 7B) [298, 300]. Based on this principle, one reaction by universal methods could theoretically transcribe all the miRNAs in a given sample [298, 300].

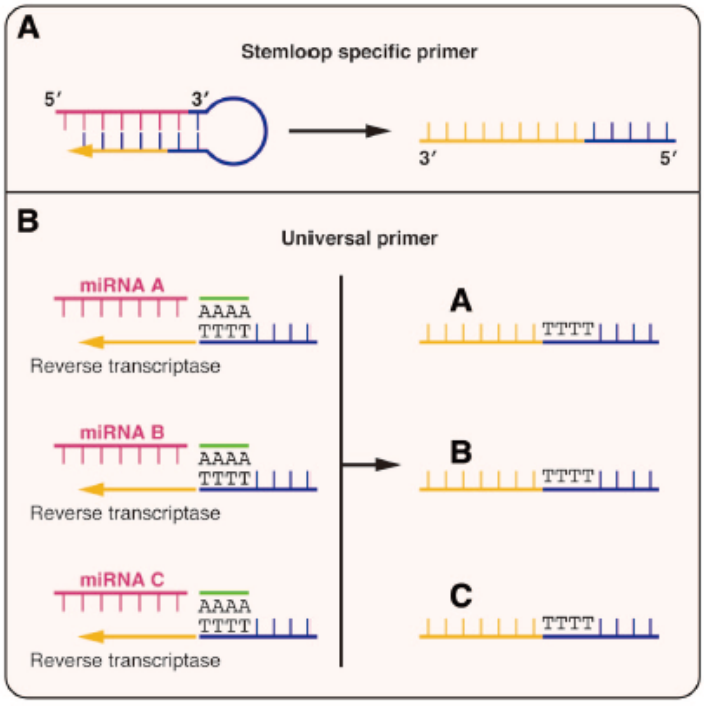


Figure 7. Different approaches for miRNA quantification by real-time RT-PCR. A. Reverse transcription of miRNAs by "stem loop" RT primers. B. Reverse transcription of miRNAs by universal RT primers; note that miRNAs are first tailed with poly "A" sequence prior to reverse transcription. Adapted from van Rooij E et al. [247].

#### 1.6.6.3.4 Quantification of MiRNAs by Northern blot

Northern blotting is another technique that allows individual quantification of specific miRNAs [303-305]. One obvious advantage of using northern blotting to detect a given miRNA is that it allows the visualization of both mature miRNA and precursor miRNA [304, 305]. However, this technique is generally time-consuming and requires large amounts of RNA sample (8ug or more), which poses a challenge for experiments with limited amount of samples [303]. Another potential drawback of the technique is the cross reaction of the detection probe with miRNAs that share high sequence homology [303]. Consequently, results obtained from northern blotting should ideally be verified by other detection methods, for example, real-time RT-PCR.

## 1.6.7 Regulation of MiRNA Expression and MiRNA Interference

### 1.6.7.1 Transcriptional Regulation of MiRNA Expression

Similar to protein-coding genes, the transcription of miRNA genes is also tightly controlled by their 5' proximal regulatory sequences (promoters) in coordination with a variety of DNA-binding factors (transcription factors, TFs) [252, 306]. However, depending on the type of miRNAs, miRNA genes can be transcribed by using either their own promoters (for intergenic miRNAs) or their host gene promoters (for exonic and intronic miRNAs) [307, 308]. Interestingly, it appears that the promoters of miRNA genes and protein coding genes share many similarities, such as initiator elements, the presence of TATA box, transcription factor II B (TFIIB) recognition, the occurrence of CpG islands and histone modifications [252, 306, 308]; and more importantly, the TFs that regulate the transcription of miRNA genes or protein coding genes can largely overlap [252, 253, 306]. For example, the proto-oncogene c-myc is found to positively regulate transcription of miR-17, while it can also promote the transcription of E2F1 [309]. Another example is p53, a well defined pro-apoptotic factor, which has been found to control both the transcription of miR-34 genes and various tumor genes [310].

In cardiomyocytes, several cardiac-specific TFs have been implicated in the control of miRNA transcription. For example, serum response factor (SRF) and myocytes enhancer

factor 2 (MEF2) have been well characterized to transcriptionally activate the expression of two muscle-specific miRNAs, miR-1 and miR-133, during cardiac development [246, 282, 311]. GATA-4, another important TF in the heart, directly binds to the promoters of miR-144 and miR-451 and promotes the transcription of these two miRNAs [312]. Nkx2.5 regulates the transcription of miR-143 and miR-145, which are important for the differentiation of cardiac progenitor cells [287].

In addition to the cardiac-specific TFs, many of other non cardiac-specific TFs have also been found to regulate the transcription of miRNAs in cardiomyocytes. A typical example is nuclear factor of activated T cells (NFAT). A recent study has shown that NFAT transcriptionally activates miR-23a expression [313], and similarly, in another recent study, NFAT was found to be a direct transcriptional activator for miR-199b [314].

#### 1.6.7.2 MiRNA Interference

##### 1.6.7.2.1 In Vitro MiRNA Interference

Transient overexpression or inhibition of miRNA in a cell-based system is the initial step towards functional studies of miRNAs. Several transfection-based approaches are currently used to overexpress miRNA in vitro: synthesized double-stranded miRNA mimics [279, 280, 282, 315], miRNA precursors [316, 317] or vectors that overexpress the miRNA of interest [247, 315]. For cells with low transfection efficiency, such as adult cardiomyocytes, a virus-based infection approach can be used [248, 279, 315]. For in vitro miRNA inhibition, the most commonly used strategy is to transfect cells with the miRNA antisense, namely antimiRs, which are the modified DNA oligos with the perfect complementarity to the guide-strand of a given miRNA that can antagonize the endogenous mature miRNAs and prevent them from binding to their targets [279, 282, 315, 317]. Alternatively, knockdown can be achieved by using either a regular vector or a viral-vector that expresses transcripts containing multiple miRNA target sites, by which the miRNA of interest can be functionally blocked or decoyed thereby being prevented from affecting its endogenous targets [318-321].

#### 1.6.7.2.2 In Vivo MiRNA Interference

The in vivo function of a specific miRNA can be elucidated by gain- and/or loss-of-function studies, which generally rely on three different approaches: 1) generation of transgenic animals with genetic modifications (either overexpression or knockout/down) of the targeted miRNA; 2) application of virus-based overexpression or knockdown techniques; and 3) the oligos-based antimiRs knockdown technique [247, 248, 321, 322]. Although many studies have revealed that genetic manipulation is a powerful approach to define the function of miRNA in vivo, some potential drawbacks with this approach should be taken into account. In some cases, forced overexpression of a miRNA could result in off-target effects due to the supraphysiological level of the miRNA expression [247, 248, 315, 317]. In other cases, genetic deletion of a miRNA could cause fetal lethality because the deletion might also disrupt a protein-coding gene, given that ~40% of miRNA genes are located within the introns of the protein coding genes that are potentially important for development [247, 248, 315, 317]. To overcome these problems, one alternative strategy is to overexpress or knockdown a miRNA by systemic delivery of the adenoviral vector expressing transcripts that contain either the miRNA precursor or multiple miRNA binding sites in the adult animals [247, 248, 315, 317]. However, due to the lack of tissue-specific expression inherent to the regular adenoviral approach, there is a growing interest of using different serotypes of adeno-associated viruses (AAVs) to achieve the tissue-specific expression, among which, AAV serotype 9 (AAV9) has been found to preferentially target cardiac tissues [248, 321, 322]. In addition to the genetic manipulation and viral expression approaches, a series of recently-developed miRNA knockdown oligos (antimiRs) have emerged as potent in vivo miRNA inhibitors with great therapeutic potential [248, 322]. Generally, these synthetic antimiRs are chemically-modified antisense oligos bearing the full or partial reverse complementary sequence of a mature miRNA that can either degrade or functionally block the endogenous miRNA upon binding [321, 323, 324]. The most commonly-used chemical modifications include 2'-O-methyl (2'-OMe)-modified oligonucleotides (Figure 8B) and locked nucleic acid (LNA)-modified oligonucleotides (Figure 8C), in which the 2'-O-oxygen is connected to the 4' position by a methylene linker to form a tight bicycle and is locked into the C3'-endo (RNA) sugar conformation, favoring the formation of a thermodynamically strong duplex with the complementary RNA [323,

324]. Both 2'-OMe and LNA modifications aim to increase the stability of oligonucleotides, improve the nuclease resistance, and enhance binding affinity to the target RNA [323, 324]. They can also be combined with some other chemical modifications to further improve cellular stability or uptake [247, 321]. For example, addition of phosphosrothioate backbone (Figure 8D) between nucleotides makes the oligonucleotides more resistant to nuclease [325]; the use of cholesterol conjugated oligonucleotides is proven to facilitate cellular uptake [326].

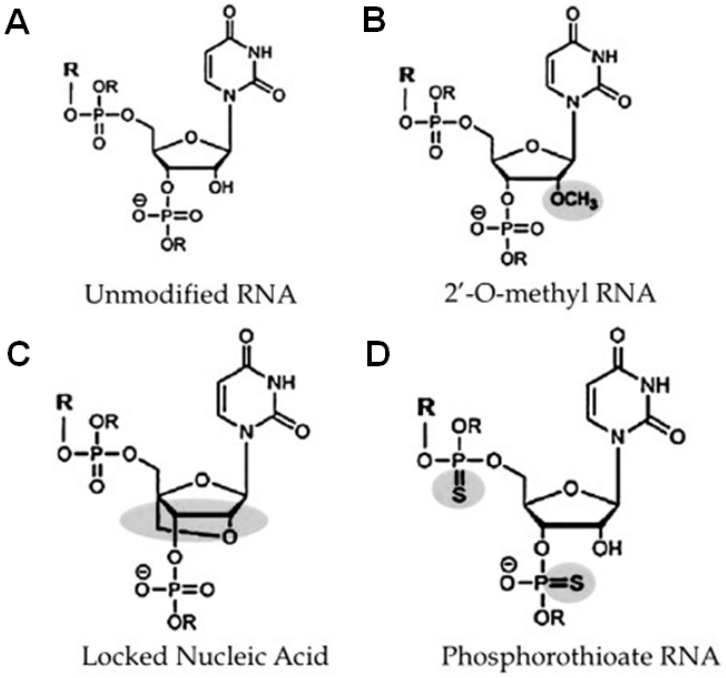


Figure 8. Different chemical modifications of in vivo miRNA knockdown oligos. A. Conformation of unmodified RNA. B. Conformation of 2'-O-methyl RNA (a methyl group bound to the 2′ oxygen of the ribose, highlighted in grey). C. Conformation of LNA monomer (methylene bridge between 2'-O and 4' in the ribose, highlighted in grey). D. Conformation of phosphorothioate RNA (S indicates sulfur substitution of a non-bridging oxygen to make a phosphorothioate linkage between nucleotides). (Adapted from Ruberti F et al. [327] with modifications).

## 1.6.8 Role of MiRNAs in the Heart

The complexity of the cardiac system is manifested by the fact that the normal function and formation of the heart are finely controlled by networks of transcriptional factors and signaling systems that govern the expression of cardiac genes that are essential for cardiogenesis, morphogenesis, and contractility [328]. The discovery of miRNAs as novel gene regulators during various biological processes has added a new layer of complexity to the cardiac system [322, 329]. It has now become clear that miRNAs tightly interact with a variety of cardiac signaling and transcriptional pathways to regulate cardiac development, function, and disease [275, 322, 329].

### 1.6.8.1 Implications of MiRNAs in Cardiac Development

Table 2. Summary of miRNAs related to cardiac development.

| miRNAs and cardiac development | | | |
|---|---|---|---|
| miRNA | Cell Type | Functions | Refs |
| miR-1 | Cardiomyocytes and skeletal muscle cells | Promotion of myocardial differentiation and negative regulation of cardiomyocyte proliferation | 333; 334 |
| miR-133 | Cardiomyocytes and skeletal muscle cells | Repression of myocardial differentiation and cardiomyocyte proliferation | 334; 335 |
| miR-17~92 | Cardiomyocytes | Promotion of myogenic differentiation | 336; 337 |
| miR-126 | Endothelial cells | Promotion of vasculogenesis | 286; 338; 339 |
| miR-143 | Smooth muscle cells | Promotion of smooth muscle cell differentiation and proliferation; vessel formation | 287; 340; 341 |
| miR-145 | Smooth muscle cells | Promotion of smooth muscle cell differentiation and proliferation; vessel formation | 287; 340; 341 |
| miR-138 | Cardiomyocytes | Cardiac morphogenesis | 342 |

The first direct evidence supporting the requirement of miRNAs for cardiac development and function came from studies using mice with cardiac-specific deletion of *Dicer* genes, which encode a protein that is essential for miRNAs processing [330-332]. The germline deletion of *Dicer* in myocardium or cardiovascular smooth muscle resulted in an aberrant expression of cardiac contractile proteins and embryonic lethality, indicating the crucial roles of miRNAs in earlier cardiac development [330, 331]. Interestingly, a subsequent study, which aimed to circumvent the embryonic lethality with germline deletion of *Dicer* by using mice with conditional *Dicer* knockout in postnatal myocardium, also observed the premature death of the animals shortly after inducing the deletion [332]. The lethal consequence of *Dicer* knockout is likely due to a joint-function of multiple miRNAs rather than a single miRNA, because, thus far, no embryonic lethality was observed when a specific miRNA was deleted [322].

To date, many of the cardiac-enriched miRNAs have been individually investigated for their potential roles in various aspects of cardiac development (e.g. myocardial differentiation and vasculogenesis), as summarized in Table 2. Muscle-specific miR-1, the most abundantly-expressed miRNA in cardiac tissue, was found to promote the formation of cardiac or skeletal muscle cells, whereas another muscle-specific miRNA, miR-133, was reported to negatively regulates myocardial differentiation [333-335]. Interestingly, both miR-1 and miR-133 were found to negatively regulate cardiomyocyte proliferation [334, 335]. Several miRNAs that belong to the miR-17-92 cluster, have also been reported to play an important role in mediating the myocardial differentiation of cardiac progenitor cells [336, 337]. In addition to myocardial differentiation, the involvement of miRNAs has also been seen in vasculogenesis during cardiac development. MiR-126, a cardiac-enriched miRNA that is selectively expressed in endothelial cells (ECs), was found to be crucially involved in angiogenic signaling and contribute importantly to vascular formation [286, 338, 339]. Interestingly, evidence supporting the potential contribution of miRNAs to vascular development has been found not only in ECs but also in smooth muscle cells (SMCs). SMC-specific miRNAs, miR-143 and miR-145, were reported to cooperatively regulate differentiation and proliferation of vascular smooth muscle cells (VSMCs) and determine VSMC cell fate, thereby contributing to the blood vessel formation [287, 340, 341]. Apart from the above various aspects of cardiac development, miRNAs are also

involved in the regulation of cardiac patterning. Evidence from a recent study using a genetic approach to delete miRNAs in zebrafish heart suggested that miR-138, a broadly conserved miRNA in mammals, is required for the proper formation of heart chambers through controlling chamber-specific gene expression patterns during cardiac morphogenesis [342].

### 1.6.8.2 Implications of MiRNAs in Cardiac Pathologies

Although tremendous efforts have been devoted to deciphering the underlying mechanisms responsible for a variety of cardiovascular diseases (e.g. cardiac hypertrophy, heart failure, ischemia, and arrhythmia), miRNAs have only recently been shown to play important roles during these pathological conditions [322, 329, 343]. It has become clear that there is a distinct expression pattern of miRNAs associated with different cardiac diseases and in some cases, the deregulation of a single miRNA is sufficient to result in a cardiac pathological condition [275, 322, 329, 343-346].

#### 1.6.8.2.1 Roles of MiRNAs in Cardiac Hypertrophy and Heart Failure

Table 3. Summary of miRNAs related to cardiac hypertrophy and heart failure.

| miRNAs in cardiac hypertrophy and failure | | | | |
|---|---|---|---|---|
| miRNA | Disease/Expression | Targets | Function | Refs |
| miR-195 | CH and HF / Upregulated | Unknown | Induction of cardiac hypertrophy and failure | 347 |
| miR-208a | CH / Unaltered | Myostatin; THRAP1 | Essential for hypertrophic response | 283; 348 |
| miR-1 | CH / Downregulated | IGF1; Calmodulin; Mef2a | Inhibition of cellular hypertrophy | 320; 349-352 |
| miR-133 | CH and HF / Downregulated | RhoA; CTGF; Col1A1 | Anti-hypertrophic (? Inconsistent *); anti-fibrotic | 320; 334; 347; 353; 355-357 |

| | | | | |
|---|---|---|---|---|
| miR-23a | CH and HF / Upregulated | MuRF1 | Promotion of cellular hypertrophy | 313 |
| miR-199b | CH and HF / Upregulated | Dyrk1a | Promotion of cellular hypertrophy | 314 |
| miR-21 | CH / Upregulated | Spry1 | Profibrotic | 284; 354 |
| miR-29b | CH and HF / Downregulated | Col1A1; Col1A2; Col3A1; FBN1; ELN | anti-fibrotic | 285 |

CH: Cardiac hypertrophy; HF: Heart Failure.
* Note that inconsistent results were reported for the anti-hypertrophic role of miR-133.

To date, the contribution of miRNAs to pathogenesis of cardiac hypertrophy and heart failure has been highlighted in numerous studies, as summarized in Table 3. The first study was done in mice subjected to transverse aortic constriction (TAC) or cardiac overexpression of activated calcineurin [347]. A series of deregulated miRNAs exhibiting a distinct expression pattern was observed in the cardiac tissues from these mice [347]. Interestingly, among these deregulated miRNAs, the cardiac-specific overexpression of miR-195 recapitulated the phenotypic changes associated with cardiac hypertrophy and heart failure, suggesting the pathogenetic role of miRNAs in these disease conditions [347]. Subsequently, a cardiac-specific miRNA, miR-208a, was found to play an essential role in cardiac hypertrophy [283, 348]. Mice with genetic deletion of miR-208a failed to demonstrate hypertrophic response to stress and hypothyroidism [283], whereas cardiac-specific overexpression of miR-208a induced cardiac hypertrophy [348]. Subsequent experiments demonstrated that the pro-hypertrophic effect of miR-208a is attributable to the repression of its targets, thyroid hormone receptor associated protein 1 (THRAP1) and myostatin, both of which function as negative regulators of muscle growth and hypertrophy [283, 348]. In addition to miR-208a, other cardiac-specific miRNAs, miR-1 and miR-133, have been reported to be involved in cardiac hypertrophy and failure [320, 349, 350]. The expression of miR-1 and miR-133 has been consistently found to be downregulated during cardiac hypertrophy in animal models and humans [320, 349, 350]. In vivo and in vitro inhibition of miR-1 in cardiomyocytes resulted in the increases in cell size and cell mass, suggesting an anti-hypertrophic role of miR-1 [320, 350]. The anti-hypertrophic effect of miR-1 may be attributed to its targeting of several signaling factors that are known to be

important to the development of cardiac hypertrophy, including insulin-like growth factor-1 (IGF-1) [351, 352], calmodulin [349], and myocytes enhancer factor 2A (MEF2A) [349]. As for miR-133, several studies have consistently documented a reduced expression of this miRNA in hypertrophied heart [320, 347, 353]. In vivo knockdown of miR-133 by systemic administration of its antagomir in the normal mouse hearts, was found to induce cardiac hypertrophy, presumably through the release of inhibition on its target, RhoA, a guanosine diphosphate-guanosine triphosphate exchange protein that can induce cardiac hypertrophy when its expression is elevated [320]. However, the exact role of miR-133 in cardiac hypertrophy remains controversial, as a subsequent study reported that mice with cardiac-specific knockout of miR-133 fail to develop cardiac hypertrophy [334]. The causes for this obvious discrepancy remain yet to be determined. More recently, two separate studies have suggested that miR-23a and miR-199b might also play important roles in cardiac hypertrophy and failure [313, 314]. The expression of both miRNAs was found to be profoundly increased in hypertrophied and failing hearts [313, 314]. In vivo inhibition of miR-23a completely abrogated the hypertrophic response upon isoproterenol stimulation [313]. The pro-hypertrophic effect of miR-23a is thought to be mediated by an anti-hypertrophic protein, muscle specific ring finger protein 1 (MuRF1), which is experimentally established as a target for miR-23a [313]. Similarly, miR-199b was also reported to positively regulate cardiac hypertrophy and failure, presumably through a relief of its repression on nuclear NFAT kinase dual-specificity tyrosine-(Y)-phosphorylation regulated kinase 1a (Dyrk1a), which functions as a negative regulator for cardiac hypertrophy [314]. Indeed, transgenic mice with overexpression of miR-199b demonstrated an enhanced hypertrophic response to pressure overload, whereas in vivo inhibition of miR-199b was able to reverse the phenotypic changes (cellular hypertrophy and fibrosis) observed in the mouse models of heart failure [314].

In addition to the direct pathogenetic roles in cardiac hypertrophy and failure, miRNAs have also been found to participate in fibrogenesis during cardiac hypertrophy and failure. The first documented fibrosis-related miRNA during cardiac hypertrophy is miR-21 [284]. A significant increase of miR-21 expression was observed during cardiac hypertrophy and this increase was found more profound in myofibroblasts than in myocytes [284]. In vivo inhibition of miR-21 with its antagomir in mice successfully prevented the fibrosis and

cardiac hypertrophy in response to pressure overload, suggesting a profibrotic role of miR-21 during cardiac hypertrophy [284]. The profibrotic effect of miR-21 is likely attributable to its targeting of sprouty homolog 1 (Spry1), which functions as a negative regulator for extracellular signal-regulated kinase 1/2 (ERK1/2) phosphorylation and myofibroblast survival [284]. However, a recent study questioned the necessity of miR-21 in hypertrophy-induced fibrosis. In this study, in vivo interference of miR-21 in the hearts was found to have no impact on fibrosis in three different mouse models of cardiac hypertrophy [354]. Thus, further studies are needed to resolve these obvious contradictions. Expression levels of miR-133 and miR-29b have also been repeatedly reported to be downregulated in hypertrophied and failing hearts [285, 355, 356]. Restoration of miR-133 to normal levels in mouse models of cardiac hypertrophy was able to prevent the fibrosis [356]. The anti-fibrotic effect of miR-133 is likely due to its repression on collagen 1A1 (Col1A1) and connective tissue growth factor (CTGF), a well-known profibrotic factor [355, 357]. Similarly, miR-29b has also been found to play an anti-fibrotic role during cardiac hypertrophy through direct targeting of multiple collagen isoforms, fibrillin, and elastin [285]. Accordingly, in vivo inhibition of miR-29b in mice was able to promote fibrogenesis in the heart [285].

#### 1.6.8.2.2 Roles of MiRNAs in Myocardial Ischemia

Table 4. Summary of miRNAs related to myocardial ischemia.

| miRNAs in cardiac ischemia | | | | |
|---|---|---|---|---|
| miRNA | Expression | Targets | Function | Refs |
| miR-199a | Downregulated | Hif-1α | Anti-apoptotic | 358 |
| miR-320 | Downregulated | HSP-20 | Anti-apoptotic | 359 |
| miR-21 | Downregulated (in CMs) | PDCD4; PTEN; FasL | Anti-apoptotic | 360; 361 |
| | Upregulated (in MFs) | PTEN | Profibrotic | 370 |
| miR-494 | Downregulated | PTEN; ROCK1; CAMKIIδ | Anti-apoptotic | 362 |

| | | | | |
|---|---|---|---|---|
| miR-24 | Downregulated (in CMs) | Bim | Anti-apoptotic | 364 |
| | Upregulated (in ECs) | GATA2; PAK4 | Proapoptotic and anti-angiogenic | 363 |
| miR-15 | Upregulated | Bcl2; Arl2 | Proapoptotic | 365-367 |
| miR-29 | Downregulated | Col1A1; Col1A2; Col3A1; FBN1; ELN | Anti-fibrotic | 285 |
| miR-92a | Downregulated (in ECs) | ITGA5 | Anti-angiogenic | 369 |
| miR-126 | Upregulated (in ECs) | Spred1 | Proangiogenic | 286; 368 |

CMs: cardiomyocytes; MFs: myofibroblasts; ECs: endothelial cells

Aberrant miRNA expression has been repeatedly observed in cardiac ischemia. Cardiac ischemia is a result of insufficient supply of blood flow to the heart, which may cause many abnormalities, affecting apoptosis, angiogenesis, fibrosis and contractile dysfunction in the myocardium. Several miRNAs that affect cell viability were reported to be perturbed during cardiac ischemia, including miR-199a [358], miR-320 [359], miR-21 [360, 361], miR-494 [362], miR-24 [363, 364], and miR-15 [365], as summarized in Table 4. Among these deregulated miRNAs, reduced expression of miR-199a, miR-21, miR-494, and miR-24 was found within the infarct zone [358, 360-362, 364]. Interestingly, when restoring the expression of these miRNAs in the ischemic heart, a reduced infarct size and improved cell viability were observed [358, 360-362, 364]. At the cellular level, overexpression of miR-199a, miR-21, miR-494, or miR-24 alone was able to inhibit hypoxia-induced apoptosis in cardiomyocytes [358, 361, 362, 364]. The underlying mechanisms responsible for their anti-apoptotic effects are likely attributable to the inhibition of various proapoptotic factors, such as hypoxia-inducible factor 1 alpha (Hif-1α, target of miR-199a) [358], phosphatase and tensin homolog (PTEN, target of miR-21 and miR-494) [361, 362], Fas ligand (FasL, target of miR-21) [361], programmed cell death 4 (PDCD4, target of miR-21) [361], Rho-associated coiled-coil containing protein kinase-1 (ROCK1, target of miR-494) [362], calcium/calmodulin-dependent protein kinase II delta (CAMKIIδ, target of miR-494) [362], and BH3-only protein (Bim, target of miR-24) [364]. Unlike the decrease of miR-199a, miR-21, miR-494, or miR-24, which deteriorates cell viability during ischemia, the observed downregulation of miR-320 during myocardial ischemia appears to be

cardioprotective, as in vivo suppression of this miRNA was found to reduce infarct area after ischemia reperfusion (IR) [359]. The cardioprotective effect of miR-320 downregulation during IR is likely due to an increased expression of heat shock protein 20 (HSP20), a well known cardioprotective protein that is targeted by miR-320 [359]. Upregulated miRNAs are also seen within the infarct zone, one example is miR-15b. In vivo inhibition of miR-15b during ischemia resulted in reduced infarct size and improved cardiac function [365]. The mechanism underlying the beneficial role of miR-15b knockdown is likely related to the increased levels of cell death suppressor proteins, ADP-ribosylation factor-like 2 (Arl2) and B-cell lymphoma 2 (Bcl2), both of which are validated targets of miR-15b [366, 367].

Deregulated miRNAs seen in myocardial ischemia are implicated not only in cell viability but also in angiogenesis. A typical example is miR-126, which was found to be highly enriched and upregulated in endothelial cells during cardiac ischemia [368]. The enhanced expression of miR-126 was proven to be required for reparative angiogenesis in response to ischemic insult through repression of an anti-angiogenic protein, sprouty-related EVH1 domain-containing protein 1 (Spred-1) [286, 368]. Interestingly, for miR-24, in contrast to its downregulation in cardiomyocytes during myocardial ischemia, a significant increase in its expression was observed in endothelial cells, where it induced apoptosis of these cells [363]. Accordingly, in vivo inhibition of miR-24 during myocardial ischemia was found to prevent endothelial cells from undergoing apoptosis and increases angiogenesis, suggesting an anti-angiogenic role of miR-24 [363]. The observed anti-angiogenic effect of miR-24 is likely caused by an increased expression of miR-24 conserved targets, GATA2 and p21-activated kinase-4 (PAK4), both of which are known to positively regulate angiogenesis [363]. MiR-92a was also found to be downregulated during myocardial ischemia [369]. This downregulation was shown to promote reparative angiogenesis, which is likely due to an increased level of alpha-5 integrin (ITGA5), a proangiogenic protein that is targeted by miR-92a [369].

Similar to cardiac hypertrophy, miRNAs are also involved in fibrogenesis during myocardial ischemia. Two miRNAs have so far been implicated in control of fibrosis during cardiac ischemia: miR-21 and miR-29. Both of these miRNAs are highly enriched in fibroblasts [285, 370]. While miR-21 was reported to be dramatically increased in the

infarcted region during cardiac ischemia [370], downregulation of miR-29 was consistently observed in the same context [285]. Increased level of miR-21 in cardiac fibroblasts during cardiac ischemia was found to promote fibrosis by repressing the expression of PTEN (a validated target of miR-21), which in turn stimulates the synthesis of metalloproteinase-2 (MMP-2), a well-known profibrotic factor [370]. Likewise, decreased expression of miR-29 in the ischemic heart is also thought to promote fibrosis [285]. This is likely attributable to an increased expression of various ECM proteins that are validated as targets of miR-29, including collagens, fibrillins, and elastin [285].

#### 1.6.8.2.3 Roles of MiRNAs in Arrhythmia

Table 5. Summary of miRNAs related to cardiac arrhythmia.

| Roles of miRNAs in cardiac arrhythmia | | | | |
|---|---|---|---|---|
| miRNA | Disease/Expression | Targets | Function | Refs |
| miR-1 | Ischemia / Upregulated | Cx43; KCNJ2 | Proarrhythmic | 204 |
| | AF / Downregulated | KCNJ2 | To be determined | 96 |
| | HF / Upregulated | Ppp2r5a; | Abnormal $Ca^{2+}$ handling | 373; 374 |
| miR-133 | CH / Downregulated | KChIP2 | Prolongation of QT interval | 356 |
| | Nicotin-induced AF / Downregulated | TGF-β1; TGF-βRII | Atrial fibrosis | 375 |
| miR-590 | Nicotin-induced AF / Downregulated | TGF-β1; TGF-βRII | Atrial fibrosis | 375 |
| miR-328 | AF / Upregulated | CACNA1C; CACNB1 | Overexpression promotes AF | 113 |

CH: Cardiac hypertrophy; HF: Heart Failure; AF: Atrial Fibrillation.

Accumulating evidence has suggested that miRNAs are implicated in arrhythmogenesis under different disease paradigms such as cardiac hypertrophy, heart failure, myocardial ischemia, and atrial fibrillation, as summarized in the Table 5. The first arrhythmia-related miRNA was discovered in a study aimed at elucidating the molecular mechanism responsible for ischemia-related arrhythmia [204]. MiR-1 was found to be dramatically

upregulated during coronary artery disease in humans and ischemic rat hearts, which coincided with an increased incidence of arrhythmia [204]. Inhibition of miR-1 in the ischemic rat heart resulted in a reduced occurrence of arrhythmia, whereas overexpressing miR-1 in the healthy rat heart induced arrhythmia [204]. This proarrhythmic effect of miR-1 in ischemic conditions is attributed to its targeting and suppression of two proteins, Connexin 43 (encoded by *GJA1*, the main form of cardiac gap junction proteins) and Kir2.1 (encoded by *KCNJ2*, subunit of $K^+$ channels carrying $I_{K1}$) [204], as the deregulation of these proteins was reported to promote arrhythmia [371, 372]. Likewise, a significant increase of miR-1 was also observed in cardiomyocytes isolated from both rat and dog failing hearts [373, 374]. Subsequent in vitro studies demonstrated that this increased level of miR-1 could result in abnormal $Ca^{2+}$ handling, which may contribute to arrhythmogenesis in failing hearts [373, 374]. In this case, miR-1 exerts its effect via suppressing the regulatory subunits of protein phosphatase 2A (Ppp2r5a), which is important for $Ca^{2+}$/calmodulin-dependent protein kinase (CaMKII)-mediated phosphorylation of ryanodine receptors (RyR2) [374].

In cardiac hypertrophy, one consistent finding is the downregulation of miR-133. In fact, a recent study suggested that this downregulation is responsible for the reduced expression of $I_{to}$ channel accessory subunit, KChIP2, which may indirectly contribute to prolonged QT interval, thereby promoting arrhythmogenesis [356].

The first evidence indicating a direct role of miRNAs in AF was obtained from a study using nicotine-induced AF dogs [375]. Severe fibrosis was observed in the atrial tissue from these dogs, accompanying with significant increase of transforming growth factor-β1 (TGF-β1) and TGF-β receptor type II (TGF-βRII), and reduced expression of miR-133 and miR-590 [375]. Further in vivo and in vitro experiments confirmed that the reduction of miR-133 and miR-590 is responsible for the enhanced expression of TGF- β1 and TGF- β RII, as these proteins are validated as targets of miR-133 and miR-590 [375]. While the above study highlights the potential role of miRNAs in atrial structural remodeling under AF [375], evidence from two other studies suggests miRNAs may also contribute to atrial electrical remodeling associated with AF [96, 113]. Upregulation of $I_{K1}$ and downregulation of $I_{CaL}$ represent the two most prominent findings during ionic remodeling associated with AF. Interestingly, a recent study indicated that miR-1 levels are significantly reduced in

persistent AF patients and this reduction may contribute to upregulation of Kir2.1 subunits (validated target of miR-1), thereby leading to increased $I_{K1}$ [96]. Nonetheless, further in vivo experiments are needed to establish a potential mechanistic link between miR-1 and AF. In another study, miR-328 was found to be upregulated in human AF patients with rheumatic disease, as well as in a canine model of AF [113]. Subsequent in vivo experiments in dogs demonstrated that overexpression of miR-328 by intracardial injection of miR-328-overexpressing adenovirus increases AF susceptibility [113]. Likewise, transgenic mice with miR-328 overexpression were more susceptible to AF induction, whereas inhibiting the overexpression of miR-328 in these mice reduced AF inducibility [113]. Mechanistically, the increased incidence of AF is attributable to the reduction in $I_{CaL}$, as both the α1c and β1 subunits of the L-type calcium channel were experimentally established as the targets of miR-328 [113].

## 1.7 Rationale for Present Studies

Atrial fibrillation is the most clinically-encountered arrhythmia, representing a major cause of morbidity and mortality. Over the past two decades, a major advancement in our understanding of the pathogenesis of AF is the recognition that AF induces both electrical and structural remodeling in the atria, which in turn promotes the recurrence and maintenance of AF. A key feature in electrical remodeling is the abbreviation of atrial effective refractory period, which is primarily due to shortening of action potential as the result of ion channel alterations. Structural remodeling, on the other hand, is mainly manifested by atrial fibrosis which may also result from the deregulation of ion channels. Interventions that prevent deregulation of ion channels and/or atrial fibrosis may adequately serve as an effective approach to prevent AF occurrence. However, the precise molecular mechanisms underlying these remodeling processes are still poorly understood. Of note, the recent discovery of miRNAs as an important regulator in various cardiac pathologies has shed light on this matter. Emerging evidence has suggested that miRNAs can directly regulate the expression of ion channel genes. More importantly, deregulation of ion channels as a result of the aberrant miRNA expression has been implicated in arrhythmogenesis under several cardiac pathological conditions. Therefore, the goals of the

studies presented herein were to gain an appreciation for the importance of miRNA in regulation of cardiac ion channel and its pathophysiological implication in AF, to improve our understanding of the basic mechanisms for electrical and structural remodeling pertaining to AF, and to ultimately identify a potential therapeutic target for the treatment of AF. To this end, three separate studies with specific focus were carried out as below:

1. As discussed in Section 1.6.5 of the introduction, currently-available experimental approaches do not permit thorough characterization of miRNA targeting. In order to acquire a comprehensive view of the miRNA regulation of cardiac ion channel in arrhythmia, a rationally-designed bioinformatics analysis was performed in conjunction with experimental approaches to identify the miRNA from the currently available miRNA databases which have the potential to regulate human cardiac ion channel genes and to validate the analysis with several pathological settings associated with the deregulated miRNAs and ion channel genes in the heart.
2. As discussed in Section 1.3.1 and 1.4.4 of the introduction, upregulation of $I_{K1}$ is a key component of AF-related electrical remodeling. In order to study the role of miRNAs in this AF-related ionic remodeling process. Both in vitro and in vivo approaches were used to identify a deregulated miRNA in experimental and clinical AF, to test whether the deregulated miRNA can target *KCNJ2* (gene encoding Kir2.1 subunit for $I_{K1}$), to investigate the arrhythmogenic potential of the deregulated miRNA, and to explore the molecular mechanisms underlying the deregulation of the selected miRNA.
3. As discussed in Section 1.3.2 and 1.5.4 of the introduction, TRP channels may contribute to fibroblast proliferation and differentiation, which are central to AF-induce fibrotic remodeling. In order to test whether TRPC3 channels play a role in AF-induce fibrosis and whether miRNAs are involved in this process. Both in vitro and in vivo approaches were used to investigate whether TRPC3 channels are deregulated during AF and whether this deregulation play a role in AF-induced fibrotic remodeling, to identify a miRNA candidate responsible for the deregulation of TRPC3, and to study the molecular mechanisms underlying the change of the selected miRNA.

# CHAPTER 2. Overview of the Role of MiRNAs in Regulation of Cardiac Ion Channel Genes and its Potential Arrhythmogenic Implication

As discussed in Section 1.6.5 of the Introduction, a single miRNA could theoretically target hundreds or thousands of potential targets, and conversely, a given protein-coding gene could be simultaneously targeted by multiple miRNAs. Currently-available experimental approaches do not permit thorough characterization of miRNA targeting; thus, bioinformatic analysis represents an ideal approach for the thorough and rapid characterization of miRNA targeting. In order to acquire a comprehensive view of the miRNA regulation of cardiac ion channel in arrhythmia, in this chapter, we carried out a rationally-designed bioinformatics analysis in conjunction with experimental approaches to identify the miRNAs from the currently-available miRNA databases which have the potential to regulate human cardiac ion channel genes and to validate the analysis with several pathological settings (e.g. cardiac hypertrophy/heart failure, myocardial ischemia, and atrial fibrillation) associated with the deregulated miRNAs and ion channel genes in the heart.

This work has been published in ***Cellular Physiology and Biochemistry*.**

**Luo X**, Zhang H, Xiao j, Wang Z. Regulation of Human Cardiac Ion Channel Genes by MicroRNAs: Theoretical Perspective and Pathophysiological Implications. ***Cell. Physiol. Biochem.*** 2010;25(6):571-86.

# 2.1 Regulation of Human Cardiac Ion Channel Genes by MicroRNAs: Theoretical Perspective and Pathophysiological Implications

**Xiaobin Luo[1,2†], Haijun Zhang[1†], Jiening Xiao[1], Zhiguo Wang[1,2*]**

[1]Research Center, Montreal Heart Institute, Montreal, PQ H1T 1C8 Canada;

[2]Department of Medicine, University of Montreal, Montreal, PQ H3C 3J7, Canada;

Running Title: miRNAs and Ion Channel Genes

*Correspondence should be addressed to Zhiguo Wang

## Abstract

Excitability is a fundamental characteristic of cardiac cells, which is delicately determined by ion channel activities modulated by many factors. MicroRNA (miRNA) expression is dynamically regulated and altered miRNA expression can render expression deregulation of ion channel genes leading to channelopathies–arrhythmogenesis. Indeed, evidence has emerged indicating the crucial role of miRNAs in controlling cardiac excitability by regulating expression of ion channel genes at the post-transcriptional level. However, the very limited experimental data in the literature hinder our understanding of the role of miRNAs and the often one-to-one interaction between miRNA and ion-channel gene in the published studies also casts a doubt about fullness of our view. Unfortunately, currently available techniques do not permit thorough characterization of miRNA targeting; computational prediction programs remain the only source for rapid identification of a putative miRNA target *in silico*. We conducted a rationally designed bioinformatics analysis in conjunction with experimental approaches to identify the miRNAs from the currently available miRNA databases which have the potential to regulate human cardiac ion channel genes and to validate the analysis with several pathological settings associated with the deregulated miRNAs and ion channel genes in the heart. We established a matrix of miRNAs that are expressed in cardiac cells and have the potential to regulate the genes encoding cardiac ion channels and transporters. We were able to explain a particular ionic remodeling process in hypertrophy/heart failure, myocardial ischemia, or atrial fibrillation with the corresponding deregulated miRNAs under that pathological condition; the changes of miRNAs appear to have anti-correlation with the changes of many of the genes encoding cardiac ion channels under these situations. These results indicate that multiple miRNAs might be critically involved in the electrical/ionic remodeling processes of cardiac diseases

through altering their expression in cardiac cells, which has not been uncovered by previous experimental studies.

## Introduction

Cardiac cells are excitable cells that can generate and propagate excitations; excitability is a fundamental characteristic of cardiac cells. Cardiac excitability is conferred by three basic elements: automaticity, cardiac conduction, and membrane repolarization. Automaticity is a measure of the ease of cells to generate excitations or spontaneous membrane depolarization. Conduction refers to the propagation of excitation within a cell and between cells, and cardiac conduction velocity is determined by the rate of membrane depolarization and the intercellular conductance. The rate of membrane repolarization determines the length of action potential duration (APD) and effective refractory period (ERP) thereby the timeframe of availability for generation of a next excitation in a cardiac cell. These three intrinsic properties are reflected by electrical activities in cardiac cells. The electrical activities of the heart are orchestrated by a matrix of ion channels and transporters, the transmembrane proteins that control the movement of ions across the cytoplasmic membrane of cardiomyocytes. Sodium ($Na^+$) channels determine the rate of membrane depolarization and connexins (Cxs) are critical for gap junction communication, being responsible for excitation generation and inter-cell conductance of excitations, respectively. Calcium channels (mainly L-type $Ca^{2+}$ channels) account for the characteristic long plateau phase of cardiac action potentials and excitation-contraction coupling, and also contribute to pacemaker activities. Potassium ($K^+$) channels govern the membrane potential and rate of membrane repolarization. Pacemaker channels, which carry the non-selective cation currents, are essential in generating sinus rhythm and ectopic heart beats as well. Intricate interplays of all these ion channels maintain the normal heart rhythm thereby contraction. Channelopathies, diseases caused by dysfunction of the ion channels, which may result

from either genetic alterations in ion channel genes or aberrant expression of these genes, can render electrical disturbances predisposing to cardiac arrhythmias [1].

Evidence has emerged indicating the crucial role of microRNAs (miRNAs) in regulating expression of ion channel genes at the post-transcriptional level. The muscle-specific miRNA *miR-1* was shown to produce cardiac conduction disturbance in myocardial infarction [2] and in genetic knockout animal [3]; these studies opened up the new opportunity for studying the pathogenesis of miRNAs in the heart [4,5]. While the role of miRNAs in oncogenesis and cardiac development has been well appreciated over the past few years, the involvement of miRNAs in the pathological process of cardiovascular system has only been recognized very recently. It is now clear that in addition to their role in cardiac development [6–12], miRNAs are also critically involved in the pathological processes of adult hearts, including cardiac hypertrophy [13–19], heart failure [14,19], cardiomyopathy [20], angiogenesis [21] and arrhythmogenesis [2,22–26]. In addition to myocardial infarction, we have also demonstrated the participation of miRNAs in other pathological settings. *miR-133*, another muscle-specific miRNA, was shown to regulate pacemaker channel HCN2 and HCN4 and contributes to the re-expression of these channels in hypertrophy heart [23]. This miRNA had also been shown to repress HERG $K^+$ channel gene KCNH2 contributing to the abnormal QT prolongation in an animal model of diabetes mellitus [24]. Both *miR-1* and *miR-133* may be involved in the spatial patterns of tissue distribution of ion channels [25].

An important message brought about by previous studies is that miRNA expression is dynamically regulated and altered miRNA expression can render expression deregulation of ion channel genes leading to channelopathies. Functional or mature miRNAs are around 22-nucleotides in length. In order for a miRNA to elicit functional consequences, its 5'–end

7 to 8 nts must have exact or nearly perfect complementarity to the target mRNA, the so-called ‘seed’ region, and partial complementarity with rest of its sequence [27–31]. A miRNA can either inhibit translation or induce degradation of its target mRNA or both, depending upon at least the following factors: (1) the overall degree of complementarity of the binding site, (2) the number of binding sites, and (3) the accessibility of the bindings sites (as determined by free energy states). The greater the complementarity of the accessible binding sites, the more likely a miRNA degrades its targeted mRNA, and those miRNAs that display imperfect sequence complementarities with target mRNAs primarily result in translational inhibition [27–31]. With better complementarity to the accessible binding sites, a miRNA could more likely degrades its targeted mRNA, and those miRNAs that display imperfect sequence complementarities with target mRNAs primarily result in translational inhibition. Greater actions may be elicited by a miRNA if it has more than one accessible binding site in its targeted miRNA, owing to the potential cooperative miRNA-mRNA interactions from different sites.

miRNAs are abundant non-coding mRNAs in terms of the species of miRNAs existing in a cell: to date, ~6400 vertebrates mature miRNAs have been registered in miRBase, an online repository for miRNA [32], among which ~5100 miRNAs are found in mammals which include 718 human miRNAs. These miRNAs are predicted to regulates ~30% of protein–coding genes [33,34]. One common concern that somewhat subsides researchers’ inner confidence on the published experimental data on miRNA-target interactions with high-level skeptics and thus hinders our understanding of the function of miRNAs is the possibility that a single protein-coding gene may be regulated by multiple miRNAs and *vice versa* an individual miRNA has the potential to target multiple protein-coding genes. For instance, in our previous study, *miR-1* was shown to target GJA1

(encoding gap junction channel protein connexin43) and KCNJ2 (encoding the Kir2.1 $K^+$ channel subunit) to cause slowing of cardiac conduction leading to ischemic arrhythmogenesis [2]. However, it is conceivable that GJA1 and KCNJ2 are not the only ion channel targets for *miR-1*; it is also able to repress other genes such as SCN5A, CACNA1C, KCND2, KCNA5 and KCNE1 [4] and whether the repression of these genes other than GJA1 and KCNJ2 also contributes to the ischemic arrhythmogenesis remained unclear. On the other hand, GJA1 is predicted to be regulated by other miRNAs in addition to *miR-1* (including *miR-101, miR-125, miR-130, miR-19, miR-23*, and *miR-30*); whether these miRNAs are also involved in the deregulation of GJA1 in myocardial infarction remained unknown either. This same uncertainty or confusion expectedly exists in the interactions between literally all miRNAs and protein-coding genes. The only way to tackle this problem is the proper experimental approaches.

However, given the laborious nature of experimental validation of targets and the limited available experimentally validated data, computational prediction programs remain the only source for rapid identification of a putative miRNA target *in silico*. While currently available experimental approaches do not allow for thorough elucidation of the complete set of target genes of a given miRNA or of the complete array of mRNAs that regulate a given protein-coding genes, appropriate theoretical analyses might aid to resolve this intricate problem. The present study aims to shed light on the issue by performing a rationally designed bioinformatics analysis in conjunction with experimental approaches to identify the miRNAs from the currently available miRNA databases which have the potential to regulate human cardiac ion channel genes and to validate the analysis with several pathological settings associated with the deregulated miRNAs and ion channel genes in the heart.

## Materials and Methods

### Canine model of atrial fibrillation (AF)

Mongrel dogs (22 to 28 kg) of either sex were randomly divided into two groups: sham control (Ctl, n=6) and atrial tachypacing (n=7) groups. For animals in the A-TP group, dogs were sedated and anesthetized with morphine (2 mg/kg SC) and α-chloralose (120 mg/kg IV load, 29.25 mg/kg/h infusion), for electrode implantation via the jugular veins and atrioventricular (AV) block was created with radiofrequency ablation. A programmable pacemaker was inserted in a subcutaneous pocket with sterile techniques, and a tined atrial pacing lead was positioned in the right atrial appendage under fluoroscopic guidance. The dogs were subjected to continuous right atrial pacing at 400 bpm for 56 days (8 weeks) before experimental studies. The control dogs were sham-operated in the same way as atrial tachypaced dogs but without tachypacing. On study days, dogs were anaesthetized with morphine and α-chloralose and ventilated to maintain physiological arterial blood gases. Body temperature was maintained at 37°C. A median sternotomy was performed, and bipolar, Teflon-coated, stainless steel electrodes were hooked into the right and left atrial appendages for recording and stimulation. A programmable stimulator was used to deliver 2-ms pulses at twice-threshold current. The surface ECG and direct atrial activation electrograms were recorded.

AF vulnerability was tested at a basic cycle length (S1−S1 interval) of 300 ms, with single premature S2 extrastimuli delivered at each site by setting the coupling interval initially to 200 ms and decreasing by 10 ms decrements until AF was induced or failure to capture occurs. For the purpose of measuring AF duration, AF was induced by burst atrial pacing with 4x threshold 4-ms pulses at 20 Hz at a basic cycle length (BCL) of 300 ms. AF

was considered sustained if it required electrical cardioversion for termination (cardioversion was performed after 30 min AF). To estimate the mean duration of AF, AF was induced 10 times if AF duration was <5 min, 5 times for AF between 5 and 20 min and 3 times for AF >20 min.

**Rat model of myocardial infarction (MI)**

Male Wistar rats (220-250 g) were randomly divided into control and MI groups. MI was established as previously described [2]. The rats were anesthetized with diethyl ether and placed in the supine position with the upper limbs taped to the table. A 1–1.5 cm incision was made along the left side of the sternum. The muscle layers of the chest wall were bluntly dissected to avoid bleeding. The thorax was cut open at the point of the most pronounced cardiac pulsation and the right side of the chest was pressed to push the heart out of the thoracic cavity. The left anterior descending (LAD) coronary artery was occluded and then the chest was closed back. All surgical procedures were performed under sterile conditions. Twelve hours after occlusion, the heart was removed for Langendorff perfusion experiments or the tissues within ischemic zone (IZ), boarder zone (BZ) and non-ischemic zone (NIZ) distal to the ischemic zone were dissected for measurement of miRNA levels. Control animals underwent open-chest procedures without coronary artery occlusion.

**Microarray analysis**

The hearts were then removed from the dogs or rats and total RNA samples were extracted with Ambion's *mir*Vana miRNA Isolation Kit for miRNA expression analysis. The RNA samples were also isolated from left ventricular walls of healthy human hearts. miRNA expression profiles were analyzed using the miRNA microarray technology miRCURY™ LNA Array (Exiqon Company, Denmark). miRCURY™ LNA Array, including 718 mature

human miRNAs plus 650 mature rodent miRNAs, incorporates Locked Nucleic Acid into an oligonucleotide probe, which greatly increases the affinity and specificity of that oligonucleotide for its complementary DNA or RNA target. Slides were scanned by the Genepix 4000B at 635 nm and the expression level was analyzed by Genepix Pro 6.0. The array output was received in Excel spreadsheets as lists of raw data and also as "simple detectable" data, which were the average of 4 signal values for each miRNA on the array. Differentially regulated miRNAs were defined as those with either <0.5- or >2-fold changes in expression for both arrays compared with the baseline expression levels from sham-operated dogs.

**Quantitative real-time RT-PCR analysis**

The *mir*Vana™ qRT-PCR miRNA Detection Kit (Ambion) was used in conjunction with real-time PCR with TaqMan for quantification of miRNAs in our study, as previously described in detail [2,22,23]. qRT-PCR was performed on a thermocycler ABI Prism® 7500 fast (Applied Biosystems) for 40 cycles. Fold variations in expression of an mRNA between RNA samples were calculated. The threshold cycle ($C_T$) is defined as the fractional cycle number at which the fluorescence passes the fixed threshold. To estimate copy numbers of transcript in a cardiac cells, a standard curve was generated by using a series of concentrations of synthetic *miR-1* and converting TaqMan $C_T$ values into absolute copy numbers using the standard curve assuming 30 pg of total RNA in each cell [35,36].

**Computational prediction of miRNA target**

We used the miRecords miRNA database and target-prediction website for our initial analysis. The miRecords is resource for animal miRNA-target interactions developed at the University of Minnesota [37]. The miRecords consists of two separate databases. The

*Validated Targets* database contains the experimentally validated miRNA targets being updated from meticulous literature curation. The *Predicted Targets* database of miRecords is an integration of predicted miRNA targets produced by 11 established miRNA target prediction programs. These algorithms include DIANA-microT, MicroInspector, miRanda, MirTarget2, miTarget, NBmiRTar, PicTar, PITA, RNA22, RNAhybrid, and TargetScan/TargetScanS.

## Results and Discussion

### Initial analysis of miRNAs with the potential to regulate cardiac ion channel genes

Our study was focused on the genes encoding cardiac cytoplasmic ion channels and electrogenic ion transporters (Table 1). The list includes $Na^+$ channel, $Ca^{2+}$ channel, inward rectifier $K^+$ channel subunits, voltage-gated $K^+$ channel pore-forming α-subunits, ACh-activated $K^+$ channel α-subunits, ATP-sensitive $K^+$ channel α-subunit and receptor subunit, pacemaker hyperpolarization-activated cyclic-nucleotide gated cation channels, gap junction channel proteins, transient receptor potential channel subunits, chloride channel subunits, $K^+$ channel β-subunits, $Na^+/Ca^{2+}$ exchanger NCX1, and $Na^+/K^+$-ATPase. These cytoplasmic ion channels and electrogenic ion transporters play the fundamental roles in generating, maintaining and shaping cardiac electrical activities (Table 1). Dysfunction of these proteins has been associated with a variety of pathological conditions of the heart.

As an initial "screening" process, we performed miRNA target prediction through the miRecords database [37]. This miRNA database integrates miRNA target predictions by 11 algorithms, as detailed in Methods section. Four of the 11 algorithms (microInspector, miTarget, NBmiRTar, and RNA22) were removed from our data analysis because they failed to predict; these websites require manual input of 3'UTR sequences of the genes.

Thus, our data analysis was based upon the prediction from seven algorithms (TargetScan, DIANA-miT3.0, miRanda, PicTar, PITA, RNAHybrid, and miRTarget2) [38-44]. These prediction techniques are based on algorithms with different parameters (such as miRNA seed:mRNA 3'UTR complementarity, thermodynamic stability of base-pairing (assessed by free energy), evolutionary conservation across orthologous 3'UTRs in multiple species, structural accessibility of the binding sites, nucleotide composition beyond the seed sequence, number of binding sites in 3'UTR, and anti-correlation between miRNAs and their target mRNAs) and each of them are expected to provide a unique dataset. Some of them have higher sensitivity of prediction but low accuracy and the other weight on the accuracy in the face of reduced sensitivity. We collected all miRNAs predicted by at least four of the seven algorithms to have the potential to target any one of the selected cardiac ion channel and ion transporter genes. Meanwhile, we also collected all ion channel and ion transporter genes that contain the potential target site(s) (the binding site(s) with favorable free energy profiles) for at least one of the 718 human miRNAs. From the above two datasets, we noticed two points. First, out of 718 mature human miRNAs registered in miRBase, 429 miRNAs find their potential target site(s) in the 3'UTR(s) of at least one of the genes encoding cardiac ion channels and ion transporters. Second, all of the genes encoding cardiac ion channels and ion transporters selected for analysis, except for CLCN2, are the potential targets for miRNA regulation.

**miRNA expression profiling in human cardiac tissue**

Expression of miRNAs in mammalian species under normal conditions is genetically programmed with certain spatial (depending on cell-, tissue-, or organ-type) and temporal (depending on developmental stage) patterns. This property generates the so-called

expression signature of a particular tissue. One approach to decrease the incidence of false positive predictions and to narrow down the list of putative miRNA targets would be to compare these *in silico* target predictions to the miRNA transcriptome signatures in the biological system of interest. We therefore conducted miRNA microarray analysis of miRNAs including all 718 human miRNAs for their expression in left ventricular tissues of five healthy human individuals. We found 220 out of 718 human miRNAs being expressed in the cardiac tissue (Supplementary Table 1S).

According to the results reported by Liang *et al* for human heart [35], the top 20 abundant miRNAs in human heart are *miR-1, miR-133a/b, miR-16*, *miR-100, miR-125a/b, miR-126, miR-145, miR-195, miR-199*, miR-20a/b, miR-21, miR-26a/b, miR-24, miR-23, miR-29a/b, miR-27a/b, miR-30a/b/c, miR-92a/b*, *miR-99*, and *let-7a/c/f/g* (Fig. 1A). We verified the expression abundance of several selected miRNAs (*miR-1, miR-133a/b, miR-125a/b, miR-30a/b/c*, *miR-26a/b, miR-24, miR-27a/b, miR-23, miR-29a/b, miR-101, miR-21, miR-150* and *miR-328*) using RNA samples isolated from left ventricular tissues of healthy human subjects (Supplementary Fig. S1). A recent study by Rao *et al* [45] reported a similar array of abundant miRNAs in mouse heart. But differences between the two species exist: e.g. *miR-1* constitutes ~40% of total miRNA content in mouse, but in human, it is ranked the 2$^{nd}$ most abundant miRNA around 1/3 of the *miR-133* level; *miR-208* was found to be one of the top 20 abundant miRNA in mouse but not in human; and *miR-22, miR-143*, *miR-499* and *miR-451* were considered the most abundant miRNAs in mouse heart but not in human heart. Our analysis was focused on the miRNA transcriptome in human heart.

We considered the miRNAs with the same seed sequence as one single miRNA for these miRNAs expectedly have the same set of target genes. This consideration might change the relative abundance of miRNAs. For instance, *miR-1* was found more abundant

than each of the *miR-30* or *miR-26* isoforms; but was considered less abundant than these latter two miRNAs when the seed family was taken as one miRNA, ranked top 4 after *miR-30a/b/c* (top 2) and *miR-26a/b* (top 3).

**Detailed analysis of the miRNAs with the potential to regulate cardiac ion channel genes**

Using this cardiac miRNA expression profiling data in conjunction with published data obtained by real-time RT-PCR by Liang et al [35], we refined the miRNA–target prediction by filtering out the miRNAs that are not expressed in the heart. In this way, we generated the modified datasets for subsequent analyses (Supplementary Table S2 & Table S3). Detailed analysis of these two datasets revealed the following notes.

(1) One hundred ninety-three out of 718 registered human miRNAs or out of 222 miRNAs expressed in the heart have the potential to target the genes encoding human cardiac ion channels and transporters.

(2) Only two genes CLCN2 and KCNE2 were predicted not to contain the target site for miRNAs expressed in the heart.

(3) It appears that the most fundamental and critical ion channels governing cardiac excitability have the largest numbers of miRNAs for their regulators. These include SCN5A for $I_{Na}$ (responsible for the upstroke of the cardiac action potential thereby the conduction of excitations), CACNA1C/CACNB2 for $I_{Ca,L}$ (accounting for the characteristic long plateau of the cardiac action potential and excitation-contraction coupling), KCNJ2 for $I_{K1}$ (sets and maintains the cardiac membrane potential), SLC8A1 for NCX1 (an antiporter membrane protein which removes $Ca^{2+}$ from cells), GJA1/GJC1 (gap junction channel responsible for intercellular conduction of excitation), and ATP1B1 for $Na^+/K^+$

pump (establishing and maintaining the normal electrochemical gradients of $Na^+$ and $K^+$ across the plasma membrane). Each of these genes is theoretically regulated by >30 miRNAs.

(4) The atrium-specific ion channels, including Kir3.4 for $I_{KACh}$, Kv1.5 for $I_{Kur}$, and CACNA1G for $I_{Ca,T}$, seem to be the rare targets for miRNAs (<5 miRNAs).

(5) All four genes for $K^+$ channel auxiliary β-subunits KCNE1, KCNE2, KCHiP, and KCNAB2 were also found to have less number of regulator miRNAs (<10).

(6) Intriguingly, 16 of these top 20 miRNAs are included in the list of the predicted miRNA-target dataset; the other four cardiac-abundant miRNAs *miR-21*, *miR-99*, *miR-100* and *miR-126* are predicted unable to regulate the genes for human cardiac ion channels and transporters.

(7) There is a rough correlation between the number of predicted targets and the abundance of miRNAs in the heart. It appears that the miRNAs within top 8 separate from the rest 12 less abundant miRNAs in their number of target genes (Fig. 1B). The muscle-specific miRNA *miR-1* was predicted to have the largest number of target genes (9 genes) among all miRNAs most abundantly expressed in the heart, followed by *miR-30a/b/c*, *miR-24* and *miR-125a/b* that have 6 target genes each. The muscle-specific miRNA *miR-133* has four target genes and three of them (KCNH2, KCNQ1 and HCN2) have been experimentally verified [22-25].

(8) Comparison of the target genes of the three muscle-specific miRNAs *miR-1*, *miR-133* and *miR-208* revealed that they might play different role in regulating cardiac excitability. It appears that *miR-1* may be involved in all different aspects of cardiac excitability: cardiac conduction by targeting GJA1 and KCNJ2, cardiac automaticity by targeting HCN2 and HCN4, cardiac repolarization by targeting KCNA5, KCND2 and

KCNE1, and $Ca^{2+}$ handling by targeting SLC8A1. By comparison, *miR-133a/b* mainly controls cardiac repolarization through targeting KCNH2 (encoding HERG/$I_{Kr}$) and KCNQ1 (encoding KvLQT1/$I_{Ks}$), the two major repolarizing $K^+$ channels in the heart. *miR-208* was predicted to target only KCNJ2 (encoding Kir2.1 for $I_{K1}$). The non-muscle-specific *let-7* seed family members seem to regulate mainly cardiac conduction by targeting SCN5A (Nav1.5 for intracellular conduction) and GJC1 (Cx45 for intercellular conduction). *miR-30a/b/c* and *miR-26a/b*, *miR-125a/b*, *miR-16*, and *miR-27a/b* were predicted to be L-type $Ca^{2+}$ channel "blockers" through repressing α1c- and/or β1/β2-subunits (Fig. 2).

**Application of the theoretical analysis to explaining the electrical remodeling processes of cardiac diseases**

Next, we intended to apply the theoretical prediction to explaining some established observations of the electrical remodeling related to deregulation of both miRNAs and the genes for ion channels and transporters. Three pathological conditions, cardiac hypertrophy/heart failure, ischemic myocardial injuries, and atrial fibrillation, were studied because the participation of miRNAs in these conditions has previously been investigated.

***Cardiac hypertrophy and heart failure***

The adult heart is susceptible to stress (such as hemodynamic alterations associated with myocardial infarction, hypertension, aortic stenosis, valvular dysfunction, etc) by undergoing remodeling process, including electrical/ionic remodeling. The remodeling process may originally be adaptive in nature, but is in the face of increased risk of arrhythmogenesis. The mechanisms for arrhythmogenesis in failing heart involve [46]: (1) Abnormalities in spontaneous pacemaking function (enhanced cardiac automaticity) as a result of increases in atrial and ventricular $I_f$ due to increased expression of HCN4 channel

may contribute to ectopic beat formation in CHF; (2) Slowing of cardiac repolarization thereby prolongation of APD due to reductions of repolarizing $K^+$ currents (including $I_{K1}$, $I_{Ks}$, and $I_{to1}$) provides the condition for occurrence of early afterdepolarizations (EADs) leading to triggered activities; (3) Delayed afterdepolarizations (DADs) due to enhanced $Na^+$-$Ca^{2+}$ exchanger (NCX1) activity in cardiac hypertrophy/CHF is a consistent finding by numerous studies. Upregulation of NCX1 expression is the major cause for the enhancement; (4) Reentrant activity due to slowing of cardiac conduction velocity.

To date, there have been seven published studies on role of miRNAs and cardiac hypertrophy [13-19]. The common finding of these studies is that an array of miRNAs is significantly altered in their expression, either up- or down-regulated, and that single miRNAs can critically determine the generation and progression of cardiac hypertrophy. The most consistent changes reported by these studies are up-regulation of *miR-21* (6 of 6 studies), *miR-23a* (4 of 6), *miR-125b* (5 of 6), *miR-214* (4 of 6), *miR-24* (3 of 6), *miR-29* (3 of 6) and *miR-195* (3 of 6), and down-regulation of *miR-1*, *miR-133*, *miR-150* (5 of 6 studies) and *miR-30* (5 of 6). These miRNAs were therefore included in our analysis of target genes encoding ion channel and transporter proteins, as shown in Figure 3. Our analyses suggest the following.

(1) It is known that cardiac myocytes are characterized with re-expression of the funny current (or pacemaker current) $I_f$ that may underlie the increased risk of arrhythmogenesis in hypertrophic and failing heart [23], which is carried by HCN2 channel in cardiac muscles. We have previously verified that downregulation of *miR-1* and *miR-133* caused upregulation of HCN2 in cardiac hypertrophy [23]. This may contribute to the enhanced abnormal cardiac automaticity and the associated arrhythmias in CHF.

(2) The NCX1 is upregulated in cardiac hypertrophy, ischemia, and failure. This upregulation can have an effect on $Ca^{2+}$ transients and possibly contribute to diastolic dysfunction and an increased risk of arrhythmias [46, 47-51]. Our target prediction indicates that SLC8A1, the gene encoding NXC1 protein, is a potential target for both *miR-1* and *miR-30a/b/c*. The downregulation of *miR-1* and *miR-30a/b/c* in hypertrophy/failure is deemed to relieve the repression of SLC8A1/NCX1 since a strong tonic repression *miR-1* and *miR-30a/b/c* is anticipated considering the high abundance of these miRNAs. On the other hand, upregulation of *miR-214* tends to repress NCX1, but the expression level of *miR-214* is of no comparison with those of *miR-1* and *miR-30a/b/c*; its offsetting effect should be minimal. Our prediction thus provides a plausible explanation for the upregulation of NCX1 through the miRNA mechanism.

(3) A variety of $Na^+$ channel abnormalities have been demonstrated in heart failure. Several studies suggest that peak $I_{Na}$ is reduced which can cause slowing of cardiac conduction and promote re-entrant arrhythmias [52-55]. It has been speculated that post-transcriptional reduction of the cardiac $I_{Na}$ α-subunit protein Nav1.5 may account for the reduction of peak $I_{Na}$ [55]. In this study, we found that the only miRNA that can target Nav1.5 and is upregulated in cardiac hypertrophy/CHF is *miR-125a/b*. As an abundantly expressed miRNA, upregulation of *miR-125a/b* could well result in repression of SCN5A/Nav1.5.

(4) The gap junction channel proteins connexin43, connexin45 and connexin40 are important for cell-to-cell propagation of excitations. Downregulation of connexin43 expression is associated with an increased likelihood of ventricular tachyarrhythmias in heart failure [56]. Other connexins, including connexin45 [57] and connexin40 [58], are upregulated in failing hearts, possibly as a compensation for connexin43 downregulation.

Our analysis indicates that the upregulation of *miR-125a/b* and *miR-23a/b* should produce repression of connexin43 and connexin45 and the down regulation of *miR-1*, *miR-30a/b/c* and *miR-150* should do the opposite. These two opposing effects may cancel out each other.

(5) Prolongation of ventricular APD is typical of heart failure to enable the improvement of contraction strength, thereby supporting the weakened heart. However, APD prolongation consequent to decreases in several repolarizing $K^+$ current ($I_{to1}$, $I_{Ks}$, and $I_{K1}$) in failing heart often results in occurrence of early afterdepolarizations (EADs) [59-64]. Our prediction failed to provide any explanation at the miRNA level: None of the upregulated miRNAs may regulate the genes encoding repolarizing $K^+$ channels. On the contrary, downregulation of *miR-1* and *miR-133* predict upregulation of KCNE1/minK and KCNQ1/KvLQT1, respectively.

(6) A majority of published studies showed a decrease in $I_{K1}$ in ventricular myocytes of failing hearts [46, 61-64]. But whether KCNJ2/Kir2.1, the major subunit underlying $I_{K1}$, is downregulated remained controversial in previous studies and the mechanisms remained obscured. One study noted decreased KCNJ2 mRNA expression but unaltered Kir2.1 protein level [64]. With our prediction, the upregulated miRNAs (*miR-125, miR-214, miR-24, miR-29*, and *miR-195*) predict reduction of inward rectifier $K^+$ channel subunits including KCNJ2/Kir2.1, KCNJ12/Kir2.2, KCNJ14/Kir2.4, and KCNK1/TWIK1, whereas the downregulated miRNAs (*miR-1* and *miR-30a/b/c*) predict increase in KCNJ2/Kir2.1.

In summary, our analysis of target genes for deregulated miRNAs in hypertrophy/CHF may explain at least partly the enhanced cardiac automaticity (relief of HCN2 repression and increased NCX1 expression) and reduced cardiac conduction (repression of Nav1.5). But the data suggest that miRNAs are hardly involved in the abnormality of cardiac repolarization in cardiac hypertrophy and heart failure since the

genes for the repolarizing $K^+$ channels were not predicted as targets for the upregulated miRNAs. The prediction of NCX1 upregulation as a result of derepression from miRNAs may be of particular importance aberrantly enhanced NXC1 activity has also been noticed in atrial fibrillation occurring in CHF.

***Myocardial infarction (MI)***

MI, a typical situation of metabolic stress, is presented as cascades of cellular abnormalities as a result of deleterious alterations of gene expression outweighing adaptive changes [65,66]. MI can cause severe cardiac injuries and the consequences are contraction failure, electrical abnormalities and even lethal arrhythmias, and eventual death of the cell. Ischemic myocardium demonstrates characteristic sequential alterations in electrophysiology with an initial shortening of APD and QT interval during the early phase (<15min) of acute ischemia and subsequent lengthening of APD/QT after a prolonged ischemic period and chronic myocardial ischemia [46,65,66]. While these alterations may be adaptive to the altered metabolic status, they occur at the cost of arrhythmogenesis consequent to ischemic ionic remodelling. To exploit if miRNAs could be involved in the remodelling process, several original studies have been published. We first identified upregulation of *miR-1* in acute myocardial infarction and the ischemic arrhythmias caused by this deregulation of *miR-1* expression [2]. Similar ischemic *miR-1* upregulation was reproduced by another two groups [67,68]. Subsequently, miRNA expression profiles in the setting of myocardial ischemia/reperfusion injuries were reported by three groups [69-71]. Here we also present the miRNA transcriptome in a rat model of acute myocardial infarction (Supplementary Fig. S2).

Extracting of the overlapping results from different laboratories and filtering with the cardiac expression profile verified by real-time RT-PCR in human hearts allowed us to

identify an array of miRNAs that are likely deregulated in the setting of myocardial ischemia. The upregulated miRNAs include *miR-1, miR-23, miR-29, miR-20, miR-30, miR-146b-5p, miR-193, miR-378, miR-181, miR-491-3p, miR-106*, *miR-199b-5p*, and *let-7f*; the downregulated miRNAs include *miR-320*, *miR-185*, *miR-324-3p,* and *miR-214* (Fig. 4). This analysis excluded some miRNAs that were found deregulated by a study but not by others and that were found deregulated in rat heart but was not expressed in human heart. Interesting to note is that some of the miRNAs demonstrated the opposite directions of changes in their expression between ischemic myocardium and hypertrophic hearts. For example, *miR-1*, *let-7*, *miR-181b*, *miR-29a* and *miR-30a/e* are upregulated in ischemic myocardium, but downregulated in hypertrophy. Similarly, *miR-214*, *miR-320* and *miR-351* are down-regulated in ischemic myocardium, but up-regulated in hypertrophy (Fig. 3). This fact further reinforces the notion that different pathological conditions have different expression profiles. Our analysis yielded the following notions.

(1) Six upregulated miRNAs (*miR-1, miR-29, miR-20, miR-30, miR-193* and *miR-181*) were predicted to target several Kir subunits (KCNJ2, KCNJ12, KCNJ, and KCNK1), but none of the downregulated miRNAs can target these genes (Fig. 4). This is in line with the previous finding that $I_{K1}$ is reduced and membrane is depolarized in ischemic myocardium [2,65,66].

(2) The cardiac slow delayed rectifier $K^+$ current ($I_{Ks}$) is carried by co-assembly of an α-subunit KvLQT1 (encoded by KCNQ1) and a β-subunit mink (encoded by KCNE1) [72,73]. Loss-of-function mutation of either KCNQ1 or KCNE1 can cause long QT syndromes, indicating the importance of $I_{Ks}$ in cardiac repolarization. In ischemic myocardium, persistent decreases in minK with normalized KvLQT1 protein expression have been observed which may underlie unusual delayed rectifier currents with very rapid

activation [73,74], resembling currents produced by the expression of KvLQT1 in the absence of minK [72,73]. We have experimentally established KCNE1 as a target for *miR-1* repression [25], which was also predicted in the present analysis. Moreover, no other miRNAs were predicted to target KCNQ1. This finding is coincident with the observations on the diminishment of minK alone without changes of KvLQT1 in ischemic myocardium.

(3) It has been observed that cells in the surviving peri-infarct zone have discontinuous propagation due to abnormal cell-to-cell coupling [76-78]. This is largely due to decreased expression and redistribution of gap junction protein connexins (Cxs). In this study, seven out of 12 upregulated miRNAs were predicted to target Cxs including GJA1/Cx43, GJC1/Cx45, and GJA5/Cx40, but only one downregulated miRNA *miR-185* may regulate GJA5/Cx40 (Fig. 5). This result clearly points to the role of miRNAs in damaging cardiac conduction in ischemic myocardium. Indeed, repression of GJA1/Cx43 to slow conduction and induce arrhythmias in acute myocardial infarction has been experimentally verified by our previous study [2].

(4) In ischemic myocardium, fast or peak $I_{Na}$ density is reduced, which may also account partly for the conduction slowing and the associated re-entrant arrhythmias [79-81]. Our analysis showed that *let-7f* and *miR-378* may target SCN5A/Nav1.5 and upregulation of these miRNAs is anticipated to cause reduction of $I_{Na}$ via downregulating SCN5A/Nav1.5 in myocardial infarction. By comparison, none of the downregulated miRNAs may repress SCN5A/Nav1.5 based on our target prediction.

(5) $I_{to1}$ is reduced in myocardial ischemia and in rats, $I_{to1}$ decreases correlate most closely with downregulation of KCND2-encoded Kv4.2 subunits [82,83]. *miR-1* is predicted to repress KCND2/Kv4.2, and *miR-29* may target KCHiP2 that is known to be critical in the formation of $I_{to1}$.

(6) $I_{Ca,L}$ is diminished in border-zone cells of dogs [46,84,85]. *miR-30* family has the potential to target CACNA1C/Cav1.2 and CACNB2/Cavβ2, and *miR-124, miR-181, miR-320* and *miR-204* to target CACNB2. Upregulation of *miR-30*, *miR-124* and *miR-181* therefore would decrease CACNA1C/Cav1.2 and CACNB2/Cavβ2 expression, but downregulation of *miR-320* and *miR-204* tends to increase the expression of these genes. Considering the relative abundance of these miRNAs, it seems that the decreasing force overweighs the increasing force with a balance towards a net inhibition of $I_{Ca,L}$.

(7) $Na^+/K^+$ ATPase is a sarcolemmal ATP-dependent enzyme transporter that transports three intracellular $Na^+$ ions to the extracellular compartment and moves two extracellular $K^+$ ions into the cell to maintain the physiological $Na^+$ and $K^+$ concentration gradients for generating the rapid upstroke of the action potential but also for driving a number of ion-exchange and transport processes crucial for normal cellular function, ion homeostasis and the control of cell volume. It is electrogenic, producing a small outward current $I_P$ [86]. We noticed that the ischemia-induced upregulation of *miR-29* and *miR181* expression might render inhibition of $Na^+/K^+$ ATPase activity as they possibly target the ATP1B1 β-subunit of the enzyme. This may contribute to the electrical and contractile dysfunction in the ischemic/reperfused myocardium due to the ischemia-induced inhibition of the $Na^+/K^+$ ATPase and the failure of intracellular $Na^+$ to recover completely on reperfusion [87].

In a whole, it appears that the expression signature of miRNAs in the setting of myocardial ischemia and the predicted gene targeting of these miRNAs coincide with the ionic remodelling process under this pathological condition (Fig. 4). The miRNAs seem to be involved in all aspects of the abnormalities of cardiac excitability during ischemia, as manifested by the slowing of cardiac conduction due to reduced $I_{Na}$ and Cx43, the depolarized membrane potential to adversely affect cardiac conduction due to reduced $I_{K1}$,

the impaired excitation-contraction coupling and contractile function due to reduced $I_{Ca,L}$ and $Na^+/K^+$ ATPase, and the delayed cardiac repolarization due to reduced $I_{Ks}$ and $I_{to1}$.

***Atrial fibrillation (AF)***

AF is the most commonly encountered clinical arrhythmia that causes tremendous health problems by increasing the risk of stroke and exacerbating heart failure. It is characterized by a process termed atrial electrical remodeling: the rapid atrial activation rate during AF can remodel the atrial electrophysiology to promote the recurrence and maintenance of AF [46,88]. A prominent finding in atrial electrical remodeling is shortening of atrial effective refractory period (ERP) favoring re-entrant arrhythmias, primarily because of the shortening of atrial APD as a result of two critical changes. The first change is the reduction of L-type $Ca^{2+}$ current ($I_{CaL}$) that serves to shorten the plateau duration. And the second change is the increase in inward rectifier $K^+$ current $I_{K1}$, which underlies the shortening of the terminal phase [89-91]. Whereas it is known that the expression of the genes for these channels is deregulated during AF, the precise molecular mechanisms remained unclear. Additionally, expression of other ion channels such as KCND3 (encoding Kv4.3 for $I_{to1}$) and KCNA5 (encoding Kv1.5 for $I_{Kur}$) has been consistently found downregulated in AF, though the role of the changes in AF is yet to be elucidated [89-91]. The present analysis, however, aids us to get some insight into the issue.

We first conducted expression profiling to identify deregulated miRNAs in the atrial tissues of a canine model of tachypacing-induce AF, using miRNA microarray analysis comparing the differential expressions of miRNAs between control and AF dogs. Four miRNAs *miR-223, miR-328, miR-664* and *miR-517* were found increased by >2 folds, and six were decreased by at least 50% including *miR-101, miR-133, miR-145, miR-320, miR-373* and *miR-499*. Real-time quantitative RT-PCR (qRT-PCR) analysis confirmed the

significant upregulation of *miR-223, miR-328* and *miR-664* (*miR-517* was undetectable), and the significant downregulation of *miR-101, miR-320*, and *miR-499* (Fig. 5). Our subsequent analysis was therefore based on the deregulated miRNAs verified by qPCR.

(1) Our prediction indicates that three miRNA *miR-328, miR-145* and *miR-320* have the potential to repress both the α1c- and β2-subunits of cardiac L-type $Ca^{2+}$ channel genes, CACNA1C and CACNB2, respectively. While increased miR-328 level should upregulate L-type $Ca^{2+}$ channel expression, decreased *miR-145* and *miR-320* levels should downregulate it. In reality, these two opposing actions may offset each other.

(2) Among the deregulated miRNAs, the only miRNA that may target KCND3 is *miR-328*. Hence, upregulation of *miR-328* predicts downregulation of Kv4.3 thereby reduction of $I_{to1}$ in AF.

(3) Increase in $I_{K1}$ is a hallmark of atrial electrical remodeling in AF. *miR-101* was predicted to target KCNJ2/Kir2.1 and downregulation of this miRNA should upregulate KCNJ2/Kir2.1 due to a relief of repression. Repression of KCNJ12/Kir2.2 due to *miR-328* upregulation may be canceled out by a derepression upon *miR-145* downregulation.

(4) Impulse initiation by automaticity and triggered activity as well as impulse initiation resulting from reentry in AF has been suggested [92]. The hyperpolarization activated cation current or funny current $I_f$ is a candidate for contributing to abnormal automaticity [93]. The downregulation of *miR-133* in AF predicts enhancement of $I_f$ through derepression of HCN2 to induce abnormal cardiac automaticity.

(5) Our data did not predict involvement of miRNAs in the alterations of the genes for $I_{Kur}$, $I_{Kr}$ and $I_{Ks}$.

Taken together, it appears that the miRNA expression signature identified in a canine model of tachypacing-induced AF is related to the atrial ionic remodelling process.

Specifically, downregulation of *miR-101* and *miR-133* may contribute to enhanced $I_{K1}$ and $I_f$, respectively, and upregulation of *miR-328* may underlie the reduction of $I_{to1}$, in AF. Whether this upregulation also contributes to the reduction of $I_{Ca,L}$ need to be examined experimentally. The characteristic decrease of $I_{Kur}$ in AF is unlikely related to miRNA deregulation.

Cardiovascular diseases remain the major cause of mortality and morbidity in developed countries. Most of the cardiac deaths are sudden, occurring secondary to ventricular arrhythmias, the electrical disturbances that can result in irregular cardiac contraction. Abnormally altered cardiac excitability suggests that for arrhythmias to arise, the normal matrix of ion channels and transporters must be perturbed by arrhythmogenic substrates to produce a proarrhythmic conditions to permit rhythmic disturbances caused by impaired excitation conduction/propagation, enhanced automaticity, or abnormal repolarization. In some cases, abnormalities of these ion channels, channelopathies, can be attributed to mutations in the genes encoding the channel proteins, which can predispose to arrhythmias. In other cases, malfunction of ion channels can also be ascribed to abnormally altered expression. The present study aims to acquire an overall picture about the potential expression regulation of ion channel and transporter genes by miRNAs and the possible implications of this regulatory mechanism. The theoretical analysis in conjunction with experimental demonstration of miRNA expression profiles under various conditions performed in this study allowed us to establish a matrix of miRNAs that are expressed in cardiac cells and have the potential to regulate the genes encoding cardiac ion channels and transporters. These miRNAs likely play an important role in controlling cardiac excitability and keeping the normal electrical activities of the heart. In other words, the ion channel genes may normally be under the post-transcriptional regulation of a group of miRNAs in

addition to the muscle-specific miRNAs *miR-1* and *miR-133* as already demonstrated experimentally. Also were we able to link a particular ionic remodeling process in hypertrophy/heart failure, myocardial ischemia, or atrial fibrillation to the corresponding deregulated miRNAs under that pathological condition; the changes of miRNAs appear to have anti-correlation with the changes of many of the genes encoding cardiac ion channels under these situations. Intriguingly, the miRNA targeting under three different conditions clearly demonstrated three different patterns with that in hypertrophy/CHF showing balanced repression and derepression, in MI showing repression overweighing derepression, and in AF showing the opposite: derepression overweighing repression. Another important notion revealed by this study is that though we have elucidated role of *miR-1* and *miR-133* in controlling cardiac excitability and the associated arrhythmogenesis in the above-mentioned three pathological conditions, it is now clearly that other miRNAs that are deregulated are also likely involved in these processes. In reality, it is conceivable that the electrical/ionic remodeling processes under various conditions are caused by many miRNAs in addition to other regulatory molecules. The present study should aid us to pinpoint the individual miRNAs that can most likely take part in the remodeling processes through targeting particular genes.

It should be noted, however, that the present computational study is in no way to replace experimental approaches for understanding the role of miRNAs in regulating expression of genes for cardiac ion channels and transporters; rather it merely presents a prediction of the odds of miRNA:mRNA interactions under normal situation and in the context of electrical/ionic remodeling under the selected circumstances of the heart. This theoretical analysis like all other computational studies needs to be eventually verified with the bench-top work and should not be considered original results. Nonetheless, with sparse

experimental data published to date and the anticipated difficulties to acquire complete experimental data using the currently available techniques, this study can well serve as first-hand information, providing a framework and guideline for future experimental studies. The second limitation of the study is the possibility of underestimating the number of ion channel-regulator miRNAs because of the stringent criterion for inclusion of miRNAs with positive prediction of targets by at least four out of 11 algorithms; in the past, we had been able to experimentally verified nearly all the target genes predicted by only one algorithm miRanda for our pre-experiment analysis. However, the fact that our prediction includes all 20 most abundant miRNAs and other highly expressed miRNAs in the myocardium suggests that this limitation might not have significant negative impact on the accuracy of our analysis and inclusion of more miRNAs by more permissive criteria does not guarantee their physiological function if they are scarcely expressed in the heart. Yet it should be noted that the miRNA expression profiles were obtained from myocardium that also includes fibroblasts and caution needs to be taken when interpreting the expression data. Another important notion is that despite that our prediction of miRNA targeting coincides with the changes of ion channel expression under the pathological conditions, it does not imply that miRNAs are necessarily the important or even the only determinant of the electrical remodeling processes. Our data to the most indicate the potential contribution of miRNAs to such conditions; other molecules like transcription factors must also be involved in the regulation of expression of ion channel genes under these conditions. Finally, it is also difficult to predict the net outcome when two miRNAs target a same gene but alter in their expression in the opposite directions. Yet, with deepened and broadened understanding of miRNA targeting and action, these above limitations should eventually be worked out.

**ACKNOWLEDGEMENTS**

The authors thank XiaoFan Yang for her excellent technical supports. This work was supported by the Canadian Institute of Health Research (ZW). Dr. Z Wang is a Changjiang Scholar Endowed Professor of the Ministry of Education of China.

**Author Contributions**

Z.W. generated the idea, supervised the studies and wrote the manuscript. X.L. performed the miRNA microarray and real-time RT-PCR experiments and analyses. H.Z. performed the computational prediction and participated in preparing figures. J.X participated in miRNA microarray and real-time RT-PCR experiment.

## References

1. Marbán E: Cardiac channelopathies. Nature 2002; 415: 213–218.
2. Yang B, Lin H, Xiao J, Lu Y, Luo X, Li B, Zhang Y, Xu C, Bai Y, Wang H, Chen G, Wang Z: The muscle-specific microRNA *miR-1* regulates cardiac arrhythmogenic potential by targeting GJA1 and KCNJ2. Nat Med 2007; 13: 486–491.
3. Zhao Y, Ransom JF, Li A, Vedantham V, von Drehle M, Muth AN, Tsuchihashi T, McManus MT, Schwartz RJ, Srivastava D: Dysregulation of cardiogenesis, cardiac conduction, and cell cycle in mice lacking *miRNA-1-2*. Cell 2007 129: 303–317.
4. Yang, Lu Y, Wang Z: Control of cardiac excitability by microRNAs. Cardiovasc Res 2008; 79: 571–580.

5. van Rooij E, Marshall WS, Olson EN: Toward microRNA–based therapeutics for heart disease: the sense in antisense. Circ Res 2008; 103: 919-928.

6. Zhao Y, Samal E, Srivastava D: Serum response factor regulates a muscle-specific microRNA that targets Hand2 during cardiogenesis. Nature 2005; 436: 214–220.

7. Chen JF, Mandel EM, Thomson JM, Wu Q, Callis TE, Hammond SM, Conlon FL, Wang DZ: The role of *microRNA-1* and *microRNA-133* in skeletal muscle proliferation and differentiation. Nat Genet 2006; 38: 228–233.

8. Rao PK, Kumar RM, Farkhondeh M, Baskerville S, Lodish HF: Myogenic factors that regulate expression of muscle-specific microRNAs. Proc Natl Acad Sci U S A 2006; 103: 8721–8726.

9. Kwon C, Han Z, Olson EN, Srivastava D: *MicroRNA1* influences cardiac differentiation in Drosophila and regulates Notch signaling. Proc Natl Acad Sci U S A 2005; 102: 18986–18991.

10. Sokol NS, Ambros V: Mesodermally expressed Drosophila *microRNA-1* is regulated by Twist and is required in muscles during larval growth. Genes Dev 2005; 19: 2343–2354.

11. Wienholds E, Kloosterman WP, Miska E, Alvarez-Saavedra E, Berezikov E, de Bruijn E, Horvitz HR, Kauppinen S, Plasterk RH: MicroRNA expression in zebrafish embryonic development. Science 2005; 309: 310–311.

12. Callis TE, Chen JF, Wang DZ: MicroRNAs in skeletal and cardiac muscle development. DNA Cell Biol 2007; 26: 219–225.

13. van Rooij E, Sutherland LB, Qi X, Richardson JA, Hill J, Olson EN: Control of stress-dependent cardiac growth and gene expression by a microRNA. Science 2007; 316: 575–579.

14. van Rooij E, Sutherland LB, Liu N, Williams AH, McAnally J, Gerard RD, Richardson JA, Olson EN: A signature pattern of stress-responsive microRNAs that can evoke cardiac hypertrophy and heart failure. Proc Natl Acad Sci U S A 2006; 103: 18255–18260.

15. Sayed D, Hong C, Chen IY, Lypowy J, Abdellatif M: MicroRNAs play an essential role in the development of cardiac hypertrophy. Circ Res 2007; 100: 416–424.

16. Carè A, Catalucci D, Felicetti F, Bonci D, Addario A, Gallo P, Bang ML, Segnalini P, Gu Y, Dalton ND, Elia L, Latronico MV, Høydal M, Autore C, Russo MA, Dorn GW 2nd, Ellingsen O, Ruiz-Lozano P, Peterson KL, Croce CM, Peschle C, Condorelli G: MicroRNA-133 controls cardiac hypertrophy. Nat Med 2007; 13: 613–618.

17. Cheng Y, Ji R, Yue J, Yang J, Liu X, Chen H, Dean DB, Zhang C: MicroRNAs are aberrantly expressed in hypertrophic heart. Do they play a role in cardiac hypertrophy? Am J Pathol 2007; 170: 1831–1840.

18. Tatsuguchi M, Seok HY, Callis TE, Thomson JM, Chen JF, Newman M, Rojas M, Hammond SM, Wang DZ: Expression of microRNAs is dynamically regulated during cardiomyocyte hypertrophy. J Mol Cell Cardiol 2007; 42: 1137–1141.

19. Thum T, Galuppo P, Wolf C, Fiedler J, Kneitz S, van Laake LW, Doevendans PA, Mummery CL, Borlak J, Haverich A, Gross C, Engelhardt S, Ertl G, Bauersachs J. MicroRNAs in the human heart: a clue to fetal gene reprogramming in heart failure. Circulation 2007; 116: 258–267.

20. Ikeda S, Kong SW, Lu J, Bisping E, Zhang H, Allen PD, Golub TR, Pieske B, Pu WT: Altered microRNA expression in human heart disease. Physiol Genomics 2007; 31: 367–373.

21. Ji R, Cheng Y, Yue J, Yang J, Liu X, Chen H, Dean DB, Zhang C: MicroRNA expression signature and antisense-mediated depletion reveal an essential role of MicroRNA in vascular neointimal lesion formation. Circ Res 2007; 100: 1579–1588.

22. Xiao L, Xiao J, Luo X, Lin H, Wang Z, Nattel S: Feedback remodeling of cardiac potassium current expression. A novel potential mechanism for control of repolarization reserve. Circulation 2008; 118: 983–992.

23. Luo X, Lin H, Pan Z, Xiao J, Zhang Y, Lu Y, Yang B, Wang Z: Downregulation of *miRNA-1/miRNA-133* contributes to re-expression of pacemaker channel genes HCN2 and HCN4 in hypertrophic heart. J Biol Chem 2008; 283: 20045–20052.

24. Xiao J, Luo X, Lin H, Zhang Y, Lu Y, Wang N, Zhang Y, Yang B, Wang Z: MicroRNA *miR-133* represses HERG $K^+$ channel expression contributing to QT prolongation in diabetic hearts. J Biol Chem 2007; 282: 12363–12367.

25. Luo X, Xiao J, Lin H, Li B, Lu Y, Yang B, Wang Z: Transcriptional activation by stimulating protein 1 and post-transcriptional repression by muscle-specific microRNAs of $I_{Ks}$-encoding genes and potential implications in regional heterogeneity of their expressions. J Cell Physiol 2007; 212: 358–367.

26. Wang Z, Luo X, Lu Y, Yang B: miRNAs at the heart of the matter. J Mol Med 2008; 86: 772–783.

27. Brennecke J, Stark A, Russell RB, Cohen SM: Principles of microRNA-target recognition. PLoS Biol 2005; 3: 404–418.

28. Jackson RJ, Standart N: How do microRNAs regulate gene expression? Sci STKE 2007; 23: 243–249.

29. Lewis BP, Shih I-H, Jones-Rhoades MW, Bartel DP, Burge CB: Prediction of mammalian microRNA targets. Cell 2003; 115: 787–798.

30. Nilsen TW: Mechanisms of microRNA-mediated gene regulation in animal cells. Trends Genet 2007; 23: 243–249.

31. Pillai RS, Bhattacharyya SN, Filipowicz W: Repression of protein synthesis by miRNAs: how many mechanisms? Trends Cell Biol 2007; 17: 118–126.

32. Griffiths-Jones S, Saini HK, van Dongen S, Enright AJ: miRBase: tools for microRNA genomics. Nucleic Acids Res 2008; 36: D154–D158.

33. Lewis BP, Burge CB, Bartel DP: Conserved seed pairing, often flanked by adenosines, indicates that thousands of human genes are microRNA targets. Cell 2005; 120: 15–20.

34. Miranda KC, Huynh T, Tay Y, Ang YS, Tam WL, Thomson AM, Lim B, Rigoutsos I: A pattern-based method for the identification of MicroRNA binding sites and their corresponding heteroduplexes. Cell 2006; 126: 1203–1217.

35. Liang Y, Ridzon D, Wong L, Chen C: Characterization of microRNA expression profiles in normal human tissues. BMC Genomics 2007; 8: 166.

36. Chen C, Ridzon DA, Broomer AJ, Zhou Z, Lee DH, Nguyen JT, Barbisin M, Xu NL, Mahuvakar VR, Andersen MR, Lao KQ, Livak KJ, Guegler KJ: Real-time quantification of microRNAs by stem-loop RT-PCR. Nucleic Acids Res 2005; 33: e179.

37. Xiao F, Zuo Z, Cai G, Kang S, Gao X, Li T: miRecords: an integrated resource for microRNA-target interactions. Nucleic Acids Res 2009; 37: D105–D110.

38. Kiriakidou M, Nelson PT, Kouranov A, Fitziev P, Bouyioukos C, Mourelatos Z, Hatzigeorgiou A: A combined computational-experimental approach predicts human microRNA targets. Genes Dev 2004; 18: 1165–1178.

39. Enright AJ, John B, Gaul U, Tuschl T, Sander C, Marks DS: MicroRNA targets in Drosophila. Genome Biology 2003; 5: R1.

40. Wang X, El Naqa IM: Prediction of both conserved and nonconserved microRNA targets in animals. Bioinformatics 2008; 24: 325–332.

41. Krek A, Grün D, Poy MN, Wolf R, Rosenberg L, Epstein EJ, MacMenamin P, da Piedade I, Gunsalus KC, Stoffel M, Rajewsky N: Combinatorial microRNA target predictions. Nat Genet 2005; 37: 495–500.

42. Kertesz M, Iovino N, Unnerstall U, Gaul U, Segal E: The role of site accessibility in microRNA target recognition, Nature Genetics 2007; 39: 1278–1284.

43. Rehmsmeier M, Steffen P, Hochsmann M, Giegerich R: Fast and effective prediction of microRNA/target duplexes. RNA 2004; 10: 1507–1517.

44. Lewis BP, Shih IH, Jones-Rhoades MW, Bartel DP, Burge CB: Prediction of mammalian microRNA targets. Cell 2003; 115: 787–798.

45. Rao PK, Toyama Y, Chiang HR, Gupta S, Bauer M, Medvid R, Reinhardt F, Liao R, Krieger M, Jaenisch R, Lodish HF, Blelloch R: Loss of cardiac microRNA-mediated regulation leads to dilated cardiomyopathy and heart failure. Circ Res 2009; 105: 585–594.

46. Nattel S, Maguy A, Le Bouter S, Yeh Y-H: Arrhythmogenic ion-channel remodeling in the heart: heart failure, myocardial infarction, and atrial fibrillation. Physiol Rev 2007; 87: 425–456.

47. Studer R, Reinecke H, Bilger J, Eschenhagen T, Böhm M, Hasenfuss G, Just H, Holtz J, Drexler H: Gene expression of the cardiac $Na^{+}$-$Ca^{2+}$ exchanger in end-stage human heart failure. Circ Res 1994; 75: 443–453.

48. Flesch M, Schwinger RH, Schiffer F, Frank K, Südkamp M, Kuhn-Regnier F, Arnold G, Böhm M: Evidence for functional relevance of an enhanced expression of the $Na^{+}$-$Ca^{2+}$ exchanger in failing human myocardium. Circulation 1996; 94: 992–1002.

49. O'Rourke B, Kass DA, Tomaselli GF, Kääb S, Tunin R, Marbán E: Mechanisms of altered excitation-contraction coupling in canine tachycardia-induced heart failure. I: experimental studies. Circ Res 1999; 84: 562–570.

50. Li D, Melnyk P, Feng J, Wang Z, Petrecca K, Shrier A, Nattel S: Effects of experimental heart failure on atrial cellular and ionic electrophysiology. Circulation 2000;101: 2631–2638.

51. Pogwizd SM, Bers DM: Na/Ca exchange in heart failure: contractile dysfunction and arrhythmogenesis. Ann NY Acad Sci 2002; 976: 454–465.

52. Kuryshev YA, Brittenham GM, Fujioka H, Kannan P, Shieh CC, Cohen SA, Brown AM: Decreased sodium and increased transient outward potassium currents in iron-loaded cardiac myocytes. Implications for the arrhythmogenesis of human siderotic heart disease. Circulation 1999; 100: 675–683.

53. Ufret-Vincenty CA, Baro DJ, Lederer WJ, Rockman HA, Quinones LE, Santana LF: Role of sodium channel deglycosylation in the genesis of cardiac arrhythmias in heart failure. J Biol Chem 2001; 276: 28197–28203.

54. Valdivia CR, Chu WW, Pu J, Foell JD, Haworth RA, Wolff MR, Kamp TJ, Makielski JC: Increased late sodium current in myocytes from a canine heart failure model and from failing human heart. J Mol Cell Cardiol 2005; 38: 475–483.

55. Zicha S, Maltsev VA, Nattel S, Sabbah HN, Undrovinas AI: Post-transcriptional alterations in the expression of cardiac $Na^+$ channel subunits in chronic heart failure. J Mol Cell Cardiol 2004; 37: 91–100.

56. Kitamura H, Ohnishi Y, Yoshida A, Okajima K, Azumi H, Ishida A, Galeano EJ, Kubo S, Hayashi Y, Itoh H, Yokoyama M. Heterogeneous loss of connexin43 protein in nonischemic dilated cardiomyopathy with ventricular tachycardia. Cardiovasc Electrophysiol 2002;13: 865–870.

57. Yamada KA, Rogers JG, Sundset R, Steinberg TH, Saffitz JE: Up-regulation of connexin45 in heart failure. J Cardiovasc Electrophysiol 2003; 14: 1205–1212.

58. Dupont E, Matsushita T, Kaba RA, Vozzi C, Coppen SR, Khan N, Kaprielian R, Yacoub MH, Severs NJ: Altered connexin expression in human congestive heart failure. J Mol Cell Cardiol 2001; 33: 359–371.

59. Tsuji Y, Opthof T, Kamiya K, Yasui K, Liu W, Lu Z, Kodama I: Pacing-induced heart failure causes a reduction of delayed rectifier potassium currents along with decreases in calcium and transient outward currents in rabbit ventricle. Cardiovasc Res 2000; 48: 300–309.

60. Li GR, Lau CP, Ducharme A, Tardif JC, Nattel S: Transmural action potential and ionic current remodeling in ventricles of failing canine hearts. Am J Physiol 2002; 283: H1031–H1041.

61. Beuckelmann DJ, Nabauer M, Erdmann E: Alterations of $K^+$ currents in isolated human ventricular myocytes from patients with terminal heart failure. Circ Res 1993; 73: 379–385.

62. Kääb S, Nuss HB, Chiamvimonvat N, O'Rourke B, Pak PH, Kass DA, Marban E, Tomaselli GF: Ionic mechanism of action potential prolongation in ventricular myocytes from dogs with pacing-induced heart failure. Circ Res 1996; 78: 262–273.

63. Rozanski GJ, Xu Z, Whitney RT, Murakami H, Zucker IH: Electrophysiology of rabbit ventricular myocytes following sustained rapid ventricular pacing. J Mol Cell Cardiol 1997; 29: 721–732.

64. Rose J, Armoundas AA, Tian Y, DiSilvestre D, Burysek M, Halperin V, O'Rourke B, Kass DA, Marbán E, Tomaselli GF: Molecular correlates of altered expression of potassium currents in failing rabbit myocardium. Am J Physiol 2005; 288: H2077–H2087.

65. Carmeliet E: Cardiac ionic currents and acute ischemia: from channels to arrhythmias. Physiol Rev 1999; 79: 917–1017.

66. Pinto JM, Boyden PA: Electrical remodeling in ischemia and infarction. Cardiovasc Res 1999; 42: 284–297.

67. Shan ZX, Lin QX, Fu YH, Deng CY, Zhou ZL, Zhu JN, Liu XY, Zhang YY, Li Y, Lin SG, Yu XY: Upregulated expression of *miR-1/miR-206* in a rat model of myocardial infarction. Biochem Biophys Res Commun 2009; 381: 597–601.

68. Tang Y, Zheng J, Sun Y, Wu Z, Liu Z, Huang G: *MicroRNA-1* regulates cardiomyocyte apoptosis by targeting Bcl-2. Int Heart J 2009; 50: 377–387.

69. Dong S, Cheng Y, Yang J, Li J, Liu X, Wang X, Wang D, Krall TJ, Delphin ES, Zhang C: MicroRNA expression signature and the role of *microRNA-21* in the early phase of acute myocardial infarction. J Biol Chem 2009; 284: 29514–29525.

70. Ren XP, Wu J, Wang X, Sartor MA, Qian J, Jones K, Nicolaou P, Pritchard TJ, Fan GC: MicroRNA-320 is involved in the regulation of cardiac ischemia/reperfusion injury by targeting heat-shock protein 20. Circulation 2009;119: 2357–2366.

71. Roy S, Khanna S, Hussain SR, Biswas S, Azad A, Rink C, Gnyawali S, Shilo S, Nuovo GJ, Sen CK: MicroRNA expression in response to murine myocardial infarction: miR-21 regulates fibroblast metalloprotease-2 via phosphatase and tensin homologue. Cardiovasc Res 2009; 82: 21–29.

72. Barhanin J, Lesage F, Guillemare E, Fink M, Lazdunski M, Romey G: KvLQT1 and lsK (minK) proteins associate to form the $I_{Ks}$ cardiac potassium current. Nature 1996; 384: 78–80.

73. Sanguinetti MC, Curran ME, Zou A, Shen J, Spector PS, Atkinson DL, Keating MT: Coassembly of KvLQT1 and minK (IsK) proteins to form cardiac I(Ks) potassium channel. Nature 1996; 384: 80–83.

74. Dun W, Boyden PA: Diverse phenotypes of outward currents in cells that have survived in the 5-day-infarcted heart. Am J Physiol 2005; 289: H667–H673.

75. Jiang M, Cabo C, Yao J, Boyden PA, Tseng G: Delayed rectifier K currents have reduced amplitudes and altered kinetics in myocytes from infarcted canine ventricle. Cardiovasc Res 2000; 48: 34–43.

76. Peters NS: Myocardial gap junction organization in ischemia and infarction. Microsc Res Tech 1995; 31: 375–386.

77. Spear JF, Michelson EL, Moore EN: Reduced space constant in slowly conducting regions of chronically infarcted canine myocardium. Circ Res 1983; 53: 176–185.

78. Gardner PI, Ursell PC, Fenoglio JJ Jr, Wit AL: Electrophysiologic and anatomic basis for fractionated electrograms recorded from healed myocardial infarcts. Circulation 1985; 72: 596–611

79. Spear JF, Horowitz LN, Hodess AB, MacVaugh H 3rd, Moore EN: Cellular electrophysiology of human myocardial infarction. 1. Abnormalities of cellular activation. Circulation 1979; 59: 247–256.

80. Friedman PL, Fenoglio JJ, Wit AL: Time course for reversal of electrophysiological and ultrastructural abnormalities in subendocardial Purkinje fibers surviving extensive myocardial infarction in dogs. Circ Res 1975; 36: 127–144.

81. Pu J, Boyden PA: Alterations of $Na^+$ currents in myocytes from epicardial border zone of the infarcted heart. A possible ionic mechanism for reduced excitability and postrepolarization refractoriness. Circ Res 1997; 81: 110–119.

82. Gidh-Jain M, Huang B, Jain P, el-Sherif N: Differential expression of voltage-gated $K^+$ channel genes in left ventricular remodeled myocardium after experimental myocardial infarction. Circ Res 1996; 79: 669–675.

83. Nerbonne JM, Kass RS: Molecular physiology of cardiac repolarization. Physiol Rev 2005; 85: 1205–1253.

84. Aggarwal R, Boyden PA: Diminished $Ca^{2+}$ and $Ba^{2+}$ currents in myocytes surviving in the epicardial border zone of the 5-day infarcted canine heart. Circ Res 1995; 77: 1180–1191.

85. Dun W, Baba S, Yagi T, Boyden PA: Dynamic remodeling of $K^+$ and $Ca^{2+}$ currents in cells that survived in the epicardial border zone of canine healed infarcted heart. Am J Physiol 2004; 287: H1046–H1054.

86. Neumann J, Eschenhagen T, Jones LR, Linck B, Schmitz W, Scholz H, Zimmermann N: Increased expression of cardiac phosphatases in patients with end-stage heart failure. J Mol Cell Cardiol 1997; 29: 265–272.

87. Fuller W, Parmar V, Eaton P, Bell JR, Shattock MJ: Cardiac ischemia causes inhibition of the Na/K ATPase by a labile cytosolic compound whose production is linked to oxidant stress. Cardiovasc Res 2003; 57: 1044–1051.

88. Nattel S: New ideas about atrial fibrillation 50 years on. Nature 2002; 415:219–226.

89. Van Wagoner DR, Pond AL, McCarthy PM, Trimmer JS, Nerbonne JM: Outward $K^+$ current densities and Kv1.5 expression are reduced in chronic human atrial fibrillation. Circ Res 1997; 80: 772–781.

90. Bosch RF, Zeng X, Grammer JB, Popovic CM, Kuhlkamp V: Ionic mechanisms of electrical remodelling in human atrial fibrillation. Cardiovasc Res 1999; 44: 121–131.

91. Workman AJ, Kane KA, Rankin AC: The contribution of ionic currents to changes in refractoriness of human atrial myocytes associated with chronic atrial fibrillation. Cardiovasc Res 2001 52: 226–235.

92. Wit AL, Boyden PA: Triggered activity and atrial fibrillation. Heart Rhythm 4 2007; (Suppl): S17–S23.

93. Zorn-Pauly K, Schaffer P, Pelzmann B, Lang P, Mächler H, Rigler B, Koidl B: If in left human atrium: a potential contributor to atrial ectopy. Cardiovasc Res 2004; 64: 250–259.

## Figure Legends

**Figure 1.** miRNA expression signature in the heart. (**A**) Relative levels of the top 20 most abundantly expressed miRNAs in myocardium. (**B**) Number of predicted target genes of the top 20 most abundantly expressed miRNAs in myocardium. Note that *miR-126, miR-21, miR-99* and *miR-100* are not predicted to target any genes encoding cardiac ion channels and transporters.

**Figure 2.** Predicted gene targeting of the top 20 most abundantly expressed miRNAs in myocardium. The arrows indicate repression of the genes by the connected miRNAs. The target genes are roughly divided into groups in three different colors: the genes for cardiac conduction in blue, the genes for cardiac automaticity in green, and the genes for cardiac repolarization in yellow.

**Figure 3.** Predicted gene targeting of the miRNAs deregulated in their expression in cardiac hypertrophy and congestive heart failure (CHF). The arrows in red indicate repression of the genes by the upregulated miRNAs (top row in blue) and those in blue indicate derepression of the genes by the downregulated miRNAs (bottom row in yellow). The target genes are roughly divided into groups in three different colors: the genes for cardiac conduction in blue, the genes for cardiac automaticity in green, and the genes for cardiac repolarization in yellow.

**Figure 4.** Predicted gene targeting of the miRNAs deregulated in their expression in ischemic myocardial injuries. The arrows in red indicate repression of the genes by the upregulated miRNAs (top rows in blue) and those in blue indicate derepression of the genes by the downregulated miRNAs (bottom row in yellow). The target genes are roughly divided into groups in three different colors: the genes for cardiac

conduction in blue, the genes for cardiac automaticity in green, and the genes for cardiac repolarization in yellow.

**Figure 5.** Predicted gene targeting of the miRNAs deregulated in their expression in experimental atrial fibrillation. The arrows in red indicate repression of the genes by the upregulated miRNAs (top row in blue) and those in blue indicate derepression of the genes by the downregulated miRNAs (bottom row in yellow). The target genes are roughly divided into groups in three different colors: the genes for cardiac conduction in blue, the genes for cardiac automaticity in green, and the genes for cardiac repolarization in yellow.

**Figures**

Figure 1

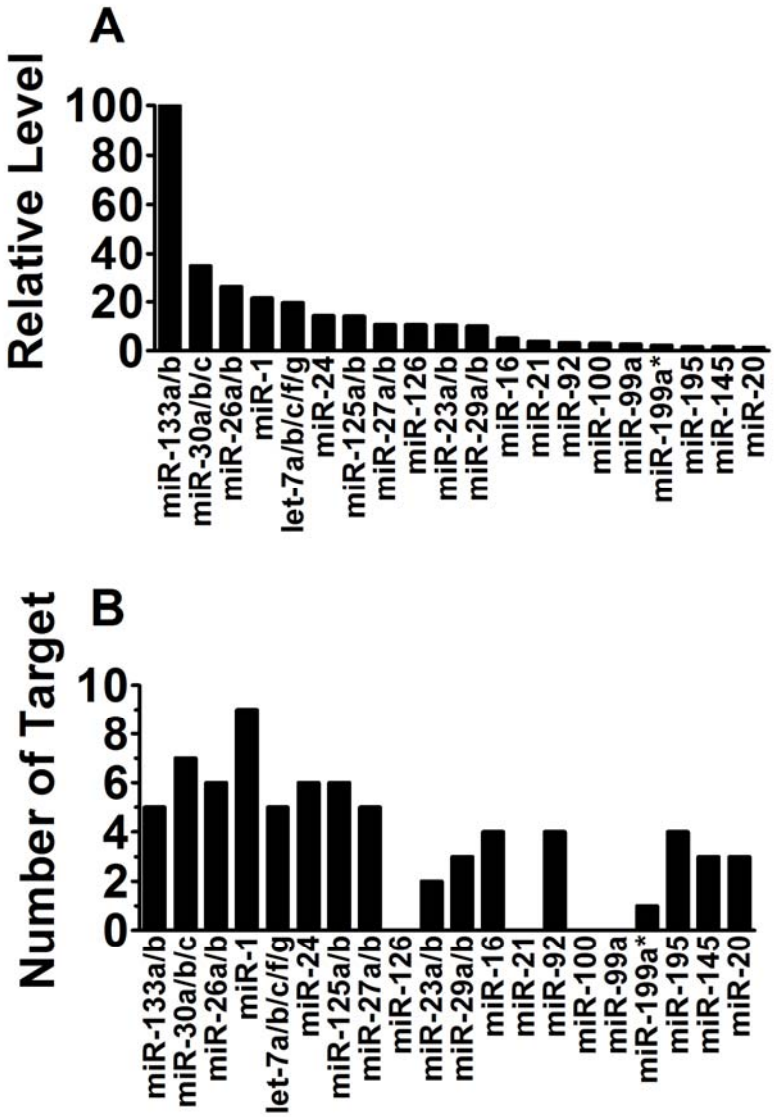

Figure 2

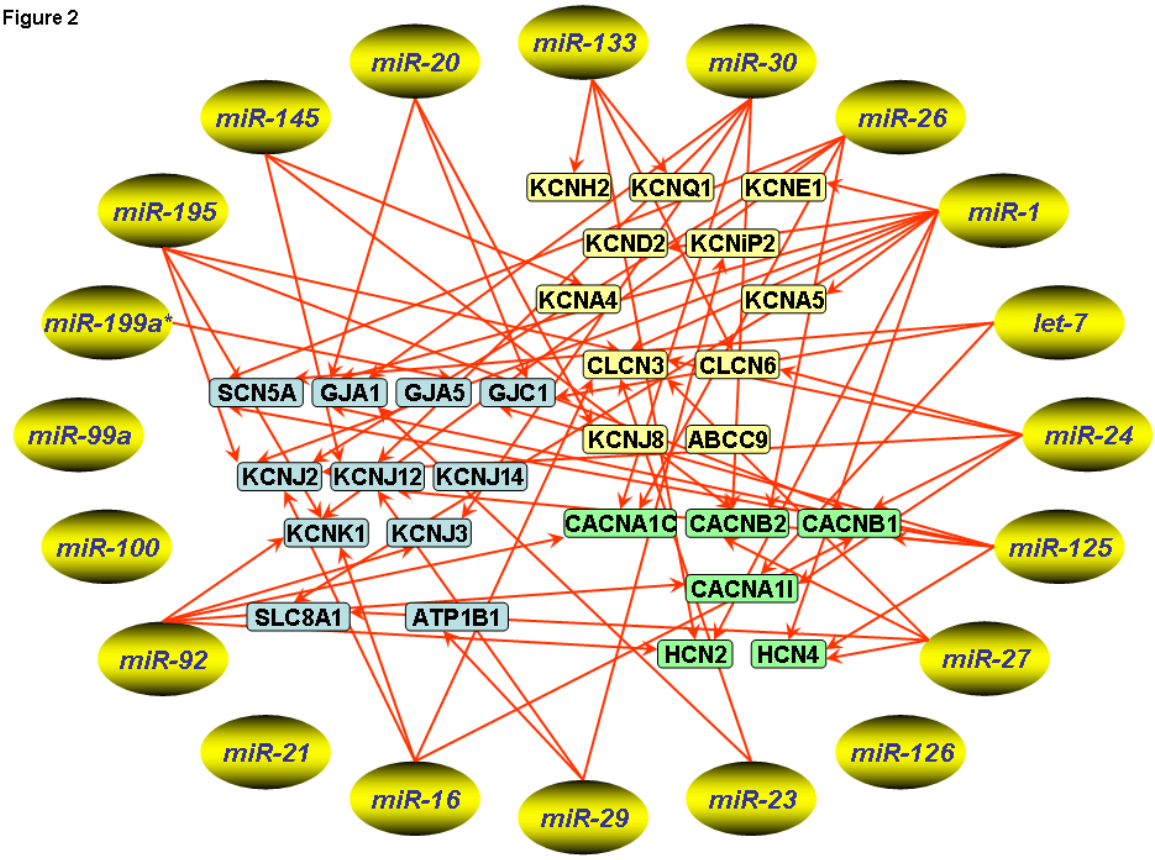
miR-133
miR-20
miR-30
miR-145
miR-26
KCNH2
KCNQ1
KCNE1
miR-195
miR-1
KCND2
KCNiP2
KCNA4
KCNA5
miR-199a*
let-7
CLCN3
CLCN6
SCN5A
GJA1
GJA5
GJC1
miR-99a
miR-24
KCNJ8
ABCC9
KCNJ2
KCNJ12
KCNJ14
CACNA1C
CACNB2
CACNB1
miR-100
KCNK1
KCNJ3
miR-125
CACNA1I
SLC8A1
ATP1B1
miR-92
HCN2
HCN4
miR-27
miR-21
miR-126
miR-16
miR-29
miR-23

Figure 3

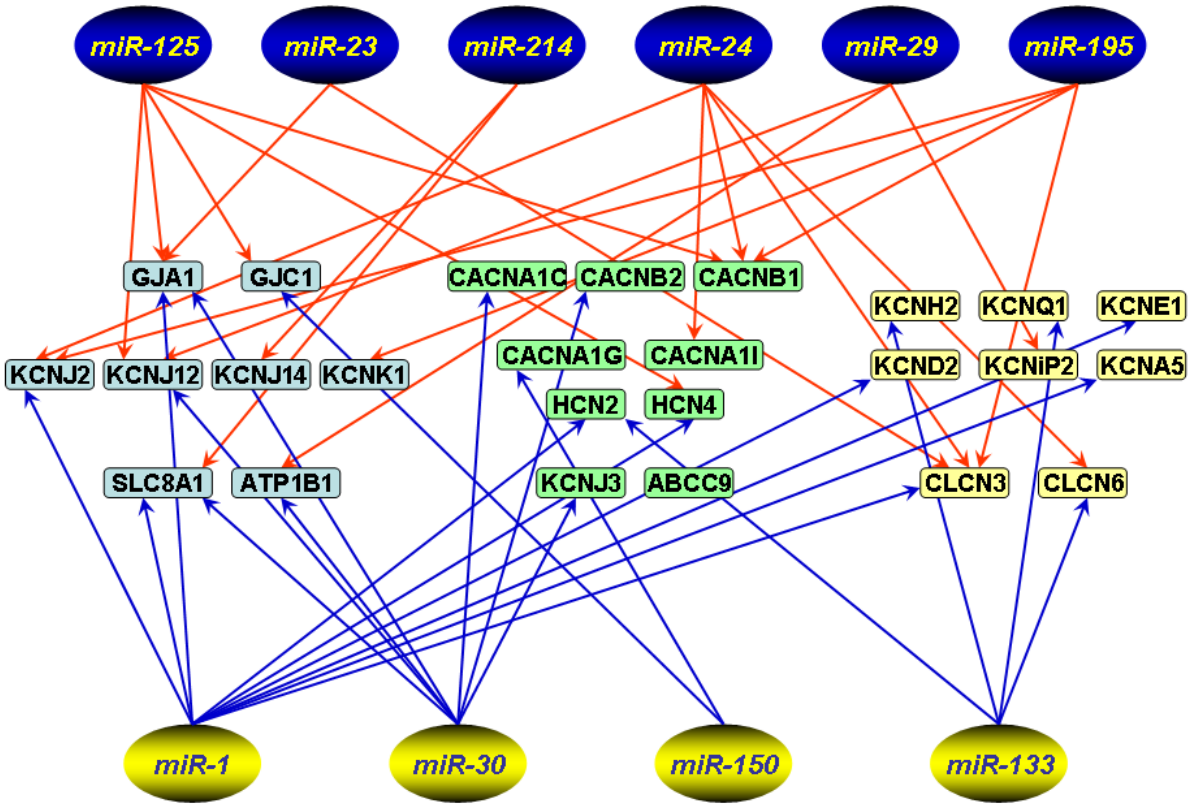
miR-125
miR-23
miR-214
miR-24
miR-29
miR-195
GJA1
GJC1
CACNA1C
CACNB2
CACNB1
KCNH2
KCNQ1
KCNE1
KCNJ2
KCNJ12
KCNJ14
KCNK1
CACNA1G
CACNA1I
KCND2
KCNiP2
KCNA5
HCN2
HCN4
SLC8A1
ATP1B1
KCNJ3
ABCC9
CLCN3
CLCN6
miR-1
miR-30
miR-150
miR-133

Figure 4

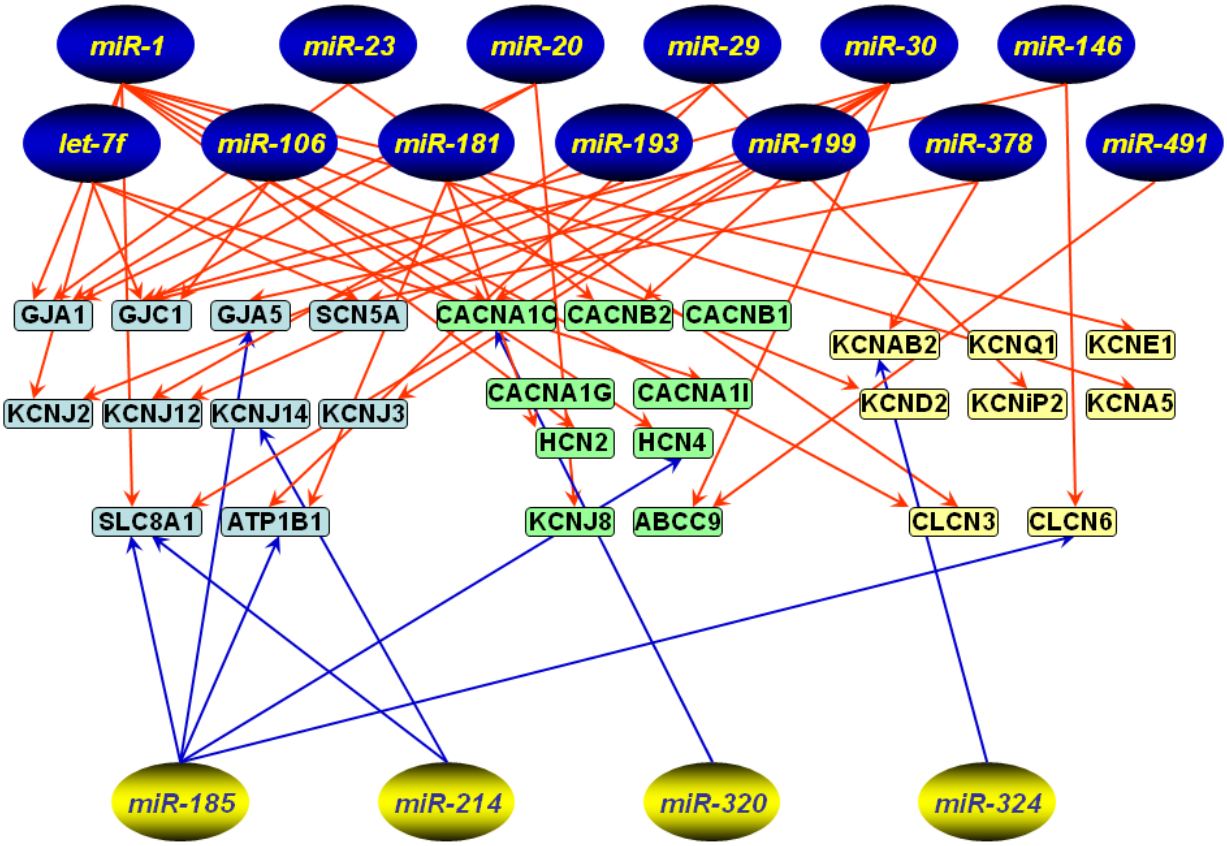
miR-1
miR-23
miR-20
miR-29
miR-30
miR-146
let-7f
miR-106
miR-181
miR-193
miR-199
miR-378
miR-491
GJA1
GJC1
GJA5
SCN5A
CACNA1C
CACNB2
CACNB1
KCNAB2
KCNQ1
KCNE1
KCNJ2
KCNJ12
KCNJ14
KCNJ3
CACNA1G
CACNA1I
KCND2
KCNiP2
KCNA5
HCN2
HCN4
SLC8A1
ATP1B1
KCNJ8
ABCC9
CLCN3
CLCN6
miR-185
miR-214
miR-320
miR-324

Figure 5

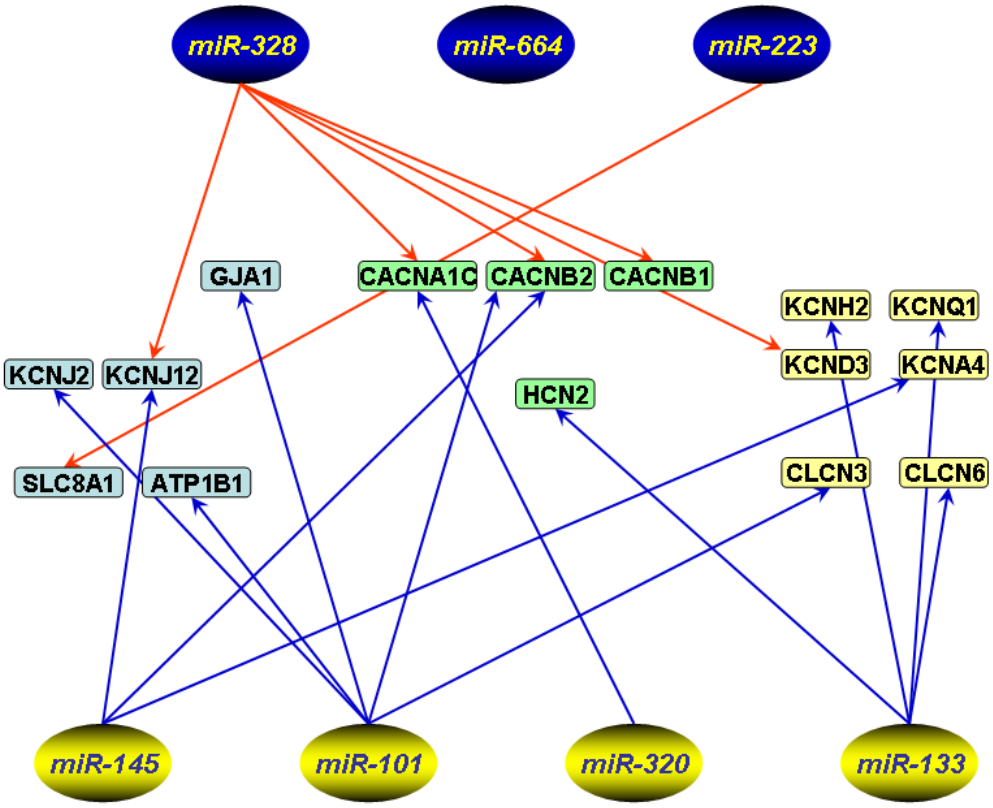
miR-328
miR-664
miR-223
GJA1
CACNA1C
CACNB2
CACNB1
KCNH2
KCNQ1
KCNJ2
KCNJ12
KCND3
KCNA4
HCN2
SLC8A1
ATP1B1
CLCN3
CLCN6
miR-145
miR-101
miR-320
miR-133

**Table 1. The genes encoding cardiac cytoplasmic ion channel proteins and electrogenic ion transporters selected for this study**

| Gene Name | IUPHAR Name | Gene ID | Description |
|---|---|---|---|
| SCN5A | Nav1.5 | ENSG00000183873 | Pore-forming α-subunit of voltage-dependent $Na^+$ channel carrying TTX-insensitive $Na^+$ current ($I_{Na}$) responsible for phase 0 membrane depolarization of a cardiac action potential thereby cardiac conduction velocity and for type 3 familial long QT syndrome (LQT3) when mutated |
| SCN4B | Navβ4 | ENSG00000105711 | β-subunit of cardiac $Na^+$ channel able to enhance α-subunit conductance and is responsible for type 10 familial long QT syndrome (LQT10) when mutated |
| | | | |
| CACNA1C | Cav1.2 | ENSG00000151067 | Pore-forming α-subunit of voltage-dependent dihyropyridine-insensitive $Ca^{2+}$ channel carrying L-type $Ca^{2+}$ current ($I_{Ca,L}$) responsible for phase 2 plateau of a cardiac action potential and excitation-contraction coupling and for type 8 familial long QT syndrome leading to Timothy's syndrome when mutated |
| CACNB1 | Cavβ1 | ENSG00000067191 | β1-subunit of $Ca^{2+}$ channel able to enhance α-subunit conductance |
| CACNB2 | Cavβ2 | ENSG00000165995 | β2-subunit of $Ca^{2+}$ channel able to enhance α-subunit conductance |
| | | | |
| CACNA1G | Cav3.1c | ENSG00000006283 | Pore-forming α-subunit of voltage-dependent $Ca^{2+}$ channel carrying T-type $Ca^{2+}$ current ($I_{Ca,T}$) contributing to pacemaker activity of sino-atrial nodal cells |

| | | | |
|---|---|---|---|
| CACNA1I | Cav3.3 | ENSG00000100346 | Pore-forming α-subunit of voltage-dependent $Ca^{2+}$ channel carrying T-type $Ca^{2+}$ current ($I_{Ca,T}$) contributing to pacemaker activity of sino-atrial nodal cells |
| | | | |
| KCNJ2 | Kir2.1 | ENSG00000123700 | Pore-forming α-subunit and the major molecular component of inward rectifier $K^+$ channel carrying inward rectifier $K^+$ current ($I_{K1}$) responsible for setting the membrane potential and late phase repolarization of cardiac cells. Mutation of KCNJ2 leads to type 7 familial long QT syndrome (LQT7) and Andersen-Tawil syndrome. |
| KCNJ12 | Kir2.2 | ENSG00000184185 | Pore-forming α-subunit of inward rectifier $K^+$ channel carrying inward rectifier $K^+$ current ($I_{K1}$) |
| KCNJ4 | Kir2.3 | ENSG00000168135 | Pore-forming α-subunit of inward rectifier $K^+$ channel carrying inward rectifier $K^+$ current ($I_{K1}$) |
| KCNJ14 | Kir2.4 | ENSG00000182324 | Pore-forming α-subunit of inward rectifier $K^+$ channel carrying inward rectifier $K^+$ current ($I_{K1}$) |
| KCNJ3 | Kir3.1 | ENSG00000162989 | Pore-forming α-subunit of acetylcholine-activated inward rectifier $K^+$ channel carrying ACh-sensitive $K^+$ current ($I_{KACh}$) |
| KCNJ5 | Kir3.4 | ENSG00000120457 | Pore-forming α-subunit of acetylcholine-activated inward rectifier $K^+$ channel carrying ACh-activated $K^+$ current ($I_{KACh}$), mainly expressed in atrial cells. It is an atrium-specific ion current |
| KCNJ8 | Kir6.1 | ENSG00000121361 | Pore-forming α-subunit of ATP-sensitive $K^+$ channel carrying ATP-sensitive, inward rectifier $K^+$ current ($I_{KATP}$) |
| ABCC9 | SUR2 | ENSG00000069431 | Sulfonylurea receptor β-subunit of ATP-sensitive $K^+$ channel |
| KCNK1 | TWIK1 | ENSG00000135750 | Pore-forming α-subunit of two-pore inward rectifier $K^+$ channel |

| | | | |
|---|---|---|---|
| KCNA5 | Kv1.5 | ENSG00000130037 | Pore-forming α-subunit of voltage-gated $K^+$ channel carrying ultrarapid delayed rectifier $K^+$ current ($I_{Kur}$), mainly expressed in human heart. It is an atrium-specific ion current |
| KCNA4 | Kv1.4 | ENSG00000182255 | Pore-forming α-subunit of voltage-gated $K^+$ channel carrying transient outward $K^+$ current ($I_{to1}$), mainly expressed in rabbit heart |
| KCND2 | Kv4.2 | ENSG00000184408 | Pore-forming α-subunit of voltage-gated $K^+$ channel carrying transient outward $K^+$ current ($I_{to1}$), mainly expressed in rodent hearts |
| KCND3 | Kv4.3 | ENSG00000171385 | Pore-forming α-subunit of voltage-gated $K^+$ channel carrying transient outward $K^+$ current ($I_{to1}$), mainly expressed in human heart. Being responsible for phase 1 rapid repolarization and the "spike and dome" morphology of cardiac action potentials |
| KCNH2 | HERG | ENSG00000055118 | Pore-forming α-subunit of voltage-gated, *ether-a-go-go*-related $K^+$ channel carrying rapid delayed rectifier $K^+$ current ($I_{Kr}$) responsible for phase 3 repolarization and drug-induced long QT syndrome and type 2 familial long QT syndrome (LQT2) when mutated |
| KCNQ1 | KvLQT1 | ENSG00000053918 | Pore-forming α-subunit of voltage-gated $K^+$ channel carrying slow delayed rectifier $K^+$ current ($I_{Ks}$) responsible for phase 3 repolarization and drug-induced long QT syndrome and type 1 familial long QT syndrome (LQT1) when mutated |
| KCHIP2 | KChIP2 | ENSG00000120049 | β-subunit of voltage-gated $K^+$ channel able to interact with Kv4.2 and Kv4.3 α-subunits to modulate transient outward $K^+$ current ($I_{to1}$) |

| | | | |
|---|---|---|---|
| KCNE1 | minK | ENSG00000180509 | β-subunit of voltage-gated $K^+$ channel carrying slow delayed rectifier $K^+$ current ($I_{Ks}$) responsible for phase 3 repolarization and drug-induced long QT syndrome and type 5 familial long QT syndrome (LQT5) when mutated |
| KCNE2 | MIRP1 | ENSG00000159197 | β-subunit of voltage-gated, *ether-a-go-go*-related $K^+$ channel carrying rapid delayed rectifier $K^+$ current ($I_{Kr}$) responsible for phase 3 repolarization and drug-induced long QT syndrome and type 6 familial long QT syndrome (LQT6) when mutated |
| KCNAB2 | Kvβ2 | ENSG00000069424 | β-subunit of voltage-gated $K^+$ channel able to co-assemble with Kv1.4 α-subunit carrying transient outward $K^+$ current ($I_{to1}$) |
| | | | |
| CLCN2 | CIC2 | ENSG00000114859 | A molecular component of $Cl^-$ channel thought to play a role in sinus nodal cells |
| CLCN3 | CIC3 | ENSG00000109572 | A molecular component of volume-sensitive outwardly rectifying $Cl^-$ channel |
| CLCN6 | CIC6 | ENSG00000011021 | A molecular component of volume-sensitive outwardly rectifying $Cl^-$ channel |
| | | | |
| GJA1 | Cx43 | ENSG00000143140 | Connexin43 gap junction channel protein mainly expressed in ventricular cells, responsible for intercellular conduction of excitation and the coordinated depolarization of cardiac muscle |
| GJA5 | Cx40 | ENSG00000152661 | Connexin40 gap junction channel protein mainly expressed in atrial cells, responsible for intercellular conduction of excitation and the coordinated depolarization of cardiac muscle |

| | | | |
|---|---|---|---|
| GJC1 | Cx45 | ENSG00000182963 | Connexin45 gap junction channel protein mainly expressed in atrio-ventricular nodal cells, responsible for intercellular conduction of excitation |
| | | | |
| HCN2 | HCN2 | ENSG00000099822 | $K^+/Na^+$ hyperpolarization-activated cyclic nucleotide-gated channel 2, the dominant isoform for ventricular funny current ($I_f$), responsible for abnormal automaticity of the heart |
| HCN4 | HCN4 | ENSG00000138622 | $K^+/Na^+$ hyperpolarization-activated cyclic nucleotide-gated channel 4, the major molecular component for sinus funny current ($I_f$), responsible for phase 4 diastolic spontaneous membrane depolarization and pacemaker activity |
| | | | |
| TRPC4 | TRPC4 | ENSG00000133107 | Member of the class C (canonical) transient receptor potential channels, activated by phospholipase C stimulation. Its expression is downregulated in cardiac hypertrophy |
| TRPM4 | TRPM4 | ENSG00000130529 | Member of the class M (melastatin) transient receptor potential channels, activated by intracellular calcium. Its expression is downregulated in cardiac hypertrophy |
| | | | |
| SLC8A1 | NCX1 | ENSG00000183023 | $Na^+/Ca^{2+}$ exchanger, an antiporter membrane protein which removes $Ca^{2+}$ from cells. The NCX removes a single $Ca^{2+}$ in exchange for the import of three $Na^+$, generating a net inward current believed to account for delayed after depolarization |
| | | | |

| | | | |
|---|---|---|---|
| ATP1A3 | Na/K ATPase α3 | ENSG00000105409 | The large catalytic α-subunit of the $Na^+/K^+$ pump, pumping three sodium ions out of the cell for every two potassium ions pumped in after each single action potential for establishing and maintaining the normal electrochemical gradients of $Na^+$ and $K^+$ across the plasma membrane |
| ATP1B1 | Na/K ATPase β1 | ENSG00000143153 | The smaller glycoprotein β-subunit of the $Na^+/K^+$ pump |

**Supplementary Figure 1**

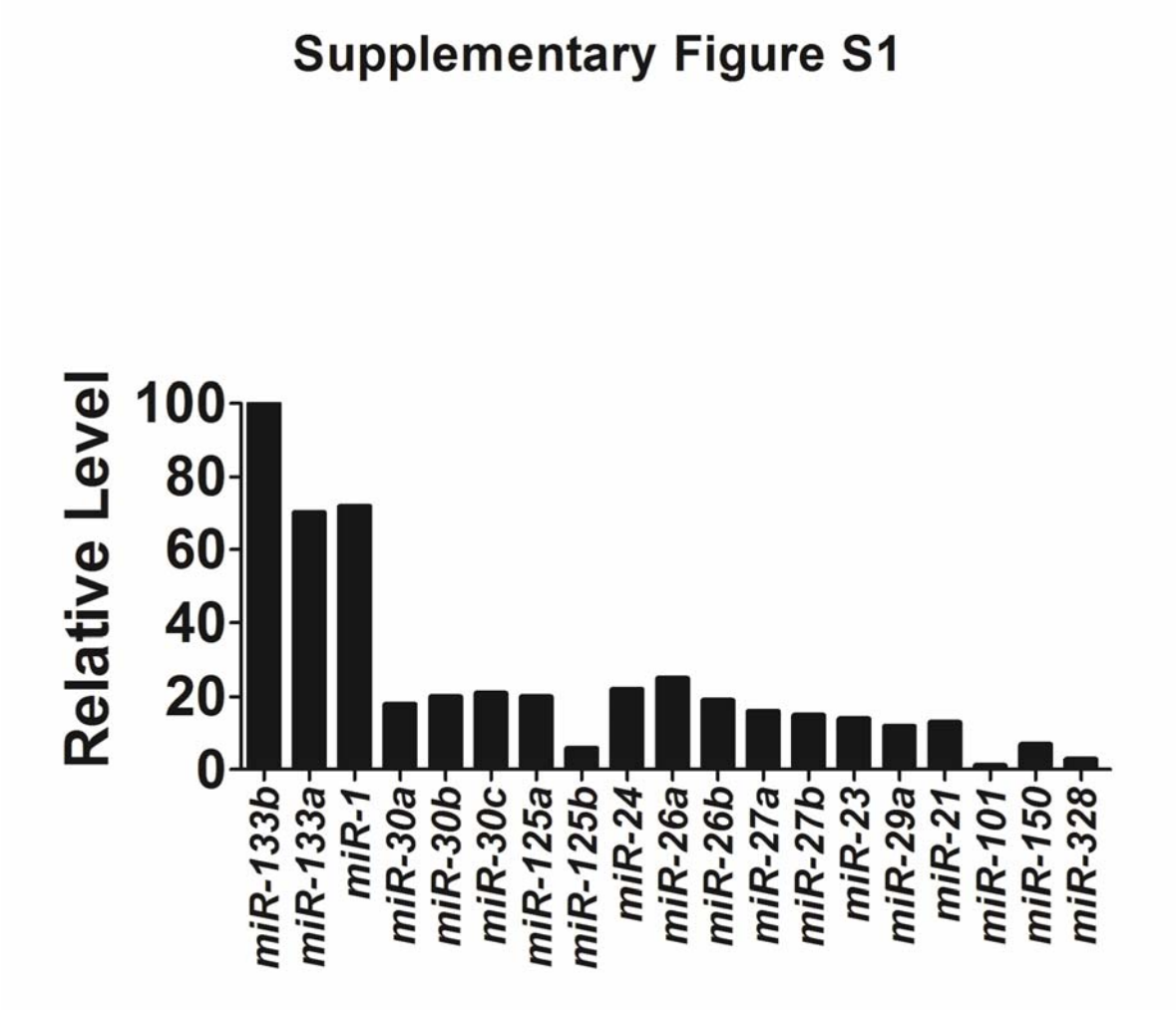

**Supplementary Figure 2**

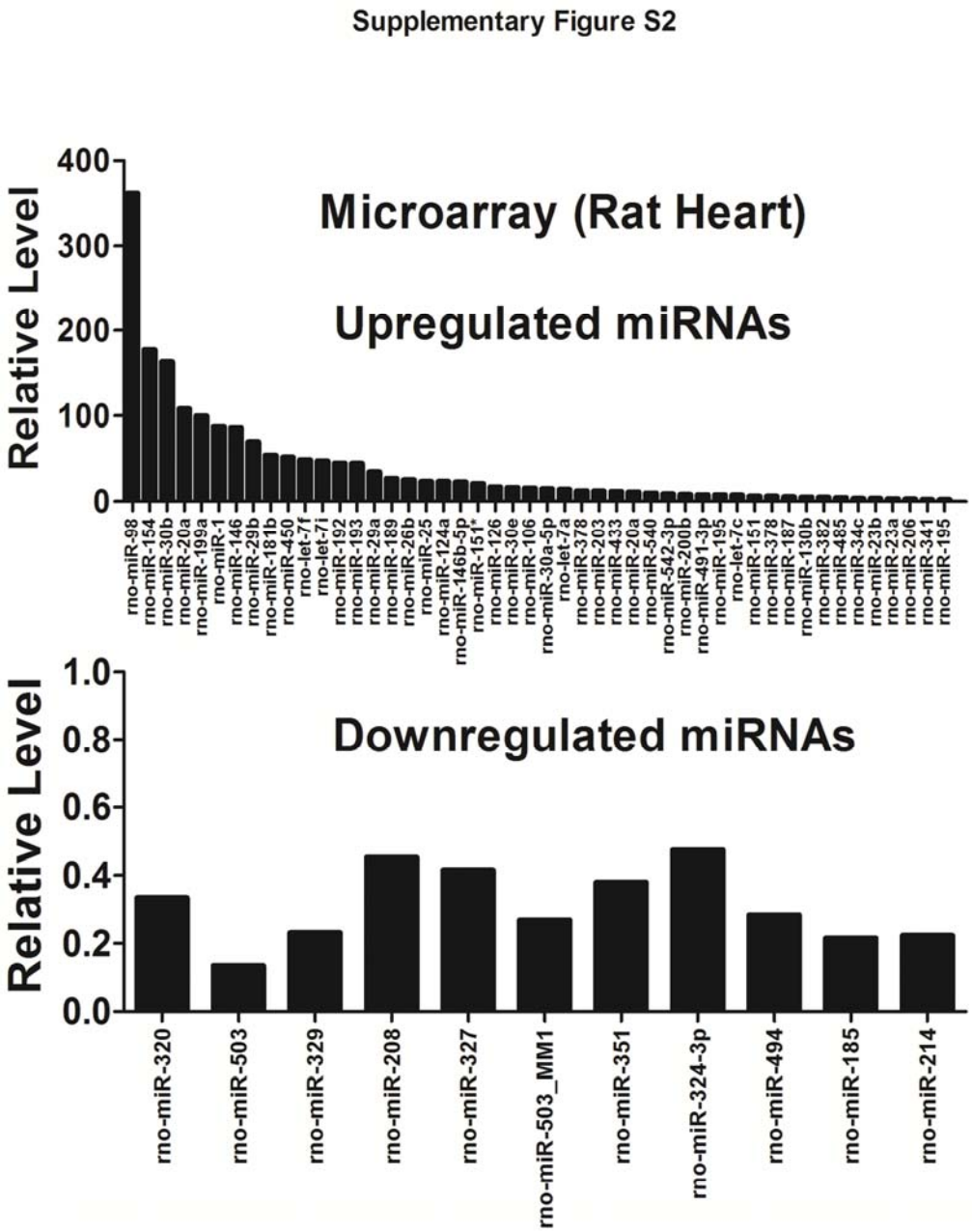

# CHAPTER 3. The Control of Adverse Electrical Remodeling by MiRNAs in AF

As noted in sections 1.3.1 and 1.4.4 of the Introduction, upregulation of $I_{K1}$ is a key component of the adverse electrical remodeling underlying AF. Although it has been suggested that the AF-induced $I_{K1}$ enhancement is likely due to the increased expression of the underlying channel subunit Kir2.1 at protein and mRNA levels, the precise molecular mechanisms underlying these expression changes are still poorly understood. Given that miRNAs have emerged as an important player in a variety of cardiac pathological conditions and a novel regulator for ion channels at post-transcriptional level, the present study was designed to study the role of miRNAs in this AF-related ionic remodeling process.

This work is currently in revision for ***Journal of Clinical Investigation*.**

**Luo X***, Pan Z*, Shan H*, Xiao J, Sun X, Wang N, Lin H, Xiao L, Maguy A, Qi X-Y, Li Y, Gao X, Dong D, Zhang Y, Bai Y, Ai J, Sun L, Lu H, Luo X, Wang Z, Lu Y, Yang B, Nattel S. MicroRNA-26 governs profibrillatory inward-rectifier potassium current changes in atrial fibrillation. ***J. Clin. Invest.*** (accepted for publication, in press).

# 3.1 MicroRNA-26 Governs Profibrillatory Inward-Rectifier Potassium Current Changes in Atrial Fibrillation

**Xiaobin Luo,[1,2,6,§] Zhenwei Pan,[4,§] Hongli Shan,[4,§] Jiening Xiao,[1] Xuelin Sun,[4] Ning Wang,[6] Huixian Lin,[1] Ling Xiao,[1,2,3] Ange Maguy,[1] Xiao-Yan Qi,[1] Yue Li,[7] Xu Gao,[5] Deli Dong,[4] Yong Zhang,[4] Yunlong Bai,[6] Jing Ai,[4] Lihua Sun,[4] Hang Lu,[6] Xiao-Yan Luo,[1] Zhiguo Wang,[4,6] Yanjie Lu,[4,6] Baofeng Yang,[4,6,*] Stanley Nattel[1,2,3,*]**

From the [1]Research Center, Montreal Heart Institute, Montreal, PQ H1T 1C8 Canada; [2]Department of Medicine, Université de Montréal, Montreal, PQ H3C 3J7, Canada; [3]Department of Pharmacology and Therapeutics, McGill University; and [4]Department of Pharmacology (the State-Province Key Laboratories of Biomedicine-Pharmaceutics of China); [5]Departments of Biochemistry; [6]Cardiovascular Research Institute (the Key Laboratory of Cardiovascular Research, Ministry of Education of China) and [7]First Affiliated Hospital, Harbin Medical University, Harbin, Heilongjiang 150081, P. R. China

**Running Title:** miR-26, *KCNJ2* regulation and AF

**Conflict of interest:** The authors have declared that no conflict of interest exists.

[§]Authors with equal contributions, to be considered co-first authors.

*Correspondence should be addressed to Stanley Nattel, 5000 Belanger St, Montreal, PQ H1T 1C8, Canada. Tel. 514-376-3330, Fax: 514-376-1355; or to Baofeng Yang, Harbin Medical University, Harbin, Heilongjiang 150086, China.

**Abstract**

Rationale: Atrial fibrillation (AF) is a highly-prevalent arrhythmia with pronounced morbidity and mortality. Inward-rectifier $K^+$-current ($I_{K1}$) is believed to be an important controller of reentrant-spiral dynamics, as well as a major component of AF-related electrical remodeling. MicroRNA (miR)-26 is predicted to target the *KCNJ2*-gene encoding $I_{K1}$. Objectives: To study the potential role of miR-26 in AF. Findings: MiR-26 was downregulated in atrial samples of AF animals and patients, accompanied by upregulation of KCNJ2-protein and $I_{K1}$. Mir-26 overexpression suppressed, while miR-26 knockdown, inhibition or binding-site mutation enhanced, expression of KCNJ2/$I_{K1}$, establishing *KCNJ2* as a target for miR-26. Knockdown of endogenous miR-26 by LNA-modified antisense promoted AF in mice, whereas adenoviral-transfer of miR-26 reduced AF-vulnerability. Anti-AF efficacy was abolished when miR-Masks that bind KCNJ2-specific target-sites were employed to eliminate miR-26's repressive effect on *KCNJ2* without altering other target-genes. When a miR-Mimic specifically targeting *KCNJ2* was co-injected into mice to prevent Kir2.1/$I_{K1}$ increases, LNA-antimiR-26 no longer promoted AF. NFAT, a known actor in AF-associated remodeling, was found to negatively regulate miR-26 transcription. Conclusions: MiR-26 controls the expression of the *KCNJ2*-gene, and its downregulation in AF may play an important role in AF-promotion. MiR-26 replacement may be a potentially-valuable novel antiarrhythmic approach.

Recent studies have uncovered an important role of microRNAs (miRNAs) in regulating cardiac excitability and arrhythmogenesis in various cardiac diseases, including myocardial infarction (1), cardiac hypertrophy (2), diabetic cardiomyopathy (3), atrial fibrillation (4,5), and other cardiac conditions (6-8). These studies have primarily focused on the muscle-specific miRNAs miR-1 and miR-133, with the exception of miR-328, which also contributes to shaping cardiac electrophysiology (5).

Atrial fibrillation (AF) is a highly prevalent condition associated with pronounced morbidity and mortality which can cause or exacerbate heart failure and is an important risk factor for stroke (9). AF is characterized by atrial electrical remodeling (mediated predominantly by ion-channel alterations), which favors arrhythmia recurrence and maintenance (9,10). A prominent feature of the electrical remodeling associated with AF is abbreviation of the effective refractory period (ERP) favoring reentry, primarily due to shortening of atrial action potential duration (APD) (9, 10). Numerous studies have demonstrated that increased inward-rectifier $K^+$ current ($I_{K1}$), along with increased expression of the principal underlying subunit *KCNJ2* mRNA and its encoded Kir2.1 protein, is a prominent feature of AF-related atrial electrical remodeling (10-17). $I_{K1}$ is the key $K^+$-current responsible for setting the resting membrane potential, controlling cardiac excitability and modulating late-phase repolarization and APD in cardiac cells. Augmentation of inward-rectifier $K^+$-currents like $I_{K1}$, which shortens atrial APD and stabilizes rotor-dynamics, is an important factor favoring AF-maintenance (18, 19). Furthermore, $I_{K1}$ is a central regulator of cardiac excitability and arrhythmogenesis and a promising target for new antiarrhythmic approaches (20).

The mechanism of $I_{K1}$-dysregulation in AF is poorly understood. We performed a computational analysis of microRNAs altered in AF to identify microRNA-candidates for

$I_{K1}$ dysregulation (See Online Supplement), which suggested that miR-26 has the potential to repress *KCNJ2*/Kir2.1/$I_{K1}$. MiR-26 belongs to a cardiac-enriched (21), but non-cardiac-specific, miRNA family composed of three members, miR-26a-1, miR-26a-2 and miR-26b, sharing identical seed sequences (2-8 nucleotides at the 5'-end determining gene-targeting) (22) and with only two nucleotide differences between miR-26a and miR-26b (Online Figure 1), suggesting that these miRNAs likely have the same set of target genes. MiR-26 sequences are highly conserved across species (Online Figure 1). The 3' untranslated region (3'UTR) of *KCNJ2* mRNA contains two binding sites for miR-26a and miR-26b (Online Figure 2). We therefore hypothesized that miR-26-family miRNAs participate in AF pathophysiology by regulating the expression of *KCNJ2*/Kir2.1/$I_{K1}$. Both miR-26a and miR-26b are downregulated in hypertrophied hearts (23) and aortic-valve disease (24). However, the potential roles of miR-26 in cardiomyocyte function and cardiac pathophysiology have not been studied.

## RESULTS

### Dysregulation of miR-26 family miRNAs and KCNJ2/Kir2.1 in atrial fibrillation

In an effort to explore the roles of miRNAs in AF, we found that miR-26 family members were significantly downregulated (>50%) in a canine AF-model (miR-26a, Figure 1A) and in AF-patients (miR-26a and miR-26b, Figure 1B; see Online Table 1 for patient information), indicating possible involvement in AF pathophysiology. The level of miR-26a is approximately 4 times higher than that of miR-26b in our canine and human preparations (Online Figure 1). In contrast, miR-1 and miR-133 levels were unaltered in AF-samples (Figures 1A and B). Moreover, in line with previous studies (10-17), we found Kir2.1 protein as well as *KCNJ2* mRNA to be upregulated in both AF dogs and patients (Figures 1C-F). These results are consistent with the notion that miR-26 might contribute to *KCNJ2*-dysregulation in AF, a possibility that we proceeded to test directly.

### Validation of KCNJ2 as a target for miR-26

Based on computational analyses revealing two miR-26 binding sites in the 3'untranslated region (3'UTR) of *KCNJ2* (Online Figure 2), we conducted Western blot analysis and luciferase reporter gene assays to experimentally clarify whether *KCNJ2* is in fact a target for miR-26. As shown in Figure 2A, transfection of miR-26a (100 nM) into H9c2 rat ventricular cells produced marked downregulation of Kir2.1 protein compared to sham-treated control (Ctl) cells. This repression was efficiently rescued by suppressing expression of miR-26 with its antisense inhibitor AMO-26a (10 nM). More strikingly, upregulation of Kir2.1 protein was consistently seen with AMO-26a or AMO-26b alone to knock down endogenous miR-26 and mimic the effect of AF (Figure 2B), indicating the relief of tonic repression of Kir2.1 by miR-26. *KCNJ2* mRNA expression was also

decreased by miR-26a, reflecting mRNA-destabilization (Figure 2C). We further went on to verify the effects of miR-26 at the functional level. $I_{K1}$ was recorded in neonatal rat ventricular cells using whole-cell patch-clamp techniques. As shown in Figure 2D, the cells transfected with miR-26 had smaller $I_{K1}$ density than control cells, and the difference was eliminated by co-transfection with AMO-26a. Application of AMO-26a alone increased $I_{K1}$ density. The regulation of the *KCNJ2*-gene by miR-26 was confirmed by luciferase assay, which indicated that both of the binding sites for miR-26 responded similarly to miR-26a expression-changes (Figure 2E). Mutation of the binding sites (Online Figure 2a) abolished the suppressant effect of miR-26 on the *KCNJ2* target-gene in luciferase assay (Figure 2E), exposing a small stimulatory effect. The specificity of miR-26 action was indicated by an absence of change with the negative control miRNA (miR-NC) and AMO (AMO-NC) (Online Figure 2b). The efficacy of miR-26a, AMO-26a or AMO-26b transfer in altering miR-26a and miR-26b expression was verified by real-time RT-PCR experiments (Figure 2F).

In subsequent control experiments, we found no effects of miR-26 on the protein levels of other $K^+$ subunits such as HERG (encoded by *KCNH2*) for rapid delayed rectifier $K^+$-current, KvLQT1 (encoded by *KCNQ1*) for slow delayed rectifier $K^+$-current, and Kv4.3 (encoded by *KCND3*) for transient outward $K^+$-current (Online Figure 3). These results are consistent with computational predictions excluding these genes as targets for miR-26 and indicate that the effect of miR-26 on *KCNJ2*/Kir2.1/$I_{K1}$ is target-specific.

**Regulation of AF-vulnerability by miR-26**

Upregulation of Kir2.1 due to downregulation of miR-26 is expected to promote AF. To test this notion, we injected locked nucleic acid-modified AMO-26 (LNA-antimiR-26;

Online Figure 4) into mice through tail veins to knock down endogenous miR-26 (mimicking the AF effect), with an approach that is documented to be highly efficient in knocking down targeted miRNAs with long-lasting efficacy under in vivo conditions (25-27). This type of LNA-modified molecule has been shown by numerous studies to have improved cellular uptake and stability, as well as target affinity and specificity. Attempts to induce AF by intracardiac pacing were then made. AF vulnerability was substantially enhanced in the mice treated with LNA-antimiR-26, as indicated by an increased proportion of animals with successful induction of AF by electrical stimulation and prolonged AF duration once induced (Figure 3A), as compared with sham-operated, age-matched wild-type (WT) mice. In contrast, with miR-26 overexpression by tail vein injection of miR-26a-expressing adenovirus (Adv-miR-26a; Online Figure 5), AF incidence was significantly reduced (Figure 3A). Mean AF duration also decreased, albeit without a statistically-significant difference from WT, likely because of the very small number of miR-26 overexpressing mice that showed quantifiable AF (n=2; Figure 3A). (Please note that for clarity of display, data for AF incidence and duration for relevant corresponding groups are shown as separate sets in Figures 3 and 4; however, all statistical comparisons were performed simultaneously for all groups, as shown in Online Figure 6). Effective cellular uptake of Adv-miR-26a was verified (Online Figure 7). Whole-cell patch-clamp recordings confirmed increased $I_{K1}$ density in atrial cells after LNA-antimiR-26a treatment and the opposite effect was seen after Adv-miR-26a treatment (Figure 3B). Corresponding effects of LNA-antimiR-26a and Adv-miR-26a on Kir2.1 protein level were confirmed by Western blot analysis (Online Figures 8A and B). The mismatched (MM)-LNA-antimiR-26 (Online Figure 4) failed to produce the changes described above, as did the adenovirus carrying the miR-26a-free vector (Online Figure 5). qPCR confirmed the downregulation

of both miR-26a and miR-26b in atrial samples from the mice injected with LNA-antimiR-26a, as well as overexpression of miR-26a in the animals infected by Adv-miR-26a (Figure 3C). Neither miR-26a upregulation with Adv-miR-26a nor downregulation with LNA-antimiR-26a altered cardiac structure or function as determined echocardiographically (Online Table 2). Of the ECG-intervals, miR-26a manipulation affected only the QT-interval, with forced miR-26a upregulation (which downregulated KCNJ2) increasing QT-interval and miR-26a downregulation decreasing QT-interval (Online Table 3).

While the above results suggested a significant role for miR-26 in controlling AF initiation and maintenance in mice, whether the effects are attributable specifically to targeting of *KCNJ2*/Kir2.1/$I_{K1}$ remained to be determined. To shed light on this issue, we conducted the following two types of experiments. First, we wanted to see if knockdown of miR-26 is still able to promote AF if Kir2.1 upregulation resulting from miR-26 downregulation is prevented by using the miRNA mimic (miR-Mimic) techniques developed in previous work (28) to specifically retain miR-26 downregulation of Kir2.1. We designed a miR-Mimic to specifically target the 3'UTR of *KCNJ2* without interacting with potential miR-26 target sites of any other transcripts of known function (Online Figure 9), thus mimicking the effect of miR-26 on *KCNJ2* without altering other targets. We began by co-injecting LNA-antimiR-26 and LNA-miR-Mimic into mice and assessed changes in vulnerability to AF. Whereas LNA-antimiR-26 enhanced AF incidence and duration relative to WT control-animals, this effect was eliminated by co-injection with LNA-miR-Mimic (Figure 4A). The ability of the miR-Mimic to prevent the Kir2.1-expression enhancement caused by LNA-antimiR-26 was confirmed by Western blot analysis showing reductions of atrial Kir2.1 protein levels to WT levels (Figure 4B). The mismatched LNA-miR-Mimic (LNA-MM-miR-Mimic) failed to alter the arrhythmia-

promoting or Kir2.1 protein-upregulating effects of LNA-antimiR-26. Second, we tested directly whether overexpression of miR-26 is still able to suppress AF if its repressive effect on *KCNJ2* is specifically prevented, while its inhibitory effects on other target genes are maintained. To achieve this goal, we used the miRNA-masking oligodeoxynucleotide (miR-Mask) strategy, or target-protection approach, that has been developed to produce target gene-specific protection against a miRNA (28). Two miR-Masks (Online Figure 9) were designed to be fully complementary to the two binding sites for miR-26 at the 3'UTR of *KCNJ2* without binding to any other functionally-identified targets, and were LNA-modified for greater in vivo efficacy. These miR-Masks are composed of single-stranded DNA, which is unable to incorporate into the RNA-induced silencing complex (RISC) that is essential for miRNA action. Thus, the miR-Masks bind specifically and tightly to the miR-26 binding-sequence of *KCNJ2* (preventing miR-26 binding) but do not bind to other miR-26 targets, and do not mimic miR-26 effects on *KCNJ2* translation or mRNA stability. Consequently, the miR-Masks prevent the effect of miR-26 on *KCNJ2* without preventing effects on other miR-26 targets. As shown in Figure 4C, in mice pretreated with the LNA-miR-Masks via tail vein injection, Adv-miR-26 failed to protect against AF induction and maintenance, in contrast to the clear protection produced by Adv-miR-26 in non-pretreated mice. Moreover, administration of the LNA-miR-Masks alone increased AF inducibility and maintenance (Figure 4C), indicating that endogenous background miR-26 expression offers significant protection against AF. The ability of the LNA-miR-Masks to prevent the repressive effect of miR-26 on Kir2.1 was verified in mice treated with the construct together with Adv-miR-26 (Figure 4D).

Figure 4 shows the ability of miR-Mimic and miR-Mask to counteract the effects of antimiR-26a and Adv-miR-26a respectively. The ability of the LNA-miR-Mimic alone

(Figure 5A) to downregulate, and the LNA-miR-Masks alone (Figure 5B) to upregulate, atrial Kir2.1 protein level in mice were also verified. Further control experiments were conducted to confirm biologically the gene-specificity of LNA-miR-Mimic and LNA-miR-Masks on *KCNJ2*, by verifying the lack of action on other miR-26 targets predicted bioinformatically not to interact (as described in Online Methods and Online Figure 9 legend). First, administration of LNA-miR-Mimic (Figures 5C and D) showed no effects on the expression of protein-products of two previously-validated target genes of miR-26, Cyclin D2 and Cyclin E2 (29). Second, in contrast to Kir2.1, the repressive effects of Adv-miR-26a on Cyclin D2 and Cyclin E2 protein-expression (Online Figures 8C and D) were not affected by co-application of the LNA-miR-Masks (Figures 5E and F), in agreement with the absence of recognition sites for the LNA-miR-Masks on these two genes.

**Potential mechanism of miR-26 downregulation in AF**

Having established the role of miR-26 in controlling AF through targeting *KCNJ2*, we went on to elucidate potential molecular mechanisms underlying the dysregulation of miR-26 in AF. We suspected that the three members of the miR-26 family, miR-26a-1, miR-26a-2 and miR-26b, might be transcriptionally regulated in man by a common transcription factor, since both miR-26a and miR-26b were significantly downregulated in AF (Figure 1B). Computational analysis using *MatInspector* V2.2 revealed a common feature of the 5'-flanking regions of the human host genes for the miR-26 family members: they all contain a cluster of putative *cis*-acting elements for NFAT (nuclear factor of activated T-cells) within 5 kb upstream of the transcriptional start sites across different species (Figure 6A; Online Table 4). Intriguingly, enhanced NFAT activity has been frequently implicated in AF promotion and is believed to couple rapid atrial activity to atrial remodeling via $Ca^{2+}$-

sensitive signaling through calcineurin (30-32). We therefore explored the role of NFAT in regulating expression of miR-26a/b.

We first identified the transcription start sites (TSSs) of the host genes using 5'RACE techniques: CtdspI for miR-26a-1, Ctdsp2 for miR-26a-2, and Cdtsp1 for miR-26b (Online Figures 10a-d). We then subcloned the promoter fragments spanning the putative NFAT binding sites upstream of the TSSs (Online Figures 10b-d) into pGL3 luciferase vector and conducted luciferase assays to assess the effects of a decoy oligodeoxyribonucleotide that contains the ideal binding site for NFAT (dODN-NFAT; for sequence, see Online Figure 11) to sequester NFAT and block its function, as well as to study the effects of siRNAs targeting NFATc3 and NFATc4 to knock down NFAT expression (Online Figure 12) and to analyze the actions of the cell-permeable NFAT inhibitor INCA6. As depicted in Figure 6B, dODN-NFAT, NFAT-siRNAs or INCA6 robustly increased luciferase activity of the miR-26 host-gene promoter constructs. Next, we evaluated the effects of INCA6 on the expression levels of miR-26a and miR-26b in H9c2 cells. As shown in Figure 6C, 24-hr incubation of cells with INCA6 produced concentration-dependent increases in both miR-26a and miR-26b expression. Similar to INCA6, transfection of H9c2 cells with dODN-NFAT or NFAT-siRNAs caused around 2-fold upregulation of both miR-26a and miR-26b (Figure 6C). As expected, the host genes demonstrated parallel changes in their expression (Figure 6D). In contrast to miR-26, miR-1 expression, as a negative control, was not significantly affected by dODN-NFAT, siRNAs and INCA6 (Online Figure 13). These results indicate that NFAT negatively regulates transcription of the miR-26 family members. Negative-control scrambled dODN and siRNA did not affect miR-26 promoter activity or the expression level of miR-26 (Figures 6B and C).

To verify the physical interaction between NFAT and the *cis*-acting elements of miR-26, we first carried out EMSA in conjunction with supershift to assess the ability of NFAT to bind the putative *cis*-acting elements in the 5'-flanking regions of the miR-26a and miR-26b host genes. We incubated each probe, a synthesized, digoxigenin-labeled putative NFAT *cis*-acting element (double-stranded oligodeoxynucleotides fragment) with nuclear extract from Hela cells. As depicted in Figure 7A, a shifted band representing protein-DNA binding was identified, which was eliminated upon addition of excessive non-labelled probes but was supershifted by the antibody to NFAT. We then subsequently conducted ChIP to further verify the protein-DNA interactions that occur inside the nucleus of living cells. Our results confirmed the binding of NFAT to each of the three *cis*-elements in the 5'-flanking regions of the three miR-26 members (Figure 7B).

We reasoned that if NFAT is indeed a negative regulator of miR-26, inhibition of NFAT activity should downregulate Kir2.1 protein by relieving the inhibitory effect on miR-26, provided that other regulatory factors are kept unchanged. This hypothesis was supported by the data shown in Figure 7C: application of INCA6 significantly decreased Kir2.1 protein expression. Finally, we confirmed NFAT-modulation in AF as evidenced by enhanced translocation of NFATc3 and NFATc4 from cytoplasm to nucleus in atrial samples of AF dogs and patients on immunohistochemical examination (Figure 7D). The experiments shown in Figures 6 and 7 indicate that NFAT is a negative regulator of miR-26 transcription and that, since NFAT is translocated to cardiomyocyte nuclei in AF, it is a strong candidate to underlie AF-induced miR-26 dysregulation.

**DISCUSSION**

Taken together, our results identify miR-26 as a potentially important regulator of *KCNJ2* gene-expression and, via $I_{K1}$, a determinant of AF-susceptibility. In addition, our findings identify miR-26 as a novel potential mediator of the electrophysiological effects of $Ca^{2+}$-dependent NFAT signaling, believed to be an important player in AF perpetuation (30-32). Our study therefore reveals novel molecular control mechanisms for AF at the miRNA level, as summarized schematically in Figure 8.

AF can be induced by a variety of factors, including atrial dilation, oxidative stress, atrial ischemia or hypoxia, and intracellular $Ca^{2+}$ overload; all of these ultimately act by altering, directly or indirectly, atrial electrical activity, principally by modulating ion channel function and/or expression (9, 10, 33). Many ion currents are altered by atrial electrical remodeling during AF (10). $I_{K1}$ is a particularly important mechanistic determinant of AF-supporting reentry because, in addition to accelerating repolarization, enhanced $I_{K1}$ increases $Na^{+}$-current availability, accelerating and stabilizing reentrant rotors (18). $I_{K1}$ enhancement is not only a potentially important contributor to AF associated with atrial remodeling (18, 33) but is also the causative factor in familial AF resulting from gain-of-function mutations associated with Kir2.1 channelopathies (34-36).

More generally, $I_{K1}$ plays a central role in cardiac excitability and arrhythmogenesis (20, 37). Although $I_{K1}$-alterations are important in the failing heart, they are not explained by changes in candidate-subunit transcript-levels (38), suggesting post-transcriptional regulation. Similarly, KCNJ2 protein-expression changes in patients with AF may exceed mRNA alterations (16), pointing to post-transcriptional mechanisms such as microRNA-induced inhibition of translation. Our findings indicate that miR-26 regulates this important $K^{+}$-channel under specific disease conditions and provide insights into the

transcriptional control of miR-26. Further studies of miR-26 dysregulation of $I_{K1}$ in other pathological contexts are clearly of potential interest.

Downregulation of L-type $Ca^{2+}$-current is well-established as an important component of the ionic remodeling associated with AF (9, 33). The $Ca^{2+}$-calcineurin-NFAT system plays a central role in detecting the rapid repetitive atrial activation that occurs during AF, and in coupling AF to L-type $Ca^{2+}$-currrent downregulation (30-32). The contribution of $I_{K1}$ upregulation has been established more recently (10), but is recognized to be of substantial importance to AF pathophysiology (18). Our findings here suggest that the calcineurin-NFAT system engaged by AF might also induce $I_{K1}$ changes via transcriptional regulation of miR-26, indicating that this $Ca^{2+}$-dependent system may be a common pathway for at least 2 of the important changes in ion-channel function associated with AF.

We found that adenoviral gene-transfer of miR-26 via tail-vein injection was able to upregulate cardiac miR-26 expression and suppress AF inducibility and maintenance. AF-therapy is presently quite inadequate, with conventional antiarrhythmic drugs having limited efficacy and potentially-significant toxicity (9, 39). There is therefore great interest in novel therapeutic approaches to the arrhythmia, one of which in early development is gene therapy (39, 40). Our findings suggest that miR-26 could conceivably be a candidate for AF-targeting gene-therapy in the future.

The expression of miR-1, which is upregulated in myocardial infarction and established by a previous study to target KCNJ2/Kir2.1/$I_{K1}$ (1), was unaltered in our samples from dogs and patients with AF (Figure 1A). Girmatsion *et al* (4), however, reported that the expression of miR-1 was reduced by approximately 86% in left atrial samples of AF patients undergoing mitral valve repair or bypass grafting. There was a

corresponding increase in Kir2.1-protein expression. Based on their data, the authors proposed that downregulation of miR-1 is responsible for upregulation of Kir2.1/$I_{K1}$ in AF patients. However, their study leaves a number of important unresolved issues. First, no direct evidence for an AF-promoting role of miR-1 downregulation was presented. Second, Kir2.1 was found to be upregulated by only 1.5-fold at the protein level but by 3-fold at the mRNA level in the Girmatsion study. These results are inconsistent with the expected effect of miR-1, because miR-1 has been documented not to affect *KCNJ2* transcript levels (1). Third, the authors showed that the expression of connexin-43, another validated target of miR-1 (1), was unaltered. Finally, whether the observed upregulation of Kir2.1 expression in their preparations was caused by miR-1 downregulation was not tested. The lack of miR-1 expression change in our patient and dog samples indicates that miR-1 changes are unlikely to have been a major contributor to AF in our subjects.

Although we identified miR-26 downregulation in AF as an important potential contributor to $I_{K1}$ upregulation and AF-promotion, we are in no way claiming that miR-26/$I_{K1}$ changes are the only factor governing AF-development. AF is clearly a complex condition that results from multiple potential etiological contributors that can interact with each other (36). In addition to $I_{K1}$ changes, the electrical disturbances in AF-related remodeling can stem from changes in $I_{CaL}$, constitutive $I_{KACh}$ and alterations in connexin function (36). Indeed, a comparison of the time-course of changes in AF-duration, miR-26 expression and Kir2.1 protein-expression in our canine AF-model (Online Figure 14) shows that AF-vulnerability is significantly increased at one week of atrial tachypacing, before significant changes in miR-26 and Kir2.1 appear, indicating that other factors are certainly involved. Nevertheless, further statistically-significant changes occur in AF-vulnerability between weeks 1 and 6, concomitant with miR-26/Kir2.1 changes, consistent

with the profibrillatory properties of miR-26 downregulation/Kir2.1 upregulation seen in our mouse model. Furthermore, structural alterations and changes in intracellular $Ca^{2+}$ handling can also play a significant role, and the mechanistic contributors to AF vary, depending on underlying diseases and genetic factors (33, 36). Nor is $I_{K1}$ the only potential target for miR-26 in AF. For example, we recently demonstrated that miR-26 also targets the nonselective cation-channel subunit TRPC3, through which it can alter fibroblast function and thereby contribute to AF-promotion (41). However, the miR-26 interaction with the TRPC3 gene is not predicted to be mimicked by the *KCNJ2*-binding miR-Mimic, nor is it blocked by the miR-Masks, that we used in the present study. Thus, the protective effects against *KCNJ2* upregulation and AF-promotion that we observed in our mouse model with the miR-Mimic, and the opposite phenomena with the miR-Masks, are not mediated by TRPC3-changes. Similarly, our miR-Mimic did not bind to any other functional transcripts in GenBank, and the miR-Mask interaction with the miR-26 binding sites on *KCNJ2* did not apply to any other functional transcript in GenBank. Therefore, our results strongly suggest that the effects of miR-26 alterations that we observed on AF in our in vivo mouse model were mediated through changes in KCNJ2/$I_{K1}$. Our observations of the AF-promoting effect of miR26-downregulation/$I_{K1}$-upregulation are limited to changes in AF-vulnerability and AF-sustainability once induced. We never saw spontaneously-initiated AF in this study and thus our observations provide no information about the mechanisms of spontaneous AF-onset in man. They rather relate to the factors determining the substrate for AF-initiation and persistence, upon induction by spontaneous atrial ectopy/tachyarrhythmia.

We demonstrated in vitro that NFAT is a negative regulator of miR-26: NFAT-inhibition upregulated miR-26-transcription and reciprocally downregulated KCNJ2-

expression. However, we were unable to create an in vivo model to test whether we could mimic the effects on miR26/KCNJ2/AF-vulnerability seen with AF by enhancing NFAT-signaling. Until this is accomplished, the role of NFAT in AF-related miR26-regulation and associated AF-promotion remains to be fully established. Another potential limitation to our findings is that the underlying heart diseases of patients from whom we obtained atrial-tissue samples (Online Table 1) could have influenced the results.

In conclusion, we have discovered that miR-26 regulates the *KCNJ2*-gene and the $I_{K1}$ channel that it encodes. The application of innovative miR-Mimic and miR-Mask methods allowed us to confirm that KCNJ2-changes are necessary and sufficient to explain AF-vulnerability increases that result from miR-26 upregulation and decreases caused by miR-26 downregulation in an in vivo mouse model. MiR-26 is significantly decreased in AF-patients and an animal-model of AF, and AF-related miR-26 dysregulation is likely due to suppression of miR-26 transcription by the $Ca^{2+}$-dependent transcription factor NFAT. These findings provide new insights into the molecular mechanisms underlying a common and important cardiac arrhythmia and may have implications for other arrhythmia conditions in which $I_{K1}$ is dysregulated.

## METHODS

### AF induction in mice

C57BL/6 mice were anesthetized with 1% sodium pentobarbital through tail vein injection (30 mg/kg). Intracardiac pacing was performed in these animals by inserting an eight-electrode catheter (1.1 F, octapolar EP catheter, Scisense) through the jugular vein and advancing it into the right atrium and ventricle with protocols similar to those reported in previous studies (5,42). Inducibility of atrial arrhythmias was tested by applying 6-second tachypacing bursts through the catheter electrodes, using an automated stimulator interfaced with the data acquisition system (GY6000, HeNan HuaNan Medical Science & Technology Ltd, China). The first 6-second burst had a cycle length of 40 ms, decreasing in each successive burst with a 2-ms decrement down to a cycle length of 20 ms. Successful induction of AF was defined as the creation of rapid irregular atrial rhythm lasting for ≥1 s, calculated from the direct atrial activation recordings.

To study AF changes with miR-26 manipulation, adenovirus carrying pre-miR-26a (Adv-miR-26a) was injected into mice through a tail vein (100 μl; titer: $10^{10}$ pfu/ml) once daily for 3 consecutive days. Manipulation of miR-26a was similarly achieved by tail vein injection of LNA-antimiR-26a and/or LNA-miR-Mimic or Adv-miR-26a and/or LNA-miR-Mask at 5 mg/kg/day once a day for three days. AF was measured and/or atrial-tissue samples for biochemical analysis were obtained three days after the last dose of the constructs.

### Human atrial samples from patients with atrial fibrillation

Human tissues (right atrium appendage) were provided by the Second Affiliated Hospital of the Harbin Medical University under procedures approved by the Ethics Committee of

Harbin Medical University. The tissues were obtained from 22 individuals undergoing heart surgery, ten in sinus rhythm and twelve with AF (Online Table 1). These preparations were used to isolate total RNA for real-time RT-PCR quantification of miRNAs and to extract cytosolic proteins for measurement of Kir2.1.

**Dog AF model**

Mongrel dogs of either sex, weighing between 15 and 25 kg, were instrumented with right atrial pacemakers (Shanghai Fudan University, Shanghai, China) under sodium pentobarbital (30 mg/kg i.v.) anesthesia. AF was induced by up to 6 weeks of atrial tachypacing at 400 bpm. Dogs with spontaneously-persisting AF, defined as continuous spontaneous AF maintenance for at least 2 hours, were used in this study (5).

**Cell culture**

The H9c2 (rat embryonic ventricular) cell line used in this study was purchased from American Type Culture Collection (ATCC, Manassas, VA) and cultured in Dulbecco's Modified Eagle Medium (DMEM).

**Cardiomyocyte isolation and primary cell culture**

The enzymatic dispersion techniques used to isolate single atrial myocytes from neonatal rats and adult mice have been previously described in detail (5). Briefly, 1-3 day old rats were decapitated and their hearts were aseptically removed. The atria were dissected, minced and trypsinized at 37°C for 10 min. Dissociated cells were plated in 24-well plates in Dulbecco's Modified Eagle Medium (DMEM, Ivitrogen) containing 10% FBS and 0.1 mM bromodeoxyuridine (Sigma) and the non-adherent cardiomyocytes were removed. The

cells ($1\times10^5$/well) were seeded in a 24-well plate for further experiments. This procedure yielded cultures with 90±5% myocytes, as assessed by microscopic observation of cell beating. The cardiomyocytes were also verified by positive staining with an anti-α-actin monoclonal antibody through immunocytochemistry.

For the isolation of adult mouse heart cells, mice that had been treated with varying constructs were anaesthetized with sodium pentobarbital (30 mg/kg ip). The hearts were rapidly removed and retrogradely perfused through the aorta using a modified Langendorff apparatus. The preparation was perfused with standard Tyrode's solution (in mM: NaCl 126, KCl 5.4, HEPES 10, $NaH_2PO_4$•$2H_2O$ 0.33, $MgCl_2$•$6H_2O$ 1.0, $CaCl_2$ 1.8, and glucose 10; pH adjusted to 7.4 with NaOH) for 5 min, then switched to $Ca^{2+}$-free Tyrode's solution until beating stopped, followed by perfusion with the same solution containing collagenase II (7 mg/50 ml) and BSA. The freshly isolated atrial myocytes were gently centrifuged and resuspended in Kraftbruhe (KB) storage solution (in mM: glutamic acid 70, taurine 15, KCl 30, $KH_2PO_4$ 10, $MgCl_2$ 0.5, EGTA 0.5, HEPES 10, and glucose 10; pH adjusted to 7.35 with KOH). All solutions were aerated with 100% oxygen and warmed to 37±0.5°C. Only single rod-shaped, $Ca^{2+}$-tolerant, and quiescent cells with clear cross-striations were selected for patch clamp recording.

**Computational prediction of miRNA target genes and cis-acting elements for transcription factors**

We used seven established miRNA target prediction algorithms: DIANA-microT3.1, miRanada, MirTarget2, PicTar, PITA, microcosm, and TargetScan5.1. Only the miRNAs that are predicted to target a given gene by at least four of the seven algorithms were considered as candidates for further analysis (43).

The binding sites for various transcription factors in the promoter regions of the host genes of miR-26a-1, miR-26a-2 and miR-26b from different species (human, canine, rat and mouse) were analyzed with *MatInspector* V2.2 (Genomatix) (44). Analyses were made to the 5'flanking regions 5 kb upstream of the transcriptional start sites of the host genes (Online Table 4).

**Synthesis of miRNAs and anti-miRNA antisense inhibitors**

miR-26a and miR-26b were synthesized by Integrated DNA Technologies Inc (IDT), and their respective antisense oligonucleotides, AMO-26a and AMO-26b, were synthesized by Exiqon (Denmark). Five nucleotides or deoxynucleotides at both ends of the antisense molecules were locked (LNA; the ribose ring is constrained by a methylene bridge between the 2'-*O*- and the 4'-C atoms). Additionally, a scrambled RNA was used as negative control. For in vivo experiments, LNA-modified constructs, LNA-antimiR-26a, LNA-miR-Mimic, and LNA-miR-Masks, were synthesized by Exiqon (Demark). The LNA-antimiR-26a and LNA-miR-Masks are single-stranded DNA analogues complementary to mature miR-26 (5'-uucaaguaauccaggauaggcu-3') and the miR-26 binding sites on *KCNJ2*, respectively, which were chemically modified with 2'-*O*Me phosphoramidites and locked nucleic acids (the ribose ring is constrained by a methylene bridge between the 2'-*O*- and the 4'-C atoms) (28). For negative control experiments, a mismatched miR-26 LNA-antimiR, MM-LNA-antimiR-26 (5'-TCCTGGATactaTGt-3'), was also synthesized. LNA-miR-Mimic is a double-stranded RNA fragment with locked nucleotides one at the 5'-end and two at the 3'-end. The LNA-antimiR-26, LNA-miR-Mimic, or LNA-miR-Masks was injected into mice through the tail vein at a dosage of 5 mg/kg/d in 0.2 ml saline once a day for three consecutive days.

**Quantitative real-time RT-PCR analysis.**

The Taqman® MicroRNA RT kit and Taqman® MicroRNA Assay kit (Applied Biosystems) were used in conjunction with real-time PCR with TaqMan for quantification of miRNAs in our study, as previously described in detail (1). Total RNA samples were isolated with Ambion's *mir*Vana miRNA Isolation Kit, from human right atrial appendages, canine left atrial preparations, cultured neonatal rat atrial myocytes, H9c2 cells, and mouse left atrium. Reactions contained Taqman® MicroRNA Assay qRT-PCR Primer sets specific for human, canine, rat and mouse miRNAs, and a scrambled miRNA as a negative control. qRT-PCR was performed on a thermocycler (Mx3005P™ Realtime PCR System; Stratagene) for 40 cycles. Fold variations in miRNA expression between RNA samples were calculated after normalizing to the internal control, snU6. The threshold cycle ($C_T$) is defined as the fractional cycle number at which the fluorescence passes the fixed threshold.

For quantification of transcripts of the host genes of the miR-26 family members, quantitative real-time RT-PCR was carried out with total RNA samples treated with DNase I. TaqMan quantitative assay of transcripts was performed with real-time two-step reverse transcription PCR, involving an initial reverse transcription with random primers and subsequent PCR amplification of the targets. Expression level of b2m was used as an internal control.

**Western blot analysis**

Protein samples (membrane and cytosolic samples separately) were extracted from canine left atria, human right atrial appendages, cultured neonatal rat atrial myocytes, and murine atrial tissues of wild-type and transgenic mice for immunoblotting analysis, with

procedures essentially the same as described in detail elsewhere (1). The protein content was determined by BCA Protein Assay Kit using bovine serum albumin as an internal standard. Protein samples (~50 μg) were fractionated by SDS-PAGE (6-12% polyacrylamide gels) and transferred to PVDF membranes (Millipore, Bedford, MA). The samples were then incubated overnight at 4°C with the primary antibodies in 1:200. Affinity purified mouse monoclonal anti-Kir2.1 antibody was purchased from UC Davis/NIH NeuroMab Facility (David, CA). Rabbit polyclonal anti-HERG1 was purchased from Alomone Labs (Israel). Goat polyclonal anti-KvLQT1 and anti-Kv4.3, mouse monoclonal anti-NFATc3 and rabbit polyclonal anti-NFATc4 were purchased from Santa Cruz Biotechnology (USA). And rabbit polyclonal anti-cyclin D2 and anti-cyclin E2 were purchased from Cell Signalling Technology (USA). The next day after incubation with the primary antibody, the membrane was incubated with secondary antibody (Santa Cruz Biotech, Inc.) diluted in PBS for 2 h at room temperature. Finally, the membrane was rinsed with PBS before scanning with an Infrared Imaging System (LI-COR Biosciences). GAPDH was used as an internal control for protein input, using anti-GAPDH monoclonal antibody (Fitzgerald Industries International Inc). Western blot bands were quantified using QuantityOne software by measuring the band intensity (Area x OD) for each group and normalizing to GAPDH. The final results are expressed as fold changes by normalizing the data to the control values.

**Construction of luciferase-miRNA-target site fusion plasmids**

To construct reporter vectors bearing miRNA-target sites, we synthesized fragments containing the exact target sites for miR-26a and miR-26b in the 3'UTR of KCNJ2, and the fragments carrying nucleotide replacement mutations at the seed sites (Online Figure 2),

through Invitrogen. Each construct contains one of the two predicted binding sites for miR-26a and miR-26b (Online Figure 2). These inserts were ligated into HindIII and SpeI sites in the pMIR-REPORT$^{TM}$ luciferase miRNA expression reporter vector (Ambion) (1).

**Construction of promoter-luciferase fusion plasmids**

Fragments corresponding to the promoter regions spanning the putative NFAT binding sites upstream to the TSSs of Ctdspl (for miR-26a-1), Ctdsp2 (for miR-26a-2) and Ctdsp1 (for miR-26b) were synthesized by Invitrogen. The fragments were subcloned into luciferase-containing pGL3-promoter vector (Promega, Madison, WI) for studying the role of NFAT in regulating transcription of the miR-26 family members and their host genes, according to procedures described elsewhere (44, 45). The sequences of the promoter fragments used are (the underlined, boldface letters indicate the NFAT binding sites):

Ctdspl (for miR-26a-1): 5'-

ATTATTCAGTCTATCTTGAATGTGCTGTAAGGACTGGGATAAA**GATATATTTTTTCCTCATG**GATAGGTACTTGTCCCAACAATTTTTGA

Ctdsp2 (for miR-26a-2): 5'-

TGTTTCCAAATTGCCTCTTACCAACCATGCAGTCAGAGAGG**CCAGAGGAAAGGGGATACA**GCAGGTAGGGAACCAAGTGAGAGTCAGTGG

Ctdsp1 (for miR-26b): 5'-

AAGACCCATTTTACAGATGAGGTAGTGCTATCTCCAAGTCCTC**AACGAGGAAACCGAGAAGC**CTCTAGTCCCGGGTCTTCAGAAAACGCA.

**Construction of adenovirus and infection**

The procedures were similar to the study reported by van Rooij *et al* (46) and our previous study (5). Mouse miR-26a-1 precursor DNA (5'-GGATCCgTTCCGGCACCGGAGCAAGTTCATT AGGTCCTATCCGACACGTCCAGGGTTCCCCGGATAAGAACCAATGAACGTGCC CCTGCGCCCGGACtttttttAAGCTT-3') was synthesized by GenScript (Nanjing, P.R. China). The fragment was first inserted into adenovirus shuttle plasmid pDC316-EGFP-U6 (Microbix Biosystems Inc, Canada). pDC316-EGFP-U6 was then cotransfected with the infectious adenovirus genomic plasmid pBHGloxΔE1,3Cre into 293 cells by liposome reagent. Following co-transfection of these two DNAs, homologous recombination occurred to generate a recombinant adenovirus in which the transgene (pre-miR-26) is incorporated into the viral genome, replacing the ΔE1 region (Online Figure 5).

**Preparation of decoy ODNs**

Single-stranded phosphorothioate decoy oligodeoxynucleotides (ODN) were synthesized by IDT incorporation (Coralville, IA; Online Figure 11). The ODN was dried and dissolved in sterilized Tris-EDTA buffer (10 mM Tris + 1 mM EDTA) (44, 47). The supernatant was purified using Micro Bio-spin30 columns (BioRad, Hercules, CA) and quantified by spectrophotometry. The double-stranded decoy ODN was then prepared by annealing complementary single stranded ODN by heating to 95°C for 10 min followed by cooling to room temperature slowly over 2 h. The decoy ODN was prepared at a concentration of 50 μM in saline. For negative control, a scrambled decoy ODN was also used.

**siRNAs to NFATc3 and NFATc4**

siRNAs (Online Figure 11 for sequences) and the scrambled negative control siRNA (Stealth™ RNAi Negative Control Duplexes, Medium GC Duplex; Cat#: 12935-300) were synthesized by Invitrogen.

**Transfection procedures**

Neonatal rat atrial myocytes and H9c2 cells were transfected with 100 nM miRNA and/or 10 nM AMOs, siRNAs, or negative control constructs with lipofectamine 2000 (Invitrogen), according to the manufacturer's instructions as in previous studies (1,48). Cells were used for luciferase assay 24 hours after the transfection or were collected for total RNA or protein purification 48 hours after the transfection.

For decoy oligodeoxynucleotides (ODN) studies, cells were washed with serum-free medium once and then incubated with 500 μl fresh fetal bovine serum (FBS)-free medium (39, 42). Decoy ODNs and lipofectamine 2000 (0.25 μl, Invitrogen, Carlsbad, CA) were separately mixed with 25 μl of Opti-MEM ® I Reduced Serum Medium (Gibco, Grand Island, NY) for 5 min. Then the two mixtures were combined and incubated for 20 min at RT. The lipofectamine: ODN mixture was added dropwise to the cells and incubated at 37°C for 5 h. Subsequently, 25 μl fresh medium containing 30% FBS was added to the well and the cells were maintained in culture until use.

**Luciferase activity assay**

For luciferase assay involving miRNA function, H9c2 cells were transfected with the pMIR-REPORT™ luciferase miRNA expression reporter vector carrying the 3'UTR of KCNJ2 or promoter-luciferase fusion plasmid pGL3, as previously described in detail (1, 44, 45).

**Chromatin immunoprecipitation assay (ChIP)**

ChIP assays were conducted with the Millipore Magna ChIP™ kit according to the manufacturer's instructions (Millipore, USA) as previously described (48). Briefly, H9c2 cells were grown to subconfluency, washed and fixed in 1% formaldehyde for 10 min to crosslink nucleoprotein complexes and scraped in phosphate buffered saline containing protease inhibitor cocktail. Pelleted cells were then lysed and sonicated in detergent lysis buffer. Sheared DNA-protein complexes were immunoprecipitated by incubating overnight the lysates with 2 μg antibodies against NFATc3 (Santa Cruz Biotechnology Inc., Santa Cruz, CA) or IgG (as a control). Magnetic Protein G beads provided with Millipore Magna ChIP™ kit (Millipore, USA) were used, and after extensive washing, crosslinks were removed at 62°C for 2 hours while agitating in 100 μl ChIP elution buffer and 1 μl Proteinase K. The DNA was isolated using the QIAquick PCR purification kit (Qiagen) and the presence of the miR-26 promoter was analyzed by PCR amplification using 10% of purified DNA. The primers used for miR-26 promoter sequences containing NFAT *cis*-acting elements are listed in Online Table 5. The PCR products were analyzed by gel electrophoreses on an 1% agarose gel and subsequent with GelRed™ Nucleic Acid Gel Stain.

**Electrophoresis mobility shift assay (EMSA)**

EMSA was performed with the DIG Gel Shift kit (Roche, Mannheim, Germany), as described previously (44, 48). Varying amounts of nuclear protein extracts from Hela cells were incubated with digoxigenin (DIG)-labeled double-stranded oligonucleotides containing the putative NFAT *cis*-acting element. For competition experiments, 100-fold excess of unlabeled double-stranded NF-AT consensus oligonucleotides, and for super-shift experiments, 1 μg of NFATc3 antibody (Santa Cruz Biotechnology Inc., Santa Cruz, CA), were added to the reaction. The generated chemiluminescent signals were recorded on X-ray film.

**Whole-cell patch-clamp recording**

Patch-clamp techniques were applied to isolated atrial myocytes from mice subjected to tail-vein injection of LNA-construct probes and/or adenovirus-transferred miRNA probes. We used procedures that have been described previously in detail (1, 5, 38). Briefly, the pipettes of patch electrodes had tip resistances of 2-3 MΩ when filled with pipette solution. Isolated cells were placed in a 1-ml chamber mounted on an inverted microscope (IX-70, Olympus) and perfused with Tyrode solution. Whole-cell recording was performed using an Axopatch 200B amplifier (Axon instrument, USA). Signals were filtered at 1 kHz and data were acquired by A/D conversion (Digidata 1320, Axon Instrument). Ion currents were recorded in the whole-cell voltage-clamp mode. For recordings of inward rectifier $K^+$ current ($I_{K1}$), the pipette solution contained (in mM) 20 KCl, 110 K-aspartate, 1 $MgCl_2$, 5 MgATP, 0.1 GTP, 5 $Na_2$ phosphocreatine, 10 EGTA, and 10 HEPES (pH 7.2 with KOH); the external Tyrode solution contained (in mM) 126 NaCl, 5.4 KCl, 2 $CaCl_2$, 0.8 $MgCl_2$, 10 HEPES, and 10 dextrose (pH 7.4 with NaOH). $CdCl_2$ (250 μM) was included to inhibit

$I_{CaL}$. Experiments were conducted at 36±1°C. Junction potentials were zeroed before formation of the membrane-pipette seal and were not corrected for data analyses. Series resistance and capacitance were compensated and leak currents were subtracted. Cells with significant leak currents were rejected for analysis. The data were collected in an IBM-compatible computer and analyzed with the use of pCLAMP 9.2.

$I_{K1}$ was recorded with 100-ms square-wave pulses to voltages ranging from -120 mV to +10 mV with a holding potential of -20 mV at a frequency of 0.1 Hz (1). For all recordings, sodium current was inactivated with the use of a holding potential of -20 mV. Since our study was designed for group comparisons of the experimental results, the currents were all recorded immediately after membrane rupture and series resistance compensation in order to minimize time-dependent rundown of currents. Individual currents were normalized to the membrane capacity to control for differences in cell size, and are expressed as current densities (pA/pF).

**Data analysis**

Group data are expressed as mean±SEM. Two-group only comparisons were performed by unpaired Student's *t*-test. Multiple-group comparisons for real-time RT-PCR and Western blot experiments were analyzed with one-way ANOVA followed by Bonferroni post-hoc tests. The statistical comparisons for AF incidence were performed with $\chi^2$-test. To account for multiple testing, we selected for comparison only results of primary biological significance and applied a correction using the Holm-Bonferroni method (Online Figure 6a). The statistical significances for multiple-group comparisons of AF duration with all the groups shown in Figures 3A, 4A and 4C were evaluated in a single one-way ANOVA

with post-hoc Tukey's tests (Online Figure 6b). A *P*-value less than 0.05 was considered significant.

**Study Approval**

All animal handling and human tissue sample procurement procedures were approved prior to study onset by the Animal Care and Use and Human Research Ethics Committees at the Harbin Medical University and the Montreal Heart Institute.

**Acknowledgments**

We thank Xiaofan Yang and Jianchun Zhang for technical support, and Dr. Marie-Claude Guertin, Director of the Biostatistics Unit of the Montreal Heart Institute Coordinating Center, for expert biostatistical advice. This work was supported in part by the Canadian Institute of Health Research (MOP 44365), the European-North American Atrial Fibrillation Research Alliance (ENAFRA; No. 07CVD03) of Fondation Leducq and the Quebec Heart and Stroke Foundation (to S. N.) and by Creative Research Groups of The National Natural Science Foundation of China (81121003 to B.Y.) and National Natural Science Foundation of China (81130088 to B.Y., 30971252 to Y.L.).

**Author contributions**

S.N. and B.Y. supervised the project and wrote the manuscript; X.L. and Z.P. were the primary investigators for this study who designed the experiments and conducted a part of the luciferase, western blot, real-time RT-PCR and in vivo experiments; X.S., J.X., H.L., L.X., D.D., J.A., A.M., X.Q., N.W. and X-Y.L. performed parts of the luciferase, real-time RT-PCR, EMSA and Western blot analyses; H.S., X.S., L.S. and Y.B. conducted patch-clamp recordings; H.L.

collected the human samples; Y-J.L., Y.L., X.G. and Y.Z. designed and conducted parts of the animal studies; Z.W. helped in the conceptualization and design of the studies.

Q:\Secrétariat Central\therfr\PUBL\J Clin Invest\miR26_SN_ft\miR26_SN_ft.doc

**References**


1. Yang B, et al. The muscle-specific microRNA *miR-1* regulates cardiac arrhythmogenic potential by targeting *GJA1* and *KCNJ2*. *Nat Med.* 2007;13**:**486-491.

2. Carè A, et al. MicroRNA-133 controls cardiac hypertrophy. *Nat Med.* 2007;13**:**613-618.

3. Feng B, et al. miR133a regulates cardiomyocyte hypertrophy in diabetes. *Diabetes Metab Res Rev.* 2010;26:40-49.

4. Girmatsion Z, et al. Changes in microRNA-1 expression and $I_{K1}$ up-regulation in human atrial fibrillation. *Heart Rhythm.* 2009;6**:**1802-1809.

*5.* Lu Y, et al. Control of experimental atrial fibrillation by microRNA-328. *Circulation.* 2010;122:2378-2387.

6. Terentyev D, et al. miR-1 overexpression enhances $Ca^{2+}$ release and promotes cardiac arrhythmogenesis by targeting PP2A regulatory subunit B56alpha and causing CaMKII-dependent hyperphosphorylation of RyR2. *Circ Res.* 2009;104:514-521.

7. Zhao Y, et al. Dysregulation of cardiogenesis, cardiac conduction, and cell cycle in mice lacking miRNA-1-2. *Cell.* 2007;119:303-317.

8. Matkovich SJ, et al. MicroRNA-133a protects against myocardial fibrosis and modulates electrical repolarization without affecting hypertrophy in pressure-overloaded adult hearts. *Circ Res.* 2010;106:166-175.

9. Nattel S. New ideas about atrial fibrillation 50 years on. *Nature.* 2002;415:219-226.

10. Nattel S, Maguy A, Le Bouter S, Yeh YH. Arrhythmogenic ion-channel remodeling in the heart: heart failure, myocardial infarction, and atrial fibrillation. *Physiol Rev.*2007;87:425-456.

11. Zhang H, Garratt CJ, Zhu J, Holden AV. Role of up-regulation of $I_{K1}$ in action potential shortening associated with atrial fibrillation in humans. *Cardiovasc Res.* 2005;66:493-502.

12. Bosch RF, Zeng X, Grammer JB, Popovic CM, Kuhlkamp V. Ionic mechanisms of electrical remodelling in human atrial fibrillation. *Cardiovasc Res.* 1999;44:121-131.

13. Workman AJ, Kane KA, Rankin AC. The contribution of ionic currents to changes in refractoriness of human atrial myocytes associated with chronic atrial fibrillation. *Cardiovasc Re*s. 2001;52:226-235.

14. Cha TJ, Ehrlich JR, Zhang L, Nattel S. Atrial ionic remodelling induced by atrial tachycardia in the presence of congestive heart failure. *Circulation.* 2004;110:1520-1526.

15. Dobrev D, et al. Human inward rectifier potassium channels in chronic and postoperative atrial fibrillation. *Cardiovasc Res.* 2002;54:397-404.

16. Gaborit N, et al. Human atrial ion channel and transporter subunit gene-expression remodeling associated with valvular heart disease and atrial fibrillation. *Circulation.* 2005;112:471-481.

17. Atienza F, et al. Activation of inward rectifier potassium channels accelerates atrial fibrillation in humans: evidence for a reentrant mechanism. *Circulation.* 2006;114:2434-2442.

18. Pandit SV, et al. Ionic determinants of functional reentry in a 2-D model of human atrial cells during simulated chronic atrial fibrillation. *Biophys J.* 2005;88:3806-3821.

19. Katsouras G, et al. Differences in atrial fibrillation properties under vagal nerve stimulation versus atrial tachycardia remodeling. *Heart Rhythm.* 2009;6:1465-1472.

20. Noujaim SF, et al. Specific residues of the cytoplasmic domains of cardiac inward rectifier potassium channels are effective antifibrillatory targets. *FASEB J.* 2010;24:4302-4312.

21. Liang Y, Ridzon D, Wong L, Chen C. Characterization of microRNA expression profiles in normal human tissues. *BMC Genomics.* 2007;8:166.

22. Lewis BP, Burge CB, Bartel DP. Conserved seed pairing, often flanked by adenosines, indicates that thousands of human genes are microRNA targets. *Cell.* 2005;120:15-20.

23. Sayed D, Hong C, Chen IY, Lypowy J, Abdellatif M. MicroRNAs play an essential role in the development of cardiac hypertrophy. *Circ Res.* 2007;100:416-424.

24. Nigam V, et al. Altered microRNAs in bicuspid aortic valve: a comparison between stenotic and insufficient valves. *J Heart Valve Dis.* 2010;19:459-465.

25. Lanford RE, et al. Therapeutic silencing of microRNA-122 in primates with chronic hepatitis C virus infection. *Science.* 2010;327:198-201.

26. Elmén J, et al. LNA-mediated microRNA silencing in non-human primates. *Nature.* 2008;452:896-899.

27. Grünweller A, Hartmann RK. Locked nucleic acid oligonucleotides: the next generation of antisense agents? *Bio Drugs.* 2007;21:235-243.

28. Wang Z. The principles of miRNA-masking antisense oligonucleotides technology. *Methods Mol Biol.* 2011;676:43-49.

29. Kota J, et al. Therapeutic microRNA delivery suppresses tumorigenesis in a murine liver cancer model. *Cell.* 2009;137:1005-1017.

30. Lin CC, et al. Activation of the calcineurin-nuclear factor of activated T-cell signal transduction pathway in atrial fibrillation. *Chest.* 2004;126:1926-1932.

31. Qi XY, et al. Cellular signaling underlying atrial tachycardia remodeling of L-type calcium current. *Circ Res.* 2008;103:845-854.

32. Tavi P, et al. Pacing-induced calcineurin activation controls cardiac $Ca^{2+}$ signaling and gene expression. *J Physiol.* 2004;554:309-320.

33. Nattel S, Burstein B, Dobrev D. Atrial remodelling and atrial fibrillation: Mechanisms and implications. *Circulation: Arrhythm and Electrophysiol.* 2008;1**:**62-73.

34. Priori SG, et al. A novel form of short QT syndrome (SQT3) is caused by a mutation in the KCNJ2 gene. *Circ Res.* 2005;96:800-804.

35. Xia M, et al. A Kir2.1 gain-of-function mutation underlies familial atrial fibrillation. *Biochem Biophys Res Commun.* 2005;332:1012-1019.

36. Wakili R, Voigt N, Kääb S, Dobrev D, Nattel S. Recent advances in the molecular pathophysiology of atrial fibrillation. *J Clin Invest*. 2011;121:2955-2968.

37. Dhamoon AS, Jalife J. The inward rectifier current ($I_{K1}$) controls cardiac excitability and is involved in arrhythmogenesis. *Heart Rhythm.* 2005;2:316-324.

38. Wang Z, Yue L, White M, Pelletier G, Nattel S. Differential expression of inward rectifier potassium channel mRNA in human atrium versus ventricle and in normal versus failing hearts. *Circulation.* 1998;98:2422-2428.

39. Dobrev D, Carlsson L, Nattel S. Novel molecular targets for atrial fibrillation therapy. *Nat Rev Drug Discov*. 2012;11:275-291.

40. Amit G, Qin H, Donahue JK. Biological therapies for atrial fibrillation. *J Cardiovasc Pharmacol.* 2008;52:222-227.

41. Harada M, et al. Transient receptor potential canonical-3 channel-dependent fibroblast regulation in atrial fibrillation. *Circulation.* 2012;126:2051-2064.

42. Schrickel JW, et al. Induction of atrial fibrillation in mice by rapid transesophageal atrial pacing. *Basic Res Cardiol.* 2002;97:452-460.

43. Luo X, Zhang H, Xiao J, Wang Z. Regulation of human cardiac ion channel genes by microRNAs: Theoretical perspective and pathophysiological implications. *Cell Physiol Biochem.* 2010;25:571-586.

44. Lin H, Xiao J, Luo X, Pan Z, Yang B, Wang Z. Transcriptional control of pacemaker channel genes *HCN2* and *HCN4* by Sp1 and implications in re-expression of these genes in hypertrophic heart. *Cell Physiol Biochem.* 2009;23:317-326.

45. Luo X, Xiao J, Lin H, Lu Y, Yang B, Wang Z. Genomic structure, transcriptional control and tissue distribution of human *ERG1* and *KCNQ1* genes. *Am J Physiol.* 2007;294:H1371-H1380.

46. van Rooij E, et al. A signature pattern of stress-responsive microRNAs that can evoke cardiac hypertrophy and heart failure. *Proc Natl Acad Sci USA.* 2006;103:18255-18260.

47. Gao H, et al. A single decoy oligodeoxynucleotides targeting multiple oncoproteins produces strong anti-cancer effects. *Mol Pharmacol.* 2006;70:1621-1629.

48. Xiao J, Lin H, Luo X, Luo X-Y, Wang Z. *miRNA-605* joins the p53 network to form a p53:*miRNA-605*:Mdm2 positive feedback loop in response to cellular stress. *EMBO J.* 2011;30:534-532.

**Figure Legends**

**Figure 1**. Downregulation of miR-26 and upregulation of *KCNJ2*/Kir2.1 in atrial fibrillation (AF). **A** and **B**. Quantitative real-time RT-PCR (qPCR) for various microRNAs showing downregulation of miR-26 in atrial samples from a canine model ($n$=10 for Ctl and $n$=9 for AF) and from AF and sinus-rhythm patients ($n$=5 per group), respectively. *$p$<0.05, ***$p$<0.001 *vs* Ctl. (For description of patient population, see online **Supplementary Table 1**.) **C** and **D**. Western blot analysis showing significant upregulation of Kir2.1 in atrial tissues from AF dogs ($n$=9/group) and AF patients ($n$=6 for Ctl and $n$=5 for AF). **$p$<0.01 *vs* Ctl. **E** and **F**. qPCR showing significant upregulation of *KCNJ2* transcripts in atrial tissues from AF dogs ($n$=9/group) and AF patients ($n$=6 for Ctl and $n$=5 for AF). *$p$<0.05 *vs* Ctl. Values are expressed as mean±SEM.

**Figure 2.** Regulation of Kir2.1-expression by miR-26. **A** and **B**. Immunoblots showing effects of miR-26a ($n$=5) and antisense (AMO-26a; $n$=6) on Kir2.1 protein-expression in H9c2 rat ventricular cells. miR-26a (100 nM) and AMO-26a (10 nM) were transfected with lipofectamine. Ctl: Mock-treated with lipofectamine; miR-NC: negative-control miRNA; AMO-NC: negative-control AMO. **$p$<0.01, ***$p$<0.001 *vs* Ctl; ϕϕ$p$<0.01 *vs* miR-26a alone. **C.** qPCR showing effects on *KCNJ2* transcript-levels in H9c2 cells. *$p$<0.05, **$p$<0.01 *vs* Ctl; $n$=4 per group. **D**. $I_{K1}$ density in cultured neonatal rat ventricular cardiomyocytes. $I_{K1}$ was elicited by 100-ms pulses to voltages indicated. *$p$<0.05 *vs* Ctl; $n$=11/group. **E**. Luciferase reporter activities from H9c2 cells co-transfected with miR-26a (10 nM) or AMO-26a (10 nM) and chimeric vectors carrying luciferase gene and a fragment containing one of the binding motifs. Ctl/WT: control with wild-type binding sites; MT: Mutated miR-26 binding sites in the 3'UTR of *KCNJ2*. *$p$<0.05, **$p$<0.01, ***$p$<0.001 *vs* Ctl; ϕϕϕ$p$<0.001 *vs* miR-26a alone; δδ $p$<0.01 *vs* miR-26a + AMO26a;

*n*=3/group for mutated constructs and 4/group for other groups. **F.** Verification of changes in miR-26 expression by qPCR. AMO-26a and AMO-26b target both miR-26a and miR-26b. ***p*<0.01, ****p*<0.001 *vs* Ctl; ϕϕ*p*<0.01, ϕϕϕ*p*<0.001 *vs* miR-26a alone; *n*=4/group. Values are mean±SEM.

**Figure 3.** **A**. Effects of miR-26 and its antisense on AF in mice. Upper panels: representative atrial electrogram recordings. WT: Control mice receiving vehicle injections. Adv-miR-Free: Adenovirus vector without miR-26; MM LNA-antimiR-26a: mismatched LNA-antimiR-26a; as negative control constructs. Burst pacing is highlighted by solid underlines, whereas dashed underlines indicate AF. Lower panels: Percentage of animals with successful AF induction (left: results are shown as (n/N), where *n*=number inducible into AF/total of N mice) and AF-duration in animals with successful AF-induction (right). **p*<0.05, ****p*<0.001 *vs* WT; ϕϕϕ*p*<0.001 *vs* LNA-antimiR-26a. Note: Here and in Figure 4, related data-sets for AF incidence and AF duration, are shown separately for clarity in display. However, statistical comparisons were performed between all animals with interventions simultaneously (see Online Figure 6 for all comparisons), with the statistical comparisons here reflecting the results of simultaneous comparisons of all data in Online Figure 6. **B.** $I_{K1}$ in atrial myocytes isolated from mice treated with various constructs. Left panels: $I_{K1}$ recordings. Right panel: $I_{K1}$ density-voltage relationships. Results for Adv-miR-26a and LNA-antimiR-26a are shown with solid lines and the symbols defined on the figure; results for their controls (Adv-miR-free and MM LNA-antimiR-26a) are shown with dashed lines. **p*<0.05 *vs* WT; *n*=12 cells/group. **C.** qPCR verification of atrial miR-26 expression-changes resulting from various constructs (NB. antimiR-26a is complementary to both miR-26a and miR-26b). ****p*<0.001 *vs* WT; *n*=8 mice/group. Values are mean±SEM.

**Figure 4**. **A**. Inhibitory effect of LNA-miR-Mimic on induction (left) and maintenance in inducible animals (right) of AF induced in mice also treated with LNA-antimiR-26a. MM LNA-miR-Mimic: mismatched miR-Mimic (negative control). Number inducible/total-used is indicated by n/N values within brackets. **p*<0.05, ****p*<0.001 *vs* WT; ϕϕ*p*<0.01, ϕϕϕ*p*<0.001 *vs* LNA-antimiR-26a alone; §*p*<0.05 *vs* LNA-antimiR-26a + LNA-miR-Mimic. **B.** Western blot verifying ability of miR-Mimic to knock down Kir2.1. ***p*<0.01 *vs* WT; ϕϕ*p*<0.01 *vs* LNA-antimiR-26a alone; §§*p*<0.01 *vs* LNA-antimiR-26a + LNA-miR-Mimic; *n*=6 for each group. **C.** LNA-miR-Mask abolishes the protective effect of Adv-miR-26a against AF induction (left) and maintenance (right). +LNA-miR-Mask: mice injected with LNA-miR-Mask (5 mg/kg/day daily for 3 days before injection of Adv-miR-26a); LNA-miR-Mask: mice injected with LNA-miR-Mask alone. MM miR-Mask: mismatched miR-Mask (negative control). **p*<0.05 *vs* WT; ϕ*p*<0.05, ϕϕ*p*<0.01 *vs* Adv-miR-26a alone; §§*p*<0.01 *vs* Adv-miR-26a + LNA-miR-Mask. **D.** Western blot verifying ability of miR-Mask to protect against Kir2.1 knockdown by Adv-miR-26a. ****p*<0.001 *vs* WT; ϕϕϕ*p*<0.001 *vs* Adv-miR-26a alone; §§§*p*<0.001 *vs* Adv-miR-26a + LNA-miR-Mask; *n*=6/group. Values are mean±SEM. Group definitions as in Figure 3. Note: The experiments shown in Figures 3A, 4A and 4C were done contemporaneously. Thus, the same WT group data serve as controls in each case, and the same LNA-antimiR-26a and Adv-miR26a data are shown in Figure 3 and Figure 4. As in Figure 3, related data-sets for AF incidence and AF duration, are shown separately for clarity in display. However, statistical comparisons were performed between all animals with interventions simultaneously (see Online Figure 6 for all comparisons), with the statistical comparisons here reflecting the results of simultaneous comparisons of all data in Online Figure 6.

**Figure 5**. **A.** and **B.** Verification of the ability of the LNA-miR-Mimic alone to reduce (**A**) and the LNA-miR-Mask alone to increase (**B**) atrial Kir2.1 protein level, by Western blot on protein samples from atrial tissues. The respective negative control constructs were also examined. $^{**}p<0.01$ *vs* WT; $n=6$ /group. **C.** and **D.** Verification of the specificity of the LNA-miR-Mimic to repress Kir2.1 without affecting the other untargeted genes, Cyclin D2 and Cyclin E2. $^{**}p<0.01$ *vs* WT; $n=5$/group. **E.** and **F.** Verification of the specificity of the LNA-miR-Masks to block action of miR-26 on Kir2.1 without altering its effects on two other proven target genes, Cyclin D2 and Cyclin E2 (27). miR-26a: Adv-miR-26a; miR-Masks: LNA-miR-Masks; MM miR-Mask: mismatched LNA-miR-Mask. $^{**}p<0.01$ *vs* WT; $n=6$/group. Values are expressed as mean±SEM.

**Figure 6**. **A**. Schematic genomic maps of the 3 miR-26 family members showing human host genes, intronic locations of pre-miR-26a/b, and putative NFAT binding sites (indicated by arrows) in the 5'flanking regions. TSS: transcription start site. **B**. Effects of NFAT-inhibition on promoter activities of the host genes of human miR-26 family members: Ctdspl/miR-26a-1, Ctdsp2/miR-26a-2, and Ctdsp1/miR-26b, determined by luciferase activity assay using pGL3 vector carrying the promoter regions containing NFAT binding sites. NFAT was inhibited by INCA6 (100 nM), or sequestered by decoy oligodeoxyribonucletotide (dODN-NFAT; 10 nM), or silenced by siRNAs to NFATc3 and NFATc4 (10 nM). Negative controls failed to affect luciferase activity (data not shown). $^{*}p<0.05$, $^{**}p<0.01$, $^{***}p<0.001$ *vs* Ctl; $n=4$/group. **C**. Effects of NFAT inhibition by INCA6 (left panel; $n=5$/group), dODN-NFAT (10 nM; middle panel; $n=6$/group), and siRNA (10 nM; right panel; $n=6$/group) on miR-26a and miR-26b levels, determined by qPCR in H9c2 cells. $^{*}p<0.05$, $^{**}p<0.01$ *vs* Ctl. **D**. Effects of NFAT inhibition on expression of miR-26 host genes, determined by qPCR in H9c2 cells. Note that NFAT

inhibition does not affect miR-1 levels (**Supplementary Figure 13** online). *$p$<0.05 *vs* Ctl; *n*=6/group. Values are mean±SEM.

**Figure 7**. **A**. EMSA to test in vitro binding of NFATc3 to its *cis*-acting element in the promoter region of human host genes for miR-26a-1, miR-26a-2, and miR-26b. Note shifted band representing protein-DNA binding (arrows), abolished with excess non-labeled probe. Supershifted band (hollow arrows) represents NFATc3-*cis*-element binding in presence of anti-NFATc3 antibody. **B**. Chromatin immunoprecipitation (ChIP) testing in vivo binding of NFAT to human host genes of miR-26a-1, miR-26a-2, and miR-26b. Top: PCR products of 5'-flanking region encompassing NFAT binding sites following immunoprecipitation with anti-NFATc3 antibody. Bottom: Host gene binding measured by qPCR following ChIP, expressed as fold-changes over IgG negative-control. Input: genomic DNA without immunoprecipitation. **$p$<0.01, ***$p$<0.001 *vs* IgG; *n*=3/group. **C**. Western blot showing Kir2.1 downregulation by INCA6 (100 nM). **$p$<0.01 *vs* Ctl; *n*=5/group. Values in **B** and **C** are mean±SEM. **D.** Immunohistochemical images showing nuclear translocation of NFATc3 and NFATc4 in atrial samples from AF dogs (CA) and patients (HA). Blue: nuclear staining (DAPI); Red: NFAT staining; Violet: NFAT nuclear localization in merged images. Findings similar to those in D were obtained in 3 subjects per group. Scale bar: 25 um.

**Figure 8.** Molecular mechanism underlying the AF-promoting effect of miR-26 downregulation (shown in blue). AF activates NFAT, enhancing NFAT translocation into the nucleus, where it transcriptionally represses the expression of miR-26 genes. Reduced miR-26 expression then derepresses its target gene KCNJ2 at both mRNA and protein levels, causing an augmentation of $I_{K1}$. The augmented $I_{K1}$ favors the maintenance of AF. Note: The roles of components illustrated in darker blue were shown by manipulation both

in vivo and in vitro; those in lighter blue were demonstrated in vitro only. In green are the underlying pathophysiological contributors to initial AF occurrence, which also contribute to the properties and probability of AF in the presence of enhanced $I_{K1}$.

**Figures**

**Figure 1**

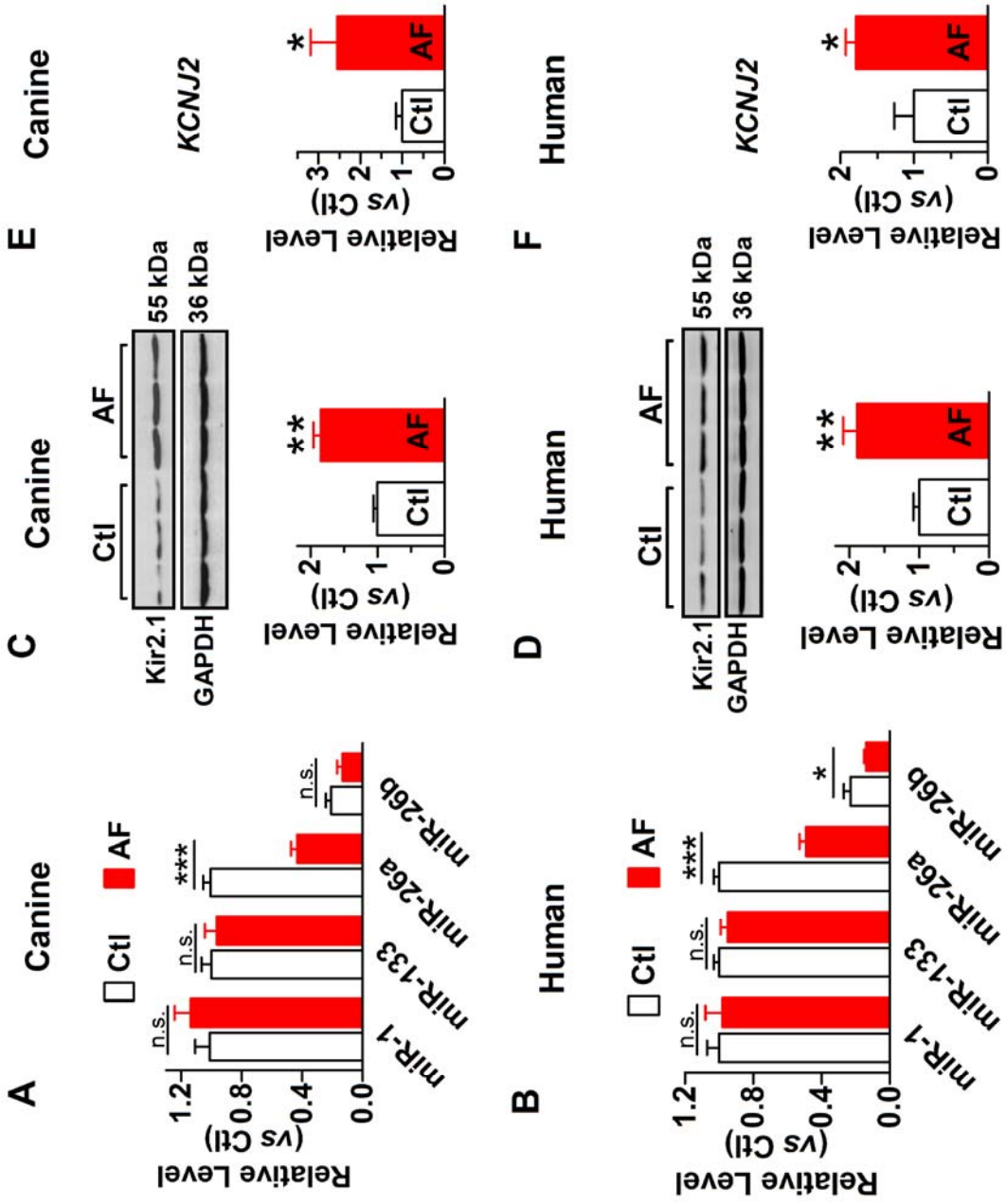

**Figure 2**

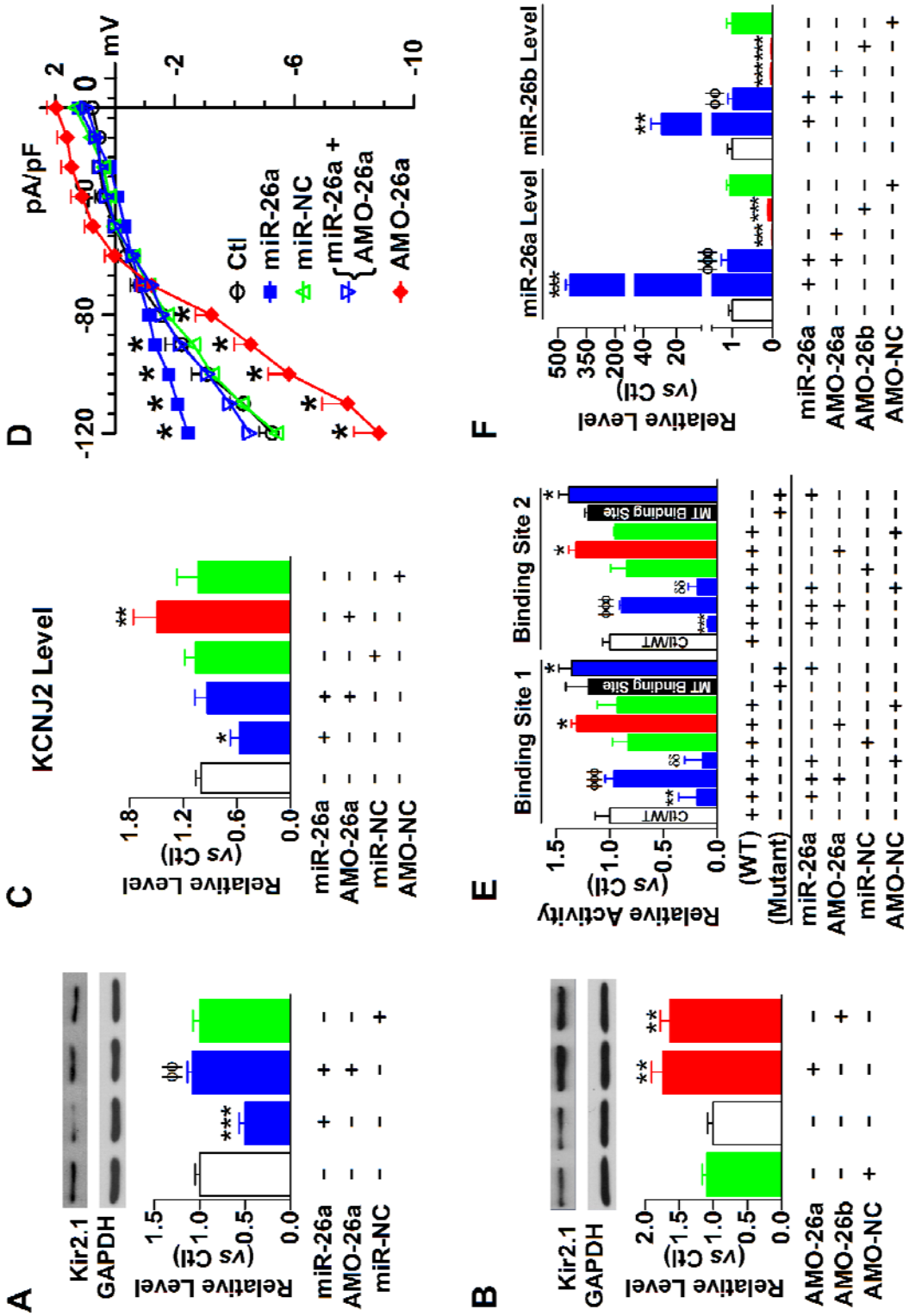
A
Kir2.1
GAPDH
Relative Level (vs Ctl)
miR-26a
AMO-26a
miR-NC
B
Kir2.1
GAPDH
Relative Level (vs Ctl)
AMO-26a
AMO-26b
AMO-NC
C
KCNJ2 Level
Relative Level (vs Ctl)
miR-26a
AMO-26a
miR-NC
AMO-NC
D
pA/pF
mV
Ctl
miR-26a
miR-NC
miR-26a + AMO-26a
AMO-26a
E
Binding Site 1
Binding Site 2
Relative Activity (vs Ctl)
Ctl/WT
MT Binding Site
(WT)
(Mutant)
miR-26a
AMO-26a
miR-NC
AMO-NC
F
miR-26a Level
miR-26b Level
Relative Level (vs Ctl)
miR-26a
AMO-26a
AMO-26b
AMO-NC

**Figure 3**

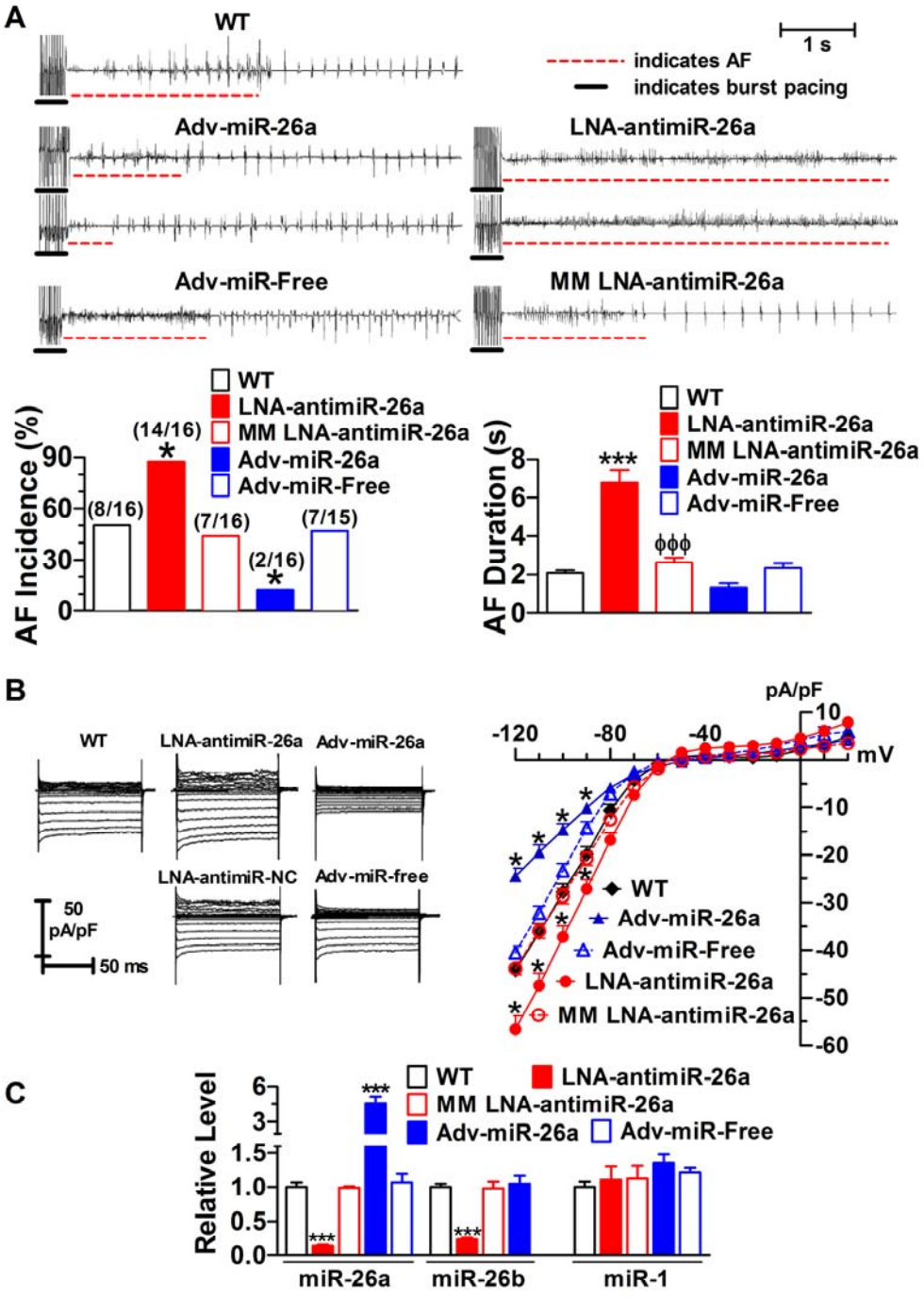
A
WT
1 s
indicates AF
indicates burst pacing
Adv-miR-26a
LNA-antimiR-26a
Adv-miR-Free
MM LNA-antimiR-26a
WT
LNA-antimiR-26a
MM LNA-antimiR-26a
Adv-miR-26a
Adv-miR-Free
AF Incidence (%)
(8/16)
(14/16)
(7/16)
(2/16)
(7/15)
AF Duration (s)
B
WT
LNA-antimiR-26a
Adv-miR-26a
LNA-antimiR-NC
Adv-miR-free
50 pA/pF
50 ms
pA/pF
mV
WT
Adv-miR-26a
Adv-miR-Free
LNA-antimiR-26a
MM LNA-antimiR-26a
C
Relative Level
miR-26a
miR-26b
miR-1

**Figure 4**

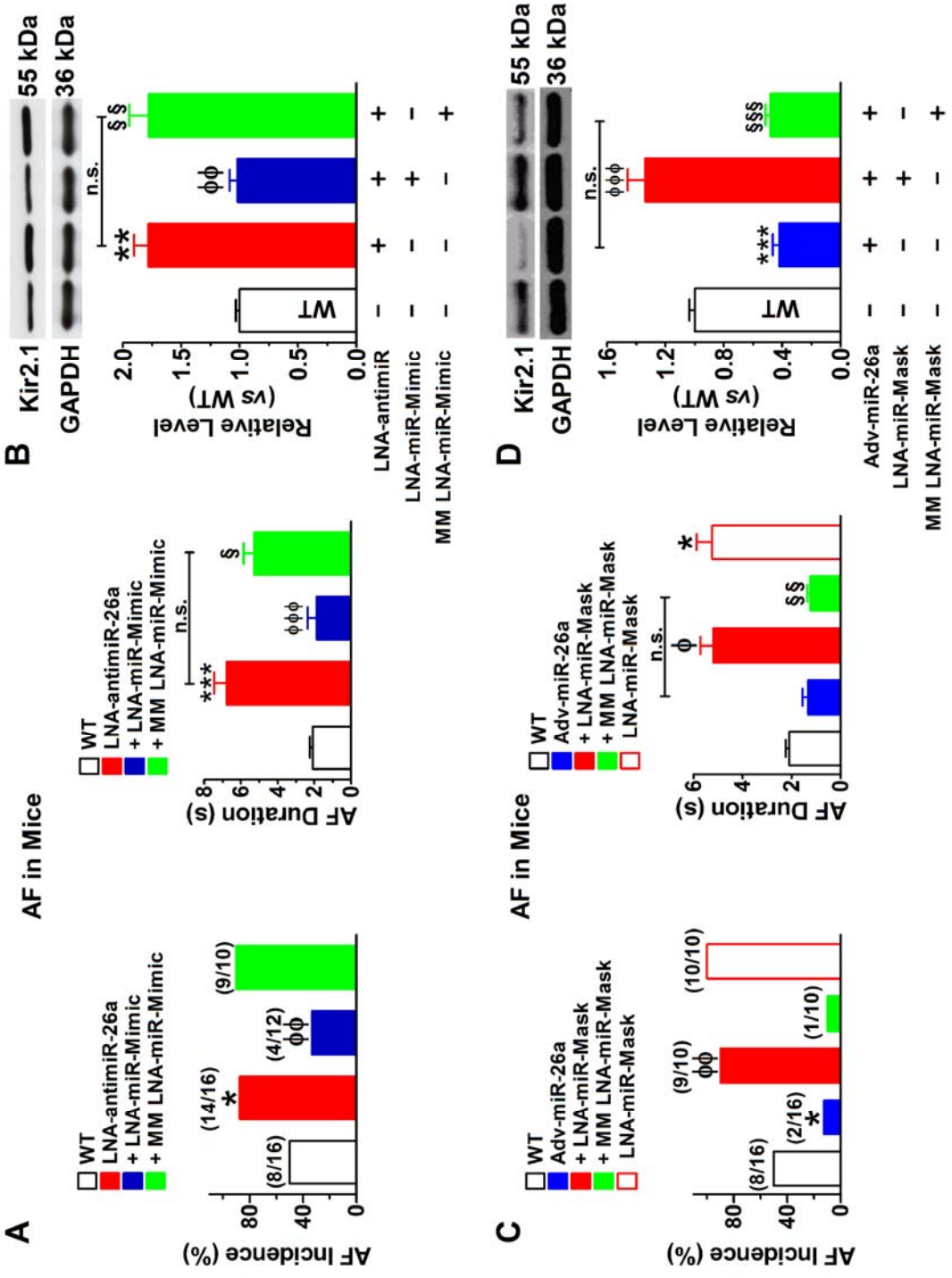
A
AF in Mice
WT
LNA-antimiR-26a
+ LNA-miR-Mimic
+ MM LNA-miR-Mimic
AF Incidence (%)
(8/16)
(14/16)
(4/12)
(9/10)
AF Duration (s)
n.s.
B
Kir2.1
GAPDH
55 kDa
36 kDa
Relative Level (vs WT)
LNA-antimiR
LNA-miR-Mimic
MM LNA-miR-Mimic
C
AF in Mice
WT
Adv-miR-26a
+ LNA-miR-Mask
+ MM LNA-miR-Mask
LNA-miR-Mask
AF Incidence (%)
(8/16)
(2/16)
(9/10)
(1/10)
(10/10)
AF Duration (s)
n.s.
D
Kir2.1
GAPDH
55 kDa
36 kDa
Relative Level (vs WT)
Adv-miR-26a
LNA-miR-Mask
MM LNA-miR-Mask

**Figure 5**

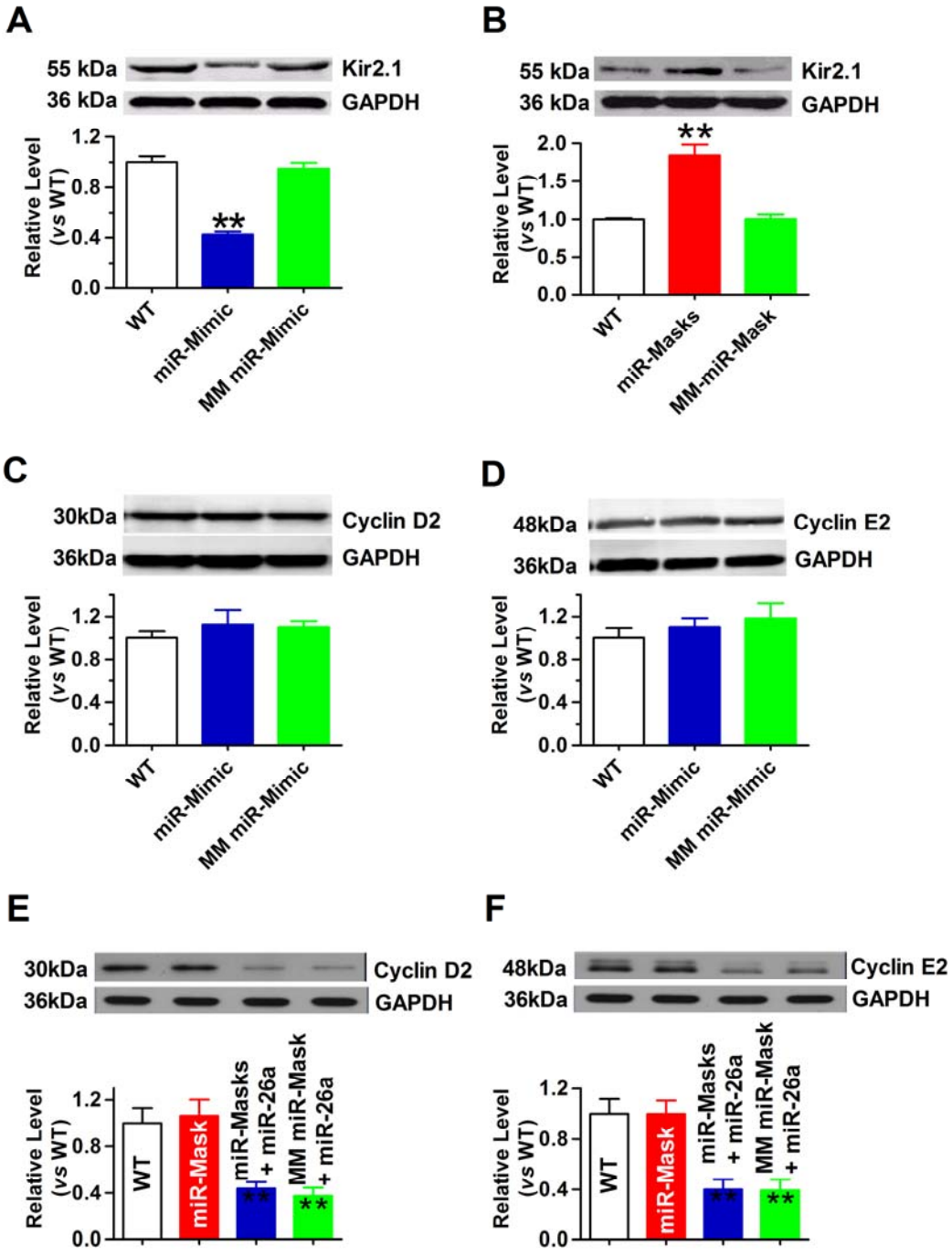
A
55 kDa
Kir2.1
36 kDa
GAPDH
Relative Level (vs WT)
1.2
0.8
0.4
0.0
**
WT
miR-Mimic
MM miR-Mimic
B
55 kDa
Kir2.1
36 kDa
GAPDH
Relative Level (vs WT)
2.0
1.5
1.0
0.5
0.0
**
WT
miR-Masks
MM-miR-Mask
C
30kDa
Cyclin D2
36kDa
GAPDH
Relative Level (vs WT)
1.2
0.8
0.4
0.0
WT
miR-Mimic
MM miR-Mimic
D
48kDa
Cyclin E2
36kDa
GAPDH
Relative Level (vs WT)
1.2
0.8
0.4
0.0
WT
miR-Mimic
MM miR-Mimic
E
30kDa
Cyclin D2
36kDa
GAPDH
Relative Level (vs WT)
1.2
0.8
0.4
0.0
WT
miR-Mask
miR-Masks + miR-26a
MM miR-Mask + miR-26a
**
**
F
48kDa
Cyclin E2
36kDa
GAPDH
Relative Level (vs WT)
1.2
0.8
0.4
0.0
WT
miR-Mask
miR-Masks + miR-26a
MM miR-Mask + miR-26a
**
**

**Figure 6**

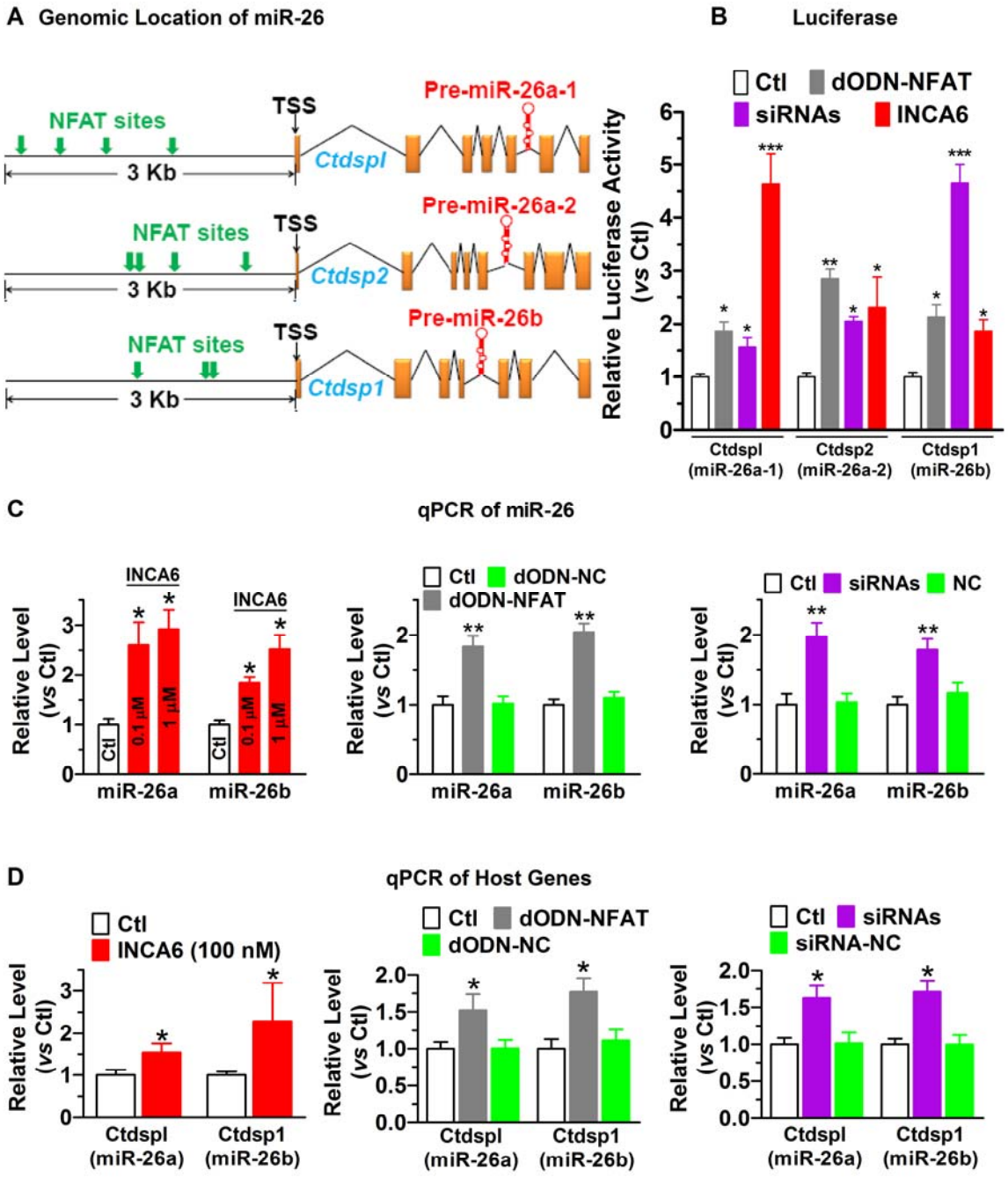
A Genomic Location of miR-26
NFAT sites
TSS
Pre-miR-26a-1
Ctdspl
3 Kb
Pre-miR-26a-2
Ctdsp2
Pre-miR-26b
Ctdsp1
B Luciferase
Ctl
dODN-NFAT
siRNAs
INCA6
Relative Luciferase Activity (vs Ctl)
Ctdspl (miR-26a-1)
Ctdsp2 (miR-26a-2)
Ctdsp1 (miR-26b)
C
qPCR of miR-26
INCA6
Relative Level (vs Ctl)
0.1 μM
1 μM
miR-26a
miR-26b
dODN-NC
siRNAs
NC
D
qPCR of Host Genes
INCA6 (100 nM)
siRNA-NC

**Figure 7**

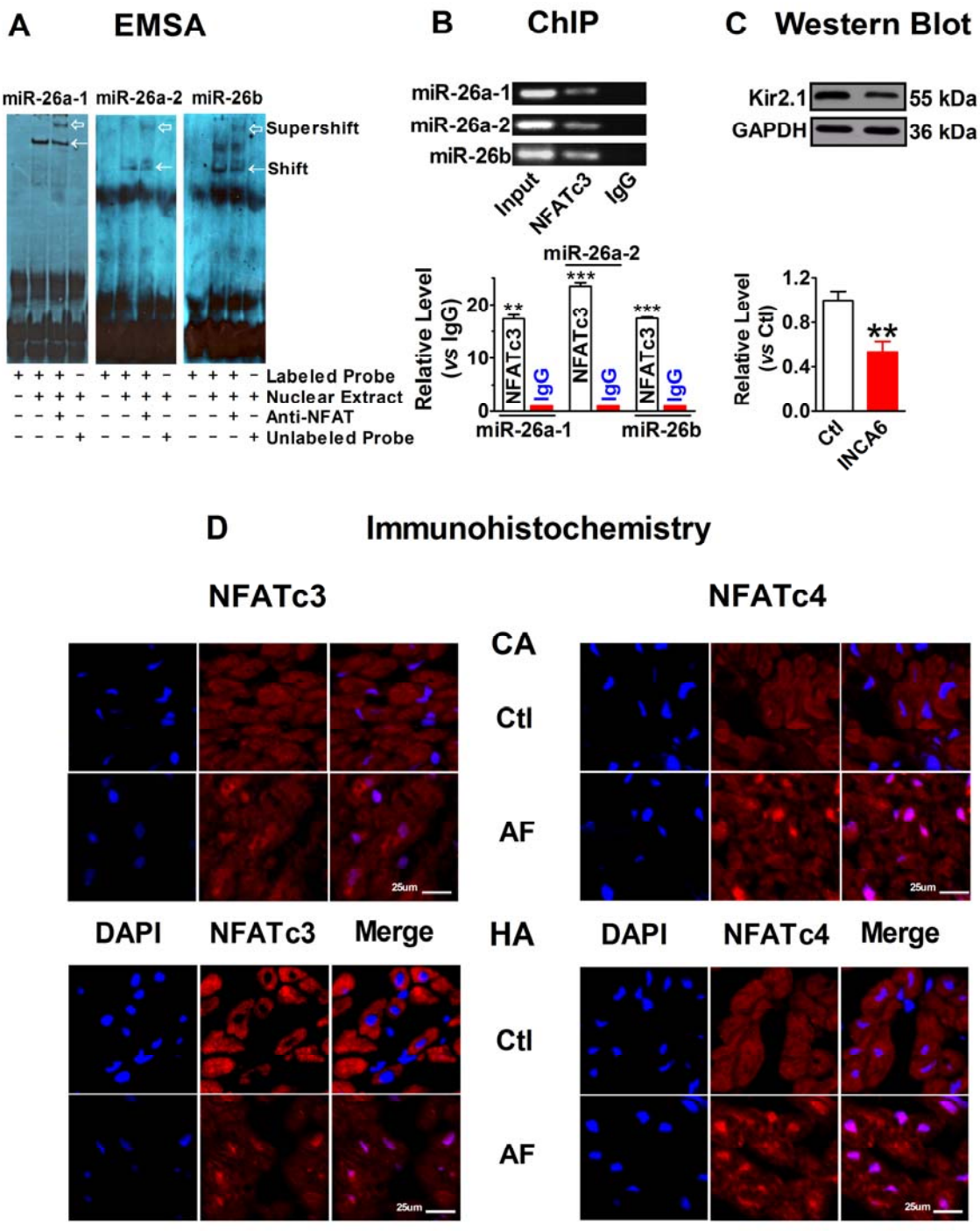
A EMSA
miR-26a-1 miR-26a-2 miR-26b
Supershift
Shift
Labeled Probe
Nuclear Extract
Anti-NFAT
Unlabeled Probe
B ChIP
miR-26a-1
miR-26a-2
miR-26b
Input
NFATc3
IgG
Relative Level (vs IgG)
miR-26a-2
miR-26a-1
miR-26b
C Western Blot
Kir2.1
55 kDa
GAPDH
36 kDa
Relative Level (vs Ctl)
Ctl
INCA6
D Immunohistochemistry
NFATc3
NFATc4
CA
Ctl
AF
DAPI
NFATc3
Merge
HA
DAPI
NFATc4
Merge
25um

**Figure 8**

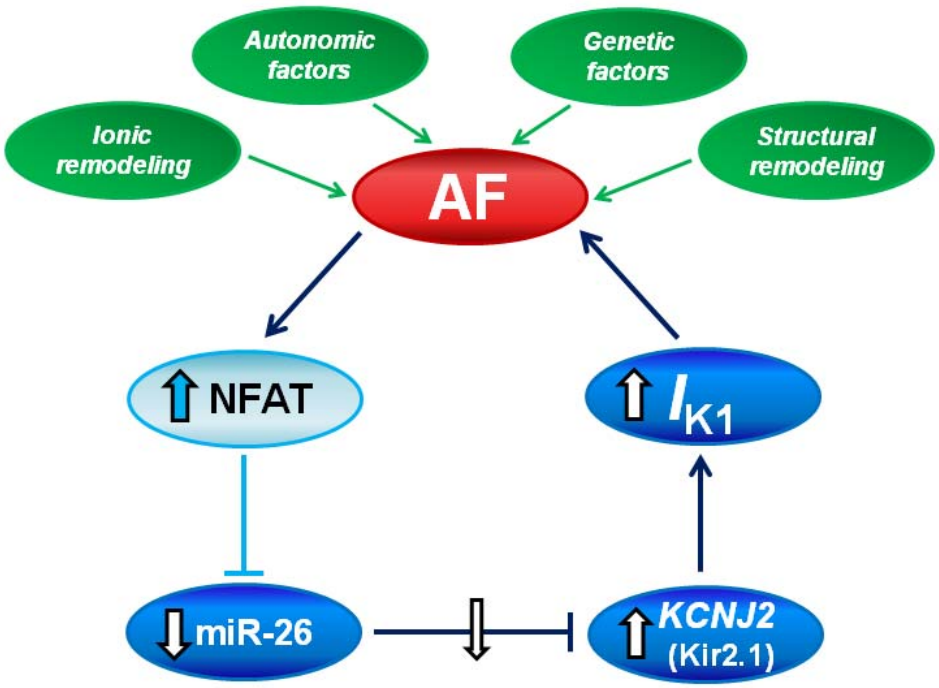
Autonomic factors
Genetic factors
Ionic remodeling
Structural remodeling
AF
NFAT
$I_{K1}$
miR-26
KCNJ2 (Kir2.1)

## Supplementary Material

### Online Methods

**Computational prediction of miRNA target genes and cis-acting elements for transcription factors.**

We used seven established miRNA target prediction algorithms: DIANA-microT3.1, miRanada, MirTarget2, PicTar, PITA, microcosm, and TargetScan5.1. Only the miRNAs that were predicted to target *KCNJ2* gene by at least four of the seven algorithms were considered as candidates for further analysis (1).

The binding sites for various transcription factors in the promoter regions of the host genes of miR-26a-1, miR-26a-2 and miR-26b from different species (human, canine, rat and mouse) were analyzed with *MatInspector* V2.2 (Genomatix) (2). Analyses were made to the 5'flanking regions 5 kb upstream of the transcriptional start sites of the host genes (Online Table 4).

**Bioinformatic identification of miR-26 as a candidate KCNJ2-regulating microRNA of interest.**

We first performed an initial miRNA screening microarray analysis of AF samples (described in one of our previous publications (3)) followed by a bioinformatic search for miRNAs that target *KCNJ2*. Initially, we suspected miR-101 as the primary candidate miRNA for *KCNJ2* regulation. However, in followup experiments, we found that the expression-levels of miR-101 in the human heart are very low compared to miR-1 or miR-26a/b (Figure A below), which makes miR-101 unlikely to be the principal regulator of *KCNJ2*. Therefore, we changed our strategy and measured the expression levels of all

the highly-conserved potential *KCNJ2*-targeting miRNAs in our atrial-tachypaced (ATP) dog samples, including miR-1, miR-16, miR-24, miR26a/b, miR-101 and miR-195, as shown in Figure B. After this screening, we selected miR-26a/b for study, based on the fact that it is the only microRNA that both targets *KCNJ2* and is highly expressed in the heart, with an expression-level that is downregulated in AF-models like the ATP dog.

**Figure A**

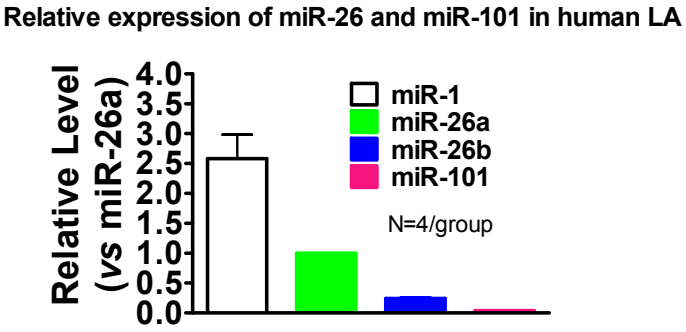


**Figure B**

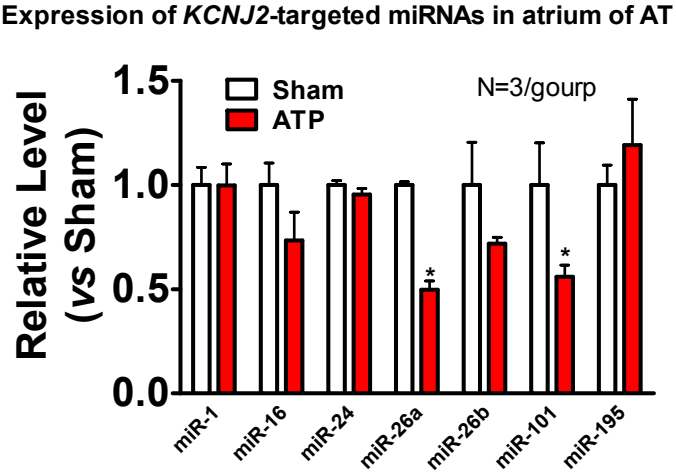


**Rapid amplification of cDNA ends (5'-RACE).** The transcription start sites (TSS) of the host genes CtdspI (for miR-26a-1), Ctdsp2 (for miR-26a-2) and

Ctdsp1 (for miR-26b) were determined with Marathon cDNA Amplification Kit, as previously described (2, 4). Human RNA sample was purchased from Clontech (Mountain View, CA). The gene-specific primers (GSPs) used for 5'RACE are shown in Online Table 5.

**Verification of miR-Mask and miR-Mimic specificity.** Searches for complementarity of the sequences of miR-Mimic and miR-Masks to other functionally-known transcripts in the mouse genome were performed by BLAST to confirm the specificity for the *KCNJ2* gene. No significant complementarity was found to any other transcript with known function. The effectiveness and specificity of miR-Mask and miR-Mimic constructs was tested by assessing their ability to prevent and mimic (respectively) the effects of miR-26 on Kir2.1-expression and AF-vulnerability, as well as a lack of effect on miR-26 targets (cyclin D2 and E2) documented in the literature (5) as well as in the present study.

**Data analysis.** Group data are expressed as mean ± SEM. Two-group only comparisons were performed by unpaired Student's *t*-test. Multiple-group comparisons for real-time RT-PCT and western blot experiments were analyzed by one-way ANOVA with Bonferroni -adjusted post-hoc *t*-tests. Differences in AF incidence were analyzed using $\chi^2$-test. To account for multiple testing, we selected for comparison only results of primary biological significance and applied a correction using the Holm-Bonferroni method. The statistical significances of multiple-group comparisons for AF duration were obtained with one-way ANOVA on all data, followed by post-hoc Tukey tests. A two-tailed $p<0.05$ was taken to indicate a statistically significant difference.

**Online References**


1. Luo X, Zhang H, Xiao J, Wang Z. Regulation of human cardiac ion channel genes by microRNAs: Theoretical perspective and pathophysiological implications. *Cell. Physiol. Biochem.* 2010;25:571-586.
2. Lin H, Xiao J, Luo X, Pan Z, Yang B, Wang Z. Transcriptional control of pacemaker channel genes *HCN2* and *HCN4* by Sp1 and implications in re-expression of these genes in hypertrophic heart. *Cell. Physiol. Biochem.* 2009;23:317-326.
3. Lu Y, et al. MicroRNA-328 contributes to adverse electrical remodeling in atrial fibrillation. *Circulation* 2010;122:2378-2387.
4. Luo X, Xiao J, Lin H, Lu Y, Yang B, Wang Z. Genomic structure, transcriptional control and tissue distribution of human *ERG1* and *KCNQ1* genes. *Am. J. Physiol.* 2007;294:H1371-H1380.
5. Kota J, et al. Therapeutic microRNA delivery suppresses tumorigenesis in a murine liver cancer model. *Cell.* 2009;137:1005-1017.

**Online Figure Legends**

**Online Figure 1.** Alignment of sequences of mature miR-26 family miRNAs of different species. The sequences of miR-26a-1 and miR-26a-2 are identical among species. The seed sites (5'end 2-8 nucleotides) are highlighted in yellow. Note that the human sequences of miR-26a and miR-26b are identical to mouse (and other species as well), which justifies the use of these miRNAs in mouse experiments.

**Online Figure 2.** Sequences of miR-26a/b and their antisense molecules used in our study. (**a**) Alignment of the sequences of miR-26a/b (upper sequences) with their target sites in the 3'-UTRs of human *KCNJ2* (lower sequences). The complementarity is indicated by boldface letters highlighted in yellow and connected by "|". (**b**) Sequences of the negative control miRNA (miR-NC) and negative control miRNA antisense oligodeoxynucleotides (AMO-NC).

**Online Figure 3.** Western blot analysis of the effects of miR-26 on protein levels of several $K^+$ channel pore-forming α-subunits. (**a**) Lack of effect of miR-26a on human *ether-ago-go*-related gene (HERG) $K^+$ channel subunit responsible for the rapid delayed-rectifier $K^+$ current ($I_{Kr}$). +AMO-26a: co-transfection of miR-26a and AMO-26a; miR-NC: negative control miRNA; AMO-NC: negative control AMO. (**b**) Lack of effect of miR-26a on human voltage-gated long QT $K^+$ channel subunit 1 (KvLQT1) responsible for the slow delayed-rectifier $K^+$ current ($I_{Ks}$). (**c**) Lack of effect of miR-26a on human voltage-gated shaker-type of $K^+$ channel subunit (Kv4.3) responsible for the transient outward $K^+$ current ($I_{to1}$). n=3/group.

**Online Figure 4.** Sequences of the antisense to miR-26a (**a**) with locked nucleotides (LNA-antimiR-26a) and the mismatched LNA-antimiR-26a (MM

LNA-antimiR-26a) for negative control. The complementarity between LNA-antimiR-26a or MM LNA-antimiR-26a and miR-26a/b is highlighted in yellow. The boldface and underlined letters represent the LNA-modified nucleotides. The lower case letters indicate the mismatched nucleotides. Note that the miRNA sequence of miR-26a is 100% conserved among human, rat and mouse.

**Online Figure 5.** Schematic illustration of construction of adenovirus vector carrying mouse pre-miR-26a-1. Mouse miR-26a-1 precursor DNA (5'-GGATCCg TTCCGGCACCGGAGCAAGTTCATTAGGTCCTATCCGACACGTCCAGGGT TCCCCGGATAAGAACCAATGAACGTGCCCCTGCGCCCGGACtttttAAGCT T-3') was inserted into adenovirus shuttle plasmid pDC316-EGFP-U6. pDC316-EGFP-U6 was then co-transfected with the infectious adenovirus genomic plasmid pBHGloxΔE1,3Cre into 293 cells by lipofectamine. Following co-transfection of these two DNAs, homologous recombination occurred to generate a recombinant adenovirus in which pre-miR-26a-1 is incorporated into the viral genome, replacing the ΔE1 region. The control vector (Adv-miR-free) lacked the pre-miR-26a DNA unit.

**Online Figure 6.** One contemporaneous set of wild type controls was performed for all groups. For clarity, results are shown separately for different sets of interventions in Figures 3 and 4 of the main manuscript. However, statistical comparisons were performed considering all groups simultaneously, as shown in this figure. AF incidence comparisons (a) were by $\chi^2$, with correction for multiple testing by the Holm-Bonferroni method. AF durations (b) were compared by one-way ANOVA with post-hoc Tukey's tests.

**Online Figure 7.** Verification of cellular uptake of Adv-miR-26a-1 in mouse atrial tissues. Adv-miR-26a-1 was administered by direct injection into tail veins. Three days after Adv-miR-26a-1 administration, the animals were scarified and atrial tissues were sliced for laser scanning confocal microscope examination. Cardiomyocytes stained in green (GFP incorporated in the viral vector) indicate successful Adv-miR-26a-1 uptake. Control samples were obtained from sham-operated, age-matched mice. The images shown are from three independent experiments from three separate animals from each group.

**Online Figure 8.** Verification of the ability of the LNA-antimiR-26a to upregulate (**A**), and adv-miR-26a to downregulate (**B**), atrial Kir2.1 protein level in mice, determined by Western blot analysis with protein samples from atrial tissues. Their respective negative control constructs were also examined. *$p$<0.05, **$p$<0.01 *vs* Ctl; n=6 for each group. **C** and **D**. Verification of Adv-miR-26a on two proven targets of miR-26, Cyclin D2 and Cyclin E2 (5). **$p$<0.01 *vs* WT; n=5/group. The LNA constructs were injected into mice via tail vein at a dosage of 5 mg/kg/day in 0.2 ml saline once a day for three consecutive days, and Adv constructs were injected through the tail vein at $10^{10}$ pfu/ml in 100 µl. The atrial tissues for the analyses were obtained 3 days after the last construct administration.

**Online Figure 9.** Sequences of the miR-Mimic (**a**) and miR-Mask (**b**) and their mismatched counterparts as negative control constructs used in our study. The complementarity between the guide strand of the miR-Mimic or miR-Mask and the 3'UTR of KCNJ2 is highlighted in yellow and connected by "|". The boldface and underlined letters represent the LNA-modified nucleotides. The lower case letters indicate the mismatched nucleotides to KCNJ2. GS: guide strand;

PS: passenger strand. The two miR-Masks were designed to fully base pair the two binding sites for miR-26 in the 3'UTR of KCNJ2 so as to protect these sites from binding miR-26. Searches for complementarity of the sequences of miR-Mimic and miR-Masks to other functionally-known transcripts in the mouse genome were performed by BLAST to confirm the specificity for the *KCNJ2* gene.

**Online Figure 10.** Identification of transcription start sites (TSSs) and genomic characteristics of the host genes of the miR-26 family miRNAs using 5'RACE techniques. (**a**) DNA gel image showing the single, discrete bands obtained by 5'RACE, indicating a single TSS for each host gene (Ctdsp2, Ctdspl or Ctdsp1). (**b**)-(**d**) Genomic sequences of Ctdspl for miR-26a-1, Ctdsp2 for miR-26a-2, and Cdtsp1 for miR-26b. TSSs are indicated; putative NFAT binding sites are shown in red letters; the fragments highlighted in green containing NFAT binding sites are those used for promoter activity analysis by luciferase assay. The outer and inner (nested) primers for 5'RACE, and the forward and reverse primers for ChIP experiments, are indicated by lines above or below the sequences.

**Online Figure 11.** The constructs used to inhibit the function of nuclear factor of activated T-cells (NFAT). (**a**) Sequences of decoy oligodeoxynucleotide (dODN) fragments used to sequestrate NFAT (dODN-NFAT) and the negative control dODN (dODN-NC). (**b**) Sequences of small interference RNA (siRNA) used to knock down the cardiac isoforms of NFAT: NFATc3 and NFATc4.

**Online Figure 12.** Verification of the efficacy of siRNAs in knocking down the cardiac isoforms of NFAT, NFATc3 and NFATc4, assessed by qPCR (**a**) and by Western blot analysis (**b**) in H9c2 rat ventricular cells. siRNA to NFATc3 and siRNA to NFATc4 were co-transfected into cells. NC: negative control siRNA. $^{**}p<0.01$, $^{***}p<0.001$ *vs* Ctl; n=4 for each group.

**Online Figure 13.** Effects of NFAT inhibition on expression of miR-1, determined by qPCR in H9c2 rat ventricular cells. Control cells were mock-treated with lipofectamine 2000 for experiments involving transfection of dODN-NFAT or siRNAs. Note that NFAT does not affect miR-1 level. n=3 for INCA group and n=4 for the other groups.

**Online Figure 14. A**. AF incidence in 1-week and 6-week atrial tachypacing (ATP) canine model. **B**. AF duration in ATP canine model. **C**. Quantitative RT-PCR measurement of miR-26a in atrium and ventricle of 1-wk and 6-wk ATP dogs. **D**. Western blot analysis of Kir2.1 protein in atrium and ventricle of 1-wk and 6-wk ATP dogs. n=5/group; *$p$<0.05, **$p$<0.01, ***$p$<0.001.

# ***Online Figures***

## Online Figure 1

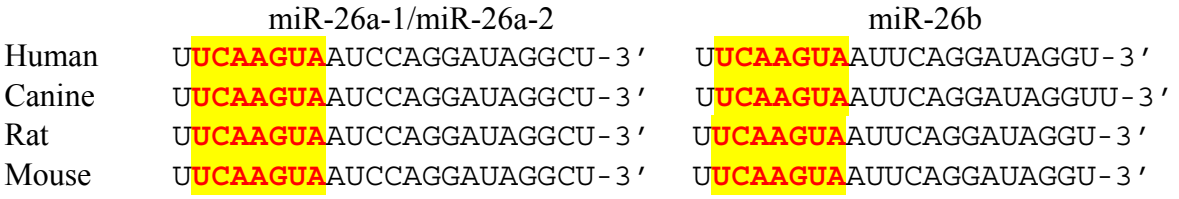


**Online Figure 1.** Alignment of sequences of mature miR-26 family miRNAs of different species. The sequences of miR-26a-1 and miR-26a-2 are identical among species. The seed sites (5'end 2-8 nucleotides) are highlighted in yellow. Note that the human sequences of miR-26a and miR-26b are identical to mouse (and other species as well), which justifies the use of these miRNAs in mouse experiments.

**Online Figure 2**

## a. miR-26:KCNJ2 Complementarity

### miR-26a

```
 3'-UCGGAUAGGACCUAAUGAACUU-5'
      |::| |||    |  |||||||
254-UGUUUUUCC---AAAACUUGAA-272
254-UGUUUUUCC---AAActgctgA-272

  3'-UCGGAUAGGACCUAAUGAACUU-5'
       |||  |    |  ||||||||
3132-UCCCUCUAAGAGUAUACUUGAA-3153
3132-UCCCUCUAAGAGUAUctgctgA-3153
```

miR-26a
3'UTR of KCNJ2 (Binding Site 1)
Mutant 3'UTR of KCNJ2

miR-26a
3'UTR of KCNJ2 (Binding Site 2)
Mutant 3'UTR of KCNJ2

### miR-26b

```
 3'-UGGAUAGGACUUAAUGAACUU-5'
    :::| |||    |  |||||||
255-GUUUUUCC---AAAACUUGAA-272
255-GUUUUUCC---AAActgctgA-272

  3'-UGGAUAGGACUUAAUGAACUU-5'
       |||  |        ||||||||
3133-CCCUCUAAGAGUAUACUUGAA-3153
3133-CCCUCUAAGAGUAUctgctgA-3153
```

miR-26b
3'UTR of KCNJ2 (Binding Site 1)
Mutant 3'UTR of KCNJ2

miR-26b
3'UTR of KCNJ2 (Binding Site 2)
Mutant 3'UTR of KCNJ2

## b. Negative Control miRNA and AMO miR-NC

### miR-NC

```
5'-UCAUAAAGCUGAUAACCUCUAGAU-3'
3'-UAAGUAUUUCGACUAUUGGAGAUC-5'
```

### AMO-NC

```
5'-TCATACAGCTAGATAACCAAAGA-3'
```

**Online Figure 2.** Sequences of miR-26a/b and their antisense molecules used in our study. (**a**) Alignment of the sequences of miR-26a/b (upper sequences) with their target sites in the 3'-UTRs of human *KCNJ2* (lower sequences). The complementarity is indicated by boldface letters highlighted in yellow and connected by "|". (**b**) Sequences of the negative control miRNA (miR-NC) and negative control miRNA antisense oligodeoxynucleotides (AMO-NC).

**Online Figure 3**

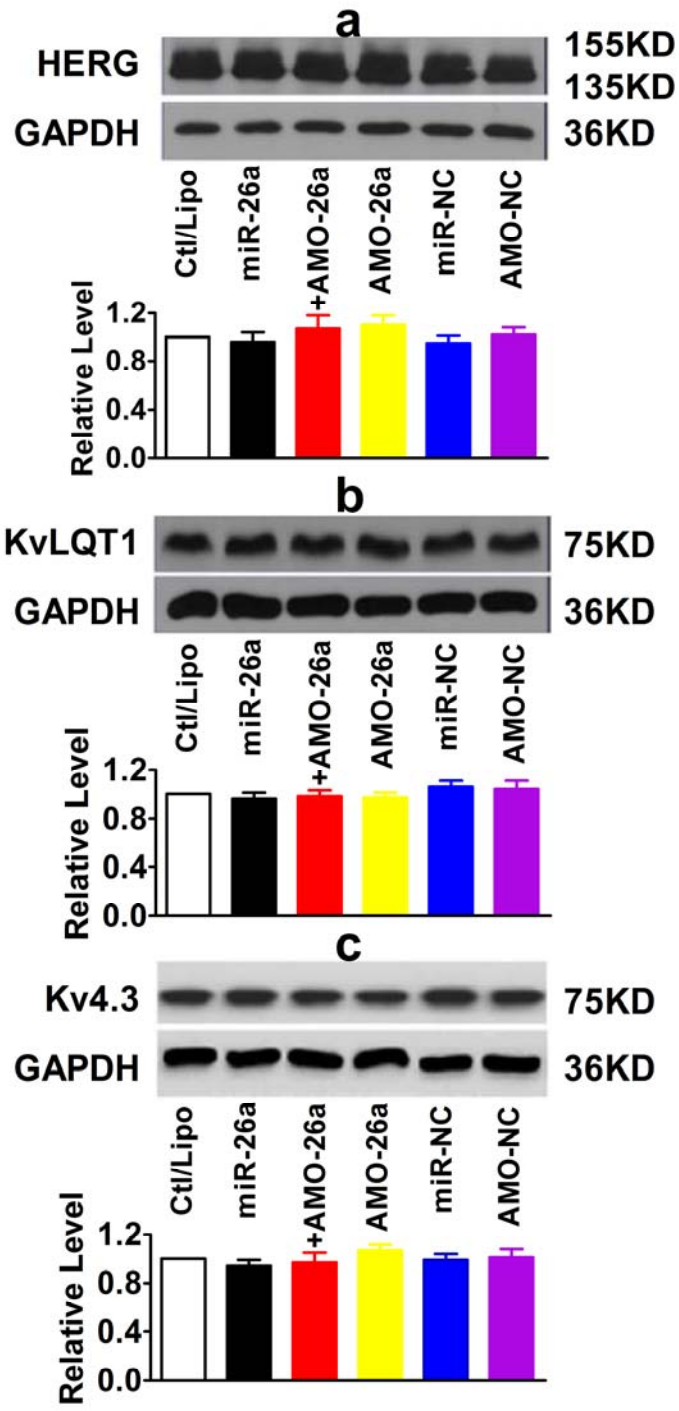


**Online Figure 3.**

Western blot analysis of the effects of miR-26 on protein levels of several $K^+$ channel pore-forming α-subunits. (**a**) Lack of effect of miR-26a on human *ether-ago-go*-related gene responsible for the rapid delayed-rectifier $K^+$ current ($I_{Kr}$). +AMO-26a: co-transfection of miR-26a and AMO-26a; miR-NC: negative control miRNA; AMO-NC: negative control AMO. (**b**) Lack of effect of miR-26a on human voltage-gated long QT $K^+$ channel subunit 1 (KvLQT1) responsible for the slow delayed-rectifier $K^+$ current ($I_{Ks}$). (**c**) Lack of effect of miR-26a on human voltage-gated shaker-type of $K^+$ channel subunit (Kv4.3) responsible for the transient outward $K^+$ current ($I_{to1}$). n=3/group.

**Online Figure 4**

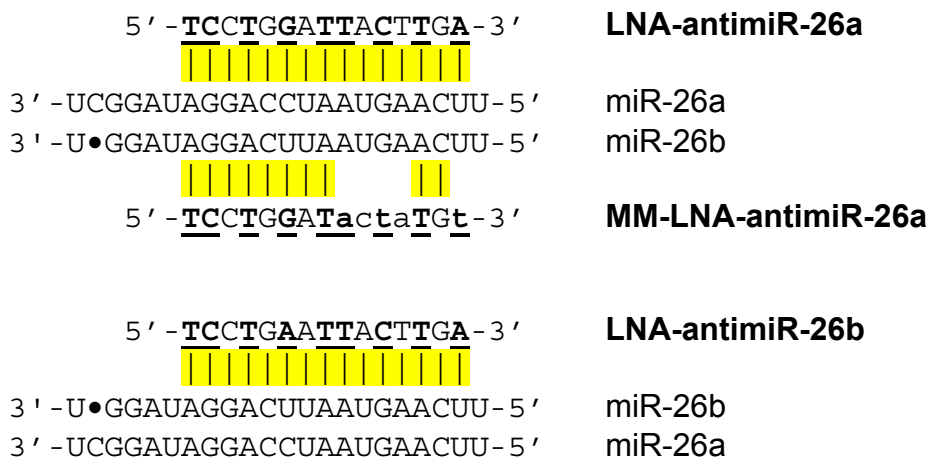


**Online Figure 4.** Sequences of the antisense to miR-26a (**a**) with locked nucleotides (LNA-antimiR-26a) and the mismatched LNA-antimiR-26a (MM LNA-antimiR-26a) for negative control. The complementarity between LNA-antimiR-26a or MM LNA-antimiR-26a and miR-26a/b is highlighted in yellow. The boldface and underlined letters represent the LNA-modified nucleotides. The lower case letters indicate the mismatched nucleotides. Note that the miRNA sequence of miR-26a is 100% conserved among human, rat and mouse.

## Online Figure 5

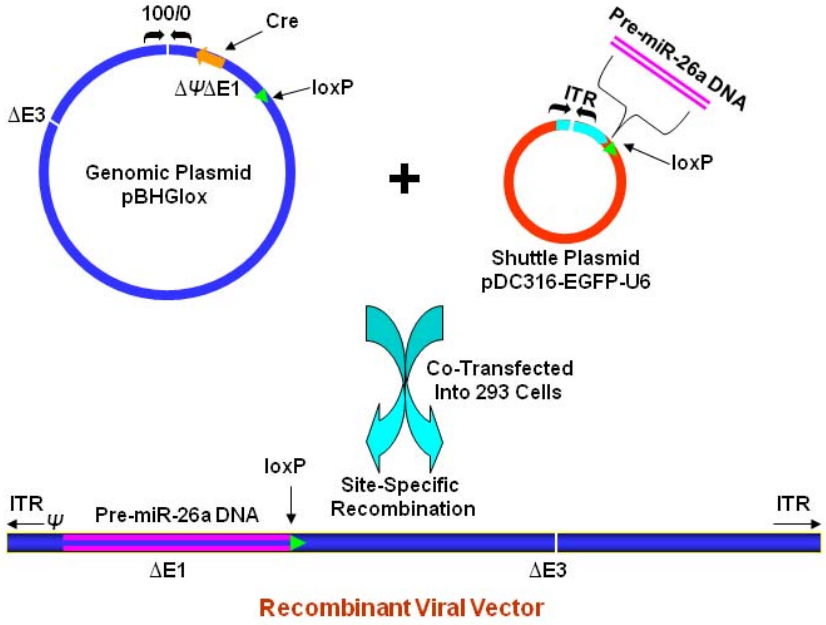


**Online Figure 5.** Schematic illustration of construction of adenovirus vector carrying mouse pre-miR-26a-1. Mouse miR-26a-1 precursor DNA (5'-GGATCCg TTCCGGCACCGGAGCAAGTTCATTAGGTCCTATCCGACACGTCCAGGGTTCCC CGGATAAGAACCAATGAACGTGCCCCTGCGCCCGGACtttttAAGCTT-3') was inserted into adenovirus shuttle plasmid pDC316-EGFP-U6. pDC316-EGFP-U6 was then co-transfected with the infectious adenovirus genomic plasmid pBHGloxΔE1,3Cre into 293 cells by lipofectamine. Following co-transfection of these two DNAs, homologous recombination occurred to generate a recombinant adenovirus in which pre-miR-26a-1 is incorporated into the viral genome, replacing the ΔE1 region. The control vector (Adv-miR-free) lacked the pre-miR-26a DNA unit.

**Online Figure 6**

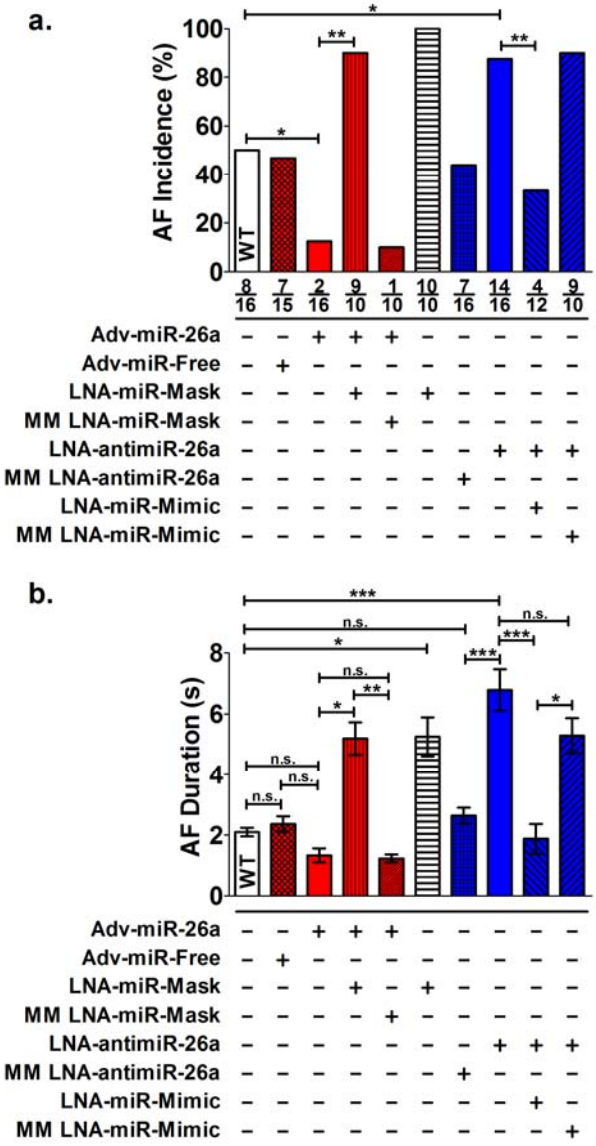


**Online Figure 6.** One contemporaneous set of wild type controls was performed for all groups. For clarity, results are shown separately for different sets of interventions in Figures 3 and 4 of the main manuscript. However, statistical comparisons were performed considering all groups simultaneously, as shown in this figure. AF incidence comparisons (a) were by $\chi^2$, with correction for multiple testing by the Holm-Bonferroni method. AF durations (b) were compared by one-way ANOVA with post-hoc Tukey's tests.

**Online Figure 7**

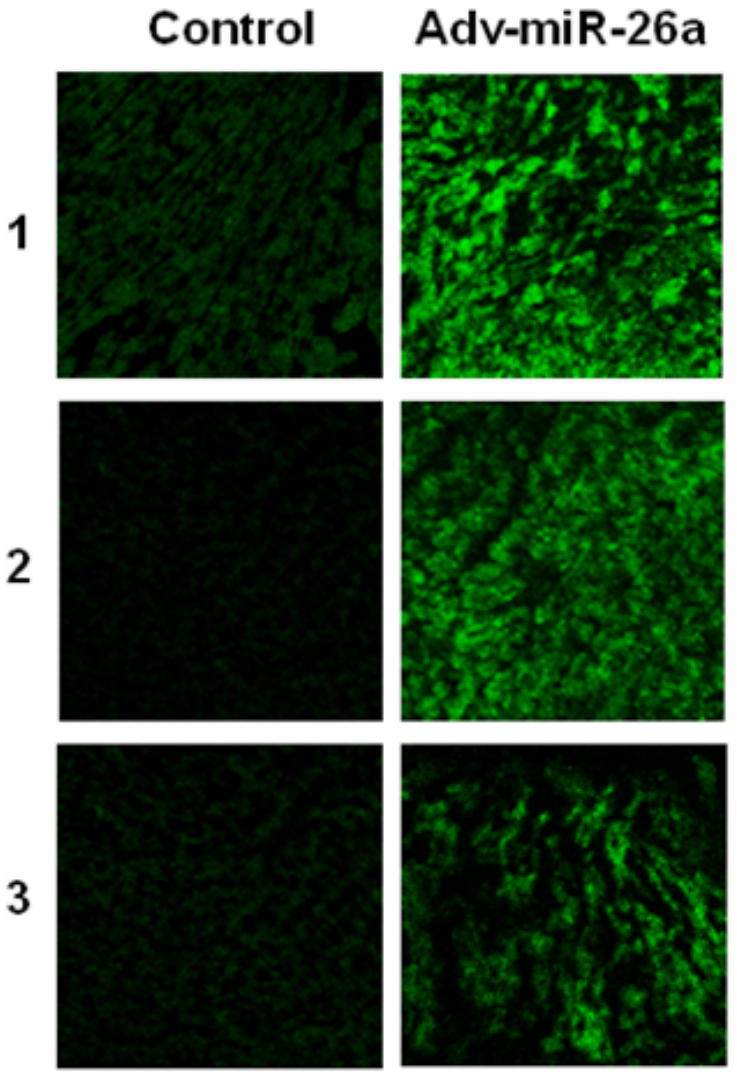


**Online Figure 7.** Verification of cellular uptake of Adv-miR-26a-1 in mouse atrial tissues. Adv-miR-26a-1 was administered by direct injection into tail veins. Three days after Adv-miR-26a-1 administration, the animals were sacrificed and atrial tissues were sliced for laser scanning confocal microscope examination. Cardiomyocytes stained in green (GFP incorporated in the viral vector) indicate successful Adv-miR-26a-1 uptake. Control samples were obtained from sham-operated, age-matched mice. The images shown are from three independent experiments from three separate animals from each group.

**Online Figure 8**

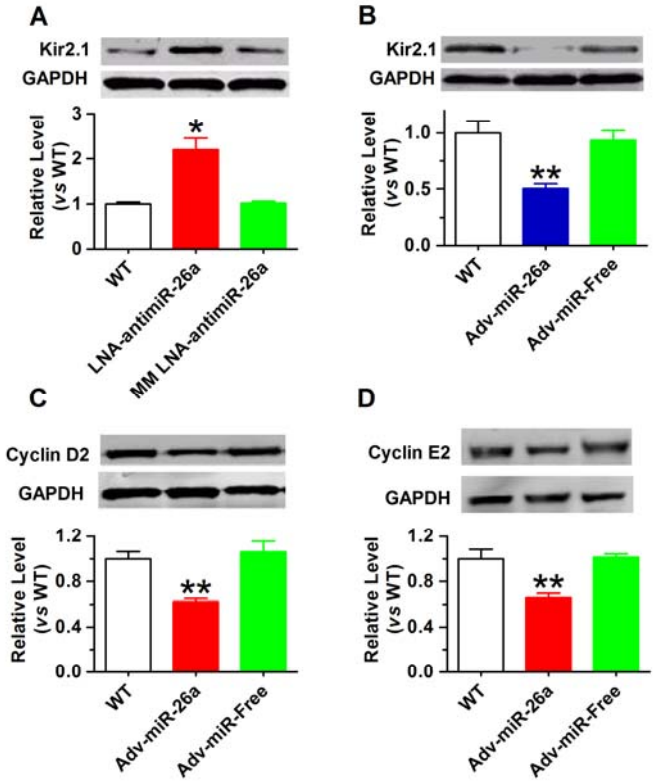


**Online Figure 8.** Verification of the ability of the LNA-antimiR-26a to upregulate (**A**), and adv-miR-26a to downregulate (**B**), atrial Kir2.1 protein level in mice, determined by Western blot analysis with protein samples from atrial tissues. Their respective negative control constructs were also examined. *$p$<0.05, **$p$<0.01 *vs* Ctl; n=6 for each group. **C** and **D**. Verification of Adv-miR-26a on two proven targets of miR-26, Cyclin D2 and Cyclin E2 (5). **$p$<0.01 *vs* WT; n=5/group. The LNA constructs were injected into mice via tail vein at a dosage of 5 mg/kg/day in 0.2 ml saline once a day for three consecutive days, and Adv constructs were injected through the tail vein at $10^{10}$ pfu/ml in 100 µl. The atrial tissues for the analyses were obtained 3 days after construct administration.

**Online Figure 9**

**a. miR-Mimic**

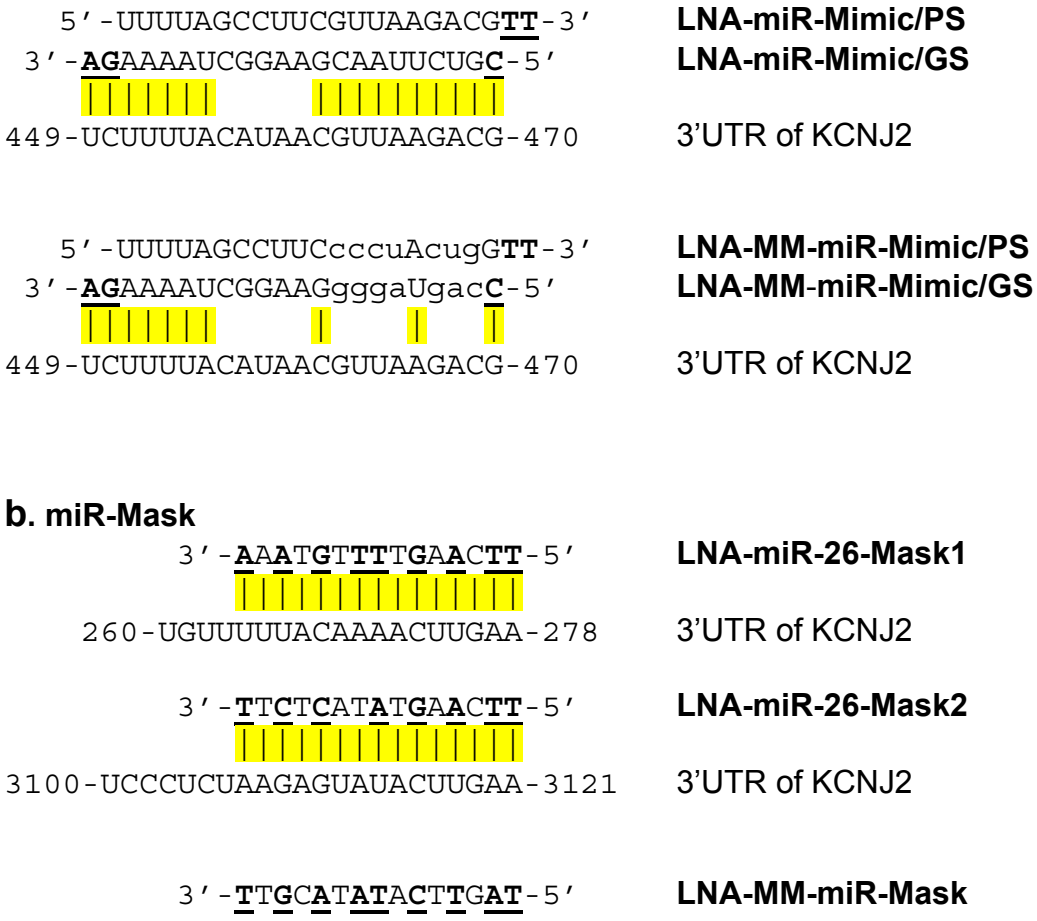


**b. miR-Mask**




**Online Figure 9.** Sequences of the miR-Mimic (**a**) and miR-Mask (**b**) and their mismatched counterparts as negative control constructs used in our study. The complementarity between the guide strand of the miR-Mimic or miR-Mask and the 3'UTR of KCNJ2 is highlighted in yellow and connected by "|". The boldface and underlined letters represent the LNA-modified nucleotides. The lower case letters indicate the mismatched nucleotides to KCNJ2. GS: guide strand; PS: passenger strand. The two miR-Masks were designed to fully base pair the two binding sites for miR-26 in the 3'UTR of KCNJ2 so as to protect these sites from binding miR-26. Searches for complementarity of the sequences of miR-Mimic and miR-Masks to other functionally-known transcripts in the mouse genome were performed by BLAST to confirm the specificity for the *KCNJ2* gene.

**Online Figure 10**

## a. DNA gel

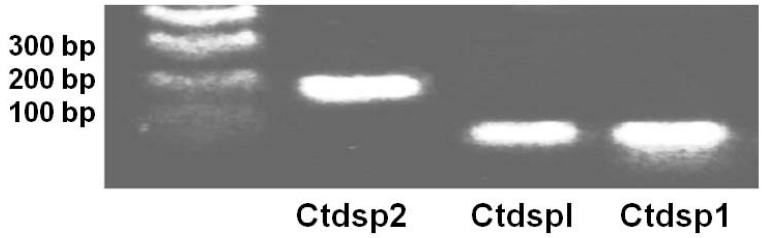


**Online Figure 10.** Identification of transcription start sites (TSSs) and genomic characteristics of the human host genes of the miR-26 family miRNAs using 5'RACE techniques. (**a**) DNA gel image showing the single, discrete bands obtained by 5'RACE, indicating a single TSS for each host gene (Ctdsp2, Ctdspl or Ctdsp1). (**b**)-(**d**) See below. Genomic sequences of Ctdspl for miR-26a-1, Ctdsp2 for miR-26a-2, and Cdtsp1 for miR-26b. TSSs are indicated; putative NFAT binding sites are shown in red letters; the fragments highlighted in green containing NFAT binding sites are those used for promoter activity analysis by luciferase assay. The outer and inner (nested) primers for 5'RACE, and the forward and reverse primers for ChIP experiments, are indicated by lines above or below the sequences.

**Online Figure 10**

## b. Ctdspl/miR-26a-1

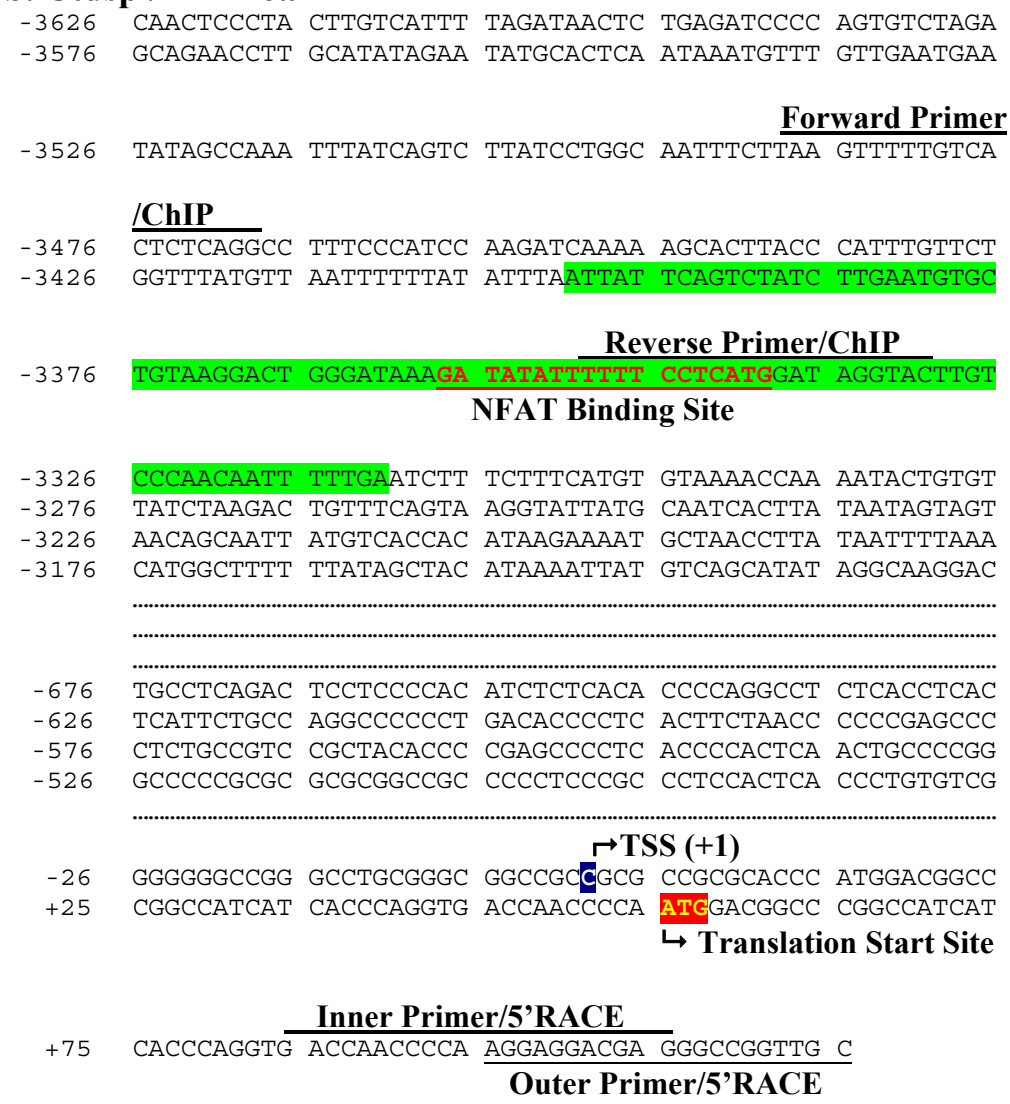


**Online Figure 10b.** Identification of transcription start sites (TSSs) and genomic characteristics of the host genes of the miR-26 family miRNAs using 5'RACE techniques. Genomic sequences of Ctdspl for miR-26a-1. TSSs are indicated; putative NFAT binding sites are shown in red letters; the fragments highlighted in green containing NFAT binding sites are those used for promoter activity analysis by luciferase assay. The outer and inner (nested) primers for 5'RACE, and the forward and reverse primers for ChIP experiments, are indicated by lines above or below the sequences.

**Online Figure 10**

## c. Ctdsp2/miR-26a-2

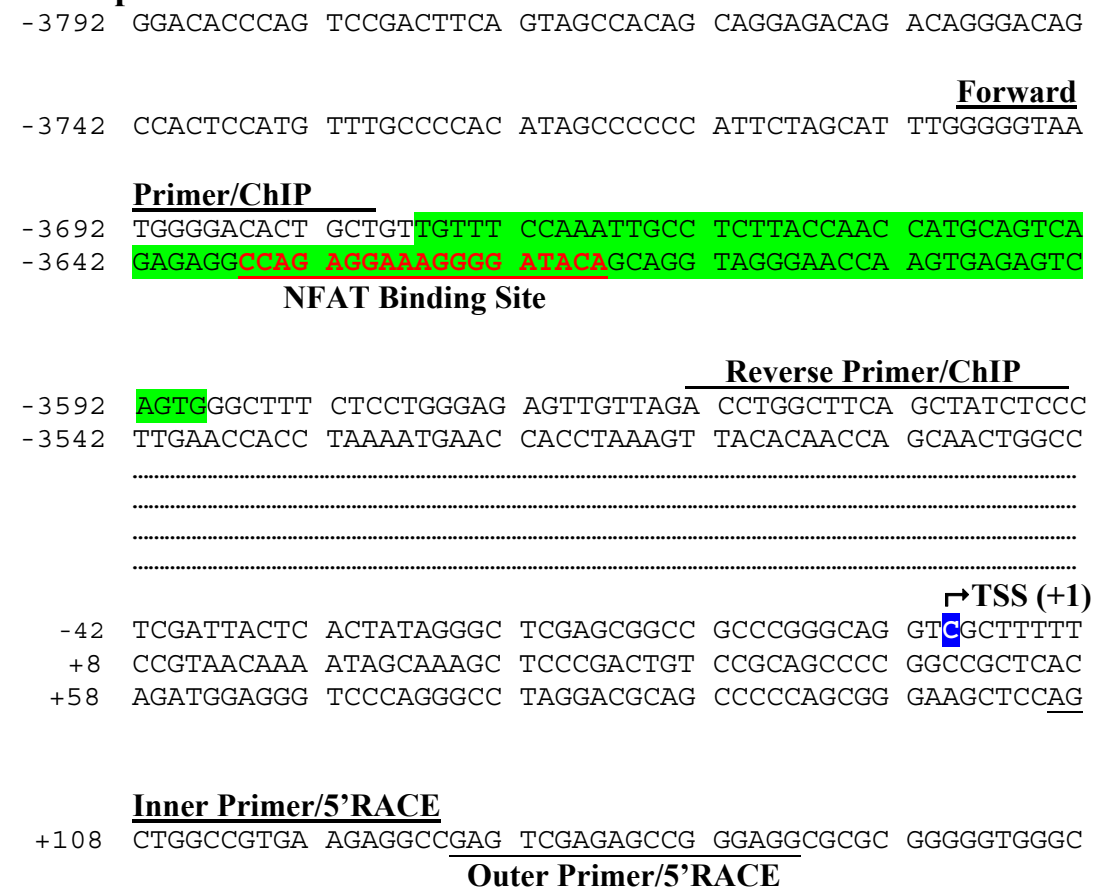


**Online Figure 10c.** Identification of transcription start sites (TSSs) Genomic sequence of Ctdsp2 for miR-26a-2. TSSs are indicated; putative NFAT binding sites are shown in red letters; the fragments highlighted in green containing NFAT binding sites are those used for promoter activity analysis by luciferase assay. The outer and inner (nested) primers for 5'RACE, and the forward and reverse primers for ChIP experiments, are indicated by lines above or below the sequences.

**Online Figure 10**

## d. Ctdsp1/miR-26b

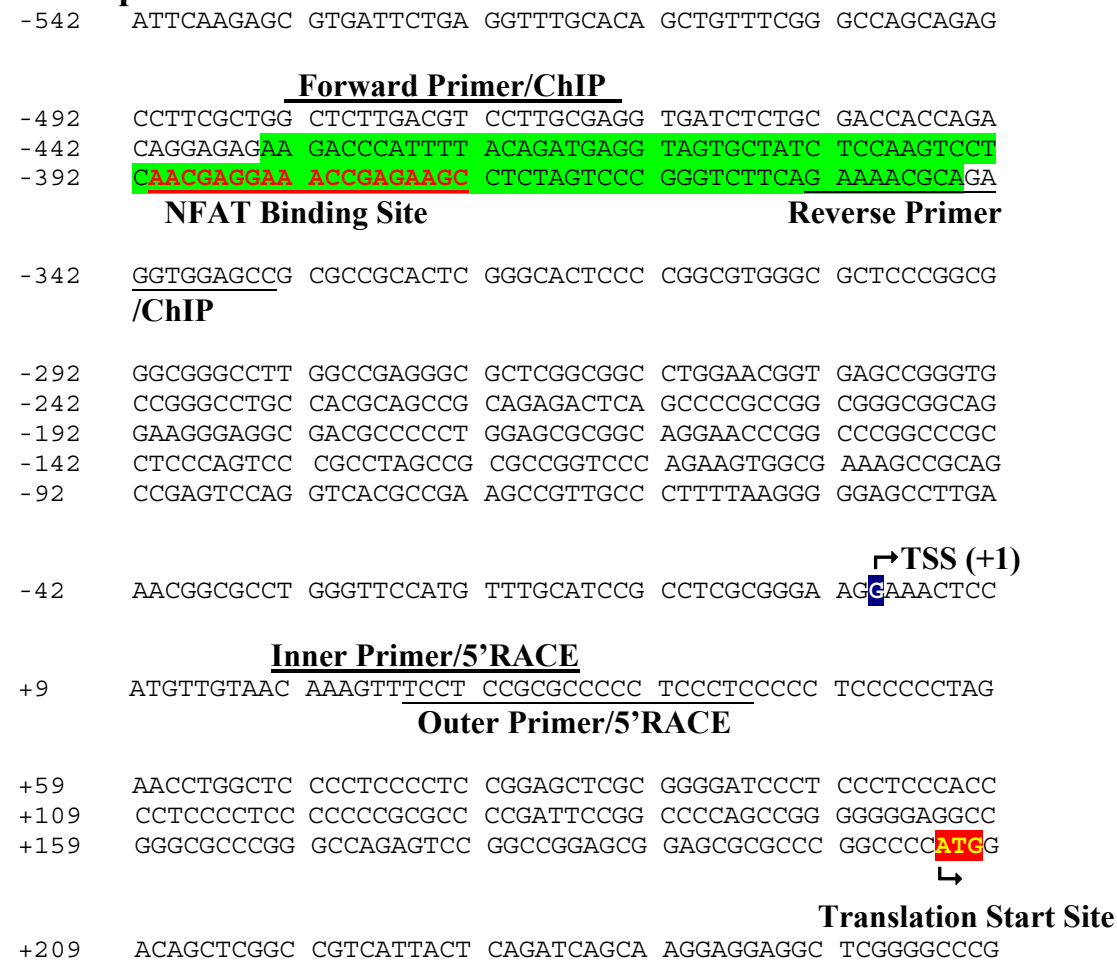


**Online Figure 10d.** Identification of transcription start sites (TSSs) and genomic characteristics of the host genes of the miR-26 family miRNAs using 5'RACE techniques. (**d**) Genomic sequence of Cdtsp1 for miR-26b. TSSs are indicated; putative NFAT binding sites are shown in red letters; the fragments highlighted in green containing NFAT binding sites are those used for promoter activity analysis by luciferase assay. The outer and inner (nested) primers for 5'RACE, and the forward and reverse primers for ChIP experiments, are indicated by lines above or below the sequences.

**Online Figure 11**

## a. Decoy Oligodeoxynucleotides (dODN)

### dODN-NFAT

5′-CGCCCAAAGA**GGAA**AATTTGTTTCATA-3′
3′-GCGGGTTTCTCCTTTTAAACAAAGTAT-5′

### dODN-NC

5′-TAGTTATGCATCACGACCTGAT-3′
3′-ATCAATACGTAGTGCTGGACTA-5′

## b. Small Interfering RNA (siRNA)

### siRNA-NFATc3

5′-UUAUCUUCCCUUCUACCUCCCACUG-3′
3′-AAUAGAAGGGAAGAUGGAGGGUGAC-5′

### siRNA-NFATc4

5′-ACCGAGUCACGAAUCUCCCAUCUAA-3′
3′-UGGCUCAGUGCUUAGAGGGUAGAUU-5′

**Online Figure 11.** The constructs used to inhibit the function of nuclear factor of activated T-cells (NFAT). (**a**) Sequences of decoy oligodeoxynucleotide (dODN) fragments used to sequestrate NFAT (dODN-NFAT) and the negative control dODN (dODN-NC). (**b**) Sequences of small interference RNA (siRNA) used to knock down the cardiac isoforms of NFAT: NFATc3 and NFATc4.

**Online Figure 12**

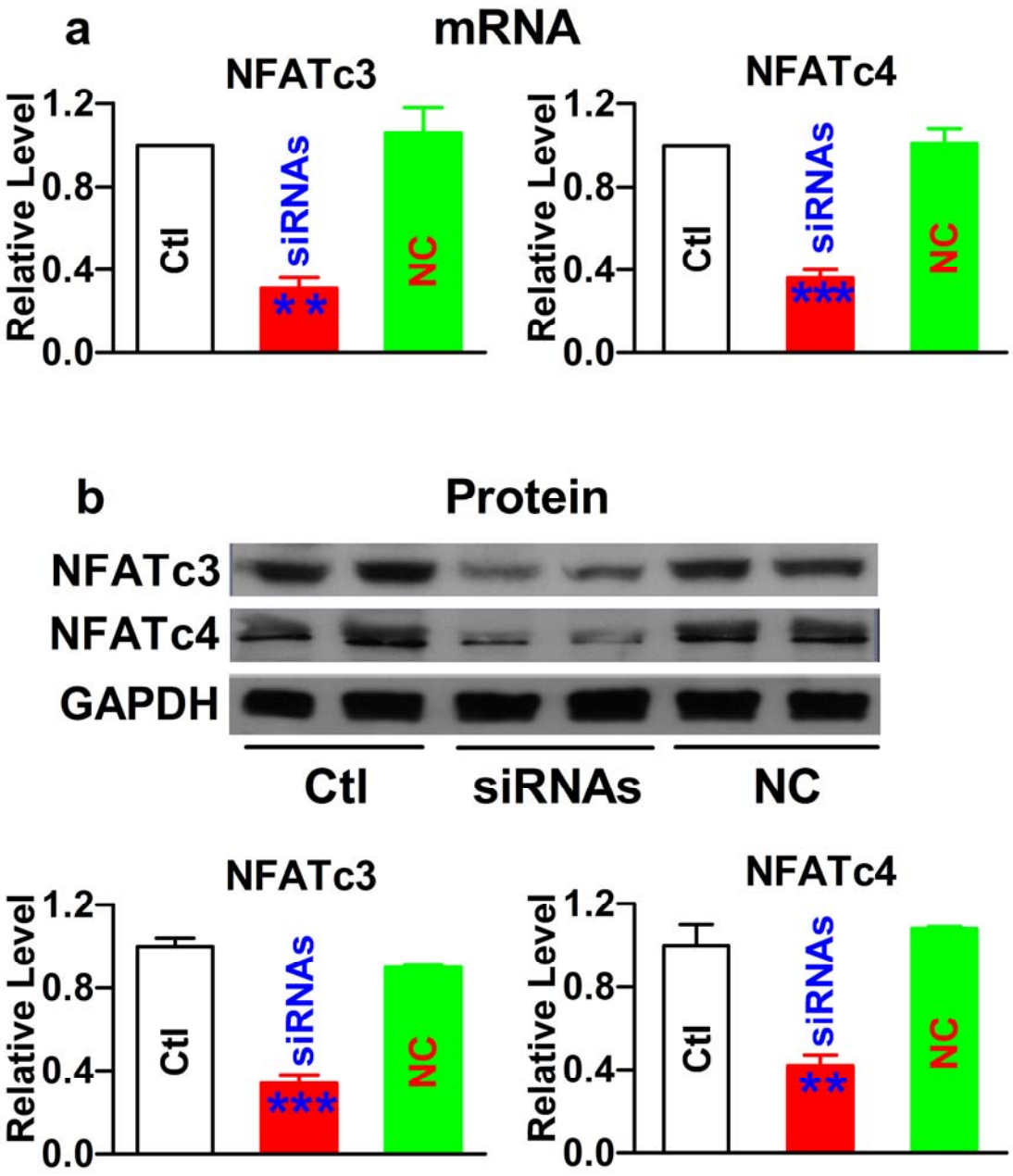


**Online Figure 12.** Verification of the efficacy of siRNAs in knocking down the cardiac isoforms of NFAT, NFATc3 and NFATc4, assessed by qPCR (**a**) and by Western blot analysis (**b**) in H9c2 rat ventricular cells. siRNA to NFATc3 and siRNA to NFATc4 were co-transfected into cells. NC: negative control siRNA. $^{**}p<0.01$, $^{***}p<0.001$ *vs* Ctl; n=4 for each group.

**Online Figure 13**

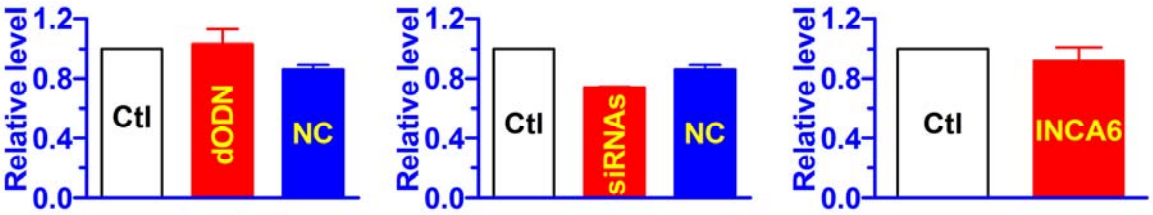


**Online Figure 13.** Effects of NFAT inhibition on expression of miR-1, determined by qPCR in H9c2 rat ventricular cells. Control cells were mock-treated with lipofectamine 2000 for experiments involving transfection of dODN-NFAT or siRNAs. Note that NFAT does not affect miR-1 level. n=3 for INCA group and n=4 for the other groups.

**Online Figure 14**

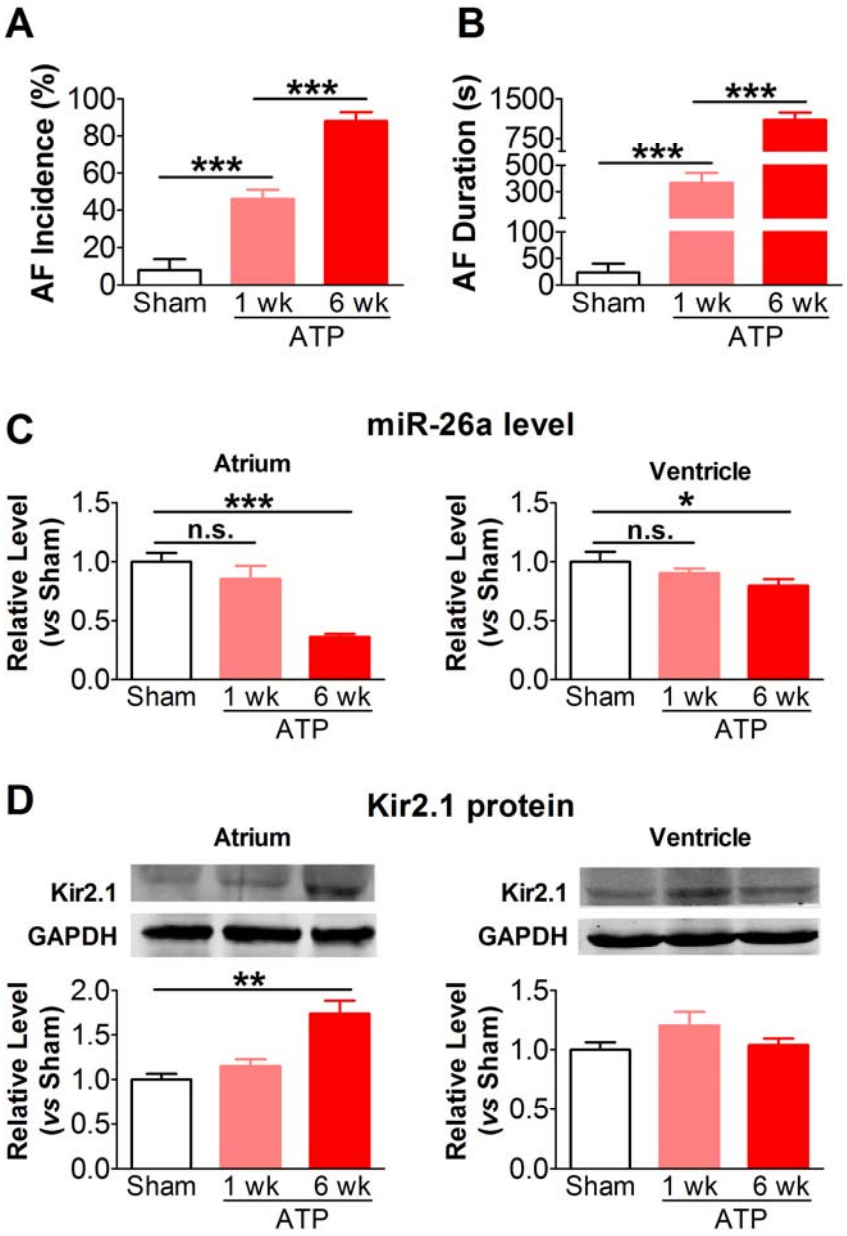


**Online Figure 14. A**. AF incidence in 1-week and 6-week atrial tachypacing (ATP) canine model. **B**. AF duration in ATP canine model. **C**. Quantitative RT-PCR measurement of miR-26a in atrium and ventricle of 1-wk and 6-wk ATP dogs. **D**. Western blot analysis of Kir2.1 protein in atrium and ventricle of 1-wk and 6-wk ATP dogs. n=5/group; *$p$<0.05, **$p$<0.01, ***$p$<0.001.

# ***Online Tables***

**Online Table 1. Clinical characteristics of the patients used* in our study**

| Patient No. | Gender | Age | Diagnosis | Surgery |
|---|---|---|---|---|
| **Non-AF (NAF) Patients** | | | | |
| NAF 1 | male | 43 | Left atrial myxoma **(SR)** | Resection operation |
| NAF 2 | male | 52 | CAD, Tricuspid incompetence. **(SR)** | TVP |
| NAF 3 | female | 46 | RHD, MVS **(SR)** | MVR |
| NAF 4 | female | 22 | CHD **(SR)** | CHD repair. |
| NAF 5 | female | 37 | CAD, Tricuspid incompetence, Cardiac hypertrophy **(SR)** | TVP |
| NAF 6 | male | 55 | Hypertension, MVP **(SR)** | MVR |
| NAF 7 | male | 44 | Infective endocarditis **(SR)** | MVR |
| NAF 8 | female | 23 | CHD **(SR)** | CHD repair. |
| NAF 9 | male | 30 | Tricuspid incompetence **(SR)** | TVP |
| NAF 10 | female | 36 | ASD **(SR)** | ASD closure. |
| **AF Patients** | | | | |
| AF 1 | male | 39 | RHD **(AF)** | AVR |
| AF 2 | female | 68 | RHD, MVS **(AF)** | MVR, RFA |
| AF 3 | male | 55 | MVD, **AF** | MVR, RFA |
| AF 4 | female | 56 | CAD, AVS **(AF)** | AVR |
| AF 5 | male | 52 | RHD **(AF)** | MVR, RFA |
| AF 6 | female | 56 | RHD **(AF)** | MVR |
| AF 7 | female | 55 | RHD, MVS **(AF)** | MVR, RFA |
| AF 8 | female | 66 | RHD, MVS **(AF)** | MVR, RFA |
| AF 9 | female | 50 | RHD, MVD **(AF)** | MVR, RFA |
| AF 10 | female | 59 | RHD, MVD **(AF)** | MVR, RFA |
| AF 11 | male | 57 | RHD, MVD **(AF)** | MVR, RFA |

| | | | | |
|---|---|---|---|---|
| AF 12 | female | 54 | RHD, MVD **(AF)** | MVR, RFA |

*Samples from a total of 22 patients were obtained (10 SR, 12 AF). Of these, 10 (NAF 1-5 and AF 1-5) were used for miRNA expression characterization; 11 (NAF 2-5, 6 and 7; AF 4, 6-9) were used for *KCNJ2* mRNA/protein expression measurement; 6 (NAF 8-10; AF 10-12) were used for immunohistochemical analyses of NFAT translocation.

Abbreviations: AF, atrial fibrillation; ASD, atrial septal defect; AVR, aortic valve replacement; AVS, aortic valve stenosis; CAD, coronary artery disease; CHD, congenital heart disease; MVP, mitral valve prolapse; MVR, mitral valve replacement; MVD, mitral valve disease; MVS, mitral valve stenosis; RFA**,** radiofrequency ablation; RHD, rheumatic heart disease; SR, sinus rhythm; TVP, tricuspid valvuloplasty.

**Online Table 2. Echocardiographic data for mice subjected to miR-26a overexpression or knockdown**

| | WT | Adv-miR-26a | Adv-miR-Free | LNA-antimiR-26a | MM LNA-antimiR-26a |
|---|---|---|---|---|---|
| BW (g) | 29.87±0.81 | 29.66±1.11 | 29.18±0.69 | 29.87±0.81 | 28.42±0.44 |
| HW (g) | 0.13±0.01 | 0.13±0.01 | 0.13±0.002 | 0.12±0.004 | 0.12±0.003 |
| HW/BW (mg/g) | 4.21±0.18 | 4.37±0.17 | 4.40±0.10 | 4.15±0.12 | 4.29±0.10 |
| LAID (cm) | 0.20±0.01 | 0.20±0.02 | 0.21±0.01 | 0.20±0.01 | 0.21±0.01 |
| IVSd (cm) | 0.10±0.01 | 0.09±0.01 | 0.10±0.01 | 0.10±0.003 | 0.11±0.003 |
| IVSs (cm) | 0.12±0.003 | 0.13±0.01 | 0.14±0.01 | 0.13±0.01 | 0.12±0.005 |
| LVIDd (cm) | 0.33±0.01 | 0.32±0.02 | 0.37±0.02 | 0.35±0.02 | 0.30±0.01 |
| LVIDs (cm) | 0.21±0.01 | 0.21±0.03 | 0.24±0.02 | 0.22±0.01 | 0.20±0.01 |
| LVPWd (cm) | 0.11±0.01 | 0.09±0.01 | 0.09±0.005 | 0.11±0.01 | 0.11±0.01 |
| LVPWs (cm) | 0.11±0.01 | 0.09±0.01 | 0.11±0.01 | 0.12±0.01 | 0.13±0.01 |
| EDV (ml) | 0.09±0.01 | 0.09±0.01 | 0.14±0.02 | 0.11±0.02 | 0.08±0.01 |
| ESV (ml) | 0.03±0.01 | 0.03±0.01 | 0.04±0.01 | 0.03±0.03 | 0.02±0.003 |
| EF (%) | 70.0±6.0 | 68.9±7.5 | 70.5±3.0 | 71.3±1.9 | 68.9±4.6 |
| SV (ml) | 0.07±0.01 | 0.06±0.01 | 0.09±0.01 | 0.08±0.01 | 0.05±0.01 |
| FS (%) | 35.4±4.4 | 35.4±5.7 | 34.8±2.1 | 35.2±1.5 | 34.0±3.6 |

BW(g): Body Weight; HW(g): Heart Weight; LAID(cm): Left Atrial Internal Diameter; IVSd(cm): Interventricular Septum thickness at end-diastole; IVSs(cm): Interventricular Septum thickness at end-systolic; LVIDd(cm): Left Ventricular Internal Diameter at end-diastole; LVIDs(cm): Left Ventricular Internal Diameter at end-systolic; LVPWd(cm): LV Posterior Wall thickness in diastole; LVPWs(cm): LV Posterior Wall thickness in systolic; EDV(ml): End Diastolic Volume; ESV(ml): End Systolic Volume; EF(%): Ejection Fraction; SV (ml): Stroke Volume; FS(%): Fractional Shortening. n=5 per group; Data are mean ± SEM.

**Online Table 3. Effects of miR-26a manipulation on electrophysiological parameters of mice**

| | QTc Interval (ms) | QRS Duration (ms) | P-R Interval (ms) |
|---|---|---|---|
| Control/WT | 49.4±1.5 | 9.3±0.5 | 45.7±2.2 |
| Adv-miR-26a | 56.3±2.1* | 10.8±0.7 | 49.1±1.1 |
| Adv-miR-Free | 47.8±1.7 | 9.8±0.5 | 46.9±1.8 |
| LNA-antimiR-26a | 42.8±1.4* | 9.8±0.6 | 45.4±1.2 |
| MM LNA-antimiR-26a | 49.2±2.2 | 9.4±0.5 | 47.5±1.5 |
| Adv-miR-26a + miR-Mask | 48.2±1.9† | 9.4±0.5 | 47.1±2.1 |
| LNA-antimiR-26a + miR-Mimic | 48.5±1.4¶ | 9.5±0.4 | 46.8±1.9 |

Adv-miR-26a: adenovirus vector carrying pre-miR-26a; Adv-miR-Free: empty adenovirus vector; MM LNA-antimiR-26a: mismatched LNA-antimiR-26a; MM LNA-antimiR-1: mismatched LNA-antimiR-1; P-R interval: indicating atrioventricular conduction, mainly determined by L-type $Ca^{2+}$ current; QRS complex: indicating the excitation conduction time in ventricular tissues, mainly determined by $Na^{+}$ current; QTc: heart rate-corrected QT interval; Ctl/WT: control (wild-type) mice without gene-transfer.. *$p$<0.05 *vs* Control/WT; †$p$<0.05 *vs* Adv-miR-26a; ¶$p$<0.05 *vs* LNA-antimiR-26a; Student *t*-test; n=12 mice per group.

**Online Table 4. Predicted NFAT binding motifs in the promoter regions of the host genes for the miR-26 family miRNAs of various species**

| miRNA | Human | Canine | Rat | Mouse |
|---|---|---|---|---|
| **Host gene** | **Ctdspl; Chr3** | **Ctdspl; Chr23** | **Ctdspl; Chr8** | **Ctdspl; Chr9** |
| **miR-26a-1** | | | | |
| **NFAT Binding Sites** | 4430-GTGATGGAAACAT TTGGAG (1/0.97)<br>†4040-ATGGAGGAAATT AGAGATG (1/1)‡<br>3992-CAGGTGGAAAGGC ACTCCA (1/0.95)<br>**3340-CATGAGGAAAAAA TATATC** (1/0.96) | 2922-GCGGAGGAAAAAG TAGCTG (1/0.99)<br>1590-GCTGAGGAAATAA ACTAGG (1/1)<br>1479-CCTCAGGAAACAG TGGTCA (1/0.95)<br>1173-CACGGAAATTCAC ATGAAA (1/0.88) | 2651-TATGGAAAGCTTA ACTCTG (1/0.89)<br>2466-TTTGGAAACAGGC CCACTC (1/0.87)<br>2285-AGAGGAAAGAGAA TGGCTG (1/0.87)<br>2283-GGAGAGGAAAGAG AATGGC (1/0.99) | 2480-GTTGGAAATATCA CCTGTT (1/0.89)<br>1293-GTTGGAAAGAAAC TTCCAG (1/0.88)<br>1213-CGTGGAAAAGTAA GGAAGT (1/0.92)<br>59-AAGGAGGAAAGCGAG GAGG (1/0.97) |
| **Host Gene** | **Ctdsp2; Chr12** | **Ctdsp2; Chr10** | | **Ctdsp2; Chr10** |
| **miR-26a-2** | | | | |
| **NFAT Binding Sites** | 4480-TTGGAGGAAAGGA GAATGA (1/0.97)<br>**3618-CCAGAGGAAAGGG GATACA** (1/0.97)<br>3385-CTATAGGAAAGAG GCCCAC (1/0.96)<br>3361-TCTGGAAAGCTCT GTAGGG (1/0.92) | 2529-GTTGGAAACAGGG AAGCCT (1/0.99) | | 2507-GGGGGAAAAAGAC AGGGTG (1/0.85)<br>1535-GAAGAGGAAATGA ACAGGA (1/0.97)<br>1177-AGGGGAAAAAAGA GCAGTG (1/0.83)<br>304-GTCGGAAACACAAA CACCC (1/0.83) |
| **Host Gene** | **Ctdsp1; Chr2** | **Ctdsp1; Chr37** | **Ctdsp1; Chr9** | **Ctdsp1; Chr1** |
| **miR-26b** | | | | |
| **NFAT Binding Sites** | 1134-GGAGAGGAAAGCG CGCCAC (1/0.97)<br>**373-AACGAGGAAAAAGA CCAAC** (1/0.99)<br>371-AACGAGGAAACCGA GAAGC (1/0.84) | 209-GGGGAGGAAACTCC ATGTT (1/0.97)<br>190-GCGGAGGAAACTTT GTTAC (1/0.97) | 2999-TTTAAGGAAAGAG GCCCAC (1/0.98)<br>2557-TGTGAGGAAACAA ACAAAC (1/1)<br>107-GGGGAGGAAACTCC ATGTT (1/0.97)<br>88-GCGGAGGAAACTTTG TTAC (1/0.97) | 2751-TTTAAGGAAAGAG GCCTAC (1/0.98)<br>2271-TGCAAGGAAACAA ACAAAC (1/0.96)<br>1454-ACAGGAAAAATAA AAAATA (1/0.88)<br>434-GCTGGAAAAATGGC TCAGG (1/0.92) |

Ctdsp: carboxy-terminal domain RNA polymerase II polypeptide A small phosphatase; Chr: chromosome; †The numbers before the sequences indicate the relative positions of the putative NFAT binding sites in the genome. ‡The numbers in the brackets indicate the scores for similarity of the putative NFAT *cis*-acting elements in the promoter regions of the host genes for the miR-26 family miRNAs to the canonical core binding sites and overall matrix for NFAT action, respectively; the sequences highlighted in yellow with boldface are the ones used for EMSA experiments.

**Online Table 5. The primers used for PCR-amplification of miR-26 promoter sequences spanning NFAT *cis*-elements for chromatin immunoprecipitation assay (ChIP)**

| Host Gene /miRNA | Forward Primer | Reverse Primer |
|---|---|---|
| **Ctdspl/miR-26a-1** | 5′-AAGTTTTTGTCACTCTCAGG-3′ | 5′-GTACCTATCCATGAGGAAAA-3′ |
| **Ctdsp2/miR-26a-2** | 5′-GGGGTAATGGGGACACTGCT-3′ | 5′-GGAGATAGCTGAAGCCAGGT-3′ |
| **Ctdsp1/miR-26b** | 5′-GCTCTTGACGTCCTTGCGAG-3′ | 5′-GGCTCCACCTCTGCGTTTTC-3′ |

**Online Table 6. The gene-specific primers (GSP) used for 5'RACE to identify the transcription start sites of the host genes for miR-26 miRNA family members**

| Host Gene /miRNA | GSP1 (Outer) | GSP2 (Nested) |
|---|---|---|
| **Ctdspl/miR-26a-1** | 5′-GCAACCGGCCCTCGTCCTCCT-3′ (40 bp downstream of ATG) | 5′-CTCGTCCTCCTTGGGGTTGGTC-3′ (30 bp downstream of ATG) |
| **Ctdsp1/miR-26b** | 5′-GAGGGAGGGGGCGCGGAGGA-3′ (161 bp upstream to ATG) | 5′-GGCGCGGAGGAAACTTTG-3′ (170 bp upstream to ATG) |
| **Ctdsp2/miR-26a-2** | 5′-CCTCCCGGCTCTCGACTC-3′ (387 bp upstream to ATG) | 5′-TCTCGACTCGGCCTCTTCAC-3′ (396 bp upstream to ATG) |

"ATG" indicates translational start site of the host genes.

# CHAPTER 4. The Control of Adverse Structural Remodeling by MiRNAs in AF

As noted in Sections 1.3.2 and 1.5.4 of the Introduction, atrial fibrosis is a key component of AF-associated adverse atrial structural remodeling and is critically determined by fibroblast activation, which requires cellular $Ca^{2+}$ entry. TRP channels are well known to be responsible for $Ca^{2+}$ entry in various cell types; thus, they may likely contribute to atrial fibrotic remodeling. Emerging evidence from a recent study has indicated an important role of TRPM7 channels in AF-associated fibrotic remodeling [168]. However, whether other TRP channels are also involved in this remodeling process remain unclear. This is a potentially-important question, given the fact that many TRP channels including TRPM7 are known to be abundantly expressed in cardiac fibroblasts with similar functions and structure [164, 168]. Notably, a recent study showed that, unlike other TRP members, TRPC3 is mainly enriched in freshly-isolated atrial fibroblasts and this enrichment diminishes upon fibroblast differentiation to myofibroblasts, suggesting a potentially-important role of TRPC3 in determining fibroblast function [237]. Hence, in this Chapter, we carried out studies to determine whether TRPC3 plays a role in AF-induced fibrosis by promoting fibroblast activation and whether miRNAs are also involved in this process.

This work has been accepted for publication in ***Circulation***.

Harada M, **Luo X**, Qi X, Tadevosyan A, Maguy A, Ordog B, Ledoux J, Kato T, Naud P, Voigt N, Shi Y, Kamiya K, Murohara T, Kodama I, Tardif J, Schotten U, Van Wagoner D, Dobrev D, Nattel S. TRPC3-dependent Fibroblast Regulation in Atrial Fibrillation. ***Circulation.*** 2012 (in press).

## 4.1 TRPC3-dependent Fibroblast Regulation in Atrial Fibrillation

Masahide Harada, MD, PhD; Xiaobin Luo, MSc; Xiao Yan Qi, PhD; Artavazd Tadevosyan, MSc; Ange Maguy, PhD; Balazs Ordog, PhD; Jonathan Ledoux, PhD; Takeshi Kato, MD, PhD; Patrice Naud, PhD; Niels Voigt, MD; Yanfen Shi, PhD; Kaichiro Kamiya, MD, PhD; Toyoaki Murohara, MD, PhD; Itsuo Kodama, MD, PhD; Jean-Claude Tardif, MD; Ulrich Schotten, MD, PhD; David R. Van Wagoner, PhD; Dobromir Dobrev, MD; Stanley Nattel, MD

**Short title:** Harada−TRPC3-channels and cardiac fibroblast function

**Subject Codes:** [132] Arrhythmias-basic studies; [152] Ion channels/membrane transport

**Word Count:** 7000 (excluding Short title, Subject Codes and Word Count)

---

From Department of Medicine and Research Center (M.H.; X.L; X.Y.Q.; A.T.; A.M.; B.O.; J.L.; T.K.; P.N.; Y.S.; J.C.T.; S.N.); Montreal Heart Institute and Université de Montréal, Montreal, Quebec, Canada; Division of Experimental Cardiology (N.V.; D.D.), Medical Faculty Mannheim, University of Heidelberg, Mannheim, Germany; Department of Cardiovascular Research (K.K.; I.K.), Research Institute of Environmental Medicine, Nagoya University, Japan; Department of Cardiology (T.M.), Nagoya University Graduate School of Medicine, Nagoya, Japan; Department of Physiology (U.S.), Maastricht University, Maastricht, Netherlands; Department of Molecular Cardiology (D.R.V.W.), Cleveland Clinic, Cleveland, Ohio.

Correspondence to Stanley Nattel, 5000 Belanger St E, Montreal, Quebec, H1T 1C8, Canada

## Abstract

**Background:** Fibroblast proliferation and differentiation are central in atrial fibrillation (AF)-promoting remodeling. Here, we investigated fibroblast regulation by $Ca^{2+}$-permeable transient receptor potential canonical-3 (TRPC3) channels. **Methods and Results:** Freshly-isolated rat cardiac-fibroblasts abundantly expressed TRPC3 and had appreciable non-selective cation currents ($I_{NSC}$) sensitive to a selective TPRC3-channel blocker, pyrazole-3 (3-μmol/L). Pyrazole-3 suppressed angiotensin-II-induced $Ca^{2+}$-influx, proliferation and α-smooth-muscle actin (αSMA) protein-expression in fibroblasts. $Ca^{2+}$-removal and TRPC3-blockade suppressed extracellular-signal regulated kinase (ERK)-phosphorylation, and ERK-phosphorylation inhibition reduced fibroblast-proliferation. TRPC3-expression was upregulated in atria from AF-patients, goats with electrically-maintained AF and tachypacing-induced heart-failure dogs. TRPC3-knockdown (shRNA-based) decreased canine atrial-fibroblast proliferation. In left-atrial (LA) fibroblasts freshly isolated from dogs kept in AF for 1 week by atrial-tachypacing, TRPC3 protein-expression, currents, ERK-phosphorylation and extracellular-matrix gene-expression were all significantly increased. In cultured LA-fibroblasts from AF-dogs, proliferation-rates, αSMA-expression and ERK-phosphorylation were increased, and suppressed by pyrazole-3. MicroRNA-26 was downregulated in canine AF-atria; experimental micro-RNA-26 knockdown reproduced AF-induced TRPC3-upregulation and fibroblast-activation. MicroRNA-26 has Nuclear Factor of Activated T-cells (NFAT) binding-sites in the 5'-promoter-region. NFAT-activation increased in AF-fibroblasts and NFAT negatively regulated microRNA-26 transcription. In vivo pyrazole-3 administration suppressed AF while decreasing fibroblast proliferation and extracellular-matrix gene-expression.

**Conclusions:** TRPC3-channels regulate cardiac fibroblast proliferation and differentiation, likely by controlling $Ca^{2+}$-influx that activates ERK-signaling. AF increases TRPC3-channel expression by causing NFAT-mediated downregulation of microRNA-26 and causes TRPC3-dependent enhancement of fibroblast proliferation and differentiation. In vivo TRPC3-block prevents AF-substrate development in a dog model of electrically-maintained AF. TRPC3 likely plays an important role in AF-promoting fibroblast pathophysiology and is a novel potential therapeutic target.

**Keywords:** arrhythmia – calcium – ion channels – fibrillation – remodeling

## Introduction

Atrial fibrillation (AF) is the most common arrhythmia in clinical practice, increasing both morbidity and mortality.[1,2] As the utility of conventional anti-arrhythmic agents targeting cardiac ion-channels is limited by inefficacy and side effects, new treatment strategies are required.[1-3] An improved understanding of underlying mechanisms may help in designing novel therapies.[2] Under pathological conditions, cardiac fibroblasts first proliferate and then differentiate into myofibroblasts that secrete profibrotic extracellular-matrix.[3,4] Atrial fibrotic remodeling causes conduction abnormalities and may promote fibroblast-cardiomyocyte electrical interactions that favor AF occurrence and maintenance.[5,6] Therefore, fibroblast control mechanisms could constitute novel antiarrhythmic targets. While it is known that cellular $Ca^{2+}$-homeostasis regulates fibroblast-function,[6] the precise regulatory mechanisms remain unclear.

Transient receptor potential (TRP)-channels, activated by cell-stretch and other pathological stimuli, regulate cellular $Ca^{2+}$entry.[6] TRP-channels modulate fundamental cell-functions like cell proliferation and death.[6-8] Mechanical stretch and related stimuli contribute to arrhythmic substrates;[3] TRP-channels are candidates to link arrhythmic-remodeling stimuli to arrhythmia-promoting cardiac-fibroblast responses. In preliminary studies (Supplemental Figure 1), we noted cell-selective expression of TRPC3 in freshly-isolated fibroblasts, along with TRPC3-downregulation upon fibroblast-differentiation to myofibroblasts, identifying TRPC3 as a potential modulator of fibroblast function. We undertook the present study to test the following hypotheses: (1) TRPC3-subunits play a role in fibroblast function in normal hearts and in an AF-model; (2) fibroblast TRPC3-expression is upregulated in AF under the control of discrete microRNA-related molecular mechanisms; and (3) in vivo TRPC3-inhibition can suppress AF-associated remodeling.

## Methods

A detailed description of methods used in this study is available in the online Data Supplement.

### Cardiac fibroblast isolation and culture

Fibroblasts were isolated from adult rat or dog hearts as previously described.[9] Tissues were digested with collagenase-II and cardiomyocytes removed by low-speed centrifugation and passage through a 20-μm nylon filter. Fibroblasts were concentrated by high-speed centrifugation (2,000 rpm, 10 min). Freshly-isolated fibroblasts or cells in primary culture within 3 days of isolation (Supplemental Figure 2A) were used in most experiments. Long-term cultured first-passage cells (2-3 weeks), which express alpha-smooth muscle actin (αSMA) and show actin-fiber organization (Supplemental Figure 2B) were used in rat-myofibroblast studies.

### Atrial tissue-samples from humans, goats, and dogs

Right-atrial appendage biopsies were obtained from patients in sinus rhythm and with chronic AF during coronary-artery bypass-graft surgery following informed consent as approved by the ethical-review committee of Dresden University of Technology. AF was induced in chronically-instrumented goats using repetitive burst-pacing for 10 days.[10] Congestive heart failure (CHF) dogs with an AF substrate were created by ventricular tachypacing (240 bpm, 2 weeks).[11] Normal goats and dogs were used as controls. Right-atrial tissue samples were collected and fast-frozen in liquid-$N_2$.

**AF-dogs**

A total of 48 mongrel dogs (20-36 kg) were divided into control and atrial-tachypacing groups. Animal-care procedures followed National Institutes of Health guidelines and were approved by the Animal Research Ethics Committee of the Montreal Heart Institute. Dogs were anesthetized with ketamine (5.3 mg/kg i.v.)/diazepam (0.25 mg/kg, i.v.)/isoflurane (1.5%), intubated, and ventilated. A unipolar pacing lead was inserted into the right-atrial appendage under fluoroscopic guidance and connected to a pacemaker in the neck. Bipolar electrodes were inserted into the right-ventricular apex and right-atrial (RA) appendage for electrogram-recording. Atrioventricular-block/ventricular-pacing (employed in many studies of atrial-tachycardia remodeling[12]) were not performed, to more closely mimic spontaneous clinical AF-episodes. The atrial pacemaker was programmed to stimulate the RA at 600-bpm for 1 week, with fibrillatory atrial activity maintained during pacing as assessed by daily ECG and intracardiac recordings. Echocardiography was performed on Day 0 (baseline) and Day 7 to assess left-atrial (LA) dimension, LA systolic function and left-ventricular diastolic volume.

For in vivo pyrazole-3-treatment of AF-dogs, Alzet osmotic pumps were implanted subcutaneously in the back to continuously-administer intravenous pyrazole-3 (0.1-mg/kg/day in DMSO and polyethylene glycol) or vehicle during atrial-tachypacing (Supplemental Figure 3).

**Electrophysiological studies**

A terminal open-chest electrophysiological study (EPS) was performed on Day 7. Dogs were anesthetized with morphine (2 mg/kg, s.c.) and α-chloralose (120 mg/kg, i.v., followed by 29.25 mg/kg/h), and ventilated. After median sternotomy, atrial effective refractory

period (ERP) and mean AF-duration induced by burst pacing were measured as previously described.[12]

**TaqMan low-density arrays**

RNA was extracted using TRIzol. RNA-integrity was assessed via Agilent Bioanalyzer. (RIN>7.5 required). cDNA was synthesized with High-Capacity cDNA Reverse Transcription Kit and random-hexamer primers. TaqMan low-density arrays (TLDAs) were used in two-step RT-PCR.[13] Real-time PCR was performed on the 7900HT Fast Real-Time PCR System. TRP-subunit genes were investigated using inventoried Taqman assays. The mean expression of genes with a Ct-value <30 was used as the reference.[14]

**Whole-cell patch clamping**

Whole-cell voltage-clamp was performed to record non-selective cation-current ($I_{NSC}$) at 37°C. The pipette-solution contained (mmol/L): 135 CsCl, 0.1 $CaCl_2$, 10 EGTA, 4.0 MgATP, 1.0 $MgCl_2$, 10 HEPES, 6.6 sodium-phosphocreatine, 0.3 Na-GTP (pH 7.4/CsOH). The bath-solution contained (mmol/L): 140 NaCl, 5.4 TEA-Cl, 2.0 $CaCl_2$, 1.0 $MgCl_2$, 10 HEPES, 10.0 glucose (pH 7.4/CsOH). Nifedipine (5-µmol/L) was used to block any L-type $Ca^{2+}$-current. $Na^{+}$-current was inactivated with a holding-potential of 0 mV. Currents were elicited with 3-s voltage-ramp protocols (1 mV/ms, from -110 mV to 100 mV, 0.1 Hz), at a holding potential of 0 mV.[15]

**Cell-proliferation and cell-cycle analysis**

Cardiac fibroblasts were cultured in T25 culture-flasks ($2.0\times10^5$ cells/flask, 25 $cm^2$ growth-area) for each treatment-group. After incubation, cells were harvested following trypsinization, and then fixed with ice-cold 75% ethanol. Samples were stored at -20°C

until analysis. Pelleted cells were re-suspended and incubated (4°C, 30 minutes) in staining solution containing propidium-iodide. Cell-numbers and DNA content-frequency histograms were obtained via FACScan (constant flow-rate, 60 µl/min, 5-min acquisition time).

**Western blots**

Protein was extracted, quantified, and processed.[12,16] Cytoplasmic and nuclear protein-fractions were extracted from fresh fibroblasts with ProteoExtract Subcellular Proteome Extraction Kit (Calbiochem, Darmstadt, Germany). Protein-samples were separated by gel-electrophoresis and transferred to polyvinylidene-difluoride membranes. Membranes were blocked and incubated with mouse anti-α smooth-muscle actin, anti-phospho-p44/42-MAP-kinase, anti-TRPM7, anti-NFATc3, anti-HSP70, anti-Lamin A/C and anti-vimentin, rabbit anti-TRPC3, anti-TRPC1 (1/200, Alomone), anti-calsequestrin and anti-NFATc4antibodies. Secondary antibodies conjugated to horseradish-peroxidase were used for detection via chemiluminescence.

**Confocal-imaging**

Cultured/freshly-isolated fibroblasts or left atrial tissue cryosections were fixed with 2%-paraformaldehyde, washed with PBS, and incubated with mouse anti-alpha SMA, goat anti-vimentin, mouse anti-NFATc3, rabbit anti-NFATc4, followed by donkey anti-mouse IgG-Alexa Fluor-555, donkey anti-rabbit IgG-Alexa Fluor-488, donkey anti-goat IgG-Alexa Fluor-488, and/or TOPRO-3 iodide. Apoptosis was assessed by TUNEL-assay with ApopTag. Fluorescent-images were obtained via Zeiss LSM-710 or OLYMPUS Fluoview FV1000 inverted confocal microscope.

**$Ca^{2+}$-imaging**

Primary cultured rat-fibroblasts (1-day culture) were loaded with Fluo-4 (10-μmol/L) in phenol-free M199-medium in the presence of pluronic acid (2.5 μg/ml) for 50 min. $Ca^{2+}$-imaging was obtained with an Andor Revolution confocal system and a Xion camera (Andor Technologies) mounted on an upright Nikon FN-1 microscope. Fluo-4 was excited at 488-nm; emitted fluorescence collected at 495 nm. Images (512×512 pixels) were acquired at 15 frames/sec. $F_O$ was determined by averaging fluorescence from 10 consecutive baseline images.[17]

**qPCR**

To study microRNA, RNA/microRNA were extracted with TRIzol/mirVana miRNA Extraction Kit (Ambion). Real-time RT-PCR was performed with 6-carboxy-fluorescein (FAM)-labeled fluorogenic Taq-Man primers. Fluorescence-signals were detected in duplicate, normalized to β2-microglobulin RNA for total RNA and to U6 snRNA for microRNA, and quantified with MxPro qPCR-software (Stratagene).[16]

**TRPC3-knockdown**

TRPC3-knockdown lentivirus-vector plasmid was obtained from Open Biosystems (Oligo ID: V2LMM_11490). A scrambled shRNAmir over-expressing virus was used as a negative control. For lentivirus-infection, 3-day cultured fibroblasts were plated in T25 culture flasks at $4\times10^3$ cells/$cm^2$, infected at 50 m.o.i. and incubated for 3 days before experiments.

**microRNA (miR) overexpression/knockdown**

For overexpression, sense and antisense oligoribonucleotides were synthesized by Invitrogen and the double-stranded RNA was created by annealing. A scrambled RNA was the negative control. For knockdown, antisense anti-miR oligonucleotides (AMO26a) with locked nucleic acid (LNA)-technology were synthesized by Exiqon (Woburn, MA). Scrambled oligonucleotides with methylene bridges were used as negative controls. Dog LA-fibroblasts in primary culture were transfected with miR-26a duplex (100-nmol/L), AMO26a (10-nmol/L), and/or control-sequences with lipofectamine-2000 (Invitrogen).[18]

**Dual luciferase-reporter assay**

A fragment containing the miR target-sequence was synthesized by Invitrogen and was used as a template for PCR amplification. The PCR product was subcloned in the pMIR-REPORT luciferase miR-expression reporter vector. HEK293 cells were transfected with 50-ng pMIR-REPORT, 0.5ng pRL-TK (for internal control) and miR-26a duplex (10-nmol/L) and/or AMO26a (3-nmol/L) with lipofectamine-2000.

**Statistical analysis**

Data are presented as mean±SEM. Two-way ANOVA with multiple-group comparisons (Bonferroni-corrected t-test) was applied to data with two or more main-effect factors. One-way ANOVA was applied for single main-effect factor experiments. Repeated-measure analyses were used when the same set of subjects/materials were exposed to multiple interventions. Students' *t*-tests were used for comparisons involving only two groups. For multiple comparisons with Bonferroni correction, adjusted *P*-values were calculated by multiplying original *P*-values by the number of comparisons (*N*) performed; values shown are adjusted values ($N \times P$). Two-tailed $P<0.05$ was considered statistically significant. For

additional details, see Online Supplement.

## Results

### TRPC3-mediated $I_{NSC}$ and $Ca^{2+}$ entry

$I_{NSC}$-recordings from freshly-isolated rat fibroblasts are shown in Figure 1A and Supplemental Figure 2C. $I_{NSC}$ was substantially suppressed by superfusion with the TRPC3-selective blocker pyrazole-3 (Figure 1B)[19] and by the general TRP-channel blocker, gadolinium ($Gd^{3+}$, 100-μmol/L, Supplemental Figure 2C). Passage-cultured myofibroblasts (Supplemental Figure 2B) showed larger membrane-capacitance than fibroblasts (16.8±1.4 pF vs. 6.4±0.4 pF, $P<0.01$) but had much smaller $Gd^{3+}$- and Pyr3-sensitive $I_{NSC}$, consistent with qPCR-data (Supplemental Figure 2D-F).

We then tested whether TRPC3-channels contribute to $Ca^{2+}$-entry in cardiac fibroblasts. Because diacylglycerol (DAG) has been suggested to be a physiological activator of TRPC3,[20] we examined the effect of TRPC3-blockade on $Ca^{2+}$-entry induced by 1-oleoyl-2-acetyl-sn-glycerol (OAG) and angiotensin-II, which activate DAG-receptors directly and indirectly respectively. Both angiotensin-II (Figures 1C-D) and OAG (Supplemental Figures 4A-B) induced fibroblast $Ca^{2+}$-entry, which was prevented by Pyr3, suggesting that TRPC3-channels are needed for OAG- and angiotensin-II-induced $Ca^{2+}$-entry.

### Role in fibroblast proliferation and differentiation

We next examined whether TRPC3-channel block affects cardiac fibroblast proliferation. Rat cardiac fibroblasts were maintained in the presence or absence of $Gd^{3+}$, Pyr3 or control-vehicle for up to 1 day in primary culture. After 24-hour culture in vehicle-medium (CTL), the number of fibroblasts increased substantially (Figure 1E). After 1-hour and 24-hour treatment, fibroblasts were collected for proliferation-analysis using flow cytometry. Representative DNA-content histograms showing the G2/M-phase

cell-content, an index of DNA-duplication, are provided in Supplemental Figures 5A-B. Pyr3 significantly slowed the increase in fibroblast-number and G2/M-phase cell-content (Figures 1E-F), as did $Gd^{3+}$ (Supplemental Figures 5C-D). Pyr3 also significantly increased the percentage of TUNEL-positive fibroblasts versus control (Supplemental Figure 6). These data suggest that TRPC3-channels regulate cardiac fibroblast survival and proliferation.

After fibroblasts proliferate, they differentiate into extracellular-matrix (ECM)-secreting myofibroblasts characterized by altered morphology and increased αSMA-expression. Supplemental Figure 7A shows confocal images of rat fibroblasts, cultured with or without Pyr3, stained with anti-αSMA-antibodies. The spindle-shaped expansion and αSMA-enhanced expression associated with myofibroblast-differentiation was inhibited by 3-μmol/L Pyr3. Figure 1G shows representative α-SMA-immunoblots on cultured rat-fibroblasts: αSMA protein-expression was significantly decreased by Pyr3 (Figure 1H). Thus, TRPC3-channels participate in fibroblast differentiation into myofibroblasts. We also examined the effect of TRPC3-blockade on already-differentiated myofibroblasts. Consistent with downregulation of TRPC3 in myofibroblasts, their cell-number, G2/M-phase cell-content and αSMA-expression were unchanged by Pyr3 (Supplemental Figures 7B-D). Thus, once fibroblasts differentiate into myofibroblasts, TRPC3-channels appear no longer to be involved their regulation.

**TRPC3-mediated $Ca^{2+}$-entry, ERK-1/2 phosphorylation and fibroblast activation**

We then examined whether TRPC3-mediated $Ca^{2+}$-entry acts by modulating $Ca^{2+}$-dependent ERK-1/2-activation, which affects cell-survival and fibroblast-activation.[21,22] Fibroblasts were cultured for 24 hours in three conditioned media: 1) 0.4-mmol/L $Ca^{2+}$, 2) 2.4-mmol/L $Ca^{2+}$, and 3) 2.4-mmol/L $Ca^{2+}$ with Pyr3.

ERK-1/2-phosphorylation was significantly decreased in low-[$Ca^{2+}$] medium and with exposure to Pyr3 (Figure 2A). Next, we examined the effect of extracellular $Ca^{2+}$-concentration on fibroblast proliferation. The increase in cell-number of cultured fibroblasts and the G2/M-phase cell-content were significantly smaller with lower [$Ca^{2+}$] in the culture-medium (Figures 2B-C). A selective ERK-pathway inhibitor, PD98058 (50-μmol/L), also significantly reduced the number of fibroblasts and the G2/M-phase cell-content after 24-hour culture (Figures 2D-E). The data in Figure 2 suggest that TRPC3-mediated $Ca^{2+}$-influx contributes to ERK-1/2-activation that regulates fibroblast proliferation.

**TRPC3-knockdown suppresses atrial-fibroblast proliferation**

We were unable to study TRPC3-knockdown in rat-fibroblasts because spontaneous TRPC3-downregulation in culture was almost complete over the time-period needed for lentiviral-mediated knockdown. However, we noted that TRPC3-downregulation was slower in cultured dog-atrial fibroblasts, which were used to study the effects of TRPC-knockdown. TRPC3-subunit mRNA and protein expression significantly decreased in TRPC3-shRNA-infected fibroblasts; TRPC6 mRNA remained unchanged (Supplemental Figures 8A-B). The fold-increase in cultured-fibroblast cell-number was significantly attenuated in TRPC3-shRNA-infected fibroblasts (Supplemental Figure 8C), as was the G2/M-phase cell-content (Supplemental Figure 8D), indicating that TRPC3-channels are involved in canine atrial-fibroblast proliferation.

**Atrial TRPC3-expression in large animal/human AF-substrates**

To assess a potential role in the AF-substrate, we examined the protein-expression of TRPC1, TRPC3, and TRPM7-subunits in RA tissue-samples from AF-patients, AF-goats, and CHF-dogs with an AF-substrate. Atrial TRPC3-expression significantly increased in all groups with AF-substrates (Supplemental Figures 9A-C) whereas TRPC1 and TRPM7 remained unchanged (Supplemental Figures 9D-I).

**Atrial remodeling in dogs with electrically-maintained AF**

To examine further the potential role of TRPC3 in AF, we used a canine model of electrically-maintained AF. Representative surface and intracardiac day-7 ECG-recordings showing irregular/rapid atrial activity and irregular ventricular responses typical of AF are shown in Figure 3A. Spontaneous AF was maintained after pacing-cessation. Fibrillatory electrical activity and spontaneous post-pacing AF were consistently observed during the 1-week pacing period (Supplemental Figure 10). Immediately following tachypacing-onset (recordings at 6.0±0.2 mins post-onset), ventricular activation rate increased by 55%, but ventricular rate then returned to control values by Day 3 (Supplemental Figure 11A). At end-study, atrial and ventricular-filling pressures were slightly but significantly increased in AF-dogs (Supplemental Table 1). Supplemental Figure 11B illustrates atrial structural remodeling in AF-dogs, with significant changes in LA diastolic area and fractional area-change (Supplemental Figures 11C-D).

AF-dogs showed electrical remodeling manifested by reduced ERPs (Figure 3B) and increased duration of burst-pacing induced AF (Figure 3C). LA fibrosis and vimentin-staining (index of fibroblast-density) were assessed by histomorphometry (Figure 3D). Fibrous-tissue content was unchanged (Figure 3E), but vimentin-positive area

(Figure 3F) and protein-expression (immunoblots, Figure 3G) increased significantly in AF-dogs.

**TRPC3-regulation of atrial-fibroblast activation in AF-dogs**

Figure 4A shows $I_{NSC}$ before and after 3-μmol/L Pyr3 in freshly-isolated LA-fibroblasts. Pyr3-sensitive current increased significantly in LA-fibroblasts of AF-dogs (Figure 4B), corresponding to increased TRPC3-subunit protein-expression in freshly-isolated LA-fibroblasts (Figure 4C). ERK-phosphorylation (Figure 4D) and ECM gene-expression (Figure 4E) were also significantly increased in LA-fibroblasts of AF-dogs.

The cell-number increase-rate, G2/M-phase cell-content and αSMA protein-expression all increased in LA-fibroblasts of AF-dogs (Figure 5A-C), indicating increased fibroblast proliferation and differentiation. In vitro treatment of AF-fibroblasts with Pyr3 significantly decreased these fibroblast-activation indices (Figures 5D-F). ERK-activation was significantly increased in AF (Figure 5G). ERK-phosphorylation in AF-dogs was significantly reduced after 24-hour treatment with Pyr3 (Figure 5H). These data suggest that TRPC3-channels are an important contributor to fibroblast-activation in AF.

**MiR-26 regulation of TRPC3 channels**

MicroRNAs post-transcriptionally regulate protein-expression in many pathological conditions.[1] MiR-target prediction (Target scan) suggested that miR-26 targets the TRPC3-gene (Supplemental Figure 12A). Expression of the 2 miR-26 isoforms, miR-26a and b, which have identical seed-sequences, was significantly decreased in freshly-isolated LA-fibroblasts from AF-dogs (Figure 6A). Other miRs involved in cardiac remodeling[1] were studied and miR-133 was also downregulated; however, miR-26 was particularly

strongly-expressed in fibroblasts (Figure 6B) whereas miR-133 expression was cardiomyocyte-selective (Figure 6C). Neither miR-1 nor miR-133 target TRPC3.

We then examined post-transcriptional regulation of TRPC3 by miR-26a with dual luciferase reporter assay. Luciferase vectors carrying the miR-26a target gene-sequence of TRPC3 were cotransfected along with miR-26a duplex and/or antisense anti-miR-26a oligonucleotides (AMO26a, Supplemental Figure 12B) into HEK-293 cells. MiR-26a overexpression significantly decreased luciferase-readout whereas knockdown of endogenous miR-26a by AMO26a significantly increased luciferase-fluorescence (Figure 6D), indicating that miR-26a regulates TRPC3 translation.

Using immunoblotting, we further validated the effect of miR-26a on TRPC3 protein-expression in cultured canine LA- fibroblasts. MiR-26a overexpression significantly decreased TRPC3 protein-expression whereas miR-26a knockdown to mimic AF-related miR-26 downregulation increased TRPC3-protein (Figure 6E). We then assessed the regulation of fibroblast proliferation by miR-26a. MiR-26a overexpression significantly decreased fibroblast-number (Figure 6F) as well as G2/M-cell percentage (Figure 6G) whereas miR-26a knockdown increased these fibroblast-proliferation indices. These data indicate that miR-26a controls TRPC3-expression by downregulating TRPC3 protein, producing parallel changes in fibroblast proliferation-indices.

**NFATc3 regulation of miR-26a**

We next looked for the potential mechanism of fibroblast miR-26 control in AF. Nuclear-translocation of the Nuclear Factor of Activated T-cells (NFAT), subsequent to dephosphorylation by $Ca^{2+}$/calmodulin-dependent calcineurin activation, is important in AF-related cardiomyocyte-remodeling.[1] The promoter regions of the host genes for miR-26a/b in humans and dogs are predicted to have multiple binding motifs for NFAT

(Supplemental Figure 12D). We therefore evaluated cellular localization of NFAT in fibroblasts from AF and control dogs. Figure 7A shows representative confocal images of freshly-isolated LA-fibroblasts stained with vimentin, TOPRO3 (nuclear stain) and NFATc3/c4-antibodies. Nuclear localization of NFATc3 increased significantly in AF (Figure 7B). We also quantified nuclear NFAT-localization by immunoblotting on isolated canine fibroblast-nuclei. AF significantly reduced the cytosolic and increased the nuclear protein fraction of NFATc3 (Figure 7C). To assess NFAT-regulation of miR26 gene-expression, we examined the effect of incubation with a selective membrane-permeable NFATc3/c4 blocker, INCA6 (2.5-μmol/L), on miR-26 and TRPC3 expression in canine atrial fibroblasts. INCA6 significantly increased miR-26a/b expression (Figure 7D) and decreased TRPC3 protein-expression (Figure 7E), consistent with an inhibitory effect of NFAT on miR-26 transcription. These data suggest that AF-induced NFATc3-translocation suppresses miR-26a-transcription, thereby reducing miR-26a inhibition of TRPC3-translation and resulting in TRPC3 protein-upregulation.

**Effects of in vivo TRPC3 blockade on the AF-substrate**

To more directly assess the role of TRPC3 in the AF-promoting remodeling of our AF-dogs, additional AF-dogs were treated with Pyr3 (0.1-mg/kg/day by continuous intravenous infusion) or vehicle for the entire period of atrial tachypacing (Supplemental Figure 3). At the terminal electrophysiological study, Pyr3-treated dogs showed significantly-reduced AF-duration (Figure 8A). They also had slightly but significantly greater ERP-values at short cycle-lengths (Figure 8B). Consistent with in vivo TRPC3-control of fibroblast function, Pyr3 significantly decreased LA vimentin-expression (Figure 8C), as well as fibroblast-number on Day 3 (Figure 8D) and G2/M-cell content on Day 2 (Figure 8E) in

LA-fibroblasts cultured from AF-dogs. Pyr3 also decreased ECM gene-expression in LA-fibroblasts freshly-isolated from AF-dogs (Figure 8F).

## Discussion

This study shows that TRPC3-channels control fibroblast-function via $Ca^{2+}$-dependent ERK-phosphorylation resulting from $Ca^{2+}$-entry through $I_{NSC}$. In addition, atrial TRPC3-expression is upregulated in AF, inducing fibroblast proliferation, differentiation and activation. TRPC3-upregulation in AF is due to downregulation of its regulatory microRNA, miR-26, under the control of NFATc3. Infusion of a highly-selective TRPC3-inhibitor, Pyr3, suppresses development of the AF-substrate in a canine model.

### Comparison with Previous Studies on TRP Channel-dependent Regulation of Fibroblast Function

TRPC3 is a $Ca^{2+}$-permeable ion channel that shows 75% homology with TRPC6 and 7.[20] These channels show substantial $Ca^{2+}$-permeability and mediate receptor-activated extracellular $Ca^{2+}$-entry.[20,23,24] TRPC3/6/7-channels are directly activated by DAG liberation into the plasma-membrane, triggered by agonist-binding to G protein-coupled receptors like angiotensin-II and endothelin-1 (ET-1) receptors.[20,23] TRPC-channels are widely expressed and are involved in diverse biological functions, such as neuronal cell survival,[24] blood vessel constriction,[25] immune cell maturation,[26] and cardiac hypertrophy.[27,28] However, the regulatory role of TRPC3-channels in cardiac fibroblast function has not been previously reported.

Rose et al. demonstrated that a TRP channel-like $I_{NSC}$ is elicited by C-type natriuretic peptide in freshly-isolated rat ventricular fibroblasts.[15] Transcripts encoding TRPC3-subunits were highly expressed in the fresh fibroblasts and $I_{NSC}$ was activated by

phorbol esters. However, the role of $I_{NSC}$ in fibroblast function was not examined.

Nishida et al. reported thatTRPC1, 3, 6, and 7 mRNAs are detected in neonatal rat fibroblasts and TRPC6-channels contribute to the regulation of ET-1-induced myofibroblast formation through JNK and NFAT signaling.[29] However, in contrast to our observations regarding TRPC3 channels, ERK1/2-phosphorylation was not affected by ET-1-activated TRPC6 currents. Of note, the Nishida study was performed in neonatal cells and TRP-channel dependent regulation of fibroblast function may change during development from neonatal to adult conditions.

Du et al. demonstrated that current corresponding to TRP melastatin-related 7 (TRPM7), a $Ca^{2+}/Mg^{2+}$-permeable channel, is strongly expressed in fibroblasts isolated from right-atrial samples of AF patients and likely plays an important role in AF pathophysiology.[30] shRNA-based TRPM7 knockdown decreased TRPM7-mediated $Ca^{2+}$-influx in cultured atrial fibroblasts and suppressed fibroblast differentiation induced by TGFβ-stimulation. Our results showed substantial TPRC3-subunit expression and associated current, as well as significant physiological function, in fibroblasts that were freshly-isolated or kept under conditions limiting differentiation. Furthermore, TRPC3-dependent current and fibroblast-regulation were enhanced in AF-dog fibroblasts. The expression and function of TRPC3-channels disappeared following differentiation to myofibroblasts under culture conditions. In contrast, mRNA-expression of TRPM7-subunits remained high in myofibroblasts, similar to the findings of Du et al, who also showed strong mRNA expression of TRPM7 but not TRPC3 subunits in cultured human atrial fibroblasts. Cardiac fibroblast phenotype dynamically changes during proliferation and differentiation. Our findings suggest that TRPC3 controls proliferation and differentiation of fibroblasts, but is downregulated in the end-cell myofibroblast. This negative-feedback system may prevent excessive ECM-remodeling. In contrast, TRPM7

is likely the dominant TRP-channel in differentiated myofibroblasts.

Du et al. found increased TRPM7-current in fibroblasts isolated from atrial samples of AF-patients but did not have sufficient tissue to perform Western-blot studies. We found increased protein-expression of TRPC3, but not TRPC1 or TRPM7, by immunoblotting of atrial samples in AF-patients, AF-goats and CHF-dogs. This observation suggests that the increased TRPM7-function noted by Du et al. in fibroblasts from AF-patients may have been due to increased membrane-trafficking of TRPM7-subunits or altered regulation rather than increased channel-expression per se.

**Potential mechanisms**

Mio et al. established the 3-dimensional structure of TRPC3-channels with cryo-electron microscopy.[31] TRPC3-channels have both a pore-forming transmembrane domain and a large intracellular domain representing a "nested-box" structure. The latter structure may act as a molecular anchor for signaling complexes. TRPC3-mediated $Ca^{2+}$-influx and an increase in local $Ca^{2+}$-concentration may trigger protein-protein interactions that activate downstream signaling pathways that regulate fibroblast function. A recent study using B-lymphocytes demonstrated that TRPC3 channels act as a platform for protein kinase C (PKC), and that the sustained scaffolding of PKC at the plasma membrane is associated with the activation of the ERK1/2 signaling pathway.[32]

ERK1/2 is a protein kinase and intracellular signaling molecule involved in various biological functions, including cell growth and survival.[21,22] In the present study, selective inhibition of ERK1/2 signaling attenuated rat fibroblast proliferation, suggesting that ERK1/2 signaling contributes to fibroblast function. Olson et al. demonstrated that angiotensin-induced intracellular $Ca^{2+}$-increases and PKC activation in adult rat cardiac fibroblasts synergistically contribute to ERK1/2 activation and fibroblast proliferation.[33]

TRPC3-channels may be particularly important in this situation because angiotensin-II increases cellular production of DAG, which activates TRPC3-channels. Our data showed that TRPC3 blockade suppresses $Ca^{2+}$-entry caused by angiotensin-II, a well-known profibrotic agent, in rat cardiac fibroblasts.

**Novelty and potential significance**

This is the first study to show a role of TRPC3-channels in controlling fibroblast-function and the first to indicate that AF activates fibroblasts via TRPC3-related mechanisms. Furthermore, we were able to identify the mechanism of TRPC3-upregulation in AF (reduced miR-26 negative control of TRPC3-translation, due to enhanced NFATc3 nuclear-translocation in AF-fibroblasts which causes enhanced inhibitory NFATC3-regulation of miR-26), and found that a TRPC3-inhibitor suppresses AF-promoting remodeling. An emerging body of evidence indicates that TRP-channels act as important mediators for a wide variety of physiological functions and are a potential target for drug discovery. There is a need to develop novel approaches to AF treatment, and therapies that prevent fibroblast activation are of potentially-great interest.[6] Our findings point to TRPC3 as a candidate target for AF-prevention.

Although it is well-recognized that AF promotes atrial fibrosis, little information is available about how this happens. In our dog model, AF upregulated TRPC3 and caused fibroblast activation that depended on TRPC3-related $Ca^{2+}$-entry, which activated ERK-phosphorylation. Similar TRPC3-upregulation was observed in atrial samples from AF-patients, AF-goats and AF-prone CHF-dogs. TRPC3-channels acted primarily in non-differentiated fibroblasts, enhancing their ability to proliferate and differentiate into myofibroblasts. Once myofibroblasts were formed, TRPC3-channels downregulated. This behavior of TRPC3-channels has not been described previously: TRPC3-channels

promote fibrosis by causing fibroblasts to proliferate and activate, but are then downregulated in activated myofibroblasts to prevent a positive-feedback process. The effects of in vivo Pyr3-infusion to prevent enhanced proliferation and ECM-expression of fibroblasts from AF-dogs, along with the associated suppression of AF-promotion, are consistent with an important role for TRPC3 in fibroblast-mediated AF-promoting remodeling.

Although NFAT nuclear-translocation has previously been shown to occur in AF-cardiomyocytes and to be involved in cardiomyocyte-remodeling,[1,34] our study constitutes the first demonstration of AF-associated NFAT-changes in fibroblasts and their involvement in AF-related fibroblast-remodeling.

**Potential limitations**

We cannot exclude the possibility that fibroblast properties were affected by cell isolation and culture. Considering that fibroblasts lose their original properties after lengthy culture-intervals, we used cells in short-term primary culture (maximum of 3 days after isolation) in most experiments. However, this approach cannot completely reproduce the complex in vivo milieu. Any extrapolation of these results to human disease should be made cautiously.

Our patch-clamp recording conditions differed from those used by Du et al[30] in that they used pipette solutions that were virtually $Mg^{2+}$-free, whereas our pipettes contained $Mg^{2+}$ at concentrations typically used for cardiac cell patch-clamp recording. TRPM7-currents are strongly suppressed by intracellular $Mg^{2+}$,[35,36] which likely explains why most of the gadolinium-sensitive current we observed was also sensitive to Pyr3. Under our conditions, $I_{NSC}$ would not be expected to contain substantial TRPM7-current and was strongly downregulated in myofibroblasts. Thus, TRPM7-channels play a much

larger role than other TRP-channels, including TRPC3, in regulating $Ca^{2+}$-influx in differentiated myofibroblasts.

Our AF-dogs showed increased atrial fibroblast density and signs of fibroblast activation like enhanced α-SMA expression (Figure 8C) and ECM-gene upregulation (Figure 7E). However, we did not see increased fibrous-tissue content in AF-dogs. We suspect that the lack of fibrosis was due to the relatively short time (7 days) that the dogs were kept in AF, with longer intervals necessary for fibrosis-development. When AF is maintained for longer periods (>3 months), clear fibrosis develops, even when excessive ventricular rates and left-ventricular dysfunction are prevented.[37] It is important to emphasize that fibroblast-proliferation and differentiation can promote AF by a range of mechanisms that does not require enhanced fibrous-tissue content, particularly fibroblast-cardiomyocyte electrical interactions.[3] The small atrial ERP-increases we noted in Pyr3-treated AF-dogs may reflect enhanced fibroblast effects on the electrophysiology of coupled cardiomyocytes.[3] Alternatively, a direct role in cardiomyocytes cannot be excluded and should be assessed in follow-up work. Our findings raise many interesting additional questions that need to be answered, but are outside the scope of the present study.

**Acknowledgments**

The authors thank Nathalie L'Heureux, Chantal St-Cyr, Louis-Robert Villeneuve for technical help and France Thériault for secretarial assistance.

**Sources of Funding**

Supported by the Canadian Institutes of Health Research (CIHR, MOP 44365), Quebec Heart and Stroke Foundation, the MITACS Network, Japanese Heart Rhythm

Society/Medtronic Fellowship, Japan Heart Foundation/Japanese Society of Electrocardiology Scholarship, German Center for Cardiovascular Research and Fondation Leducq (ENAFRA Network, 07/CVD/03).

## Disclosures

None.

Q:/Secrétariat Central/therfr/PUBL/Circulation/TRPC3_SN_ft/TRPC3_UNMARKED VERSION_SN_ft.doc

**References**


1. Wakili R, Voigt N, Kääb S, Dobrev D, Nattel S. Recent advances in the molecular pathophysiology of atrial fibrillation. *J Clin Invest.* 2011;121:2955-2968.
2. Nattel S. From guidelines to bench: Implications of unresolved clinical issues in atrial fibrillation for basic investigations of atrial fibrillation mechanisms. *Can J Cardiol*. 2011;27:19-26.
3. Burstein B, Nattel S. Atrial Fibrosis: Mechanisms and clinical relevance in atrial fibrillation. *J Am Coll Cardiol*. 2008;51:802-809.
4. Souders CA, Bowers SL, Baudino TA. Cardiac fibroblast: the renaissance cell. *Circ Res.* 2009;105:1164-1176.
5. Burstein B, Comotois P, Michael G, Nishida K, Villeneuve L, Yeh YH, Nattel S. Changes in connexin expression and the atrial fibrillation substrate in congestive heart failure. *Circ Res*. 2009;105:1213-1222.
6. Yue L, Xie J, Nattel S. Molecular determinants of cardiac fibroblast electrical function and therapeutic implications for atrial fibrillation. *Cardiovasc Res*. 2011; 89:744-753.
7. Inoue R, Jensen LJ, Shi J, Morita H, Nishida M, Honda A, Ito H. Transient receptor potential channels in cardiovascular function and disease. *Circ Res*. 2006;99:119-131.
8. Clapham DE. TRP channels as cellular sensors. *Nature*. 2003;426:517-524.
9. Shiroshita-Takeshita A, Brundel BJ, Burstein B, Leung TK, Mitamura H, Ogawa S, Nattel S. Effects of simvastatin on the development of the atrial fibrillation substrate in dogs with congestive heart failure. *Cardiovasc Res*. 2007;74:75-84.
10. Blaauw Y, Gögelein H, Tieleman RG, van Hunnik A, Schotten U, Allessie MA. "Early" class III drugs for the treatment of atrial fibrillation: efficacy and atrial

selectivity of AVE0118 in remodeled atria of the goat. *Circulation*. 2004;110:1717-1724.

11. Li D, Fareh S, Leung TK, Nattel S. Promotion of atrial fibrillation by heart failure in dogs: atrial remodeling of a different sort. *Circulation*. 1999;100:87-95.
12. Sakabe M, Shiroshita-Takeshita A, Maguy A, Dumesnil C, Nigam A, Leung TK, Nattel S. Omega-3 polyunsaturated fatty acids prevent atrial fibrillation associated with heart failure but not atrial tachycardia remodeling. *Circulation*. 2007;116:2101-2109.
13. Gaborit N, Le Bouter S, Szuts V, Varro A, Escande D, Nattel S, Demolombe S. Regional and tissue specific transcript signatures of ion channel genes in the non-diseased human heart. *J Physiol*. 2007;582:675-693.
14. Mestdagh P, Van Vlierberghe P, De Weer A, Muth D, Westermann F, Speleman F, Vandesompele J. A novel and universal method for microRNA RT-qPCR data normalization. *Genome Biol*. 2009;10:R64.
15. Rose RA, Hatano N, Ohya S, Imaizumi Y, Giles WR. C-type natriuretic peptide activates a non-selective cation current in acutely isolated rat cardiac fibroblasts via natriuretic peptide C receptor-mediated signalling. *J Physiol*. 2007;580:255-274.
16. Burstein B, Libby E, Calderone A, Nattel S. Differential behaviors of atrial versus ventricular fibroblasts: a potential role for platelet-derived growth factor in atrial-ventricular remodeling differences. *Circulation*. 2008;117:1630-1641.
17. Ledoux J, Taylor MS, Bonev AD, Hannah RM, Solodushko V, Shui B, Tallini Y, Kotlikoff MI, Nelson MT. Functional architecture of inositol 1,4,5-triphosphate signaling in restricted spaces of myoendothelial projections. *Proc Natl Acad Sci U S A*. 2008;105:9627-9632.

18. Xiao J, Lin H, Luo X, Luo X, Wang Z. miR-605 joins p53 network to form a p53: miR-605:Mdm2 positive feedback loop in response to stress. *EMBO J.* 2011; 30:524-532.

19. Kiyonaka S, Kato K, Nishida M, Mio K, Numaga T, Sawaguchi Y, Yoshida T, Wakamori M, Mori E, Numata T, Ishii M, Takemoto H, Ojida A, Watanabe K, Uemura A, Kurose H, Morii T, Kobayashi T, Sato Y, Sato C, Hamachi I, Mori Y. Selective and direct inhibition of TRPC3 channels underlies biological activities of a pyrazole compound. *Proc Natl Acad Sci U S A*. 2009;106:5400-5405.

20. Hofmann T, Obukhov AG, Schaefer M, Harteneck C, Gudermann T, Schultz G. Direct activation of human TRPC6 and TRPC3 channels by diacylglycerol. *Nature*. 1999;397:259-263.

21. Pagès G, Lenormand P, L'Allemain G, Chambard JC, Meloche S, Pouysségur J. Mitogen-activated protein kinases p42mapk and p44mapk are required for fibroblast proliferation. *Proc Natl Acad Sci U S A*. 1993;90:8319-8323.

22. Dudley DT, Pang L, Decker SJ, Bridges AJ, Saltiel AR. A synthetic inhibitor of the mitogen-activated protein kinase cascade. *Proc Natl Acad Sci U S A*. 1995;92:7686-7689.

23. Dietrich A, Mederos y Schnitzler M, Kalwa H, Storch U, Gudermann T. Functional characterization and physiological relevance of the TRPC3/6/7 subfamily of cation channels. *Naunyn Schmiedebergs Arch Pharmacol*. 2005;371:257-265.

24. Jia Y, Zhou J, Tai Y, Wang Y. TRPC channels promote cerebellar granule neuron survival. *Nat Neurosci*. 2007;10:559-567.

25. Reading SA, Earley S, Waldron BJ, Welsh DG, Brayden JE. TRPC3 mediates pyrimidine receptor-induced depolarization of cerebral arteries. *Am J Physiol Heart*

*Circ Physiol*. 2005;288:H2055-H2061.

26. Philipp S, Strauss B, Hirnet D, Wissenbach U, Mery L, Flockerzi V, Hoth M. TRPC3 mediates T-cell receptor-dependent calcium entry in human T-lymphocytes. *J Biol Chem*. 2003;278:26629-26638.
27. Onohara N, Nishida M, Inoue R, Kobayashi H, Sumimoto H, Sato Y, Mori Y, Nagao T, Kurose H. TRPC3 and TRPC6 are essential for angiotensin II-induced cardiac hypertrophy. *EMBO J*. 2006;25:5305-5316.
28. Wu X, Eder P, Chang B, Molkentin JD. TRPC channels are necessary mediators of pathologic cardiac hypertrophy. *Proc Natl Acad Sci U S A*. 2010;107:7000-7005.
29. Nishida M, Onohara N, Sato Y, Suda R, Ogushi M, Tanabe S, Inoue R, Mori Y, Kurose H. Galpha12/13-mediated up-regulation of TRPC6 negatively regulates endothelin-1-induced cardiac myofibroblast formation and collagen synthesis through nuclear factor of activated T cells activation. *J Biol Chem*. 2007;282:23117-23128.
30. Du J, Xie J, Zhang Z, Tsujikawa H, Fusco D, Silverman D, Liang B, Yue L. TRPM7-mediated $Ca^{2+}$ signals confer fibrogenesis in human atrial fibrillation. *Circ Res*. 2010;106:992-1003.
31. Mio K, Ogura T, Kiyonaka S, Hiroaki Y, Tanimura Y, Fujiyoshi Y, Mori Y, Sato C. The TRPC3 channel has a large internal chamber surrounded by signal sensing antennas. *J Mol Biol*. 2007;367:373-383.

32. Numaga T, Nishida M, Kiyonaka S, Kato K, Katano M, Mori E, Kurosaki T, Inoue R, Hikida M, Putney JW Jr, Mori Y. $Ca^{2+}$ influx and protein scaffolding via TRPC3 sustain PKCbeta and ERK activation in B cells. *J Cell Sci*. 2010;123:927-938.

33. Olson ER, Shamhart PE, Naugle JE, Meszaros JG. Angiotensin II-induced extracellular signal-regulated kinase 1/2 activation is mediated by protein kinase C delta and intracellular calcium in adult rat cardiac fibroblasts. *Hypertension*. 2008;51:704-711.

34. Qi XY, Yeh YH, Xiao L, Burstein B, Maguy A, Chartier D, Villeneuve LR, Brundel BJJM, Dobrev D, Nattel S. Cellular signalling underlying atrial tachycardia remodeling of L-type calcium-current. *Circ Res*. 2008;103:845-854.

35. Kozak JA, Cahalan MD. MIC channels are inhibited by internal divalent cations but not ATP. *Biophys J*. 2003;84:922-927.

36. Nadler MJ, Hermosura MC, Inabe K, Perraud AL, Zhu Q, Stokes AJ, Kurosaki T, Kinet JP, Penner R, Scharenberg AM, Fleig A. LTRPC7 is a Mg.ATP-regulated divalent cation channel required for cell viability. *Nature*. 2001;411:590-595.

37. Avitall B, Bi J, Mykytsey A, Chicos A. Atrial and ventricular fibrosis induced by atrial fibrillation: evidence to support early rhythm control. *Heart Rhythm*. 2008;5:839-845.

## Figure Legends

**Figure 1.** A, Representative $I_{NSC}$-recordings with or without pyrazole3 (Pyr3, 3-µmol/L). B, Mean±SEM $Gd^{3+}$- and Pyr3-sensitive $I_{NSC}$-density (n=7 cells in $Gd^{3+}$ and 9 cells in Pyr3). C, Recordings of angiotensin-II induced intracellular $Ca^{2+}$-response in presence or absence of Pyr3. D, Mean±SEM angiotensin-II (AngII)-induced $Ca^{2+}$ fluorescence ($F/F_0$), normalized to baseline in 0-mmol/L $Ca^{2+}$ (n=18, 20 cells in AngII and AngII with Pyr3, **P*<0.05 vs. 0-mmol/L $Ca^{2+}$, #*P*<0.05 vs. 2-mmol/L $Ca^{2+}$ in AngII). E, Mean±SEM fibroblast count after 1-hour or 24-hour culture with vehicle-control, or 0.3 or 3-µmol/L Pyr3 (n=9/group, **P*<0.05 vs. CTL, #*P*<0.05 vs. 1-hour treatment). F, Mean±SEM percentage of cells in G2/M-phase after Pyr3-treatment (n=9, **P*<0.05 vs CTL, #*P*<0.05 vs. 1-hour treatment). G, Representative immunoblots for αSMA and GAPDH in rat fibroblasts cultured with or without Pyr3 (3-µmol/L) and H, mean±SEM αSMA/GAPDH expression ratio (n=8/group, **P*<0.05 vs. CTL).

**Figure 2.** A, Top: Representative immunoblots of phosphorylated-ERK-1/2 (p-ERK), total ERK-1/2 (t-ERK) and GAPDH in rat fibroblasts cultured with 0.4-mmol/L $Ca^{2+}$, 2.0-mmol/L $Ca^{2+}$ and 2.0-mmol/L $Ca^{2+}$ medium containing 3-µmol/L Pyr3. Bottom: Mean±SEM (p-ERK)/GAPDH, (t-ERK)/GAPDH and (p-ERK)/(t-ERK) (n=8/group, **P*<0.05 vs. CTL, #*P*<0.05 vs. Pyr3). B, Mean±SEM fibroblast cell-count after culture in M199-medium containing 0.4 to 4.4 mmol/L $Ca^{2+}$ (n=8/group, **P*<0.05 vs. 0.4-mmol/L $Ca^{2+}$, #*P*<0.05 vs. 1-hour treatment). C, Mean±SEM percentage of cells in G2/M-phase (n=8/group-, **P*<0.05 vs. 0.4-mmol/L $Ca^{2+}$, #*P*<0.05 vs. 1-hour treatment). D, Mean±SEM fibroblast cell-count after 1-hour and 24-hour treatment with 50-µmol/L PD98059 (n=6/group, **P*<0.05 vs. CTL, #*P*<0.05 vs. 1-hour treatment). E, Mean±SEM

percentage of cells in G2/M phase after 50-μmol/L PD98059-treatment (n=6/group, *$P$<0.05 vs. CTL).

**Figure 3.** A, Representative surface ECG (left) and intracardiac electrograms (right) in an awake AF-dog on Day 7. B, Mean±SEM atrial ERP in CTL (n=11) and AF dogs (n=12) on Day 7 (*$P$<0.05). C, Mean±SEM duration of induced AF (*$P$<0.05 vs. CTL). D, Top, Representative Masson's trichrome-stained left-atrial images from CTL (left) and AF (right) dogs. Bottom, Representative immunofluorescent images of LA free-wall tissues stained with vimentin. E, Mean±SEM fibrous-tissue content in left-atrial free-wall tissues (n=5 CTL, 5 AF dogs). F, Mean±SEM vimentin-positive area (n=5 CTL, 5 AF dogs, *$P$<0.05 vs. CTL). G, Representative immunoblots (top) and mean±SEM vimentin band-intensity normalized to GAPDH (bottom) in left-atrial samples from CTL (n=5) and AF dogs (n=5, *$P$<0.05 vs CTL).

**Figure 4.** A, Representative $I_{NSC}$-recordings before and after Pyr3 (3-μmol/L) in freshly-isolated left-atrial fibroblasts from CTL and AF dogs. B, Mean±SEM Pyr3-sensitive $I_{NSC}$-density in CTL (n=6 dogs, 8 cells) and AF dogs (n=6 dogs, 9 cells; $P$<0.05 vs. CTL). C, Representative immunoblots (top) and mean±SEM TRPC3-subunit band-intensity relative to GAPDH (bottom) in freshly-isolated left-atrial fibroblasts from CTL (n=6) and AF dogs (n=6, *$P$<0.05 vs. CTL). D, Representative immunoblots (top) and mean±SEM data (bottom) for phosphorylated (p-)ERK-1/2 and total (t-)ERK-1/2 relative to GAPDH. E, Mean±SEM extracellular matrix-gene mRNA-expression in freshly-isolated left-atrial fibroblasts (n=6 CTL and 6 AF, *$P$<0.05 vs. CTL).

**Figure 5.** A, Mean±SEM cell-count of left-atrial fibroblasts after 2-day and 3-day culture in CTL (n=7) and AF dogs (n=7, *$P$<0.05 vs. CTL). B, Mean±SEM percentage of

cells in G2/M phase (n=7 dogs/group, *$P$<0.05 vs. CTL). C, Representative immunoblots (top) and mean±SEM αSMA/GAPDH (bottom) in cultured left-atrial fibroblasts from CTL (n=6) and AF dogs (n=7, *$P$<0.05 vs. CTL). D, Mean±SEM cell-count of left-atrial fibroblasts after 1-hour or 24-hour culture with vehicle-control or Pyr3 (3-μmol/L) in AF dogs (n=6/group, *$P$<0.05 vs. DMSO). E, Mean±SEM percentage of cells in G2/M-phase (n=6/group, *$P$<0.05 vs. DMSO). F, Representative immunoblots (top) and mean±SEM αSMA/GAPDH expression-ratios (bottom) in cultured left-atrial fibroblasts from AF dogs (n=7) in the presence of vehicle (DMSO) or Pyr3 (*$P$<0.05 vs. DMSO).

G, Representative immunoblots (top) and mean±SEM phosphorylated (p-)ERK-1/2 and total (t-)ERK-1/2 relative to GAPDH (bottom) in cultured left-atrial fibroblasts of CTL and AF dogs (n=6/group, *$P$<0.05 vs. CTL). G, Representative immunoblots (top) and mean±SEM ERK in left-atrial fibroblasts from AF-dogs cultured with vehicle (DMSO) or Pyr3 (3-μmol/L, n=6/group; *$P$<0.05 vs. DMSO).

**Figure 6.** A, Mean±SEM microRNA expression in freshly-isolated left-atrial fibroblasts in AF (n=7) and CTL dogs (n=7, *$P$<0.05 vs. CTL). B, Mean±SEM relative microRNA expression in freshly-isolated left-atrial fibroblasts in CTL (n=5, *$P$<0.05 vs. miR-26a). C, Mean±SEM relative microRNA expression in freshly-isolated left-atrial cardiomyocytes in CTL (n=5, *$P$<0.05 vs. miR-26a). D, Mean±SEM relative luciferase activitiy in HEK293 cells transfected with miR-26a overexpression (miR-26a duplex)/knockdown (antisense anti-mi26a oligonucleotides, AMO26a) probes (n=7/group, $P$<0.05 vs. cells transfected without the miR-26a probes). E, Representative immunoblots (top) and mean±SEM TRPC3/GAPDH protein expression (bottom) in dog left-atrial

fibroblasts transfected with the miR-26a duplex/AMO26a (n=7, $P<0.05$ vs. cells without miR-26a probes). F, Mean±SEM fibroblast count in dog left-atrial fibroblasts transfected with miR-26a duplex/AMO26a (n=7/group, *$P<0.05$ vs. cells transfected without the miR-26a probes). G, Mean±SEM percentage of cells in G2/M-phase (n=7/group, *$P<0.05$ vs. cells transfected without the miR-26a probes).

**Figure 7.** A, Representative immunofluorescent images of freshly-isolated left-atrial fibroblasts stained with NFATc3/NFATc4, vimentin (fibroblast marker) and TOPRO-3 (nuclear marker) antibodies in AF and CTL dogs. B, Mean±SEM nuclear/cytoplasmic signal intensity ratio of NFATc3 (top) and NFATc4 (bottom, n=5, *$P<0.05$ vs. CTL). C, Top: Representative immunoblots of cytosolic and nuclear protein fractions of HSP70 (cytosolic marker), Lamin A/C (nuclear marker), NFATc3 and NFATc4 in freshly-isolated left-atrial fibroblasts in AF and CTL dogs. Bottom: Mean±SEM cytoplasmic NFATc3/NFATc4 relative to HSP70 and nuclear NFATc3/NFATc4 relative to Lamin A/C (n=4/group, *$P<0.05$ vs. CTL). D, Mean±SEM miR-26a and b expression in control-dog left-atrial fibroblasts treated with INCA6 (2.5-µmol/L) for 24 hours. (n=5/group, $P<0.05$ vs. DMSO). E, Representative immunoblots (top) and mean±SEM TRPC3/GAPDH (bottom) in control-dog left-atrial fibroblasts treated with INCA6 (2.5-µmol/L) for 24 hours (n=5, $P<0.05$ vs. DMSO).

**Figure 8.** A, Mean±SEM duration of induced AF on Day 7 in AF-dogs treated throughout the AF-pacing period with intravenous Pyr3 (n=6, 0.1 mg/kg/day) or vehicle (n=6, *$P<0.05$ vs. vehicle). B, Mean±SEM atrial ERP (*$P<0.05$ vs. vehicle). C, Representative immunoblots (top) and mean±SEM vimentin band-intensity normalized to GAPDH (bottom) in left-atrial tissue samples from Pyr3- (n=5) or

vehicle-treated AF dogs (n=5, *$P$<0.05 vs. vehicle). D, Mean±SEM cell-count of left-atrial fibroblasts after 2-day and 3-day culture in Pyr3- (n=6) or vehicle-treated AF dogs (n=6, *$P$<0.05 vs. vehicle). E, Mean±SEM percentage of cells in G2/M phase (n=6/group, *$P$<0.05 vs. vehicle). F, Mean±SEM extracellular matrix-gene mRNA-expression in freshly-isolated left-atrial fibroblasts in Pyr3- (n= 5) or vehicle-treated AF dogs (n=5, *$P$<0.05 vs. vehicle).

## Figures

### Figure 1

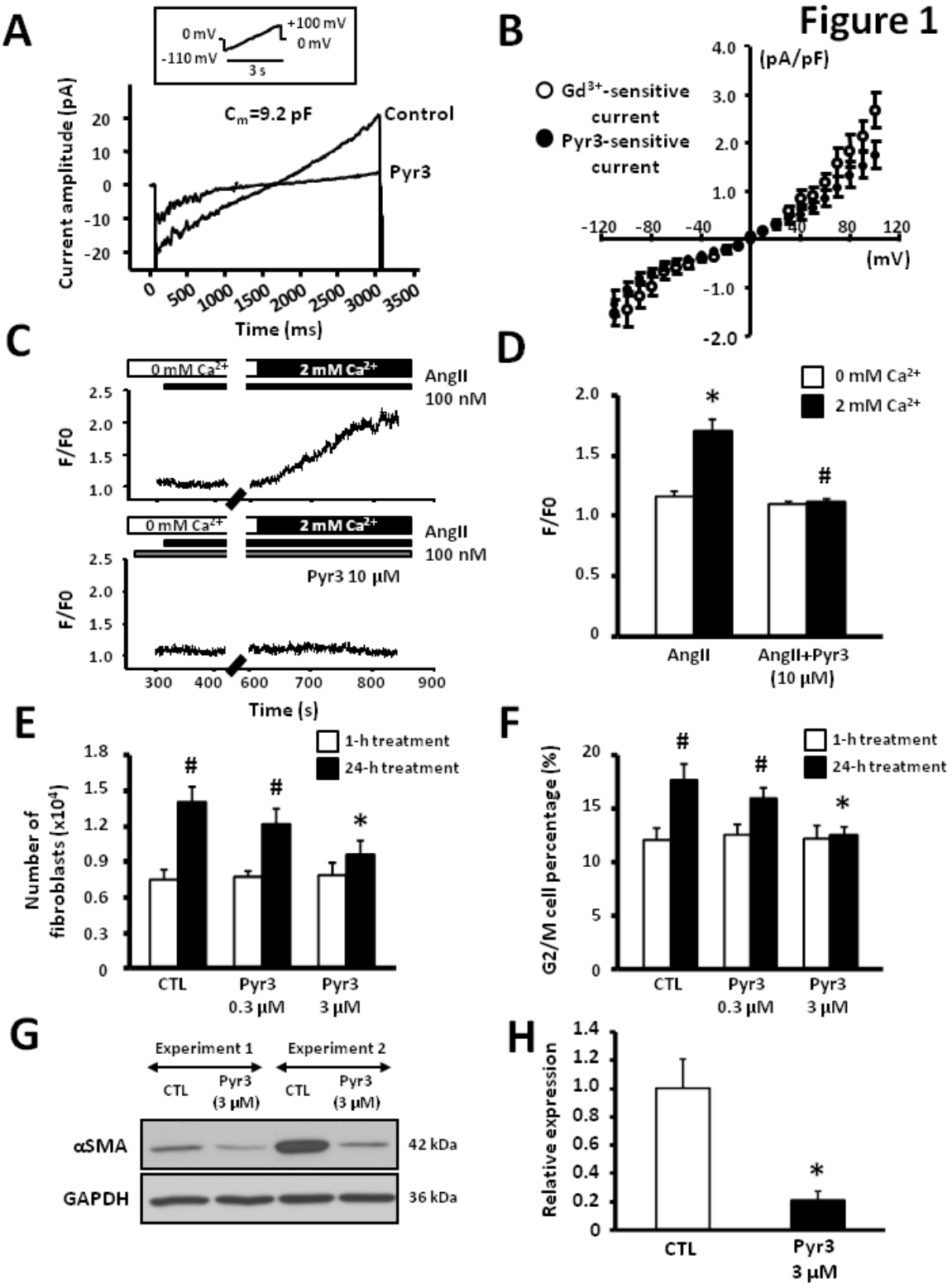

**Figure 2**

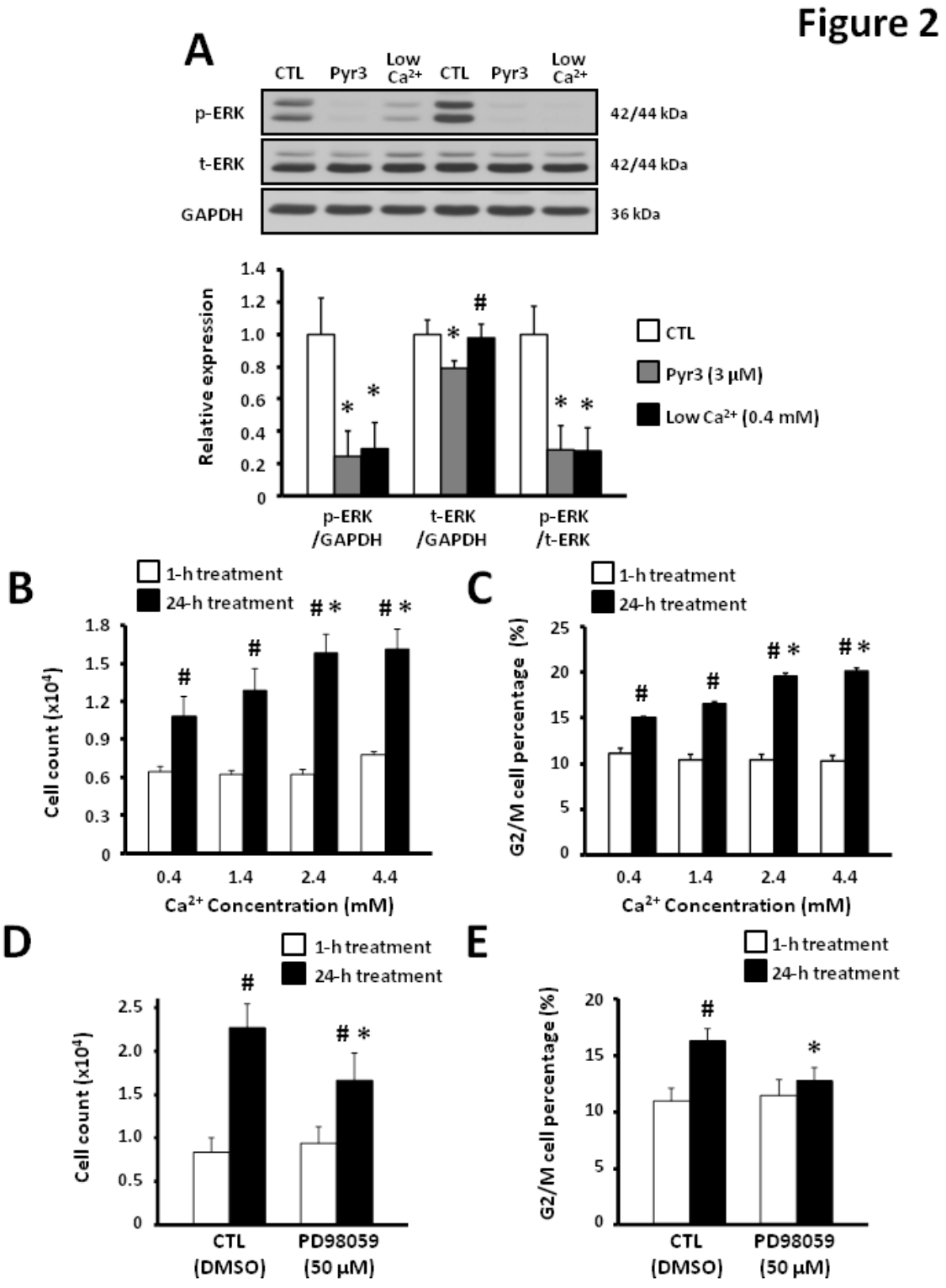
Figure 2
A
CTL
Pyr3
Low Ca2+
CTL
Pyr3
Low Ca2+
p-ERK
t-ERK
GAPDH
42/44 kDa
42/44 kDa
36 kDa
Relative expression
CTL
Pyr3 (3 μM)
Low Ca2+ (0.4 mM)
p-ERK /GAPDH
t-ERK /GAPDH
p-ERK /t-ERK
B
1-h treatment
24-h treatment
Cell count (x10⁴)
Ca2+ Concentration (mM)
C
1-h treatment
24-h treatment
G2/M cell percentage (%)
Ca2+ Concentration (mM)
D
1-h treatment
24-h treatment
Cell count (x10⁴)
CTL (DMSO)
PD98059 (50 μM)
E
1-h treatment
24-h treatment
G2/M cell percentage (%)
CTL (DMSO)
PD98059 (50 μM)

**Figure 3**

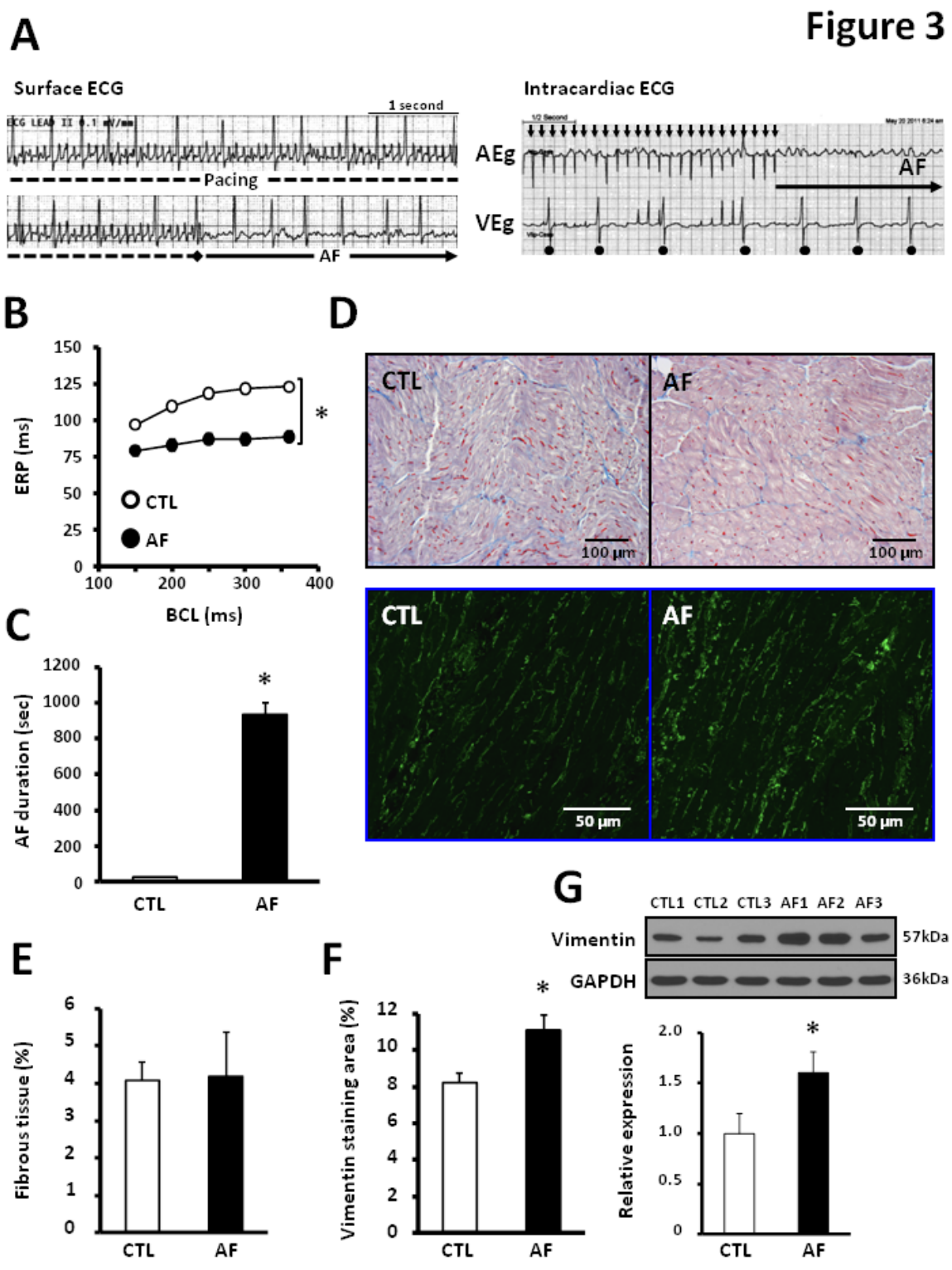
Figure 3
A
Surface ECG
1 second
Pacing
AF
Intracardiac ECG
AEg
VEg
AF
B
ERP (ms)
150
125
100
75
50
25
0
100
200
300
400
BCL (ms)
CTL
AF
*
C
AF duration (sec)
1200
1000
800
600
400
200
0
CTL
AF
*
D
CTL
AF
100 μm
100 μm
CTL
AF
50 μm
50 μm
E
Fibrous tissue (%)
6
5
4
3
2
1
0
CTL
AF
F
Vimentin staining area (%)
12
10
8
6
4
2
0
CTL
AF
*
G
CTL1 CTL2 CTL3 AF1 AF2 AF3
Vimentin
GAPDH
57kDa
36kDa
Relative expression
2.0
1.5
1.0
0.5
0
CTL
AF
*

**Figure 4**

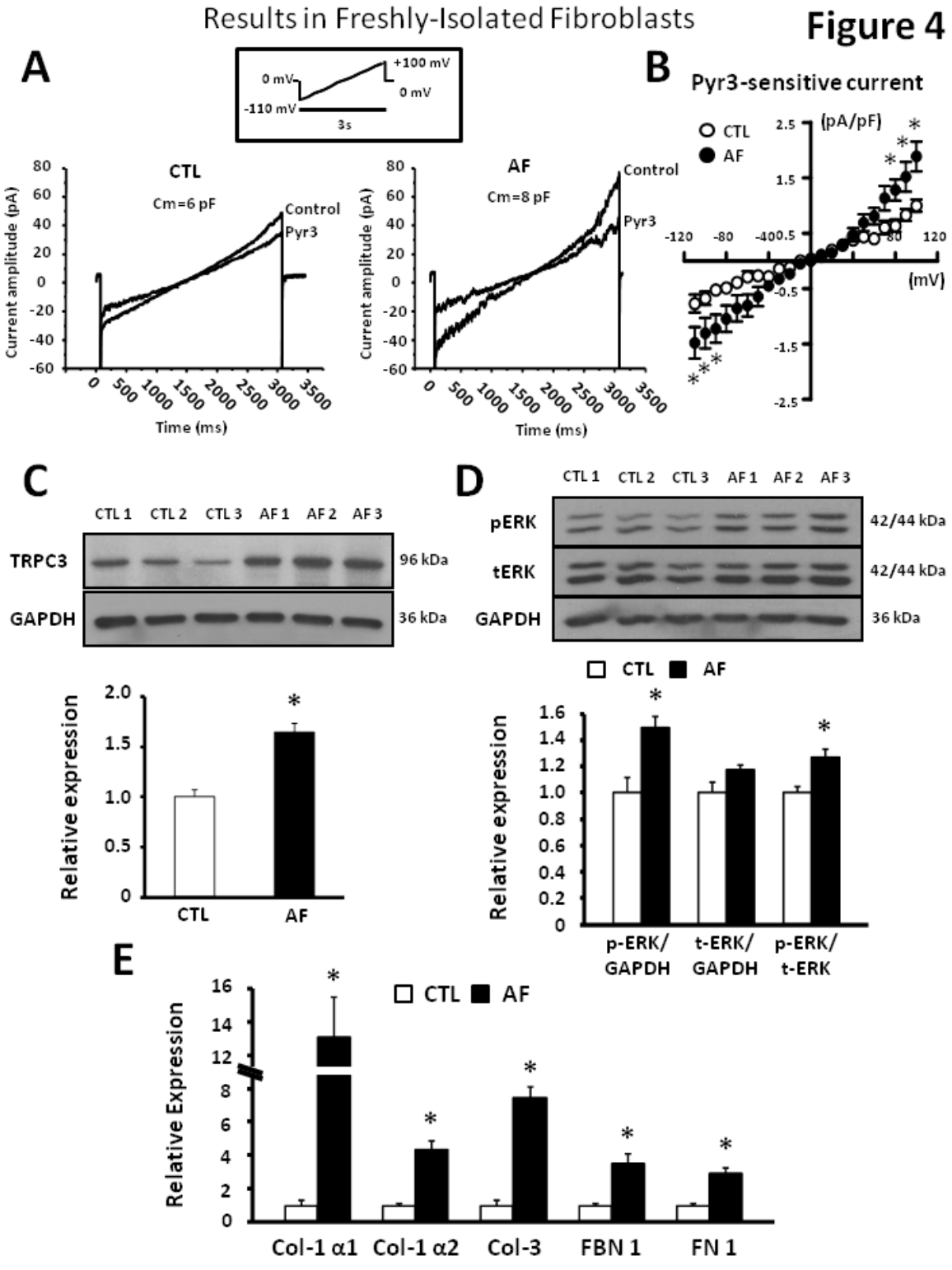
Results in Freshly-Isolated Fibroblasts
Figure 4
A
+100 mV
0 mV
0 mV
-110 mV
3s
CTL
Cm=6 pF
Control
Pyr3
AF
Cm=8 pF
Control
Pyr3
Current amplitude (pA)
Time (ms)
B
Pyr3-sensitive current
CTL
AF
(pA/pF)
(mV)
C
CTL 1
CTL 2
CTL 3
AF 1
AF 2
AF 3
TRPC3
96 kDa
GAPDH
36 kDa
Relative expression
CTL
AF
D
pERK
tERK
GAPDH
42/44 kDa
42/44 kDa
36 kDa
p-ERK/ GAPDH
t-ERK/ GAPDH
p-ERK/ t-ERK
E
Relative Expression
Col-1 α1
Col-1 α2
Col-3
FBN 1
FN 1

**Figure 5**

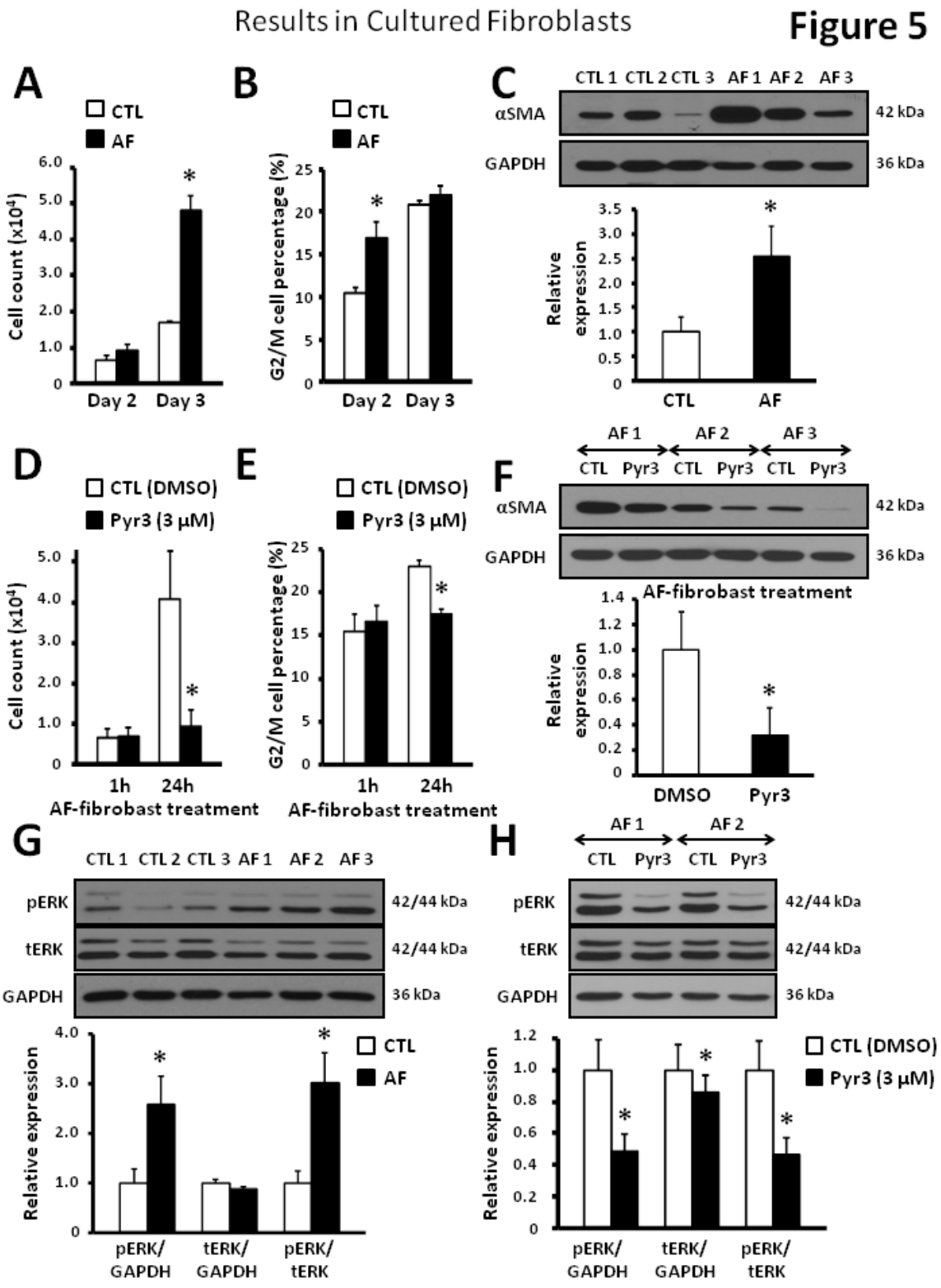
Results in Cultured Fibroblasts
Figure 5
A
CTL
AF
Cell count (x10⁴)
Day 2
Day 3
B
G2/M cell percentage (%)
C
CTL 1 CTL 2 CTL 3 AF 1 AF 2 AF 3
αSMA
GAPDH
42 kDa
36 kDa
Relative expression
D
CTL (DMSO)
Pyr3 (3 μM)
1h
24h
AF-fibrobast treatment
E
F
AF 1 AF 2 AF 3
CTL Pyr3 CTL Pyr3 CTL Pyr3
DMSO
Pyr3
G
pERK
tERK
42/44 kDa
pERK/ GAPDH
tERK/ GAPDH
pERK/ tERK
H

**Figure 6**

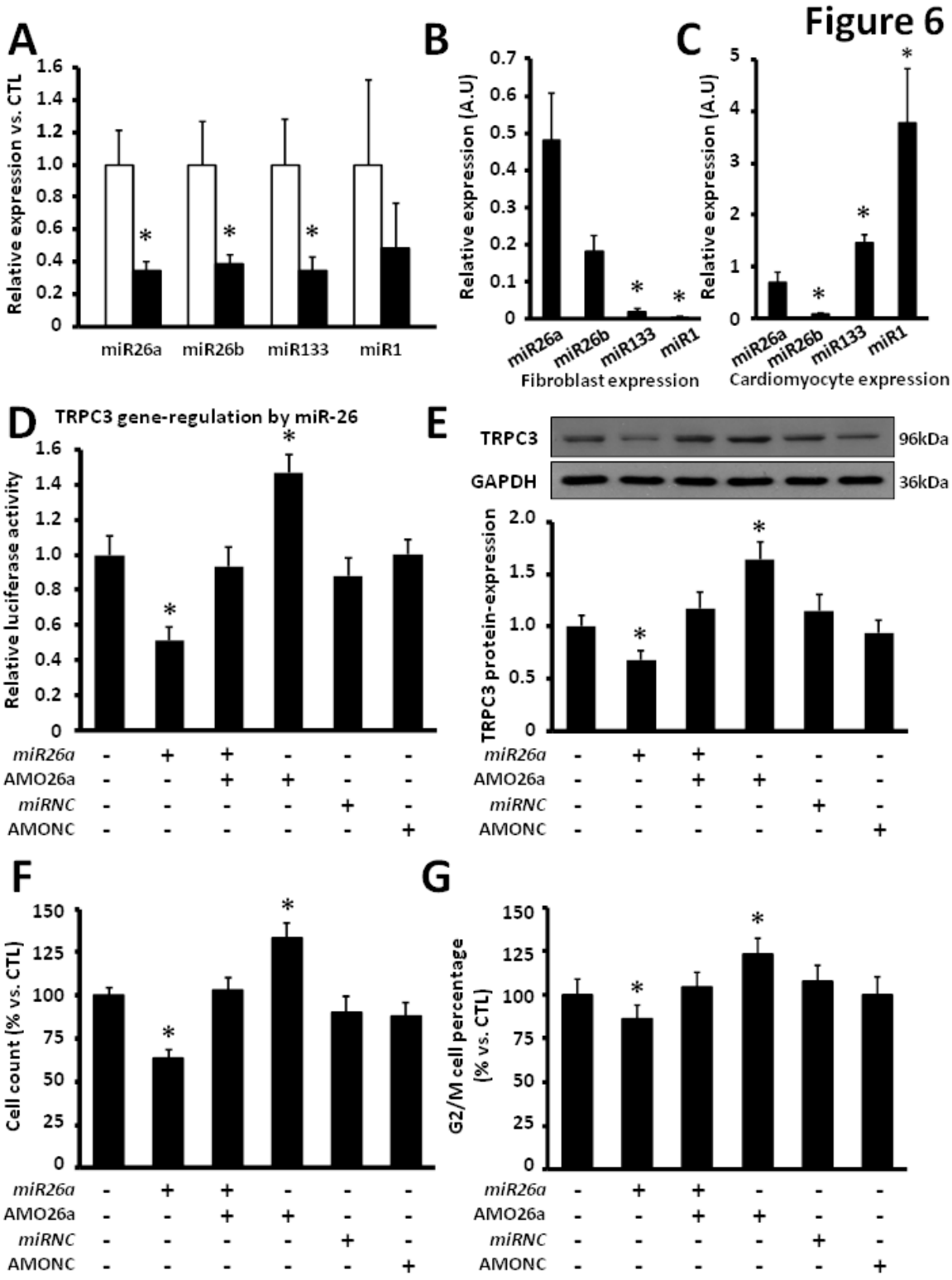
Figure 6
A
Relative expression vs. CTL
miR26a
miR26b
miR133
miR1
B
Relative expression (A.U)
Fibroblast expression
C
Relative expression (A.U)
Cardiomyocyte expression
D
TRPC3 gene-regulation by miR-26
Relative luciferase activity
miR26a
AMO26a
miRNC
AMONC
E
TRPC3
GAPDH
96kDa
36kDa
TRPC3 protein-expression
F
Cell count (% vs. CTL)
G
G2/M cell percentage (% vs. CTL)

**Figure 7**

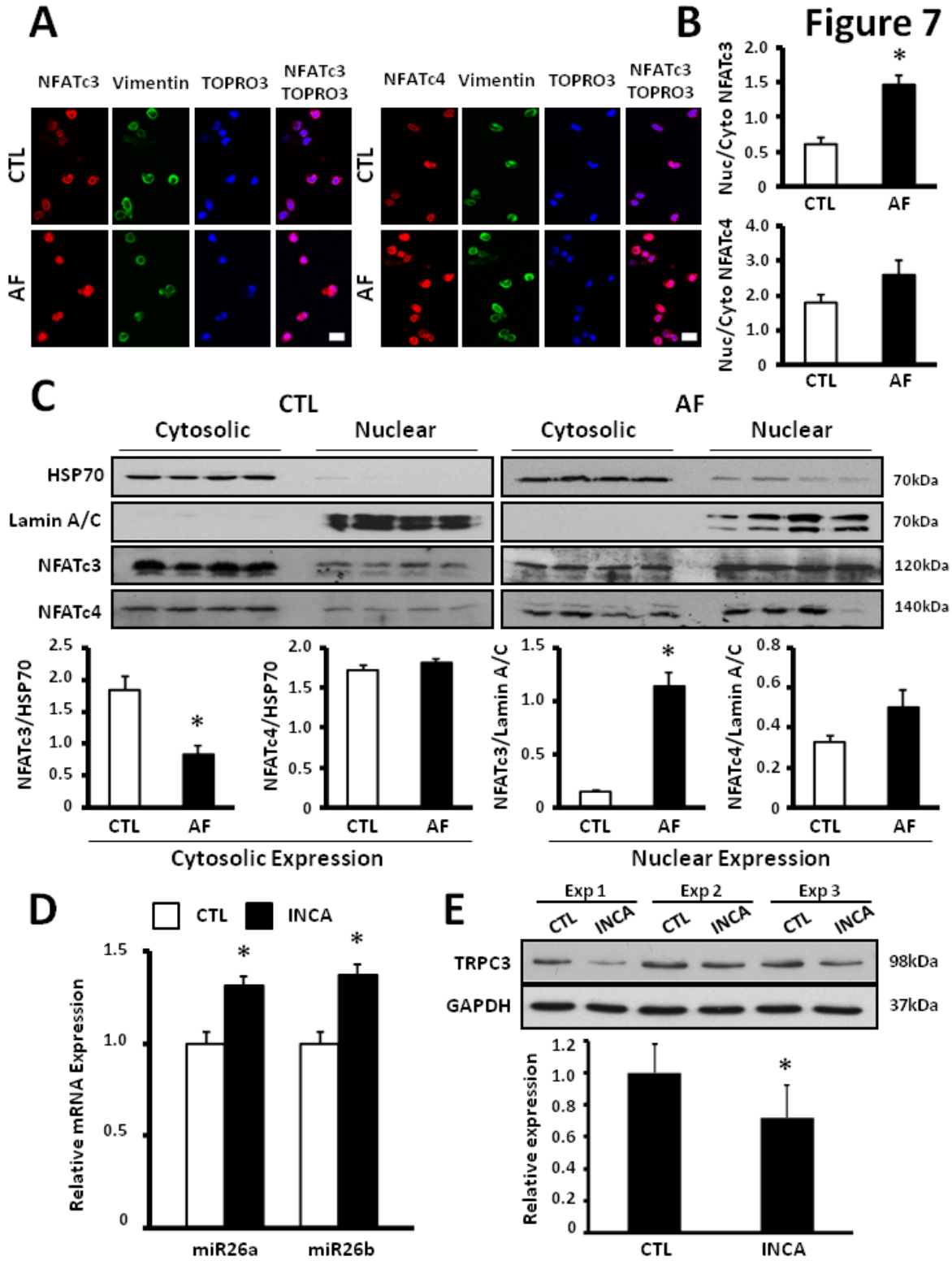
Figure 7
A
NFATc3
Vimentin
TOPRO3
NFATc3 TOPRO3
NFATc4
CTL
AF
B
Nuc/Cyto NFATc3
Nuc/Cyto NFATc4
CTL
AF
C
Cytosolic
Nuclear
HSP70
Lamin A/C
NFATc3
NFATc4
70kDa
120kDa
140kDa
NFATc3/HSP70
NFATc4/HSP70
NFATc3/Lamin A/C
NFATc4/Lamin A/C
Cytosolic Expression
Nuclear Expression
D
INCA
Relative mRNA Expression
miR26a
miR26b
E
Exp 1
Exp 2
Exp 3
TRPC3
GAPDH
98kDa
37kDa
Relative expression

**Figure 8**

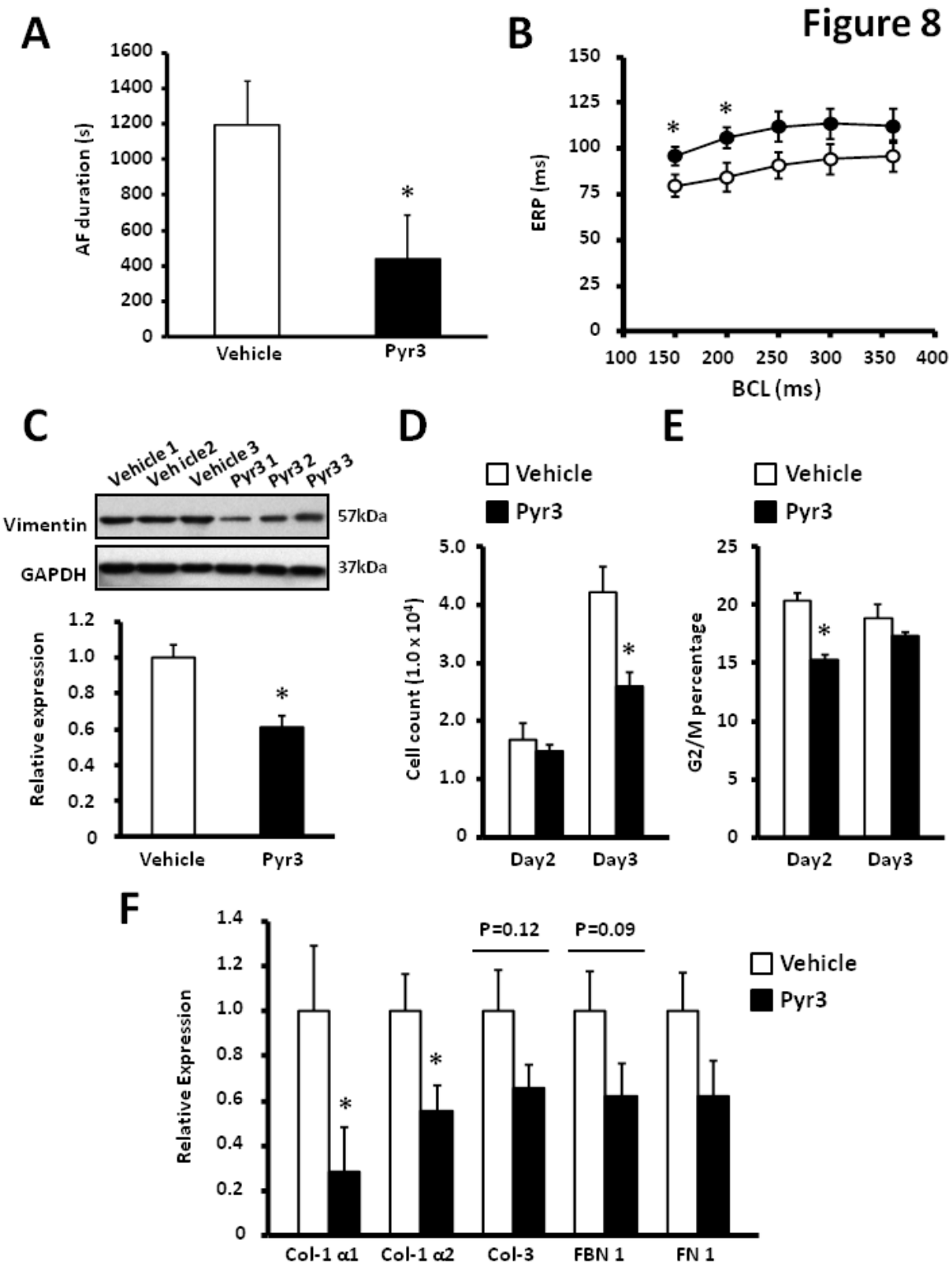
Figure 8
A
AF duration (s)
1600
1400
1200
1000
800
600
400
200
0
Vehicle
Pyr3
*
B
ERP (ms)
150
125
100
75
50
25
0
100 150 200 250 300 350 400
BCL (ms)
*
*
C
Vehicle 1
Vehicle2
Vehicle 3
Pyr3 1
Pyr3 2
Pyr3 3
Vimentin
57kDa
GAPDH
37kDa
Relative expression
1.2
1.0
0.8
0.6
0.4
0.2
0
Vehicle
Pyr3
*
D
Vehicle
Pyr3
Cell count (1.0 x 10⁴)
5.0
4.0
3.0
2.0
1.0
0
Day2
Day3
*
E
Vehicle
Pyr3
G2/M percentage
25
20
15
10
5
0
Day2
Day3
*
F
Relative Expression
1.4
1.2
1.0
0.8
0.6
0.4
0.2
0
P=0.12
P=0.09
Vehicle
Pyr3
Col-1 α1
Col-1 α2
Col-3
FBN 1
FN 1
*
*

## Supplementary Material

# TRPC3-dependent Fibroblast Regulation in Atrial Fibrillation

### Supplemental Methods

#### Rat fibroblast isolation and culture

Adult male Sprague-Dawley rats weighing 200-250 g were anesthetized with ketamine (50 mg/kg, i.p.) and xylazine (10 mg/kg, i.p.). Hearts were quickly excised via thoracotomy into ice-cold Tyrode solution containing (mol/L) 140 NaCl, 5.4 KCL, 2.0 $CaCl_2$, 1.0 $MgCl_2$, 10 HEPES, and 5.5 glucose (pH 7.35 with NaOH) and Langendorff-perfused at 37°C with 1) Tyrode solution for 5 min; 2) $Ca^{2+}$-free Tyrode solution for 5 min; 3) $Ca^{2+}$-free Tyrode solution containing 0.04 mg/ml collagenase-II for 30 min. They were then removed, minced, and homogenized in $Ca^{2+}$-free Tyrode solution. Isolated cells were centrifuged (550 rpm, 3 min), separating cardiomyocytes (primarily in the pellets) from fibroblasts (in the supernatant). Cardiomyocytes were further removed by passing the supernatant through a 20-μm nylon filter; fibroblasts were then further concentrated via centrifugation (2000 rpm, 10 min). Pellets were resuspended and washed twice in M199-medium supplemented with 10% fetal bovine serum for primary culture.

#### Atrial tissue-samples from humans, goats, and dogs

Human right-atrial appendage biopsies were obtained from patients in sinus rhythm and with chronic AF during coronary artery bypass graft surgery. The study was approved by the ethical review committee of Dresden University of Technology. All subjects gave informed consent. AF was induced in chronically-instrumented goats using repetitive burst-pacing for 10 days. Congestive heart failure (CHF) dogs with AF substrates were

created by rapid ventricular pacing (240-bpm, 2 weeks). Normal goats and dogs were used as controls. Right-atrial tissue samples were collected and fast-frozen in liquid-$N_2$.

**AF-Dogs**

A total of 48 mongrel dogs (20-36 kg) were divided into control and atrial-tachypacing groups. Animal-care procedures followed National Institutes of Health guidelines (NIH Publication No. 85-23, revised 1996) and were approved by the Animal Research Ethics Committee of the Montreal Heart Institute. Dogs were anesthetized with ketamine (5.3 mg/kg i.v.), diazepam (0.25 mg/kg, i.v.), and isoflurane (1.5%), intubated, and ventilated. A unipolar pacing lead was inserted into the right-atrial appendage under fluoroscopic guidance. The lead was connected to a pacemaker (Star Medical, Tokyo, Japan) implanted in the neck. Two bipolar electrodes were inserted into the right-ventricular apex and right-atrial appendage for internal electrocardiogram (ECG) recording. Atrioventricular-block and ventricular pacing as employed in many studies of atrial-tachycardia remodeling[1] was not performed, to more closely mimic spontaneous clinical AF-episodes. The atrial pacemaker was programmed to stimulate the right-atria at 600-bpm for 1 week, with fibrillatory atrial activity maintained during pacing as assessed by daily ECG and intracardiac recordings. Echocardiography was performed on Day 0 (before atrial pacing, baseline) and Day 7 to assess changes in LA dimension, LA systolic function and LV diastolic volume.

For in vivo treatment of the AF dogs, an Alzet osmotic pump (model 2ML1) was implanted subcutaneously in the back and a selective TRPC3 blocker, pyrazole3 (0.1 mg/kg/day, dissolved in DMSO and polyethylene glycol), or vehicle (DMSO and polyethylene glycol) was continuously administrated for the entire period of atrial tachypacing (Supplemental Figure 3).

**Dog atrial fibroblast isolation and culture**

After the open chest study, the left-atrial tissues were immersed in oxygen-saturated, $Ca^{2+}$-containing Tyrode solution at room temperature. The left circumflex coronary artery was cannulated and perfused with $Ca^{2+}$-containing Tyrode-solution (37°C, 10 min), then perfused with $Ca^{2+}$-free Tyrode-solution (15 min), followed by 50-minute perfusion with Tyrode-solution containing collagenase (Worthington, type II) and 1% bovine serum albumin (Sigma). Digested left-atrial tissue was then removed, minced, and homogenized in M199 media. Isolated cells were centrifuged (800 rpm, 3 min) to separate cardiomyocytes (primarily in the pellets) from fibroblasts (in supernatant). Cardiomyocytes were further removed by filtration of the supernatant through a 20-μm nylon filter; fibroblasts were then further concentrated via centrifugation (2000 rpm, 10 min). Pellets were resuspended and washed twice in M199-medium supplemented with 10% fetal bovine serum for primary culture.

**Terminal Open-chest Electrophysiological Study**

Dogs were anesthetized with morphine (2 mg/kg, s.c.) and α-chloralose (120 mg/kg, i.v., followed by 29.25 mg/kg/h), and mechanically ventilated. Body temperature was maintained at 37°C. A median sternotomy was performed, and bipolar electrodes were hooked into the RA appendages for recording and stimulation. Right-atrial effective refractory period (ERP) was measured at basic cycle lengths of 150, 200, 250, 300, and 360 ms with 10 basic (S1) stimuli, followed by an S2 with 5-ms decrements (all pulses twice-threshold, 2-ms). AF (irregular atrial rhythm > 400 bpm) was induced with 1-10 s atrial burst-pacing (10-20 Hz, 4×threshold, 2-ms pulses). Mean AF-duration was determined in each dog based on 10 AF-inductions for AF<5 min and 5 inductions for 5-30 min AF. AF>30 min was considered sustained: cardioversion was not performed, and

electrophysiological assessment was terminated. Haemodynamic data were obtained with fluid-filled catheters and transducers.

**qPCR**

Total RNA and microRNA were extracted with TRIzol (Invitrogen) and mirVana miRNA Extraction Kit (Ambion) from freshly isolated fibroblasts, respectively. Real-time RT-PCR was performed with 6-carboxy-fluorescein (FAM)-labeled fluorogenic Taq-Man primers and probes (Applied Biosystem). Fluorescence-signals were detected in duplicate, normalized to β2-microglobulin RNA for total RNA and to U6 snRNA for microRNA, and quantified with MxPro qPCR-software (Stratagene).

**TaqMan low-density arrays**

Total RNA was extracted using TRIzol. RNA-integrity was assessed via Agilent Bioanalyzer. (RIN>7.5 required). cDNA was synthesized using the High-Capacity cDNA Reverse Transcription Kit (Applied Biosystems) with random hexamer primers. TaqMan low-density arrays (TLDA, Applied Biosystems) were used in two-step RT-PCR as previously reported.[2] Real-time RT-PCR was performed on the 7900HT Fast Real-Time PCR System. Data were collected with SDS2.3 software and grouped with RQ Manager software. TRP-subunit genes were investigated using inventoried Taqman assays. Ct-methodology was applied to determine mRNA expression-levels. The mean expression of the genes with a Ct value below 30 (Ct<30) was selected as the reference.[3]

**Cell-Proliferation and Cell-Cycle Analysis**

Isolated cardiac fibroblasts were counted with hematocytometer and placed into T25 culture-flasks ($2.0\times10^5$ cells/flask, 25 $cm^2$ growth-area) for each treatment group. Treatment was performed on Day 2 or Day 3 unless otherwise specified. After 1-hour and 24-hour incubation, cultured fibroblasts were totally harvested from each flask following

trypsinization, then washed in ice-cold PBS and fixed in 1.0 ml of ice-cold 75% ethanol. Samples were stored at -20°C until analysis. Once pelleted, fibroblasts were re-suspended and incubated (4°C, 30 minutes) in 250 µl of staining solution containing propridium iodide (PI, Sigma) with RNAase and then 750 µl of PBS was added; the final volume in each sample was 1000 µl. In each preparation, the numbers of cells and PI fluorescence were measured with a FACScan (constant flow-rate, 60 µl/min, 5-min acquisition time, BD Bioscience) at 617-nm emission-wavelength to create a DNA content-frequency histogram. Samples were gated on fibroblast population using forward scatter vs. side scatter plot (cell size vs. granularity) and doublet discrimination gating. The percentage of cells in each phase of the cell cycle, G0/G1, S and G2/M phases, was analyzed using Flowjo software Dean-Jett-Fox model that fits G1 and G2 with Gaussian curves automatically (Tree Star Inc.).[4]

In order to confirm the accuracy of cell-counting with flowcytometry, 3-(4,5-dimethylthiazol-2-yl)-2, 5-diphenyltetrazolium bromide (MTT) cell proliferation assay was also performed with using Cell Proliferation Kit I (Roche). Two-day cultured fibroblasts were resuspended and transferred into a 96-well plate ($5.0\times10^3$ cells/well, 0.32 $cm^2$ growth-area). The cells were incubated with the same treatment protocol for the flowcytometry experiment. The assay was triplicated in each treatment group. The absorbance (550 nm-690 nm) was quantified using a scanning multiwell spectrophotometer (Synergy2, BioTek). The cell-counting with flowcytometry described above was also performed in parallel with the same passage fibroblast samples. Both proliferation assays showed similar results (Figure A and B below).

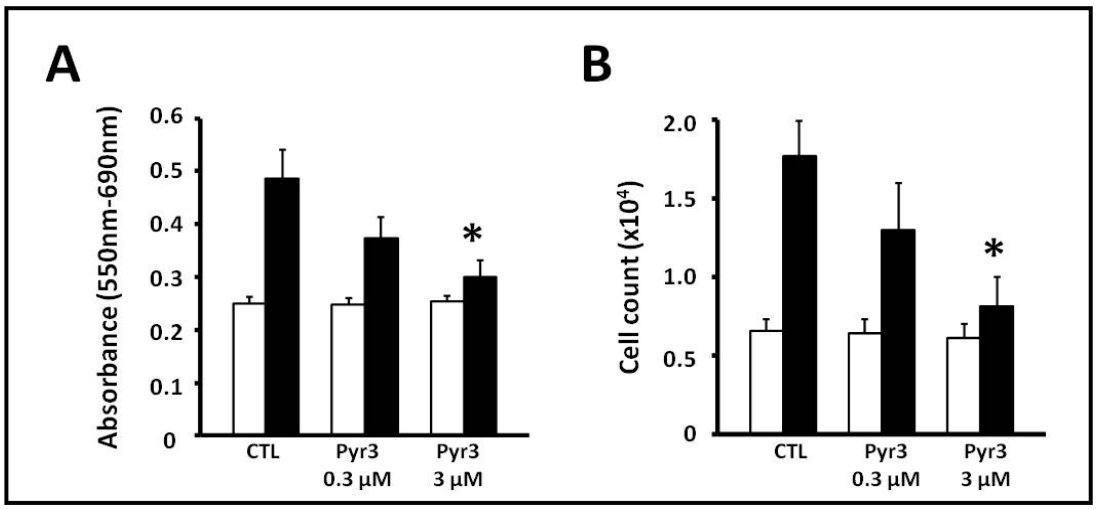


A, Cultured rat fibroblast proliferation estimated by MTT assay after 1-hour and 24-hour treatment with vehicle-control, or 0.3 or 3-µmol/L Pyr3. Mean±SEM spectrophotometrical absorbance (550 nm-690 nm) (n=6, $P<0.05$ vs. CTL). B. Mean±SEM cell-count of rat fibroblast with flowcytometry after 1-hour and 24-hour treatment with vehicle-control, or 0.3 or 3-µmol/L Pyr3. (n=6, $P<0.05$ vs. CTL).

**Western Blots**

Total protein was extracted from freshly-isolated/cultured fibroblasts or atrial tissues, quantified, and processed as previously described. Cytoplasmic and nuclear protein fractions were extracted from fresh fibroblasts with ProteoExtract Subcellular Proteome Extraction Kit (Calbiochem, Darmstadt, Germany). Protein-samples (20 µg/lane for total protein and 30 µg/lane for fractionated protein) were separated by 8% SDS-PAGE electrophoresis and then transferred to polyvinylidene-difluoride membranes. Membranes were blocked and incubated with mouse anti-α smooth-muscle actin (αSMA, 1/2000, Sigma), mouse anti-phospho p44/42-MAP-kinase (1/2000, Cell signaling), mouse anti-vimentin (1/1000, Santa Cruz), rabbit anti-TRPC3 (1/1000, Alomone), rabbit anti-TRPC1 (1/200, Alomone), mouse anti-TRPM7 (1/1000, Neuromab), mouse anti-NFATc3 (1/1000, Santa Cruz), rabbit anti-NFATc4 (1/1000, Santa Cruz), mouse anti-HSP70 (1/1000,

Stressgen), mouse anti-Lamin A/C (1/1000, Abcam), anti-GAPDH (1/10000, Fitzgerald), and rabbit anti-calsequestrin (1/2500, Dianova). Corresponding secondary antibodies conjugated to horseradish-peroxidase were used for detection. Staining was detected using chemiluminescence and quantified by video densitometry. All expression data are provided relative to GAPDH or calsequestrin staining for the same samples on the same gels.

**Confocal Imaging**

Cultured/freshly-isolated fibroblasts or left atrial tissue cryosections were fixed with 2%-paraformaldehyde, washed with PBS, and incubated with mouse anti-alpha SMA (1/400, Sigma), goat anti-vimentin (1/200, Santa Cruz), mouse anti-NFATc3 (1/200, Santa Cruz), rabbit anti-NFATc4 (1/200, Santa Cruz), followed by donkey anti-mouse IgG-Alexa Fluor 555 (1/600, Invitrogen), donkey anti-rabbit IgG-Alexa Fluor 488 (1/600, Invitrogen), donkey anti-goat IgG-Alexa Fluor 488 (1/600, Invitrogen), and TOPRO-3 iodide (1/500, Invitrogen). Apoptosis was assessed using TUNEL-assay with ApopTag plus fluorescein *in situ* apoptosis detection kits (Millipore). Fluorescent images were obtained via Zeiss LSM-710 or OLYMPUS Fluoview FV1000 inverted confocal microscope.

**Fluorescent $Ca^{2+}$-Imaging**

Primary cultured fibroblasts (1-day culture as described above) were loaded with Fluo-4 (10 μmol/L) in phenol-free M199-medium in the presence of pluronic acid (2.5 μg/ml) for 50 min at 37°C. $Ca^{2+}$-imaging was recorded with an Andor Revolution confocal system and a Xion camera (Andor Technologies) mounted on an upright Nikon FN-1 microscope with a 60× water-immersion objective (1.0 NA). Fluo-4 was excited with a 488-nm solid-state laser; emitted fluorescence was collected at 495 nm. Images (512×512 pixels) were acquired at 15 frames/sec for 5 min using iQ software (Andor Technologies). $Ca^{2+}$-associated fluorescence was analyzed with custom-designed software (A. Bonev,

University of Vermont). Regions of interest (ROIs) were determined by cell-outlines. $F_O$ was determined by averaging fluorescence of ROIs from 10 consecutive baseline images.[5] At the end of experiments, ATP (100-µmol/L) was applied to verify cell-viability. One-day cultured fibroblasts were incubated in 2-mmol/L $Ca^{2+}$-containing Tyrode solution followed by $Ca^{2+}$-free solution to induce $Ca^{2+}$-store depletion and store-dependent $Ca^{2+}$-entry. Under OAG (25-µmol/L)- or angiotensin-II (100-nmol/L)-stimulation, cell-$Ca^{2+}$ was recorded with confocal microscopy 5 minutes before and after re-administration of 2-mmol/L $Ca^{2+}$ into the extracellular solution.

**TRPC3-knockdown**

**Plasmid constructs**

The TRPC3-specific shRNAmir over-expressing pGIPZ-based lentivirus vector plasmid was obtained from Open Biosystems (Oligo ID: V2LMM_11490).

The scrambled shRNAmir over-expressing plasmid was generated as follows. The empty pGIPZ lentivirus vector plasmid carrying the mRNA-context sequence but no shRNA was obtained from Open Biosystems. The EcoRI site of pGIPZ located at position 5394 was removed by partial EcoRI digestion and Klenow fill-in, resulting in pGIPZΔEcoRI. This modification allowed the direct cloning of the scrambled shRNAmir construct in pGIPZ between XhoI, 2654 and EcoRI, 2678 sites. In the design of the scrambled shRNAmir and during the rest of the cloning procedure, we followed the methods by Paddison et al.[6] Briefly, a 97bp long synthetic oligonucleotide ( 5`TGCTGTTGACAGTGAGCG*CCGATATCAGCAGATAATGAAA*TAGTGAAGCCACA GATGTA TTTCATTATCTGCTGATATCGTTGCCTACTGCCTCGGA 3`, *passanger strand*, loop, guide strand) was PCR amplified by 5`CAGAAGGCTCGAGAAGGTATATTGCTGTTGACAGTGAGCG sense and 5`

CTAAAGTAGCCCCTTGAATTCCGAGGCAGTAGGCA antisense primers, carrying XhoI and EcoRI restriction sites, respectively. PCR product was cloned in pGIPZΔEcoRI at XhoI, EcoRI sites. Sequence identity of the resulting clone was verified by sequencing.

The psPAX2 and pMD2.G lentivirus packaging plasmids were obtained from Didier Trono`s laboratory (http://tronolab.epfl.ch/, Ecole Polytechnique Federale de Lausanne, Lausanne, Switzerland) through Addgene (Addgene plasmid 12260 and 12259).

All plasmids were amplified in *E. coli* DH5α and purified by Nucleobond anion exchange columns (Macherey-Nagel) following the manufacturer's instructions.

**Lentivirus production**

The Hek293T/17 cell line we used for producing lentivirus production was obtained from ATCC (Manassas, VA, USA) and were grown in DMEM (Invitrogen) supplemented with 10% FCS (Gibco). Lentiviruses were produced by following the protocols available from Didier Trono`s laboratory (http://tronolab.epfl.ch) with minor modifications. A subconfluent monolayer of Hek293T/17 cells (ATCC) kept in DMEM (Invitrogen) supplemented with 10% FBS (Gibco) were transfected with a mixture of plasmids containing one of the vector plasmids and the psPAX2 and pMD2.G packaging plasmids in 2:2:1 weight ratio by the calcium-phosphate precipitation method. Eight hours after transfection, the culture medium was replaced by fresh culture medium. The supernatant containing the lentivector particles was harvested two times 32 and 56 hours post-transfection. The harvested medium was clarified from cell debris by low-speed centrifugation and by filtration through a 0.45 μm pore size syringe-attached filter. Virus particles were concentrated by ultracentrifugation at 47000 g (RCF average) for 2 hours in a swinging bucket rotor, re-dissolved in sterile PBS containing 1% BSA and stored at -80°C

in aliquots. Virus preparations were titrated on Hek293T/17 cells.

***miR-26a*-Overexpression/Knockdown**

For the *miR-26a* overexpression, the sense (5` UUCAAGUAAUCCAGGAUAGGCU 3`) and antisense (5` CCUAUUCUUGGUUACUUGCACG 3`) oligoribonucleotides were synthesized by Invitrogen. The both strands were annealed by mixing the same volume of each oligoribonucleotides dissolved in annealing buffer (IDT, Coralville, IA) at a concentration of 200 μmol/L and then incubated at 95°C for 10 min, 70°C for 10 min and then 50°C for 10 min. A scrambled RNA was used as negative control (sense: 5` UCAUAAAGCUGAUAACCUCUAGAU 3`, antisense: 5` CUAGAGGUUAU CAGCUUUAUGAAU 3`).

For the *miR-26a* knockdown, the antisense anti-miRNA oligonucleotides (AMO26a: 5` AGCCTATCCTGGATTACTTGAA 3`) was synthesized by Exiqon (Exiqon, Woburn, MA). Five oligonucleotides on 5`-end of the antisense molecules and four oligonucleotides on 3`-end were locked by a methylene bridge connecting the 2'-O atom and 4' -C atom (Locked Nucleic Acid, LNA). A scrambled oligonucleotides with the same methylene bridge were used as negative control (5` ACTCAGAAGGACAAGTAGAGTCT 3`).

Dog left-atrial fibroblasts in primary culture were transfected with miR-26a (final concentration of 100 nmol/L) and/or AMO26a (final concentration of 10 nmol/L), and negative control miRNAs or AMOs with lipofectamine 2000 (Invitrogen).[7] After 48-hour transfection, cells were collected for total RNA/protein purification or proliferation analysis with a FACScan. The efficacy of miR-26a overexpression/knockdown by the miR-26a probes was confirmed by qPCR before experiments (Supplemental Figure 12C).

**Dual Luciferase Reporter Assay**

A fragment (5`

TGACTATAGCACAAATGTGGGCAATAATATTTCTAAGTATAAAATACTT GAAATGGTGTAAATTTTTAGTATTAACTACCTTTATCATGTGAATCTTTAA 3` miR-26a target site) containing miR-26a target gene of TRPC3 was synthesized by Invitrogen and was used as a template for PCR amplification with 5` GACTAGTTGACTATAGCA CAAATGT 3` and 5` CCCAAGCTTTTAAAGATTCACATGATA 3`as forward and reverse primers, respectively. The PCR product was ligated into HindIII and SpeI sites (3` UTR region of luciferase gene) in the pMIR-REPORT luciferase miRNA expression reporter vector (CMV promoter-driven Firefly luciferase expression vector, Applied Biosystems) and was subcloned.

For luciferase assay, HEK293 cells were simultaneously transfected with 50 ng of pMIR-REPORT, 0.5 ng pRL-TK (TK promoter-driven Renilla luciferase expression vector, Promega, Madison, WI) and miR-26a (final concentration of 10 nmol/L) and/or AMO26a (final concentration of 3 nmol/L) with lipofectamine 2000 (Invitrogen). After 48-hour transfection, luciferase activities were measured with a dual luciferase reporter assay kit (Promega) on a luminometer (Lumat LB9507, Berthold, Bad Wildbad, Germany).[7] The pMIR-REPORT firefly luciferase signals were normalized to the pRL-TK renilla luciferase signals as an internal control.

**Statistical Analyses**

Data are presented as mean±SEM. Two-way ANOVA with multiple-group comparisons (Bonferroni-corrected t-test) was data with two or more main-effect factors like flow-cytometry with varying culture-times (treatment and time as main-effect factors) and ERP (basic cycle length and dog-group main factors). One-way ANOVA was applied for single main-effect factor experiments like Western blots, qPCR, and luciferase assay. Repeated-measure analyses were used when the same set of subjects/materials were exposed to

multiple interventions. Students' *t*-tests were used for comparisons involving only two groups. For multiple comparisons with Bonferroni correction, adjusted *P*-values were calculated as multiplying original *P* values for each pairwise comparison by the number of comparisons (*N*) performed; values shown are adjusted values ($N \times P$). Two-tailed $P<0.05$ was considered to be statistically significant. All analyses were performed with SPSS 16.0.

**Specific Analyses for individual figures and tables:**

Two-way ANOVA with multiple comparison (Bonferroni-adjusted t-tests) was used for data with two or more factors as main effects and repeated measures (Figures 1D, 1E and 1F, Figures 2B-2E, Figure 3B, Figure 4B, Figure 5A, 5B, 5D, 5E, Figure 8B, 8D and 8E, Supplemental Figure 4B, Supplemental Figure 5C and 5D, Supplemental Figure 7B and 7C, Supplemental Fig 8C and 8D).

One-way ANOVA was applied for data with a single main-effects factor as obtained in studies of heart rate and echocardiographic data over time, with one main factor and 3 levels (groups) or more (Supplemental Fig 11A, 11C-11E). Repeated-measure analyses were used when the same set of subjects/materials were exposed to multiple interventions (Figure 2A, Figure 6B-6G, Supplemental Fig 12C).

Paired t-tests were used for Figures 1H, Figure 5F Figures 7D and 7E, and Supplemental Figures 6B, 7D, 8A and 8B.

Non-paired t-tests were used for Figures 3C, 3E-G, Figure 4CE, Figure 5C, 5G, Figure 7B, 7C, Figures 8A, 8C, and 8F, and Figures 9A-I as well as Supplemental Table 1.

**REFERENCES**

1. Sakabe M, Shiroshita-Takeshita A, Maguy A, Dumesnil C, Nigam A, Leung TK, Nattel S. Omega-3 polyunsaturated fatty acids prevent atrial fibrillation associated with heart failure but not atrial tachycardia remodeling. *Circulation*. 2007;116:2101-

2109.

2. Gaborit N, Le Bouter S, Szuts V, Varro A, Escande D, Nattel S, Demolombe S. Regional and tissue specific transcript signatures of ion channel genes in the non-diseased human heart. *J Physiol*. 2007;582:675-693.

3. Mestdagh P, Van Vlierberghe P, De Weer A, Muth D, Westermann F, Speleman F, Vandesompele J. A novel and universal method for microRNA RT-qPCR data normalization. *Genome Biol*. 2009;10:R64.

4. Fox A. A model for the computer analysis of synchronous DNA distributions obtained by flow cytometry. *Cytometry*. 1980;1:80-81.

5. Ledoux J, Taylor MS, Bonev AD, Hannah RM, Solodushko V, Shui B, Tallini Y, Kotlikoff MI, Nelson MT. Functional architecture of inositol 1,4,5-triphosphate signaling in restricted spaces of myoendothelial projections. *Proc Natl Acad Sci U S A*. 2008;105:9627-9632.

6. Paddison PJ, Cleary M, Silva JM, Chang K, Sheth N, Sachidanandam R, Hannon GJ. Cloning of Short hairpin RNAs for gene knockdown in mammalian cells. *Nature methods*. 2004;1:163-167.

7. Xiao J, Lin H, Luo X, Luo X, Wang Z. miR-605 joins p53 network to form a p53: miR-605:Mdm2 positive feedback loop in response to stress. *EMBO J.* 2011;30:524-532.

**Supplemental Table 1. Hemodynamic Data**

| | Control (n=11) | AF (n=12) |
|---|---|---|
| Body weight, kg | 26.8±0.3 | 28.2±0.2 |
| Systolic BP, mmHg | 127±2 | 120±2 |
| Diastolic BP, mmHg | 73±2 | 76±2 |
| RAP, mmHg | 1.3±0.1 | 2.5±0.1* |
| LAP, mmHg | 2.6±0.1 | 6.5±0.3* |
| RVP, mmHg | 22±0.4 | 23±0.5 |
| RVEDP ,mmHg | 1.5±0.1 | 4.2±0.3* |
| LVP, mmHg | 116±1.4 | 101±1.9 |
| LVEDP, mmHg | 3.9±0.2 | 8.0±0.5* |

*$P<0.05$ vs control.

BP indicates blood pressure; RAP and LAP, RA and LA mean pressure; RVP and LVP, RV and LV mean pressure; RVEDP and LVEDP, RV and LV end diastolic pressure.

**Supplemental Figure Legends**

**Supplemental Figure 1.** A, mRNA expression of TRP channels measured by Taqman Low-density array. B, mRNA expression of TRPC3 channel on enlarged scale.

**Supplemental Figure 2.** A, Representative immunofluorescent images of freshly-isolated rat cardiac fibroblasts. Red indicates α-smooth muscle actin (αSMA); green, vimentin; blue, TOPRO-3 (nuclear staining). B, Representative immunofluorescent images of passage-cultured myofibroblasts. C, Representative $I_{NSC}$-recordings with or without gadolinium ($Gd^{3+}$, 100-μmol/L) in freshly-isolated rat cardiac fibroblasts. Voltage-clamp protocol is shown in the inset. D and E, Representative $Gd^{3+}$- and Pyr3-sensitive $I_{NSC}$ in passage-cultured myofibroblasts. F, Mean±SEM $Gd^{3+}$- and Pyr3-sensitive $I_{NSC}$ density (n=10 cells in $Gd^{3+}$ and 8 cells in Pyr3).

**Supplemental Figure 3.** Protocol for in vivo TRPC3-blocker (pyrazole-3) treatment study in AF dogs.

**Supplemental Figure 4.** A, Recordings of OAG-induced intracellular $Ca^{2+}$-response in presence or absence of Pyr3. B, Mean±SEM OAG-induced $Ca^{2+}$ fluorescence ($F/F_0$), normalized to baseline intensity under 0-mmol/L and 2-mmol/L $Ca^{2+}$ (n=14 cells in each condition, *$P$<0.05 vs. 0-mmol/L $Ca^{2+}$, #$P$<0.05 vs. 2-mmol/L $Ca^{2+}$ in OAG-only).

**Supplemental Figure 5.** A and B, Representative DNA-content histograms and Dean-Jett-Fox model fitting of rat cultured fibroblasts with or without 24-hour treatment of $Gd^{3+}$ (100-μmol/L) or Pyr3 (3-μmol/L). C, Mean±SEM cell-count of rat fibroblasts after 1-hour and 24-hour culture with vehicle-control, or 10 or 100-μmol/L $Gd^{3+}$ (n=8/group, *$P$<0.05 vs. CTL, #$P$<0.05 vs. 1-h treatment). D, Mean±SEM percentage of cells in G2/M-phase after $Gd^{3+}$ treatment (n=8/group, *$P$<0.05 vs. CTL, #$P$<0.05 vs. 1-h

treatment).

**Supplemental Figure 6.** A, Representative images of TUNEL staining in cardiac rat fibroblasts with or without Pyr3 treatment (3-μmol/L). Red indicates TOPRO-3 (nuclear staining); yellow, TUNEL-positive cells. B, Mean±SEM percentage of TUNEL-positive cells. (n=5/group, **P*<0.05 vs. CTL).

**Supplemental Figure 7.** A, Representative immunofluorescent images of rat cardiac fibroblasts cultured with or without Pyr3 (3-μmol/L). Red indicates α-smooth muscle actin (αSMA); blue, TOPRO-3 (nuclear staining). B, Mean±SEM cell-count of culture-passaged fibroblasts after 1-hour and 24-hour treatment with 3-μmol/L Pyr3 or vehicle DMSO (n=6/group). C, Mean±SEM percentage of culture-passaged fibroblast cells in G2/M-phase after Pyr3 treatment or vehicle DMSO (n=6/group). D, Representative immunoblots (left) and mean±SEM αSMA-expression in culture-passaged fibroblasts (right, normalized to GAPDH) (n=6).

**Supplemental Figure 8.** A, Mean±SEM TRPC3 and TRPC6 mRNA-expression in scrambled (Scr)-shRNA- and TRPC3-shRNA-infected dog atrial fibroblasts (n=6/group, **P*<0.05 vs. scrambled shRNA). B, Top: Immunoblots for TRPC3 subunits and GAPDH. Bottom: Mean±SEM TRPC3/GAPDH protein-expression (n=6, **P*<0.05 vs. scramble shRNA). C, Mean±SEM fold-change over time in the number of fibroblasts, following infection with shRNA or scrambled-probe virus (n=6/group, **P*<0.05 vs. scrambled shRNA). D, Mean±SEM percentage of virus-infected fibroblast cells in G2/M-phase (n=6/group, **P*<0.05 vs. scrambled-shRNA).

**Supplemental Figure 9.** A, through C, Representative immunoblots (top) and mean±SEM (bottom) TRPC3 subunit protein-expression (normalized to calsequestrin, CSQ) in right-atrial samples from patients with AF (n=8) and in sinus rhythm (n=10), AF

model goats (n=8) and normal goats (n=5) and congestive heart failure dogs with AF substrates (n=8) and normal dogs (n=8) (*$P$<0.05 vs. control). D through F, TRPC1 subunit expression. G through I, TRPM7 subunit expression.

**Supplemental Figure 10.** A-E, Representative surface ECGs (left) and intracardiac electrograms (right) in an AF dog on Day 0 through Day 7.

**Supplemental Figure 11.** A, Mean±SEM heart rate over time during atrial tachypacing, ATP (n=7 CTL and 12 AF, *$P$<0.05 vs. CTL). B, Representative apical 4 chamber views of echocardiography on Day 0 (baseline, before pacing, left) and Day 7 (right) in an AF dog. C, Mean±SEM atrial diastolic area (n=10 CTL and 11 AF, $P$<0.05 vs. CTL). D, atrial fractional area change. E, ventricular diastolic volume.

**Supplemental Figure 12.** A, miR-26 and its complementary sequence on TRPC3 3'-UTR region. Sequences highlighted in yellow represent the seed region of miR-26a. B, Antisense anti-miR-26a oligonucleotide (AMO26a) sequence and its complementarity to miR-26. Sequences highlighted in yellow represent the seed region of miR-26. Bold characters in the AMO26a sequence indicate locked nucleic acids (LNAs). C, Results of miR-26a overexpression/knockdown by miR-26a duplex/AMO26a in dog left-atrial fibroblasts. Lipo; lipofectamine transfection without the miR-26a probes. (n=4, $P$<0.05 vs. Lipo). D, Multiple putative NFAT binding motifs in the promoter regions of the host gene for miR-26a and miR-26b in human and canine genomes. Ctdsp: Carboxy-Terminal Domain RNA polymerase II polypeptide A Small Phosphatase. The numbers before the sequences represent the relative positions of predicted NFAT binding motifs to the transcription start site (TSS) of the host gene. The numbers in the brackets stand for the scores given by Genomatix (http://www.genomatix.de) for the similarity between the putative NFAT cis-acting

elements in the promoter regions of the host genes for miR-26a/b and the perfect NFAT binding sequence; Two scores are given as core sequence similarity and overall sequence similarity. Only those with overall matrix similarity >0.95 are shown. 5000 bp upstream to the predicted TSS for miR-26a/b host genes in human and canine was analyzed.

**Supplemental Figure 1**

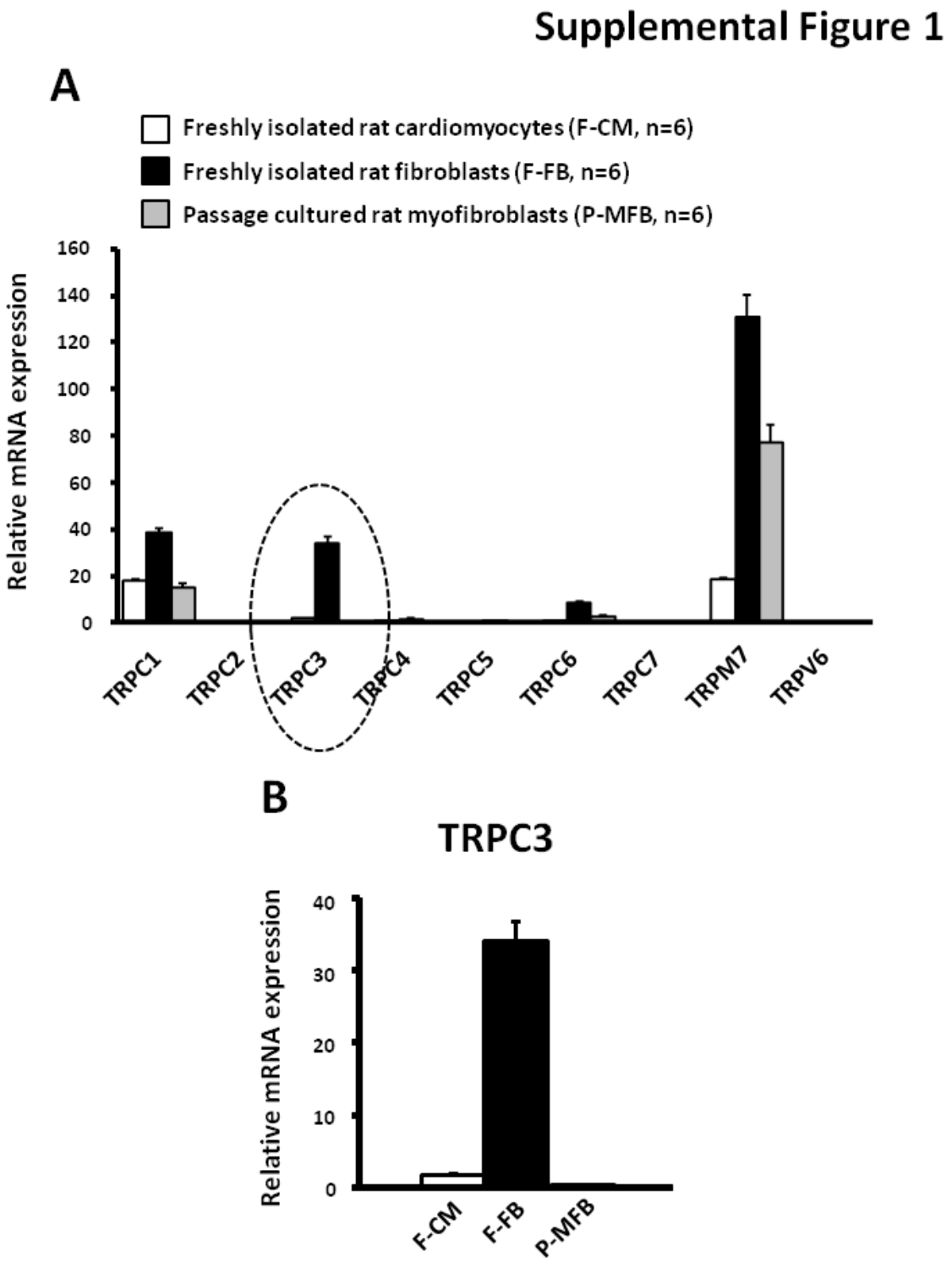

**Supplemental Figure 2**

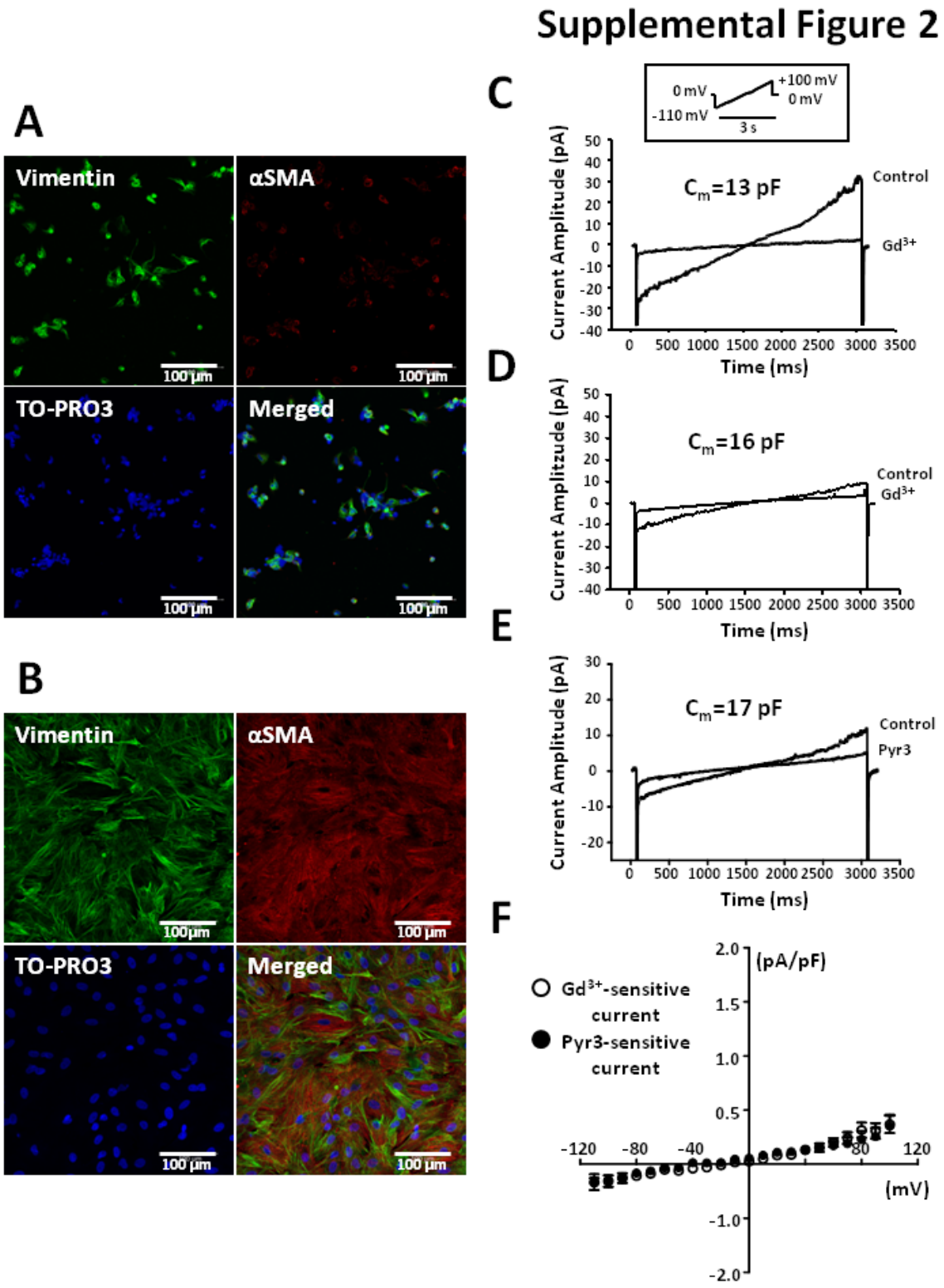

**Supplemental Figure 3**

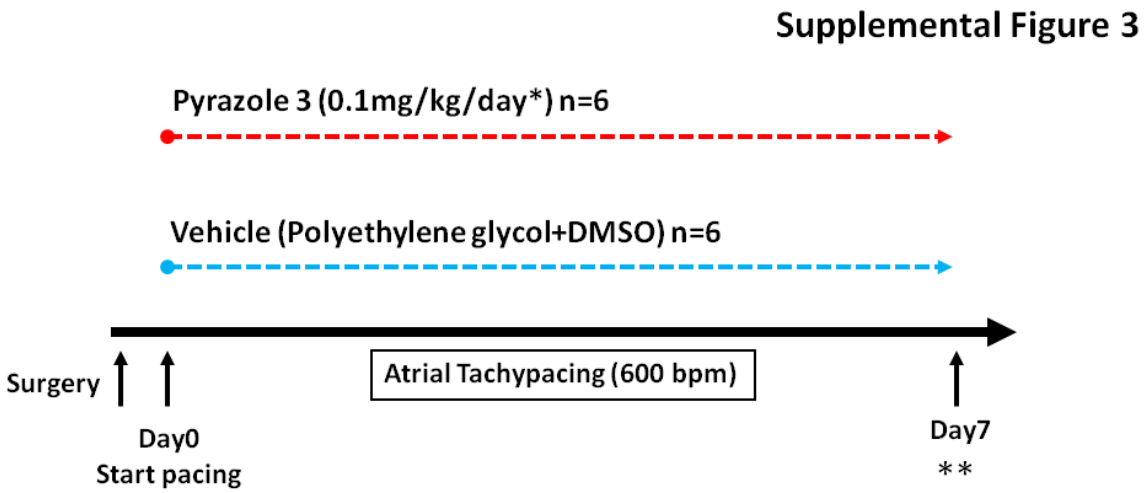


Drugs were continuously administrated with Alzet Osmotic Pump.

**Terminal Experiments

Open Chest EP study

Vimentin Western Blotting in LA tissue sample

qPCR for collagen gene in Fresh FB

Proliferation Assay in cultured FB

***Kiyonala et al PNAS 2009 106;5400-5405*

**Supplemental Figure 4**

Supplemental Figure 4

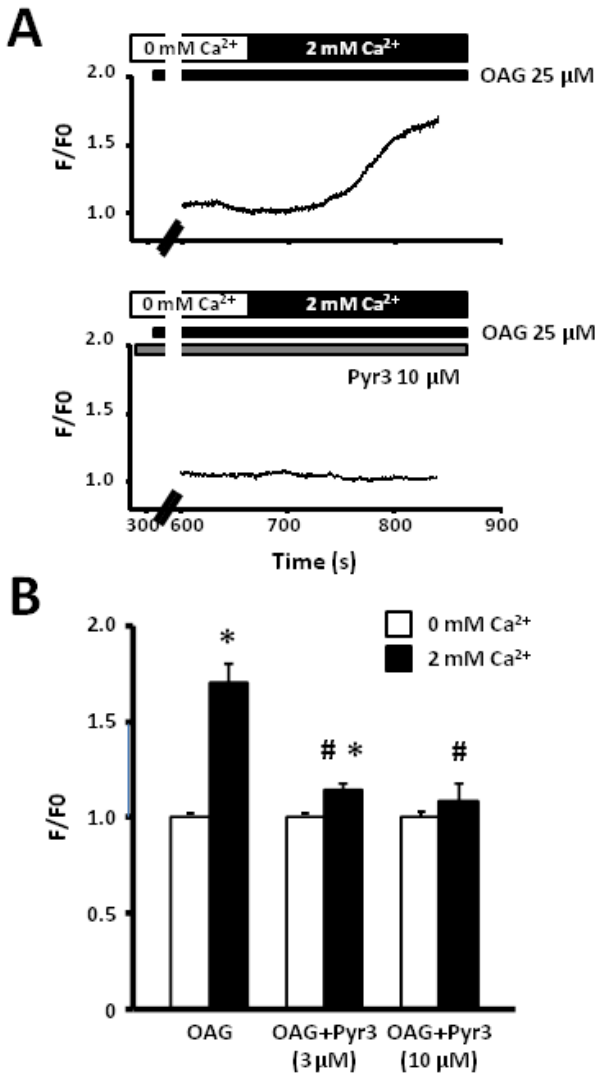

**Supplemental Figure 5**

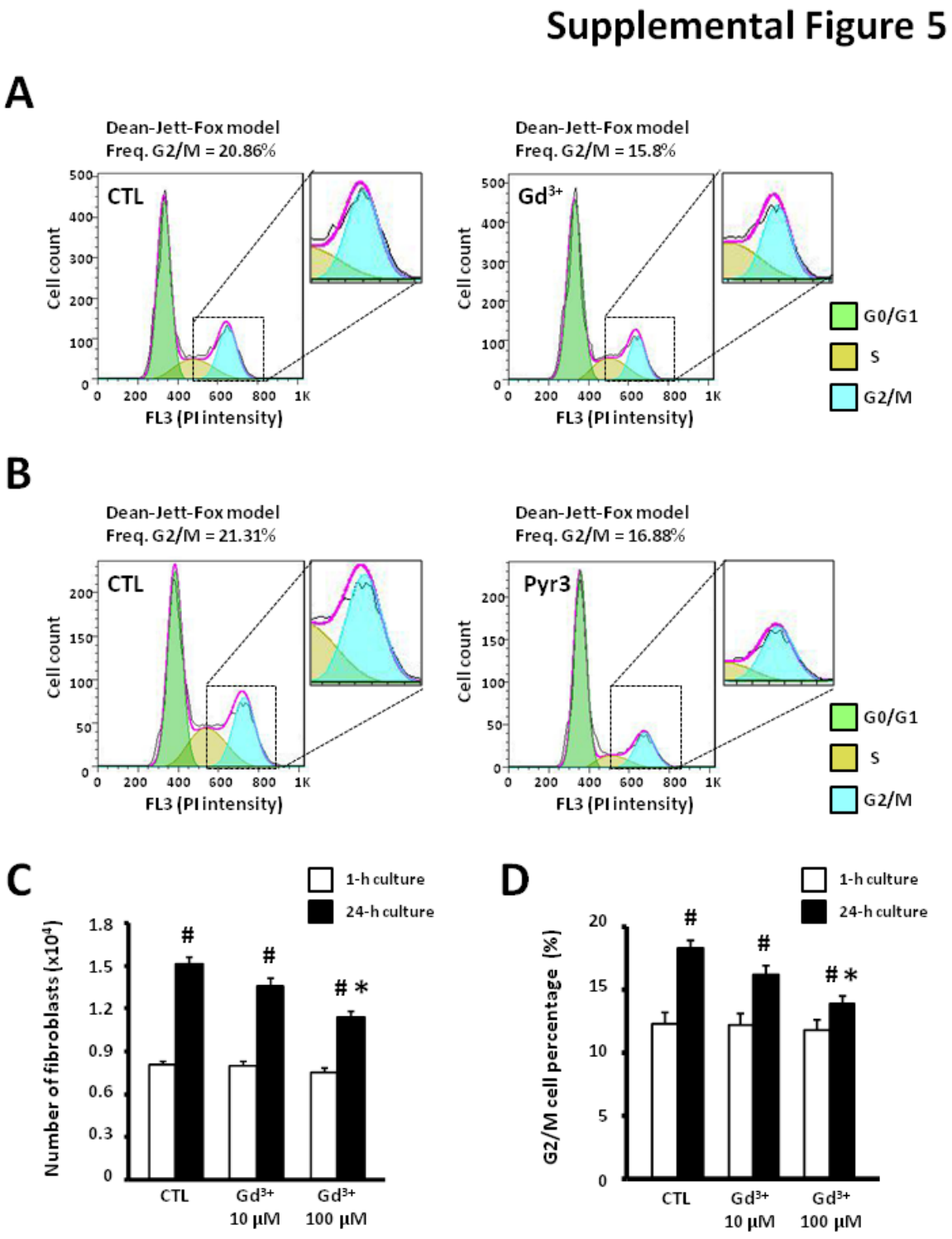

**Supplemental Figure 6**

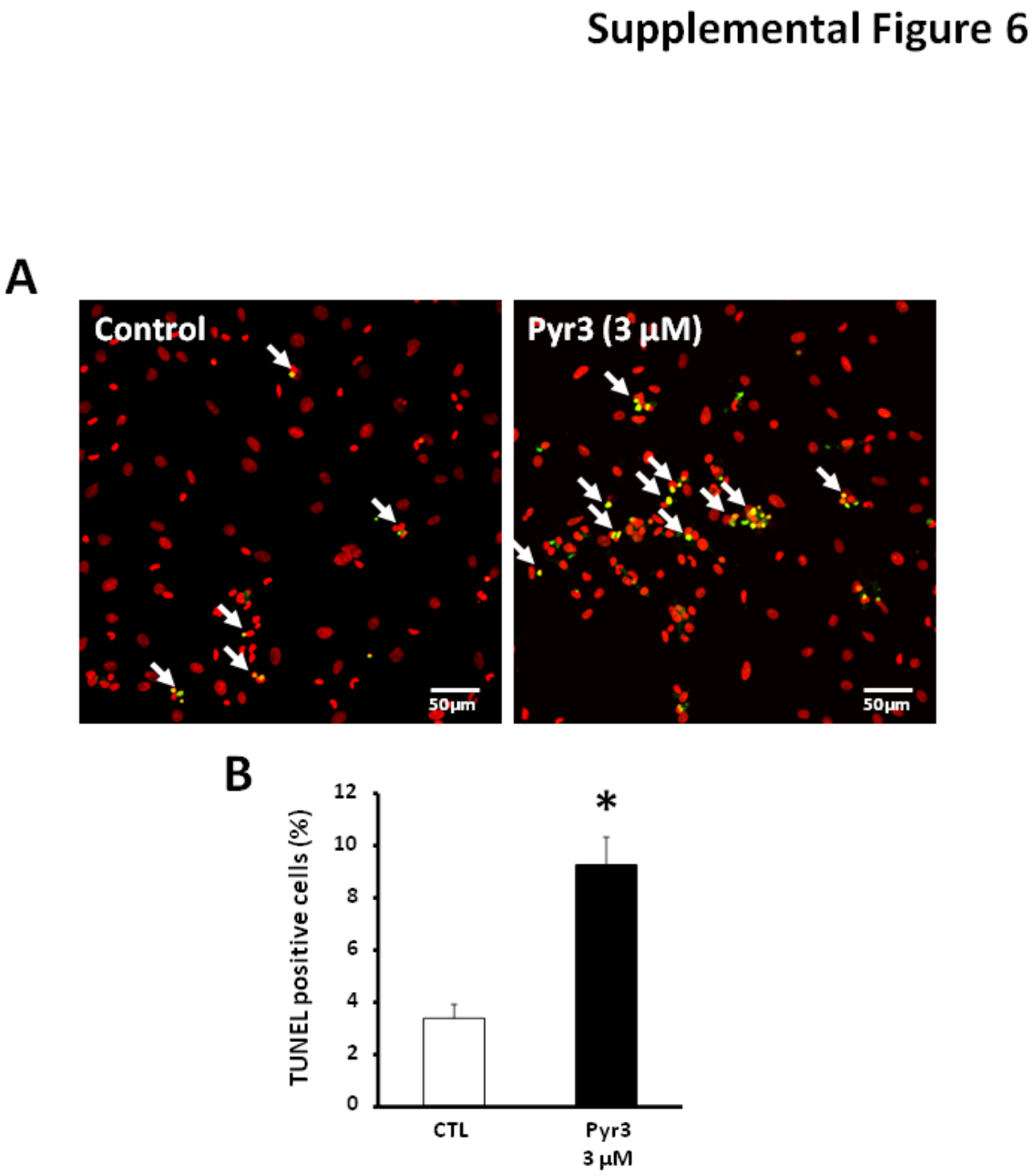

**Supplemental Figure 7**

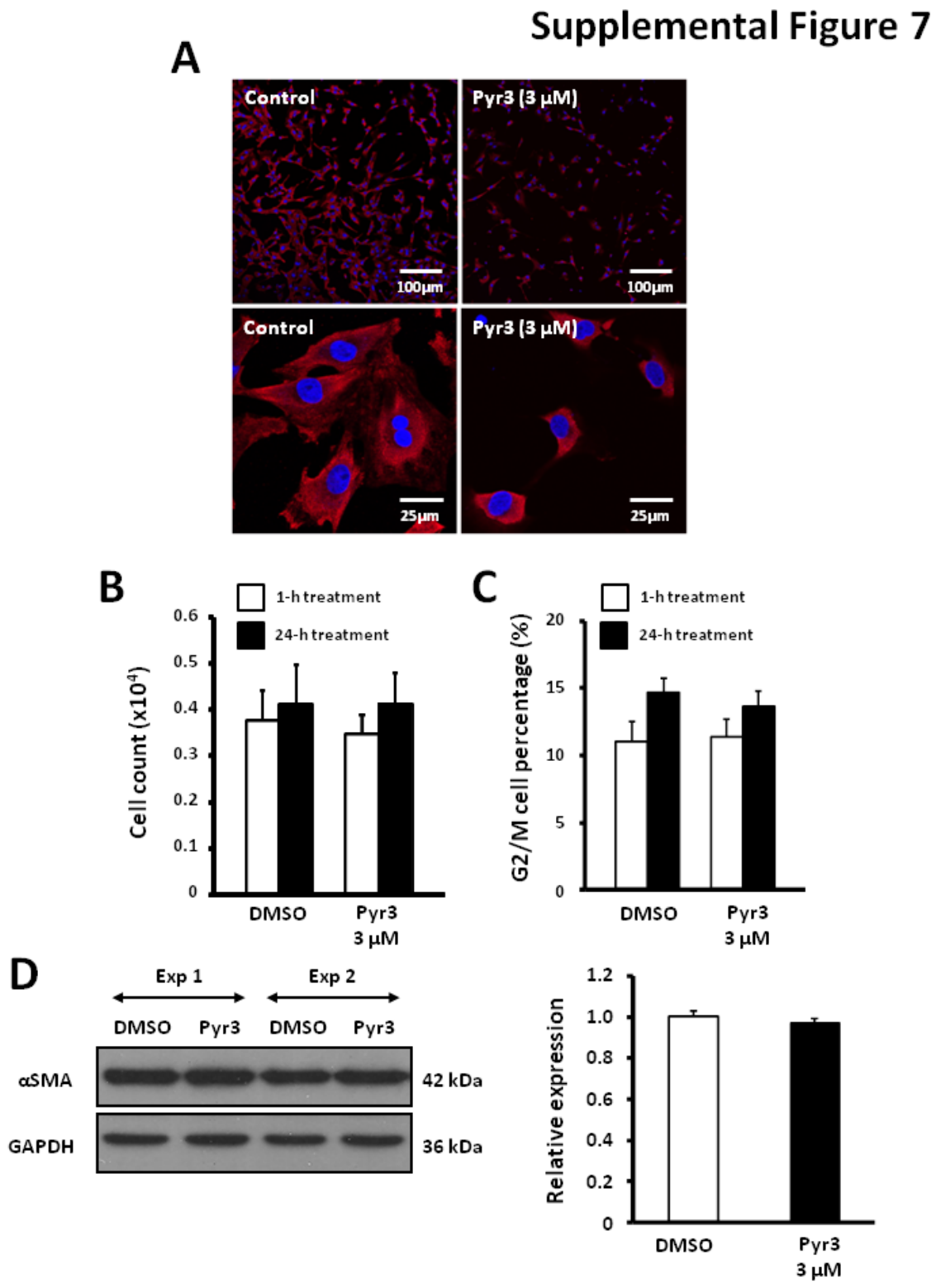

**Supplemental Figure 8**

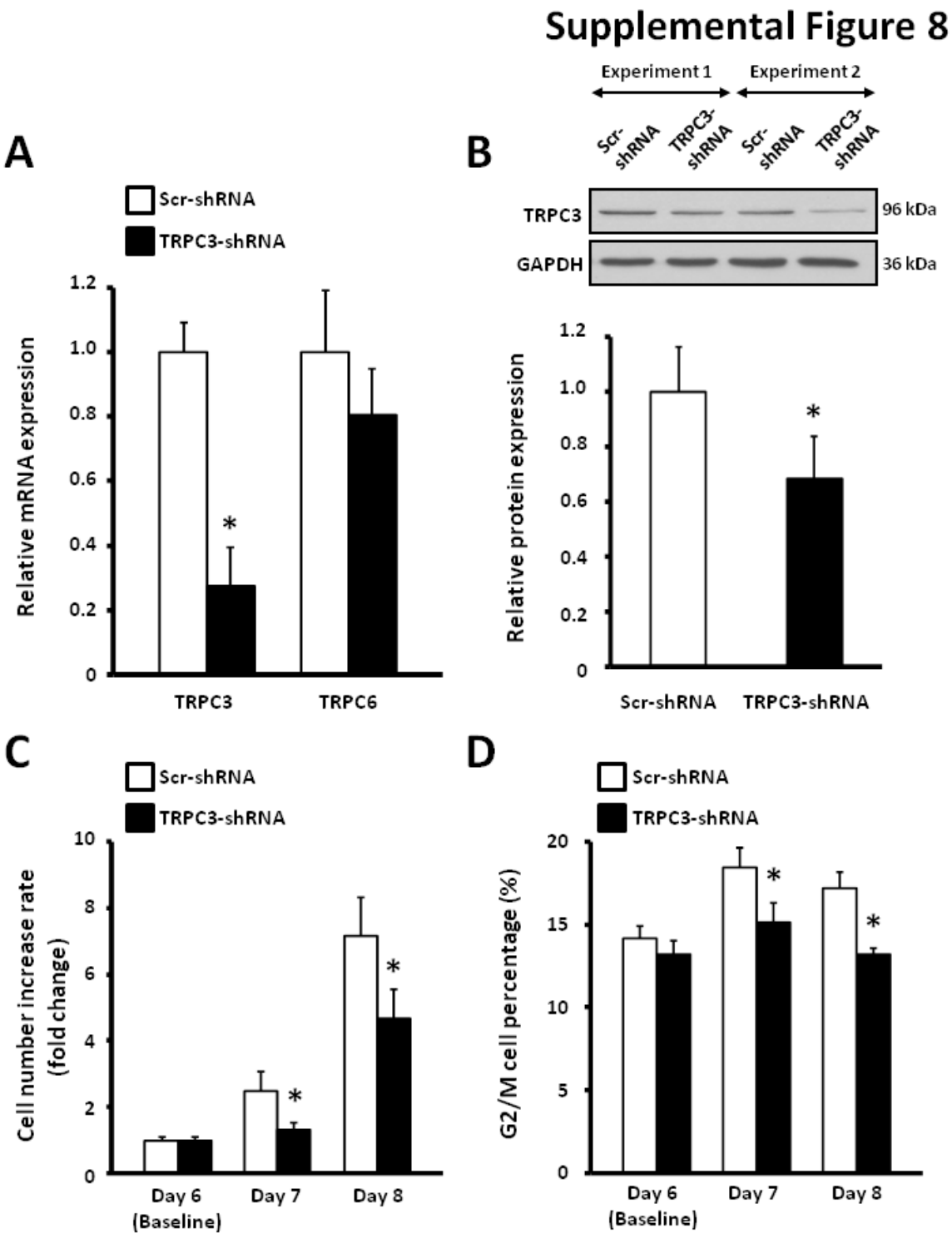

**Supplemental Figure 9**

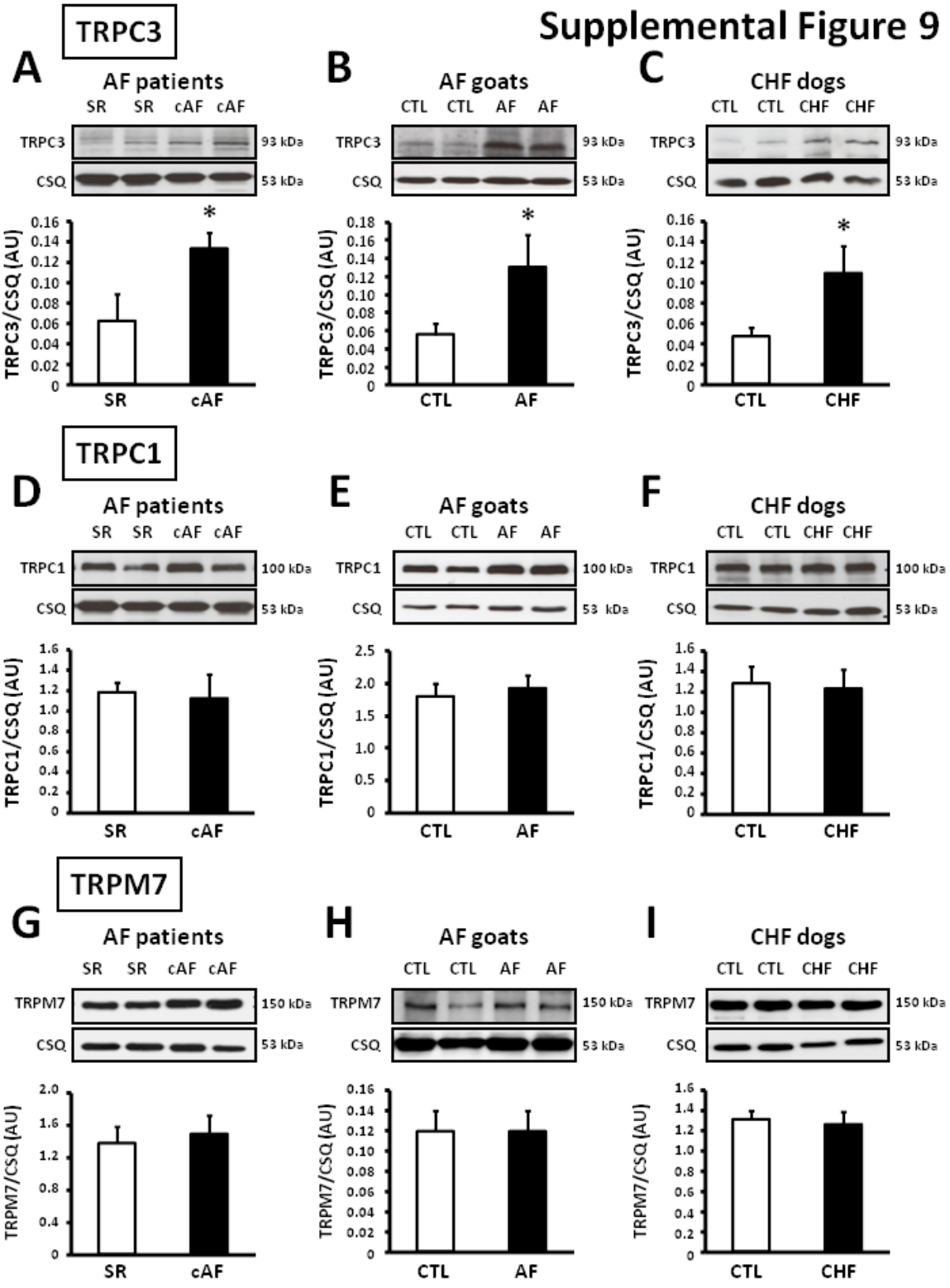

**Supplemental Figure 10**

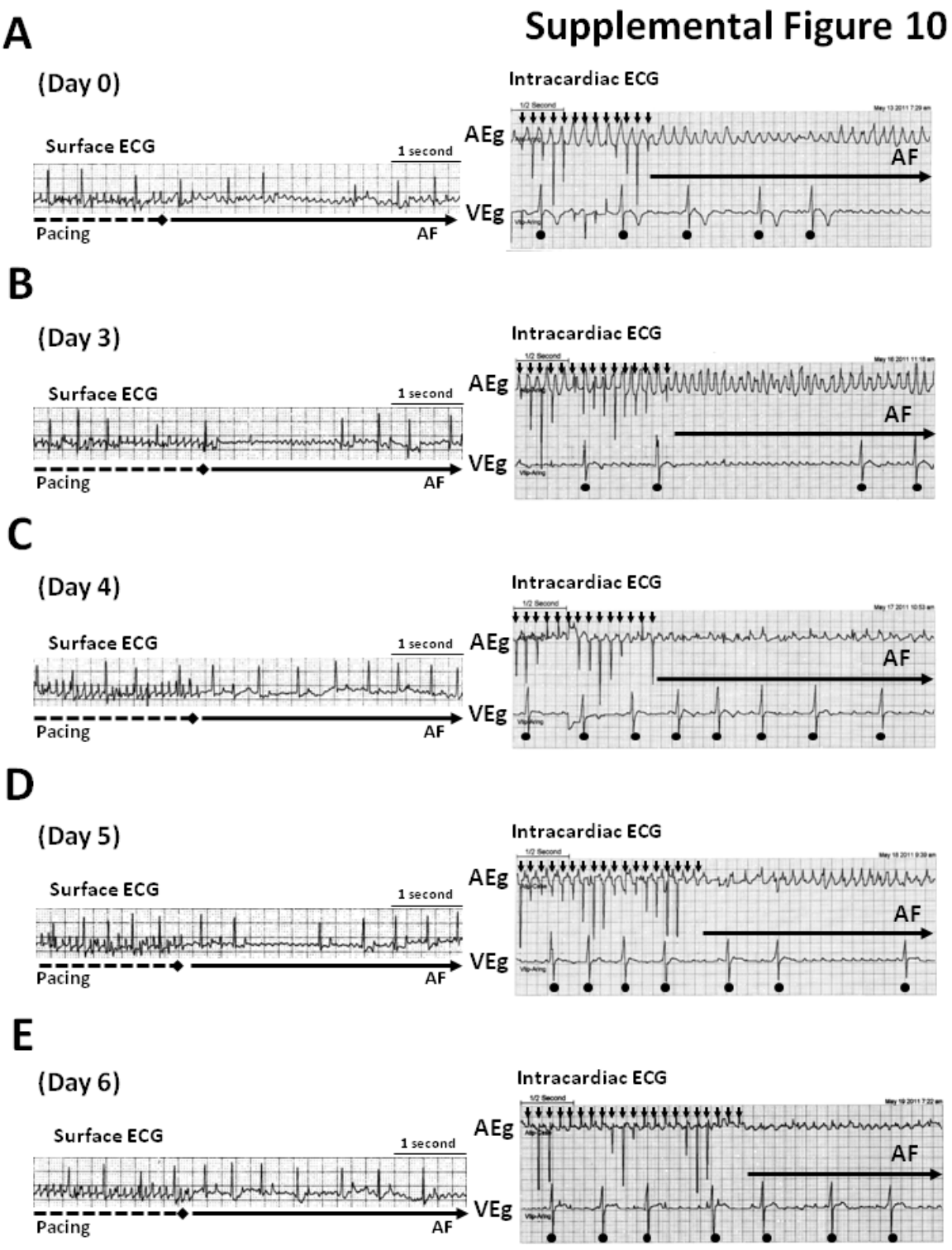

**Supplemental Figure 11**

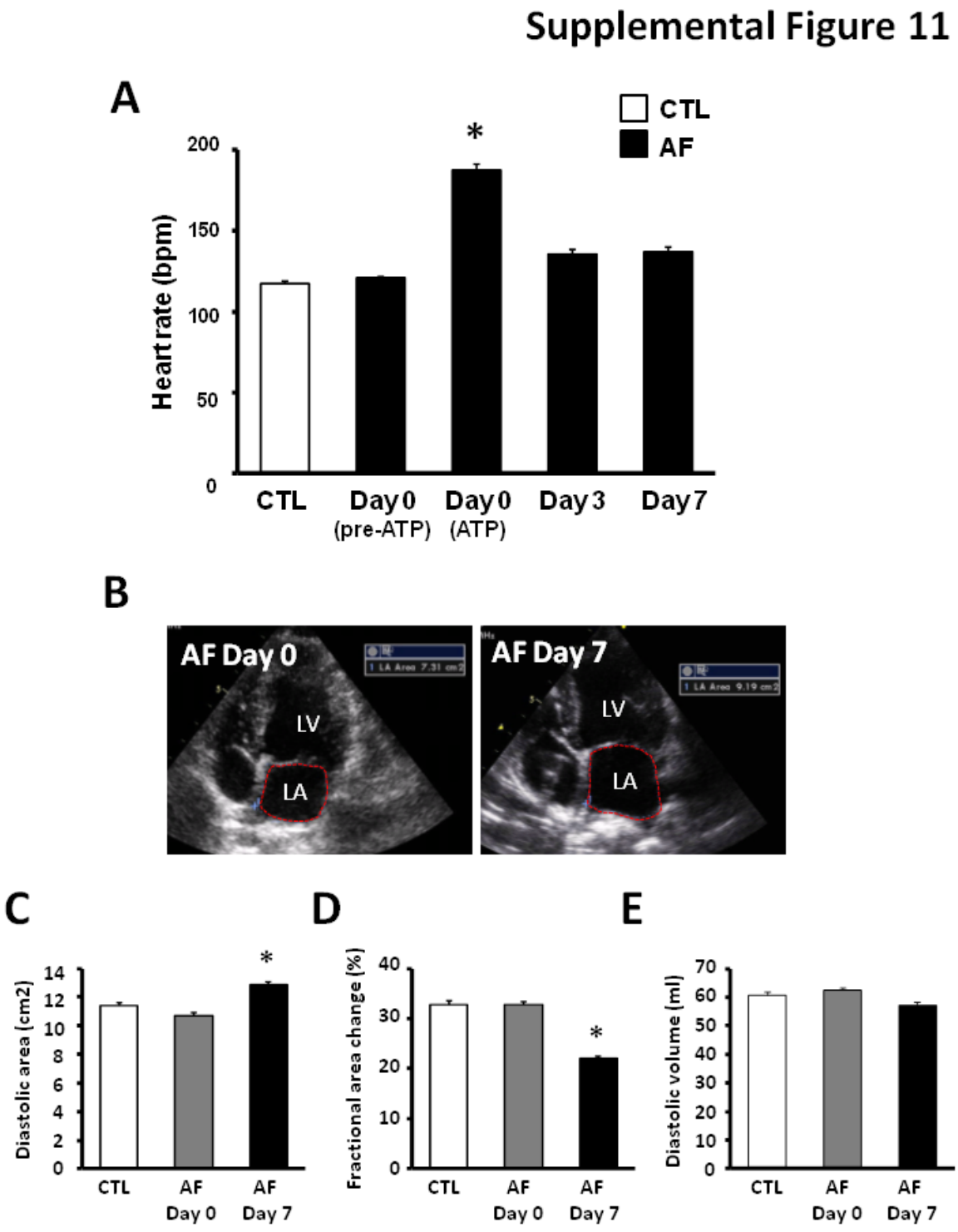

**Supplemental Figure 12**

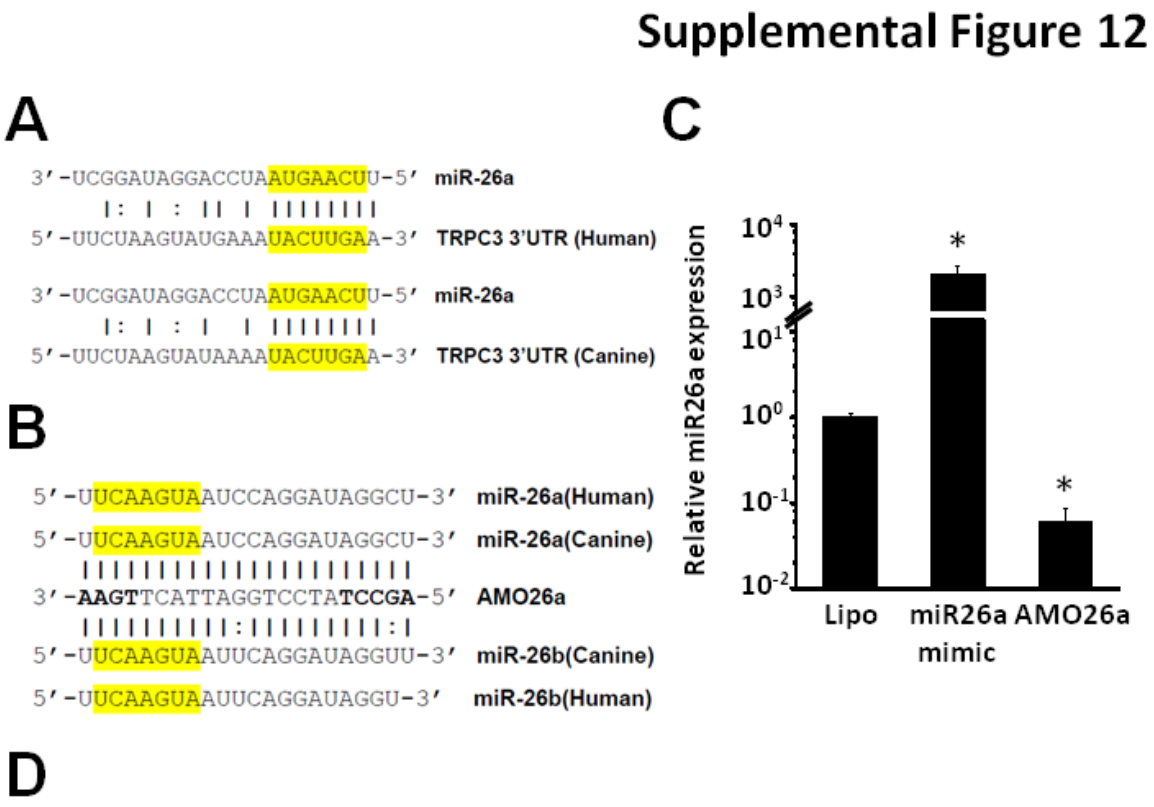


D

| Host gene (miRNA) | Human | Canine |
|---|---|---|
| Ctdspl (miR-26a-1) | 4430-GTGATGGAAACATTTGGAG (1/0.97)<br>4040-ATGGAGGAAATTAGAGATG (1/1)<br>3992-CAGGTGGAAAGGCACTCCA (1/0.95)<br>**3340-CATGAGGAAAAAATATATC** (1/0.96) | 2922-GCGGAGGAAAAAGTAGCTG (1/0.99)<br>1590-GCTGAGGAAATAAACTAGG (1/1)<br>1479-CCTCAGGAAACAGTGGTCA (1/0.95) |
| Ctdsp2 (miR-26a-2) | 4480-TTGGAGGAAAGGAGAATGA (1/0.97)<br>**3618-CCAGAGGAAAGGGGATACA** (1/0.97)<br>3385-CTATAGGAAAGAGGCCCAC (1/0.96) | 2529-GTTGGAAACAGGGAAGCCT (1/0.99) |
| Ctdsp1 (miR-26b) | 1134-GGAGAGGAAAGCGCGCCAC (1/0.97)<br>**373-AACGAGGAAAAAGACCAAC** (1/0.99) | 209-GGGGAGGAAACTCCATGTT (1/0.97)<br>190-GCGGAGGAAACTTTGTTAC (1/0.97) |

# CHAPTER 5. GENERAL DISCUSSION

## 5.1 Summary of the Novel Findings in this Thesis

In Chapter 2, we have conducted the first systematic analysis of all the cardiac-expressed miRNAs, and demonstrated that there is only a subset of these cardiac-expressed miRNAs that have the potential to target human cardiac ion channel genes. Based on this analysis, we further demonstrated that most of the deregulated expression of ion channel genes as seen in three cardiac disease states (e.g. cardiac hypertrophy/cardiac failure, myocardial ischemia, and atrial fibrillation) can be explained by the expression changes of the corresponding miRNAs. This highlights the potential significance of miRNA regulation of cardiac ion channels in arrhythmogenesis under these cardiac conditions.

In Chapter 3, we have performed the first detailed characterization of the role of miRNAs in $I_{K1}$-related atrial electrical remodeling in AF. We first identified miR-26 as a key regulator of $I_{K1}$ via controlling the expression of its underlying subunit Kir2.1. Moreover, our study demonstrated that downregulation of miR-26 due to enhanced NFATc3/c4 activities accounts for the AF-induced $I_{K1}$ enhancement. Furthermore, we observed that in vivo interference of miR-26 is able to control the AF susceptibility via regulation of $I_{K1}$.

In Chapter 4, we have presented the first study to characterize the function of TRPC3 channels in AF, and to investigate the potential role of miRNAs in regulation of this channel under the same disease paradigm. We found that TRPC3 channels regulate fibroblast function via mediating $Ca^{2+}$-entry, which results in activation of $Ca^{2+}$-dependent ERK-signaling. Moreover, we provided evidence showing that TRPC3 is upregulated in AF and this upregulation is likely due to the reduced expression of miR-26 resulting from enhanced NFATc3/c4 activities in atrial cardiac fibroblasts. Furthermore, we observed that in vivo TRPC3 channel blockade suppresses the development of the AF-promoting substrate.

## 5.2 Significance of the Major Findings in this Thesis

In general, the findings presented in this thesis provide a novel insight into how arrhythmias are generated. Specifically, they highlight the important contribution of miRNA to the AF pathogenesis and help to better understand the mechanisms underlying the remodeling processes associated with this common arrhythmic disorder. In the following section, the major findings and their potential significance will be addressed.

### 5.2.1 Discovery of miR-26 as a novel molecular and signaling mechanism for AF vulnerability and a novel therapeutic target for AF treatment

#### 5.2.1.1 MiR-26 controls AF by inhibiting $I_{K1}$-related adverse atrial electrical remodeling in atrial myocytes

$I_{K1}$ enhancement is a common observation in AF, representing one of the most important steps of ionic remodeling during AF [20, 376]. Enhanced $I_{K1}$ has been well established to play a significant role in AF pathophysiology, particularly in determining the AF-supporting reentry [20, 73]. In addition, it is also known to be a causative determinant in familial AF resulting from gain-of-function mutations associated with Kir2.1 channelopathies [95, 377]. As noted in the Introduction, numerous studies have been done to understand the molecular mechanisms for this ionic remodeling. The results strongly suggest that the functional enhancement of $I_{K1}$ in AF is likely ascribed to the increased expression of its underlying subunit Kir2.1 at protein and/or mRNA levels [83, 85]. What determines the altered expression of Kir2.1 in AF, however, remained puzzling. In this context, our study in Chapter 3 has provided a possible answer with the compelling evidence for the involvement of miRNAs. We found that miR-26 is consistently downregulated in AF dogs and AF patients, and this downregulation is accompanied by the coincided increase of Kir2.1 mRNA and protein. In addition, we experimentally validated *KCNJ2* as a cognate target of miR-26, which mechanistically accounts for the inverse changes of expression between miR-26 and Kir2.1 as seen in AF. Furthermore, we

demonstrated that in vivo interference of endogenous miR-26 is able to affect AF vulnerability and this effect is attributed to the repression of *KCNJ2*/Kir2.1/$I_{K1}$ by miR-26. Together, these findings demonstrate that miR-26 downregulation is responsible for the upregulation of Kir2.1/$I_{K1}$ in AF, revealing a novel molecular mechanism for the AF-induced electrical remodeling. Moreover, our findings also suggest that miR-26 controls AF by inhibiting the underlying adverse electrical remodeling. In addition to a previous study showing the important role of miR-328 in AF-induced $I_{CaL}$ downregulation [113], our study is the second demonstration of a crucial contribution of miRNAs to the adverse atrial electrical remodeling in AF. Given that $I_{CaL}$ downregulation and $I_{K1}$ enhancement are the two most important ionic alterations underlying AF-induced electrical remodeling [20, 62], our findings together with those from the previous study have highlighted a central role of miRNAs in the AF-associated electrical remodeling. Moreover, our data also indicates that the miRNA-mediated electrical remodeling in AF seems to be a complex process which might require the synergistic regulation of multiple miRNAs. It should be noted that downregulation of miR-26 has also been reported in cardiac hypertrophy [350, 378], whether miR-26 may also contribute to electrical abnormalities associated with cardiac hypertrophy through a similar mechanism will be of interest for further study.

While our results point to the direct involvement of miR-26 in AF-induced $I_{K1}$ augmentation, a previous study by Girmatsion et al. suggested the potential contribution of miR-1 to this adverse remodeling process [96]. The authors reported that expression of miR-1 was significantly reduced in the left atrial samples of AF patients with mitral valve diseases, along with a corresponding increase in Kir2.1-protein expression [96]. Since miR-1 was established by a previous study to target Kir2.1 [204], the authors thus proposed that reduced expression of miR-1 is responsible for upregulation of Kir2.1/$I_{K1}$ in AF patients [96]. Our studies in Chapter 3, however, found that the expression of miR-1 was unaltered in our samples from dogs and patients with AF (Chapter 3). The reason for the discrepancy in miR-1 expression in AF patients between our study and the study by Girmatsion et al. remained unclear. Various confounding factors of the patient samples such as ethnic group, age, and gender may have likely contributed to this difference. In addition, the causative role of miR-1 downregulation in AF initiation and maintenance was not established in this study, which makes the role of miR-1 in AF questionable. Further evidence against the

contribution of miR-1 downregulation to AF came from a recent study showing that downregulation of miR-1 actually improves calcium handling [374], a condition which is beneficial for AF. Nonetheless, further experiments related to the possible role of miR-1 in AF are needed to clarify the issue.

#### 5.2.1.2 MiR-26 controls AF by inhibiting TRPC3-mediated adverse atrial structural remodeling in atrial fibroblasts

Another major finding in our study is that miR-26 is abundantly expressed in atrial fibroblasts and AF-induced downregulation of miR-26 can result in upregulation of TRPC3 in atrial fibroblasts. This finding together with the finding that TRPC3 channels positively regulate atrial fibroblast proliferation and differentiation suggest that miR-26 likely contributes to atrial fibrosis via regulation of TRPC3 in AF. Our findings are in agreement with the previous studies showing the fibrogenic potential of miRNAs in the heart under different pathological conditions including AF. For example, the profibrotic effect of miR-21 and anti-fibrotic effect of miR-29 were reported in cardiac hypertrophy/heart failure and myocardial ischemia [284, 347, 354, 370]; downregulation of miR-133 and miR-590 were found to promote atrial fibrosis in experimental AF [375]. However, unlike these studies in which the fibrogenic effects of the miRNAs are primarily ascribed to the direct targeting of various ECM proteins and/or profibrotic factors, such as TGF-β1, sprouty-1, collagen, fibrillins, and elastin [284, 347, 375], our study (Chapter 4) suggests a novel mechanism: miR-26 contributes to AF-induced fibrotic remodeling by regulating fibroblast function through its targeting on TRPC3 channels. Notably, this potential mechanism may also be implicated in other cardiac pathological conditions. For example, reduced miR-26 [350, 378] and enhanced TRPC3 [222, 379] expression have been consistently reported in cardiac hypertrophy, it is conceivable that our proposed mechanism may at least partially account for the fibrotic remodeling manifested in this pathological condition.

Although, in Chapter 3, we have demonstrated a significant downregulation of miR-26 in atrial tissues obtained from AF dogs induced by atrial tachypacing as well as AF patients undergoing mitral valve disease, the cellular contribution of this miR-26 downregulation was not clearly defined. For example, the reduction of miR-26 could have resulted from its

expression changes in cardiomyocytes and/or cardiac fibroblasts, given that miR-26 is ubiquitously expressed in the heart [281]. In this regard, the study in Chapter 4 has provided direct evidence to clarify this issue. We first demonstrated that miR-26 is abundantly expressed at comparable levels in both atrial myocytes and atrial fibroblasts isolated from normal dogs (Chapter 4). Moreover, in atrial tachypacing (ATP) -induced AF dog model, we observed that miR-26 is significantly downregulated to a similar extent in both isolated atrial myocytes (unpublished data in Chapter 4) and atrial fibroblasts (Chapter 4). These findings suggest that the observed miR-26 reduction in Chapter 3 is likely the contribution from two cell types. More importantly, our findings here also suggest that miR-26 downregulation is a common phenomenon in AF, accounting for $I_{K1}$ enhancement in atrial myocytes and TRPC3 upregulation in atrial fibroblasts, and thereby contributing to AF-related electrical and structural remodeling.

#### 5.2.1.3 MiR-26 mediates the AF-promoting action of NFAT and is a key factor of two signaling pathways leading to AF

It is well known that $Ca^{2+}$-calcineurin-NFAT signaling plays a central role in detecting the rapid repetitive atrial activation that occurs during AF, and in coupling AF to L-type $Ca^{2+}$-current downregulation [109, 380, 381]. NFAT is activated upon dephosphorylation by calcineurin, a calcium/calmodulin-dependent protein phosphatase [382]. Activated NFAT is then translocated into nucleus where it functions as a transcription factor to control gene expression [382]. NFATc3 and NFATc4 are the two dominant isoforms expressed in the heart [383]. Enhanced NFATc3 and NFATc4 activities have been observed in atrial myocytes isolated from ATP-induced AF dogs [109]. Consistent with the above observations, we also found the activities of NFATc3 and NFATc4 were enhanced in our atrial tissues obtained from AF dog (Chapters 3&4) and AF patients (Chapter 3). In addition, our study in Chapter 4 further demonstrated that activation of NFAT also occurs in isolated atrial fibroblasts from our AF dogs. Notably, this is the first demonstration of AF-associated NFAT-changes in fibroblasts. Moreover, our findings suggest that enhanced NFAT activity appears to be a common cellular response to elevated $Ca^{2+}$ entry in both AF-cardiomyocytes and AF-fibroblasts.

The function of activated NFAT as a transcriptional repressor/activator has been previously described in many studies. Activation of NFATc3 was found to downregulate the expression of gene encoding Kv4.3 (main subunit underlying $I_{to}$ channel) in ventricular myocytes [384-386]. Similar repressive effect of activated NFATc3 was also observed in murine urinary bladder smooth muscle cells, where it tunes down the transcription of the gene encoding KCa1.1 (subunit underling BK channel) [387]. In AF, enhanced NFAT activity was reported to negatively regulate the expression of Cav1.2 genes in atrial myocytes [109]. Intriguingly, NFAT activation was also found to regulate the expression of miRNAs. For example, enhanced NFAT activity transcriptionally activates the expression of miR-23 and miR-199 during cardiac hypertrophy [313, 314]. In agreement with the above observations, we also found the expression of miR-26 is under the control of NFAT (Chapters 3&4). However, in contrast to the positive regulation of miR-23 and miR-199 by NFAT, we found that NFAT act as a negative regulator for miR-26 (Chapters 3&4). Our findings thus offer a mechanistic explanation for why miR-26 is downregulated in AF. In addition, our findings that in vitro NFAT inhibition is able to downregulate the expression of Kir2.1 and TRPC3 protein, suggest that the calcineurin-NFAT system may also be responsible for $I_{K1}$ and TRPC3 changes manifested during AF, indicating that this $Ca^{2+}$-dependent system is a common pathway involved in both electrical and structural remodeling associated with AF. More importantly, these findings also reveal the functional relevance of miR-26 in AF as an important mediator of the electrophysiological effects of $Ca^{2+}$-dependent NFAT signaling, highlighting a central role of miR-26 in AF control. A schematic illustration of the involvement of calcineurin-NFAT system and the central role of miR-26 in AF-induced upregulation of $I_{K1}$ and TRPC3 channels is shown in Figure 1.

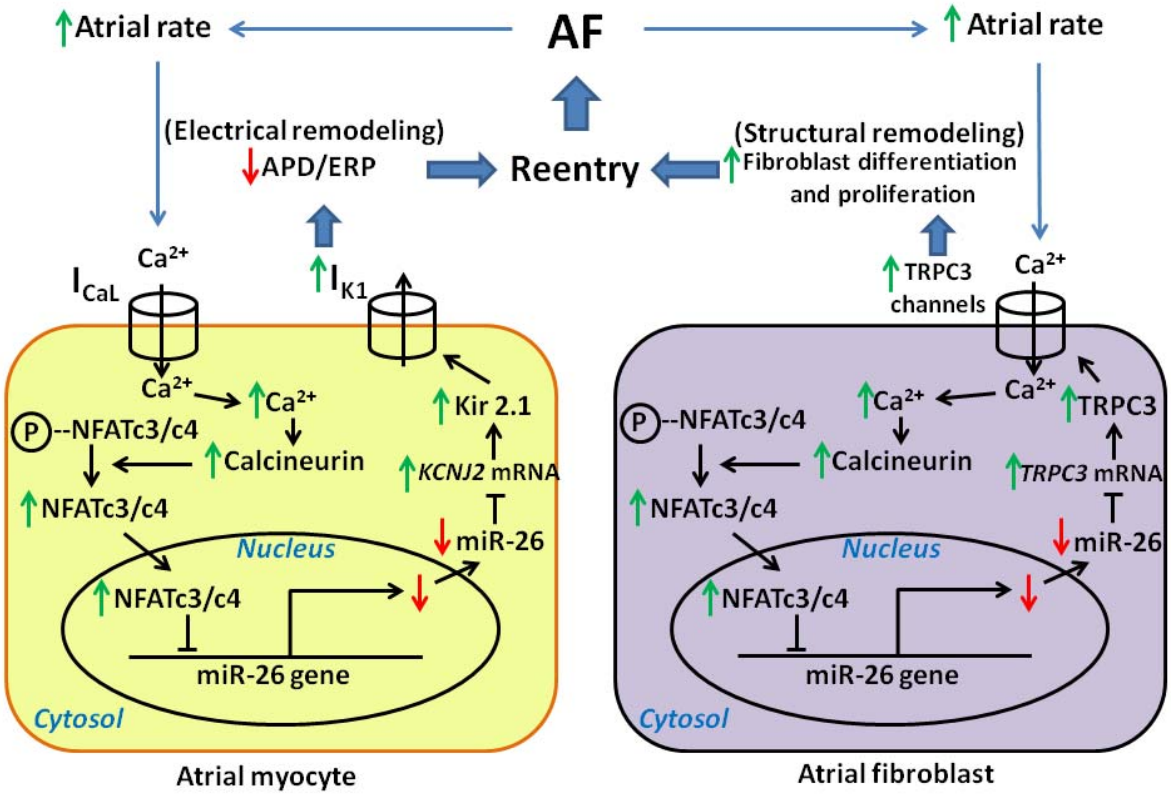


Figure 1. A schematic illustration of the involvement of calcineurin-NFAT system and the central role of miR-26 in AF-induced upregulation of $I_{K1}$ and TRPC3 channels. In AF, the rapid atrial activation causes the elevation of $[Ca^{2+}]_i$ in both atrial myocytes and atrial fibroblasts, where the calcineurin-NFAT signaling is activated in response to the increased $Ca^{2+}$ entry. Activated NFATc3 and NFATc4 are then translocated into the nucleus where they suppress the transcription of miR-26 genes. The resultant miR-26 reduction has two effects: 1) it causes the enhanced expression of Kir2.1 protein and its underlying $I_{K1}$ in atrial myocytes, contributing to APD/ERP shortening and thereby adverse electrical remodeling; and 2) it increases the expression of TRPC3 protein as well as its underlying channel in atrial fibroblasts, leading to enhanced fibroblast proliferation and differentiation and thereby adverse structural remodeling. The consequences of both cases contribute to the development of reentry substrates, favoring AF. APD: action potential duration; ERP: effective refractory period. Note: green upward arrows indicate upregulation, whereas red downward arrows indicate downregulation.

#### 5.2.1.4 Therapeutic potential of miR-26 for AF

Finally, our finding in Chapter 3 that in vivo overexpression of miR-26 is able to suppress AF induction and perpetuation, suggests the potential of miR-26 as a target for AF

management. As discussed in the introduction, AF-therapy is still a major challenge in the clinical practice, as none of the currently-available pharmacological or non pharmacological approaches is adequate to treat AF with an optimal effect [49]. Therefore, there is a great need for novel therapeutic approaches. Gene therapy may represent one of such therapeutic avenues, although it is still in its infancy. In fact, several virus-based gene therapies have already shown promises in the treatment of advanced Parkinson's disease [388] and congenital retinal disease [389, 390]. Our findings thus suggest that miR-26 could conceivably be a candidate for AF-targeting gene-therapy in the future.

### 5.2.2 Discovery of TRPC3 as a novel player in AF

Although it is not the main focus of this thesis, our findings related to the role of TRPC3 in cardiac fibroblast function in Chapter 4 help to improve our current knowledge about cardiac fibroblast biology. Previous studies have suggested that $Ca^{2+}$ entry is essential for fibroblast functions (proliferation and differentiation) [158-162]. However, the fact that cardiac fibroblasts lack voltage-gated calcium channels has led to a speculation of the existence of other $Ca^{2+}$ permeable ion channels in these cells [163]. In this context, our study in Chapter 4 has provided compelling evidence to show that TRPC3 channels may represent one of such candidates. We found that TRPC3 channels are abundantly expressed in atrial fibroblasts, where they are responsible for the $Ca^{2+}$ influx and positively regulate the atrial fibroblasts proliferation and differentiation (Chapter 4). Mechanistically, we found that TRPC3-mediated $Ca^{2+}$ entry affects atrial fibroblast functions by modulating $Ca^{2+}$-dependent ERK 1/2 phosphorylation (Chapter 4). Our findings are consistent with the previous finding that mitogen-activated protein kinase cascade is critically involved in controlling fibroblast activation [391, 392]. Collectively, our findings postulate a novel cellular mechanism for the regulation of cardiac fibroblast activation, which may also be applicable to other cardiac disorders associated with fibroblast remodeling. In addition, our results reveal a novel aspect of biological functions of TRPC3: the role in controlling fibroblast activation.

More importantly, our findings that AF enhances the expression of TRPC3 and activates fibroblast via TRPC3-dependent $Ca^{2+}$ entry mechanism (Chapter 4), provide a mechanistic explanation for why AF may itself promote atrial fibrosis, an important question related to AF pathophysiology that is insufficiently addressed by previous studies [144, 145]. A recent study has shown that TRPM7 is upregulated at mRNA and functional levels in atrial fibroblasts isolated from AF patients and may likely contribute to AF fibrogenesis via regulating the $Ca^{2+}$ entry-dependent fibroblast proliferation and differentiation [168]. However, in contrast to this study, we found that TRPM7 protein remains unchanged in the atrial samples from our AF dogs, AF goats, and AF patients (Chapter 4), suggesting that the functional enhancement of TRPM7 as observed in AF is likely determined by the other regulatory mechanisms (e.g. membrane trafficking) rather than changes in expression. In addition, our findings that in vivo TRPC3 blockade is able to prevent enhanced proliferation and ECM-expression of fibroblasts and suppresses AF (Chapter 4), are consistent with an important role in fibroblast-mediated AF-promoting remodeling and strongly suggests the therapeutic potential of TRPC3 as a candidate target for AF prevention.

### 5.2.3 Systematic identification of miRNA regulation of ion channel genes and its potential implications in arrhythmia associated with heart diseases

Previous studies have pointed out the important role of miRNAs in arrhythmia via regulation of expression of cardiac ion channel genes at the post-transcriptional level [96, 113, 204, 374]. However, due to the laborious nature of the experimental approach and the complexity of miRNA targeting activities, target identification has been a major challenge in miRNA research [250, 275] and experimental approaches, though being the ultimate path toward elucidating target genes, are low throughput and unable to provide a thorough view of miRNA targeting. One way to overcome this problem is to conduct the bioinformatic analysis by using various available computational prediction programs. In this regard, our studies in Chapter 2 took advantage of the bioinformatic tools and combined it with the miRNA expression analysis generated from experiments to obtain an overview of miRNA

targeting in regulation of cardiac ion channel genes. By applying this combinational analysis, we were able to identify a matrix of miRNAs in the heart which have the potential to regulate human cardiac ion channel genes (Chapter 2). Notably, this finding represents the first systematic analysis of miRNAs-based regulation of cardiac ion channel genes, and perhaps, one of the most important information brought up by this finding is the recognition that there is only a subset of cardiac-expressed miRNAs that could target the cardiac ion channel genes. This information may be used to rationally direct the future studies on miRNA regulation of ion channel genes. Another important finding of the study in Chapter 2 is related to the subsequent application of the above bioinformatic analysis to three specific cardiac pathological settings (e.g. cardiac hypertrophy/heart failure, cardiac ischemia, and atrial fibrillation) that are known to be associated with the aberrant miRNAs expression profile and deregulated expression of ion channel genes. This analysis allowed us to translate the bioinformatic prediction into the biological perspective. Indeed, based on the above bioinformatic analysis of miRNA targeting, we are able to explain the experimentally-observed dysregulation of ion channel gene expression by the deregulation of the miRNAs under all these three pathological conditions, suggesting a potential implication of miRNA-mediated regulation of ion channel genes in arrhythmogenesis. Taken together, our findings indicate that multiple miRNAs may be involved in the electrical/ionic remodeling processes of cardiac diseases through altering their targeted ion channel genes expression in the heart, which has not been uncovered by previous experimental studies.

## 5.3 Future Directions

1. Can miR-26 overexpression interrupt the AF maintenance when AF is established?

   We have observed in Chapter 3 that in vivo overexpression of miR-26 is able to suppress AF susceptibility, suggesting the anti-AF effect of miR-26. Given that our experiments were primarily performed in normal animals, an extension of this study to an established AF animal model will certainly help to understand whether in vivo overexpression of miR-26 could also interrupt the AF maintenance if the AF is already established. For the AF animal model, we could consider using the ATP dog model (the

one that we used in Chapter 3). In this case, the cardiac overexpression of miR-26 can be achieved by directly injecting the miR-26 over-expressing adenovirus into the atrium. Alternatively, the cardiac overexpression of miR-26 can also be introduced by using the adeno-associated virus serotype 9 (AAV9), a recently-discovered virus that shows superior cardiac selectivity [248, 321], to achieve an improved cardiac specificity.

2. What are the consequences of chronic miR-26 knockdown/overexpression in the context of AF?

We have shown in Chapter 3 that AF vulnerability is substantially enhanced when cardiac expression of miR-26 is reduced, suggesting the causative role of miR-26 reduction in AF promotion. Although, our subsequent experiments in Chapter 3 have already demonstrated that the AF-promoting effect of miR-26 knockdown is likely attributable to adverse electrical remodeling via the regulation of $I_{K1}$ (Chapter 3), it is still unknown whether in vivo miR-26 knockdown may also promote AF by inducing atrial fibrosis. Given that our experiments were performed at one week after the initial attempt of miR-26 knockdown, which might not be sufficient for the development of fibrosis, the chronic effect of in vivo miR-26 knockdown will merit further investigation. This will help us to get a clearer picture of the role of miR-26 knockdown in AF promotion and will determine more precisely how the two miR-26-mediated remodeling processes contribute to AF induction and perpetuation. On the other hand, it will be also interesting to assess whether chronic miR-26 overexpression can prevent the AF-induced atrial fibrosis.

3. What is the direct role of NFAT activation to AF susceptibility?

We have demonstrated in Chapters3&4 that NFAT is centrally involved in the two miR-26-mediated pathways (NFAT/miR-26/Kir2.1 and NFAT/miR-26/TRPC3) leading to adverse electrical and structural remodeling during AF. However, the direct role of NFAT activation on AF induction and perpetuation remains unexplored. Thus, it will be particularly interesting to determine whether in vivo NFAT activation can render AF vulnerability, as this will help to gain more insights into the functional relevance of

NFAT activation in AF pathogenesis and to better dissect the relative contribute of the above pathways to AF induction and perpetuation.

4. What is the potential implication of the synergistic interplay between miR-26 and TRPC3 in cardiac hypertrophy?

Given that reduced miR-26 [350, 378] and enhanced TRPC3 [222, 379] expression have been consistently observed in cardiac hypertrophy, it is likely that the synergistic interplay between miR-26 and TRPC3 may also contribute to the fibrotic remodeling manifested in this pathological condition. This is a potentially-interesting direction which will be worthy of further investigation.

## 5.4 Conclusion

MiRNAs may importantly participate in arrhythmogenesis through altering the expression of cardiac ion channel genes in various cardiac pathological conditions. MiR-26 is critically involved in AF-associated electrical and structural remodeling and plays a central role in determining AF susceptibility via the regulation of $I_{K1}$ and TRPC3 channel genes. Thus, our studies unravel a novel molecular control mechanism of AF at the miRNA level and reveal miR-26 as a novel and potentially-promising therapeutic target for AF.

# REFERENCES


1. **Kannel, W.B., et al., *Epidemiologic features of chronic atrial fibrillation: the Framingham study.* N Engl J Med, 1982. 306(17): p. 1018-22.**

2. **Wattigney, W.A., G.A. Mensah, and J.B. Croft, *Increased atrial fibrillation mortality: United States, 1980-1998.* Am J Epidemiol, 2002. 155(9): p. 819-26.**

3. **Chugh, S.S., et al., *Epidemiology and natural history of atrial fibrillation: clinical implications.* J Am Coll Cardiol, 2001. 37(2): p. 371-8.**

4. **Go, A.S., et al., *Prevalence of diagnosed atrial fibrillation in adults: national implications for rhythm management and stroke prevention: the AnTicoagulation and Risk Factors in Atrial Fibrillation (ATRIA) Study.* JAMA, 2001. 285(18): p. 2370-5.**

5. **Naccarelli, G.V., et al., *Increasing prevalence of atrial fibrillation and flutter in the United States.* Am J Cardiol, 2009. 104(11): p. 1534-9.**

6. **Kannel, W.B., et al., *Prevalence, incidence, prognosis, and predisposing conditions for atrial fibrillation: population-based estimates.* Am J Cardiol, 1998. 82(8A): p. 2N-9N.**

7. **Wolf, P.A., R.D. Abbott, and W.B. Kannel, *Atrial fibrillation: a major contributor to stroke in the elderly. The Framingham Study.* Arch Intern Med, 1987. 147(9): p. 1561-4.**

8. **Psaty, B.M., et al., *Incidence of and risk factors for atrial fibrillation in older adults.* Circulation, 1997. 96(7): p. 2455-61.**

9. **Benjamin, E.J., et al., *Independent risk factors for atrial fibrillation in a population-based cohort. The Framingham Heart Study.* JAMA, 1994. 271(11): p. 840-4.**

10. **Miyasaka, Y., et al., *Secular trends in incidence of atrial fibrillation in Olmsted County, Minnesota, 1980 to 2000, and implications on the projections for future prevalence.* Circulation, 2006. 114(2): p. 119-25.**

11. **Feinberg, W.M., et al., *Prevalence, age distribution, and gender of patients with atrial fibrillation. Analysis and implications.* Arch Intern Med, 1995. 155(5): p. 469-73.**

12. **Ruo, B., et al., *Racial variation in the prevalence of atrial fibrillation among patients with heart failure: the Epidemiology, Practice, Outcomes, and Costs of Heart Failure (EPOCH) study.* J Am Coll Cardiol, 2004. 43(3): p. 429-35.**

13. **Gbadebo, T.D., H. Okafor, and D. Darbar, *Differential impact of race and risk factors on incidence of atrial fibrillation.* Am Heart J, 2011. 162(1): p. 31-7.**

14. **Lahiri, M.K., et al., *Effect of race on the frequency of postoperative atrial fibrillation following coronary artery bypass grafting.* Am J Cardiol, 2011. 107(3): p. 383-6.**

15. **Rader, F., et al., *Influence of race on atrial fibrillation after cardiac surgery.* Circ Arrhythm Electrophysiol, 2011. 4(5): p. 644-52.**

16. **Fuster, V., et al., *ACC/AHA/ESC 2006 Guidelines for the Management of Patients with Atrial Fibrillation: a report of the American College of Cardiology/American Heart Association Task Force on Practice Guidelines and the European Society of Cardiology Committee for Practice Guidelines (Writing Committee to Revise the 2001 Guidelines for the Management of Patients With Atrial Fibrillation): developed in collaboration with the European Heart Rhythm Association and the Heart Rhythm Society.* Circulation, 2006. 114(7): p. e257-354.**

17. **European Heart Rhythm, A., et al., *ACC/AHA/ESC 2006 guidelines for the management of patients with atrial fibrillation--executive summary: a report of the American College of Cardiology/American Heart Association Task Force on Practice Guidelines and the European Society of Cardiology Committee for Practice Guidelines (Writing Committee to Revise the 2001 Guidelines for the Management of Patients With Atrial Fibrillation).* J Am Coll Cardiol, 2006. 48(4): p. 854-906.**

18. **Fuster, V., et al., *ACC/AHA/ESC 2006 guidelines for the management of patients with atrial fibrillation-executive summary: a report of the American College of Cardiology/American Heart Association Task Force on Practice Guidelines and the European Society of Cardiology Committee for Practice Guidelines (Writing Committee to Revise the 2001 Guidelines for the Management of Patients with Atrial Fibrillation).* Eur Heart J, 2006. 27(16): p. 1979-2030.**

19. **de Vos, C.B., et al., *Progression from paroxysmal to persistent atrial fibrillation clinical correlates and prognosis.* J Am Coll Cardiol, 2010. 55(8): p. 725-31.**

20. **Nattel, S., B. Burstein, and D. Dobrev, *Atrial remodeling and atrial fibrillation: mechanisms and implications.* Circ Arrhythm Electrophysiol, 2008. 1(1): p. 62-73.**

21. **Kida, Y., *Age and sex as independent risk factors for stroke among patients with atrial fibrillation.* JAMA, 2003. 290(22): p. 2937; author reply 2937.**

22. **Humphries, K.H., et al., *New-onset atrial fibrillation: sex differences in presentation, treatment, and outcome.* Circulation, 2001. 103(19): p. 2365-70.**

23. **Reynolds, M.R., et al., *Influence of age, sex, and atrial fibrillation recurrence on quality of life outcomes in a population of patients with new-onset atrial***

***fibrillation: the Fibrillation Registry Assessing Costs, Therapies, Adverse events and Lifestyle (FRACTAL) study.*** **Am Heart J, 2006. 152(6): p. 1097-103.**

**24. Benjamin, E.J., et al., *Impact of atrial fibrillation on the risk of death: the Framingham Heart Study.* Circulation, 1998. 98(10): p. 946-52.**

**25. Miyasaka, Y., et al., *Time trends of ischemic stroke incidence and mortality in patients diagnosed with first atrial fibrillation in 1980 to 2000: report of a community-based study.* Stroke, 2005. 36(11): p. 2362-6.**

**26. Wachtell, K., et al., *Cardiovascular morbidity and mortality in hypertensive patients with a history of atrial fibrillation: The Losartan Intervention For End Point Reduction in Hypertension (LIFE) study.* J Am Coll Cardiol, 2005. 45(5): p. 705-11.**

**27. Kowey, P.R., et al., *Management of atrial fibrillation in patients with hypertension.* J Hum Hypertens, 1997. 11(11): p. 699-707.**

**28. Verdecchia, P., et al., *Atrial fibrillation in hypertension: predictors and outcome.* Hypertension, 2003. 41(2): p. 218-23.**

**29. Capucci, A., et al., *Effectiveness of loading oral flecainide for converting recent-onset atrial fibrillation to sinus rhythm in patients without organic heart disease or with only systemic hypertension.* Am J Cardiol, 1992. 70(1): p. 69-72.**

**30. Cameron, A., et al., *Prevalence and significance of atrial fibrillation in coronary artery disease (CASS Registry).* Am J Cardiol, 1988. 61(10): p. 714-7.**

**31. Haddad, A.H., V.K. Prchkov, and D.C. Dean, *Chronic atrial fibrillation and coronary artery disease.* J Electrocardiol, 1978. 11(1): p. 67-9.**

**32. van Diepen, S., et al., *Mortality and readmission of patients with heart failure, atrial fibrillation, or coronary artery disease undergoing noncardiac surgery: an analysis of 38 047 patients.* Circulation, 2011. 124(3): p. 289-96.**

**33. Scheinman, M.M., *Atrial fibrillation and congestive heart failure: the intersection of two common diseases.* Circulation, 1998. 98(10): p. 941-2.**

**34. Hsu, L.F., et al., *Catheter ablation for atrial fibrillation in congestive heart failure.* N Engl J Med, 2004. 351(23): p. 2373-83.**

**35. Diker, E., et al., *Prevalence and predictors of atrial fibrillation in rheumatic valvular heart disease.* Am J Cardiol, 1996. 77(1): p. 96-8.**

**36. Safaie, N., et al., *New procedure for treatment of atrial fibrillation in patients with valvular heart disease.* Acta Med Iran, 2010. 48(5): p. 337-41.**

**37. Robinson, K., et al., *Atrial fibrillation in hypertrophic cardiomyopathy: a longitudinal study.* J Am Coll Cardiol, 1990. 15(6): p. 1279-85.**

**38. Doi, Y. and H. Kitaoka, *Hypertrophic cardiomyopathy in the elderly: significance of atrial fibrillation.* J Cardiol, 2001. 37 Suppl 1: p. 133-8.**

**39. Crenshaw, B.S., et al., *Atrial fibrillation in the setting of acute myocardial infarction: the GUSTO-I experience. Global Utilization of Streptokinase and TPA for Occluded Coronary Arteries.* J Am Coll Cardiol, 1997. 30(2): p. 406-13.**

**40. Hod, H., et al., *Early atrial fibrillation during evolving myocardial infarction: a consequence of impaired left atrial perfusion.* Circulation, 1987. 75(1): p. 146-50.**

**41. Klass, M. and L.J. Haywood, *Atrial fibrillation associated with acute myocardial infarction: a study of 34 cases.* Am Heart J, 1970. 79(6): p. 752-60.**

**42. Lip, G.Y. and G.I. Varughese, *Diabetes mellitus and atrial fibrillation: perspectives on epidemiological and pathophysiological links.* Int J Cardiol, 2005. 105(3): p. 319-21.**

**43. Movahed, M.R., M. Hashemzadeh, and M.M. Jamal, *Diabetes mellitus is a strong, independent risk for atrial fibrillation and flutter in addition to other cardiovascular disease.* Int J Cardiol, 2005. 105(3): p. 315-8.**

**44. Shibata, Y., et al., *Impairment of pulmonary function is an independent risk factor for atrial fibrillation: the Takahata study.* Int J Med Sci, 2011. 8(7): p. 514-22.**

**45. Villareal, R.P., et al., *Postoperative atrial fibrillation and mortality after coronary artery bypass surgery.* J Am Coll Cardiol, 2004. 43(5): p. 742-8.**

**46. Mathew, J.P., et al., *A multicenter risk index for atrial fibrillation after cardiac surgery.* JAMA, 2004. 291(14): p. 1720-9.**

**47. Daya, H., *Hyperthyroidism causing atrial fibrillation in a young man.* S Afr Med J, 1966. 40(41): p. 1007-8.**

**48. Frost, L., P. Vestergaard, and L. Mosekilde, *Hyperthyroidism and risk of atrial fibrillation or flutter: a population-based study.* Arch Intern Med, 2004. 164(15): p. 1675-8.**

**49. Nattel, S., *New ideas about atrial fibrillation 50 years on.* Nature, 2002. 415(6868): p. 219-26.**

**50. Prystowsky, E.N., *Management of atrial fibrillation: therapeutic options and clinical decisions.* Am J Cardiol, 2000. 85(10A): p. 3D-11D.**

**51. Nattel, S., et al., *New approaches to atrial fibrillation management: a critical review of a rapidly evolving field.* Drugs, 2002. 62(16): p. 2377-97.**

**52.** **Carlsson, J., et al., *Randomized trial of rate-control versus rhythm-control in persistent atrial fibrillation: the Strategies of Treatment of Atrial Fibrillation (STAF) study.* J Am Coll Cardiol, 2003. 41(10): p. 1690-6.**

**53.** **Hohnloser, S.H., K.H. Kuck, and J. Lilienthal, *Rhythm or rate control in atrial fibrillation--Pharmacological Intervention in Atrial Fibrillation (PIAF): a randomised trial.* Lancet, 2000. 356(9244): p. 1789-94.**

**54.** **Opolski, G., et al., *Rate control vs rhythm control in patients with nonvalvular persistent atrial fibrillation: the results of the Polish How to Treat Chronic Atrial Fibrillation (HOT CAFE) Study.* Chest, 2004. 126(2): p. 476-86.**

**55.** **Van Gelder, I.C., et al., *A comparison of rate control and rhythm control in patients with recurrent persistent atrial fibrillation.* N Engl J Med, 2002. 347(23): p. 1834-40.**

**56.** **Wyse, D.G., et al., *A comparison of rate control and rhythm control in patients with atrial fibrillation.* N Engl J Med, 2002. 347(23): p. 1825-33.**

**57.** **de Denus, S., et al., *Rate vs rhythm control in patients with atrial fibrillation: a meta-analysis.* Arch Intern Med, 2005. 165(3): p. 258-62.**

**58.** **Steinberg, J.S., et al., *Analysis of cause-specific mortality in the Atrial Fibrillation Follow-up Investigation of Rhythm Management (AFFIRM) study.* Circulation, 2004. 109(16): p. 1973-80.**

**59.** **Nattel, S. and L.H. Opie, *Controversies in atrial fibrillation.* Lancet, 2006. 367(9506): p. 262-72.**

**60.** **Ravens, U. and E. Cerbai, *Role of potassium currents in cardiac arrhythmias.* Europace, 2008. 10(10): p. 1133-7.**

**61.** **Iwasaki, Y.K., et al., *Atrial fibrillation pathophysiology: implications for management.* Circulation, 2011. 124(20): p. 2264-74.**

**62.** **Wakili, R., et al., *Recent advances in the molecular pathophysiology of atrial fibrillation.* J Clin Invest, 2011. 121(8): p. 2955-68.**

**63.** **Haissaguerre, M., et al., *Spontaneous initiation of atrial fibrillation by ectopic beats originating in the pulmonary veins.* N Engl J Med, 1998. 339(10): p. 659-66.**

**64.** **Yeh, Y.H., et al., *Calcium-handling abnormalities underlying atrial arrhythmogenesis and contractile dysfunction in dogs with congestive heart failure.* Circ Arrhythm Electrophysiol, 2008. 1(2): p. 93-102.**

**65.** **Pizzale, S., et al., *Sudden death in a young man with catecholaminergic polymorphic ventricular tachycardia and paroxysmal atrial fibrillation.* J Cardiovasc Electrophysiol, 2008. 19(12): p. 1319-21.**

**66.** **Johnson, J.N., et al., *Prevalence of early-onset atrial fibrillation in congenital long QT syndrome.* Heart Rhythm, 2008. 5(5): p. 704-9.**

**67.** **Nattel, S., et al., *Arrhythmogenic ion-channel remodeling in the heart: heart failure, myocardial infarction, and atrial fibrillation.* Physiol Rev, 2007. 87(2): p. 425-56.**

**68.** **Allessie, M.A., F.I. Bonke, and F.J. Schopman, *Circus movement in rabbit atrial muscle as a mechanism of tachycardia. III. The "leading circle" concept: a new model of circus movement in cardiac tissue without the involvement of an anatomical obstacle.* Circ Res, 1977. 41(1): p. 9-18.**

**69.** **Pertsov, A.M., et al., *Spiral waves of excitation underlie reentrant activity in isolated cardiac muscle.* Circ Res, 1993. 72(3): p. 631-50.**

**70.** **Comtois, P., J. Kneller, and S. Nattel, *Of circles and spirals: bridging the gap between the leading circle and spiral wave concepts of cardiac reentry.* Europace, 2005. 7 Suppl 2: p. 10-20.**

**71.** **Allessie, M.A., et al., *Pathophysiology and prevention of atrial fibrillation.* Circulation, 2001. 103(5): p. 769-77.**

**72.** **Wijffels, M.C., et al., *Atrial fibrillation begets atrial fibrillation. A study in awake chronically instrumented goats.* Circulation, 1995. 92(7): p. 1954-68.**

**73.** **Schotten, U., et al., *Pathophysiological mechanisms of atrial fibrillation: a translational appraisal.* Physiol Rev, 2011. 91(1): p. 265-325.**

**74.** **Gaspo, R., et al., *Functional mechanisms underlying tachycardia-induced sustained atrial fibrillation in a chronic dog model.* Circulation, 1997. 96(11): p. 4027-35.**

**75.** **Morillo, C.A., et al., *Chronic rapid atrial pacing. Structural, functional, and electrophysiological characteristics of a new model of sustained atrial fibrillation.* Circulation, 1995. 91(5): p. 1588-95.**

**76.** **Yue, L., et al., *Ionic remodeling underlying action potential changes in a canine model of atrial fibrillation.* Circ Res, 1997. 81(4): p. 512-25.**

**77.** **Attuel, P., et al., *Failure in the rate adaptation of the atrial refractory period: its relationship to vulnerability.* Int J Cardiol, 1982. 2(2): p. 179-97.**

**78.** **Boutjdir, M., et al., *Inhomogeneity of cellular refractoriness in human atrium: factor of arrhythmia?* Pacing Clin Electrophysiol, 1986. 9(6 Pt 2): p. 1095-100.**

**79.** **Daoud, E.G., et al., *Effect of atrial fibrillation on atrial refractoriness in humans.* Circulation, 1996. 94(7): p. 1600-6.**

**80.** **Franz, M.R., et al., *Electrical remodeling of the human atrium: similar effects in patients with chronic atrial fibrillation and atrial flutter.* J Am Coll Cardiol, 1997. 30(7): p. 1785-92.**

**81.** **Yu, W.C., et al., *Reversal of atrial electrical remodeling following cardioversion of long-standing atrial fibrillation in man.* Cardiovasc Res, 1999. 42(2): p. 470-6.**

**82.** **Bosch, R.F., et al., *Ionic mechanisms of electrical remodeling in human atrial fibrillation.* Cardiovasc Res, 1999. 44(1): p. 121-31.**

**83.** **Dobrev, D., et al., *Molecular basis of downregulation of G-protein-coupled inward rectifying K(+) current (I(K,ACh) in chronic human atrial fibrillation: decrease in GIRK4 mRNA correlates with reduced I(K,ACh) and muscarinic receptor-mediated shortening of action potentials.* Circulation, 2001. 104(21): p. 2551-7.**

**84.** **Dobrev, D., et al., *Human inward rectifier potassium channels in chronic and postoperative atrial fibrillation.* Cardiovasc Res, 2002. 54(2): p. 397-404.**

**85.** **Gaborit, N., et al., *Human atrial ion channel and transporter subunit gene-expression remodeling associated with valvular heart disease and atrial fibrillation.* Circulation, 2005. 112(4): p. 471-81.**

**86.** **Van Wagoner, D.R., et al., *Outward K+ current densities and Kv1.5 expression are reduced in chronic human atrial fibrillation.* Circ Res, 1997. 80(6): p. 772-81.**

**87.** **Workman, A.J., K.A. Kane, and A.C. Rankin, *The contribution of ionic currents to changes in refractoriness of human atrial myocytes associated with chronic atrial fibrillation.* Cardiovasc Res, 2001. 52(2): p. 226-35.**

**88.** **Van Wagoner, D.R., *Electrophysiological remodeling in human atrial fibrillation.* Pacing Clin Electrophysiol, 2003. 26(7 Pt 2): p. 1572-5.**

**89.** **Voigt, N., et al., *Differential phosphorylation-dependent regulation of constitutively active and muscarinic receptor-activated IK,ACh channels in patients with chronic atrial fibrillation.* Cardiovasc Res, 2007. 74(3): p. 426-37.**

**90.** **Cha, T.J., et al., *Atrial tachycardia remodeling of pulmonary vein cardiomyocytes: comparison with left atrium and potential relation to arrhythmogenesis.* Circulation, 2005. 111(6): p. 728-35.**

**91.** **Cha, T.J., et al., *Kir3-based inward rectifier potassium current: potential role in atrial tachycardia remodeling effects on atrial repolarization and arrhythmias.* Circulation, 2006. 113(14): p. 1730-7.**

**92.** **Cha, T.J., et al., *Atrial ionic remodeling induced by atrial tachycardia in the presence of congestive heart failure.* Circulation, 2004. 110(12): p. 1520-6.**

**93. Ehrlich, J.R., *Inward rectifier potassium currents as a target for atrial fibrillation therapy.* J Cardiovasc Pharmacol, 2008. 52(2): p. 129-35.**

**94. Zhang, H., et al., *Role of up-regulation of IK1 in action potential shortening associated with atrial fibrillation in humans.* Cardiovasc Res, 2005. 66(3): p. 493-502.**

**95. Xia, M., et al., *A Kir2.1 gain-of-function mutation underlies familial atrial fibrillation.* Biochem Biophys Res Commun, 2005. 332(4): p. 1012-9.**

**96. Girmatsion, Z., et al., *Changes in microRNA-1 expression and IK1 up-regulation in human atrial fibrillation.* Heart Rhythm, 2009. 6(12): p. 1802-9.**

**97. Skasa, M., et al., *L-type calcium currents in atrial myocytes from patients with persistent and non-persistent atrial fibrillation.* Basic Res Cardiol, 2001. 96(2): p. 151-9.**

**98. Van Wagoner, D.R., et al., *Atrial L-type Ca2+ currents and human atrial fibrillation.* Circ Res, 1999. 85(5): p. 428-36.**

**99. Christ, T., et al., *L-type Ca2+ current downregulation in chronic human atrial fibrillation is associated with increased activity of protein phosphatases.* Circulation, 2004. 110(17): p. 2651-7.**

**100. Yagi, T., et al., *Density and function of inward currents in right atrial cells from chronically fibrillating canine atria.* Cardiovasc Res, 2002. 54(2): p. 405-15.**

**101. Brundel, B.J., et al., *Ion channel remodeling is related to intraoperative atrial effective refractory periods in patients with paroxysmal and persistent atrial fibrillation.* Circulation, 2001. 103(5): p. 684-90.**

**102. Bosch, R.F., et al., *Molecular mechanisms of early electrical remodeling: transcriptional downregulation of ion channel subunits reduces I(Ca,L) and I(to) in rapid atrial pacing in rabbits.* J Am Coll Cardiol, 2003. 41(5): p. 858-69.**

**103. Brundel, B.J., et al., *Gene expression of proteins influencing the calcium homeostasis in patients with persistent and paroxysmal atrial fibrillation.* Cardiovasc Res, 1999. 42(2): p. 443-54.**

**104. Brundel, B.J., et al., *Alterations in potassium channel gene expression in atria of patients with persistent and paroxysmal atrial fibrillation: differential regulation of protein and mRNA levels for K+ channels.* J Am Coll Cardiol, 2001. 37(3): p. 926-32.**

**105. van der Velden, H.M.W., et al., *Atrial fibrillation in the goat induces changes in monophasic action potential and mRNA expression of ion channels involved in repolarization.* J Cardiovasc Electrophysiol, 2000. 11(11): p. 1262-9.**

**106. Van Gelder, I.C., et al., *Alterations in gene expression of proteins involved in the calcium handling in patients with atrial fibrillation.* J Cardiovasc Electrophysiol, 1999. 10(4): p. 552-60.**

**107. Yue, L., et al., *Molecular mechanisms underlying ionic remodeling in a dog model of atrial fibrillation.* Circ Res, 1999. 84(7): p. 776-84.**

**108. Schotten, U., et al., *The L-type Ca2+-channel subunits alpha1C and beta2 are not downregulated in atrial myocardium of patients with chronic atrial fibrillation.* J Mol Cell Cardiol, 2003. 35(5): p. 437-43.**

**109. Qi, X.Y., et al., *Cellular signaling underlying atrial tachycardia remodeling of L-type calcium current.* Circ Res, 2008. 103(8): p. 845-54.**

**110. Grammer, J.B., et al., *Atrial L-type Ca2+-channel, beta-adrenorecptor, and 5-hydroxytryptamine type 4 receptor mRNAs in human atrial fibrillation.* Basic Res Cardiol, 2001. 96(1): p. 82-90.**

**111. El-Armouche, A., et al., *Molecular determinants of altered Ca2+ handling in human chronic atrial fibrillation.* Circulation, 2006. 114(7): p. 670-80.**

**112. Levy, S., et al., *Molecular basis for zinc transporter 1 action as an endogenous inhibitor of L-type calcium channels.* J Biol Chem, 2009. 284(47): p. 32434-43.**

**113. Lu, Y., et al., *MicroRNA-328 contributes to adverse electrical remodeling in atrial fibrillation.* Circulation, 2010. 122(23): p. 2378-87.**

**114. Hove-Madsen, L., et al., *Atrial fibrillation is associated with increased spontaneous calcium release from the sarcoplasmic reticulum in human atrial myocytes.* Circulation, 2004. 110(11): p. 1358-63.**

**115. Vest, J.A., et al., *Defective cardiac ryanodine receptor regulation during atrial fibrillation.* Circulation, 2005. 111(16): p. 2025-32.**

**116. Liang, X., et al., *Ryanodine receptor-mediated Ca2+ events in atrial myocytes of patients with atrial fibrillation.* Cardiology, 2008. 111(2): p. 102-10.**

**117. Neef, S., et al., *CaMKII-dependent diastolic SR Ca2+ leak and elevated diastolic Ca2+ levels in right atrial myocardium of patients with atrial fibrillation.* Circ Res, 2010. 106(6): p. 1134-44.**

**118. Chelu, M.G., et al., *Calmodulin kinase II-mediated sarcoplasmic reticulum Ca2+ leak promotes atrial fibrillation in mice.* J Clin Invest, 2009. 119(7): p. 1940-51.**

**119. Dobrev, D., N. Voigt, and X.H. Wehrens, *The ryanodine receptor channel as a molecular motif in atrial fibrillation: pathophysiological and therapeutic implications.* Cardiovasc Res, 2011. 89(4): p. 734-43.**

**120. Ehrlich, J.R., et al., *Characterization of a hyperpolarization-activated time-dependent potassium current in canine cardiomyocytes from pulmonary vein myocardial sleeves and left atrium.* J Physiol, 2004. 557(Pt 2): p. 583-97.**

**121. Voigt, N., et al., *Changes in I K, ACh single-channel activity with atrial tachycardia remodelling in canine atrial cardiomyocytes.* Cardiovasc Res, 2008. 77(1): p. 35-43.**

**122. Dobrev, D., et al., *The G protein-gated potassium current I(K,ACh) is constitutively active in patients with chronic atrial fibrillation.* Circulation, 2005. 112(24): p. 3697-706.**

**123. Karle, C.A., et al., *Human cardiac inwardly-rectifying K+ channel Kir(2.1b) is inhibited by direct protein kinase C-dependent regulation in human isolated cardiomyocytes and in an expression system.* Circulation, 2002. 106(12): p. 1493-9.**

**124. Makary, S., et al., *Differential protein kinase C isoform regulation and increased constitutive activity of acetylcholine-regulated potassium channels in atrial remodeling.* Circ Res, 2011. 109(9): p. 1031-43.**

**125. Yue, L., et al., *Transient outward and delayed rectifier currents in canine atrium: properties and role of isolation methods.* Am J Physiol, 1996. 270(6 Pt 2): p. H2157-68.**

**126. Corradi, D., et al., *Structural remodeling in atrial fibrillation.* Nat Clin Pract Cardiovasc Med, 2008. 5(12): p. 782-96.**

**127. Boldt, A., et al., *Fibrosis in left atrial tissue of patients with atrial fibrillation with and without underlying mitral valve disease.* Heart, 2004. 90(4): p. 400-5.**

**128. Frustaci, A., et al., *Histological substrate of atrial biopsies in patients with lone atrial fibrillation.* Circulation, 1997. 96(4): p. 1180-4.**

**129. Li, D., et al., *Promotion of atrial fibrillation by heart failure in dogs: atrial remodeling of a different sort.* Circulation, 1999. 100(1): p. 87-95.**

**130. Burstein, B., et al., *Changes in connexin expression and the atrial fibrillation substrate in congestive heart failure.* Circ Res, 2009. 105(12): p. 1213-22.**

**131. Anne, W., et al., *Matrix metalloproteinases and atrial remodeling in patients with mitral valve disease and atrial fibrillation.* Cardiovasc Res, 2005. 67(4): p. 655-66.**

**132. Luo, M.H., Y.S. Li, and K.P. Yang, *Fibrosis of collagen I and remodeling of connexin 43 in atrial myocardium of patients with atrial fibrillation.* Cardiology, 2007. 107(4): p. 248-53.**

**133. Xiao, H., et al., *TGF-beta1 expression and atrial myocardium fibrosis increase in atrial fibrillation secondary to rheumatic heart disease.* Clin Cardiol, 2010. 33(3): p. 149-56.**

**134. Ohtani, K., et al., *High prevalence of atrial fibrosis in patients with dilated cardiomyopathy.* J Am Coll Cardiol, 1995. 25(5): p. 1162-9.**

**135. Prinz, C., et al., *Left atrial size and left ventricular hypertrophy correlate with myocardial fibrosis in patients with hypertrophic cardiomyopathy.* Acta Cardiol, 2011. 66(2): p. 153-7.**

**136. Gramley, F., et al., *Age-related atrial fibrosis.* Age (Dordr), 2009. 31(1): p. 27-38.**

**137. Lie, J.T. and P.I. Hammond, *Pathology of the senescent heart: anatomic observations on 237 autopsy studies of patients 90 to 105 years old.* Mayo Clin Proc, 1988. 63(6): p. 552-64.**

**138. Shiroshita-Takeshita, A., et al., *Effects of simvastatin on the development of the atrial fibrillation substrate in dogs with congestive heart failure.* Cardiovasc Res, 2007. 74(1): p. 75-84.**

**139. Li, D., et al., *Effects of angiotensin-converting enzyme inhibition on the development of the atrial fibrillation substrate in dogs with ventricular tachypacing-induced congestive heart failure.* Circulation, 2001. 104(21): p. 2608-14.**

**140. Kumagai, K., et al., *Effects of angiotensin II type 1 receptor antagonist on electrical and structural remodeling in atrial fibrillation.* J Am Coll Cardiol, 2003. 41(12): p. 2197-204.**

**141. Sakabe, M., et al., *Omega-3 polyunsaturated fatty acids prevent atrial fibrillation associated with heart failure but not atrial tachycardia remodeling.* Circulation, 2007. 116(19): p. 2101-9.**

**142. Burstein, B. and S. Nattel, *Atrial fibrosis: mechanisms and clinical relevance in atrial fibrillation.* J Am Coll Cardiol, 2008. 51(8): p. 802-9.**

**143. Yue, L., J. Xie, and S. Nattel, *Molecular determinants of cardiac fibroblast electrical function and therapeutic implications for atrial fibrillation.* Cardiovasc Res, 2011. 89(4): p. 744-53.**

**144. Xu, J., et al., *Atrial extracellular matrix remodeling and the maintenance of atrial fibrillation.* Circulation, 2004. 109(3): p. 363-8.**

**145. Avitall, B., et al., *Atrial and ventricular fibrosis induced by atrial fibrillation: evidence to support early rhythm control.* Heart Rhythm, 2008. 5(6): p. 839-45.**

**146. Xiao, H.D., et al., *Mice with cardiac-restricted angiotensin-converting enzyme (ACE) have atrial enlargement, cardiac arrhythmia, and sudden death.* Am J Pathol, 2004. 165(3): p. 1019-32.**

**147. Hunyady, L. and K.J. Catt, *Pleiotropic AT1 receptor signaling pathways mediating physiological and pathogenic actions of angiotensin II.* Mol Endocrinol, 2006. 20(5): p. 953-70.**

**148. Burstein, B. and S. Nattel, *Atrial structural remodeling as an antiarrhythmic target.* J Cardiovasc Pharmacol, 2008. 52(1): p. 4-10.**

**149. Burstein, B., et al., *Differential behaviors of atrial versus ventricular fibroblasts: a potential role for platelet-derived growth factor in atrial-ventricular remodeling differences.* Circulation, 2008. 117(13): p. 1630-41.**

**150. Verheule, S., et al., *Increased vulnerability to atrial fibrillation in transgenic mice with selective atrial fibrosis caused by overexpression of TGF-beta1.* Circ Res, 2004. 94(11): p. 1458-65.**

**151. Attisano, L. and J.L. Wrana, *Signal transduction by the TGF-beta superfamily.* Science, 2002. 296(5573): p. 1646-7.**

**152. Ponten, A., et al., *Transgenic overexpression of platelet-derived growth factor-C in the mouse heart induces cardiac fibrosis, hypertrophy, and dilated cardiomyopathy.* Am J Pathol, 2003. 163(2): p. 673-82.**

**153. Ponten, A., et al., *Platelet-derived growth factor D induces cardiac fibrosis and proliferation of vascular smooth muscle cells in heart-specific transgenic mice.* Circ Res, 2005. 97(10): p. 1036-45.**

**154. Ahmed, M.S., et al., *Connective tissue growth factor--a novel mediator of angiotensin II-stimulated cardiac fibroblast activation in heart failure in rats.* J Mol Cell Cardiol, 2004. 36(3): p. 393-404.**

**155. Cardin, S., et al., *Evolution of the atrial fibrillation substrate in experimental congestive heart failure: angiotensin-dependent and -independent pathways.* Cardiovasc Res, 2003. 60(2): p. 315-25.**

**156. Hanna, N., et al., *Differences in atrial versus ventricular remodeling in dogs with ventricular tachypacing-induced congestive heart failure.* Cardiovasc Res, 2004. 63(2): p. 236-44.**

**157. Nakajima, H., et al., *Atrial but not ventricular fibrosis in mice expressing a mutant transforming growth factor-beta(1) transgene in the heart.* Circ Res, 2000. 86(5): p. 571-9.**

**158. Kumaran, C. and K. Shivakumar, *Calcium- and superoxide anion-mediated mitogenic action of substance P on cardiac fibroblasts.* Am J Physiol Heart Circ Physiol, 2002. 282(5): p. H1855-62.**

**159. Shivakumar, K. and C. Kumaran, *L-type calcium channel blockers and EGTA enhance superoxide production in cardiac fibroblasts.* J Mol Cell Cardiol, 2001. 33(2): p. 373-7.**

**160. Colston, J.T., B. Chandrasekar, and G.L. Freeman, *A novel peroxide-induced calcium transient regulates interleukin-6 expression in cardiac-derived fibroblasts.* J Biol Chem, 2002. 277(26): p. 23477-83.**

**161. Kiseleva, I., et al., *Calcium and mechanically induced potentials in fibroblasts of rat atrium.* Cardiovasc Res, 1996. 32(1): p. 98-111.**

**162. Kiseleva, I., et al., *Electrophysiological properties of mechanosensitive atrial fibroblasts from chronic infarcted rat heart.* J Mol Cell Cardiol, 1998. 30(6): p. 1083-93.**

**163. Kohl, P. and D. Noble, *Mechanosensitive connective tissue: potential influence on heart rhythm.* Cardiovasc Res, 1996. 32(1): p. 62-8.**

**164. Clapham, D.E., *TRP channels as cellular sensors.* Nature, 2003. 426(6966): p. 517-24.**

**165. Montell, C., *The TRP superfamily of cation channels.* Sci STKE, 2005. 2005(272): p. re3.**

**166. Nilius, B., *TRP channels in disease.* Biochim Biophys Acta, 2007. 1772(8): p. 805-12.**

**167. Runnels, L.W., L. Yue, and D.E. Clapham, *The TRPM7 channel is inactivated by PIP(2) hydrolysis.* Nat Cell Biol, 2002. 4(5): p. 329-36.**

**168. Du, J., et al., *TRPM7-mediated Ca2+ signals confer fibrogenesis in human atrial fibrillation.* Circ Res, 2010. 106(5): p. 992-1003.**

**169. Thomas, S.A., R.B. Schuessler, and J.E. Saffitz, *Connexins, conduction, and atrial fibrillation.* J Cardiovasc Electrophysiol, 1998. 9(6): p. 608-11.**

**170. Thomas, S.A., et al., *Disparate effects of deficient expression of connexin43 on atrial and ventricular conduction: evidence for chamber-specific molecular determinants of conduction.* Circulation, 1998. 97(7): p. 686-91.**

**171. van der Velden, H.M., et al., *Gap junctional remodeling in relation to stabilization of atrial fibrillation in the goat.* Cardiovasc Res, 2000. 46(3): p. 476-86.**

**172. van der Velden, H.M., et al., *Altered pattern of connexin40 distribution in persistent atrial fibrillation in the goat.* J Cardiovasc Electrophysiol, 1998. 9(6): p. 596-607.**

**173. Dupont, E., et al., *The gap-junctional protein connexin40 is elevated in patients susceptible to postoperative atrial fibrillation.* Circulation, 2001. 103(6): p. 842-9.**

**174. Kanagaratnam, P., et al., *Relationship between connexins and atrial activation during human atrial fibrillation.* J Cardiovasc Electrophysiol, 2004. 15(2): p. 206-16.**

**175. Heidbuchel, H., J. Vereecke, and E. Carmeliet, *The electrophysiological effects of acetylcholine in single human atrial cells.* J Mol Cell Cardiol, 1987. 19(12): p. 1207-19.**

**176. Heidbuchel, H., J. Vereecke, and E. Carmeliet, *Three different potassium channels in human atrium. Contribution to the basal potassium conductance.* Circ Res, 1990. 66(5): p. 1277-86.**

**177. Dhamoon, A.S. and J. Jalife, *The inward rectifier current (IK1) controls cardiac excitability and is involved in arrhythmogenesis.* Heart Rhythm, 2005. 2(3): p. 316-24.**

**178. Hatem, S.N., A. Coulombe, and E. Balse, *Specificities of atrial electrophysiology: Clues to a better understanding of cardiac function and the mechanisms of arrhythmias.* J Mol Cell Cardiol, 2010. 48(1): p. 90-5.**

**179. Lopatin, A.N., E.N. Makhina, and C.G. Nichols, *Potassium channel block by cytoplasmic polyamines as the mechanism of intrinsic rectification.* Nature, 1994. 372(6504): p. 366-9.**

**180. Stanfield, P.R., et al., *The intrinsic gating of inward rectifier K+ channels expressed from the murine IRK1 gene depends on voltage, K+ and Mg2+.* J Physiol, 1994. 475(1): p. 1-7.**

**181. Stanfield, P.R., S. Nakajima, and Y. Nakajima, *Constitutively active and G-protein coupled inward rectifier K+ channels: Kir2.0 and Kir3.0.* Rev Physiol Biochem Pharmacol, 2002. 145: p. 47-179.**

**182. Preisig-Muller, R., et al., *Heteromerization of Kir2.x potassium channels contributes to the phenotype of Andersen's syndrome.* Proc Natl Acad Sci U S A, 2002. 99(11): p. 7774-9.**

**183. Schram, G., et al., *Barium block of Kir2 and human cardiac inward rectifier currents: evidence for subunit-heteromeric contribution to native currents.* Cardiovasc Res, 2003. 59(2): p. 328-38.**

**184. Kubo, Y., et al., *Primary structure and functional expression of a mouse inward rectifier potassium channel.* Nature, 1993. 362(6416): p. 127-33.**

**185. Kubo, Y., et al., *International Union of Pharmacology. LIV. Nomenclature and molecular relationships of inwardly rectifying potassium channels.* Pharmacol Rev, 2005. 57(4): p. 509-26.**

**186. Wang, Z., et al., *Differential distribution of inward rectifier potassium channel transcripts in human atrium versus ventricle.* Circulation, 1998. 98(22): p. 2422-8.**

**187. Melnyk, P., et al., *Differential distribution of Kir2.1 and Kir2.3 subunits in canine atrium and ventricle.* Am J Physiol Heart Circ Physiol, 2002. 283(3): p. H1123-33.**

**188. Zaritsky, J.J., et al., *The consequences of disrupting cardiac inwardly rectifying K(+) current (I(K1)) as revealed by the targeted deletion of the murine Kir2.1 and Kir2.2 genes.* J Physiol, 2001. 533(Pt 3): p. 697-710.**

**189. Zaritsky, J.J., et al., *Targeted disruption of Kir2.1 and Kir2.2 genes reveals the essential role of the inwardly rectifying K(+) current in K(+)-mediated vasodilation.* Circ Res, 2000. 87(2): p. 160-6.**

**190. McLerie, M. and A.N. Lopatin, *Dominant-negative suppression of I(K1) in the mouse heart leads to altered cardiac excitability.* J Mol Cell Cardiol, 2003. 35(4): p. 367-78.**

**191. Zobel, C., et al., *Molecular dissection of the inward rectifier potassium current (IK1) in rabbit cardiomyocytes: evidence for heteromeric co-assembly of Kir2.1 and Kir2.2.* J Physiol, 2003. 550(Pt 2): p. 365-72.**

**192. Hibino, H., et al., *Inwardly rectifying potassium channels: their structure, function, and physiological roles.* Physiol Rev, 2010. 90(1): p. 291-366.**

**193. Hilgemann, D.W., S. Feng, and C. Nasuhoglu, *The complex and intriguing lives of PIP2 with ion channels and transporters.* Sci STKE, 2001. 2001(111): p. re19.**

**194. Huang, C.L., S. Feng, and D.W. Hilgemann, *Direct activation of inward rectifier potassium channels by PIP2 and its stabilization by Gbetagamma.* Nature, 1998. 391(6669): p. 803-6.**

**195. Takano, M. and S. Kuratomi, *Regulation of cardiac inwardly rectifying potassium channels by membrane lipid metabolism.* Prog Biophys Mol Biol, 2003. 81(1): p. 67-79.**

**196. Lopes, C.M., et al., *Alterations in conserved Kir channel-PIP2 interactions underlie channelopathies.* Neuron, 2002. 34(6): p. 933-44.**

**197. Sato, R. and S. Koumi, *Modulation of the inwardly rectifying K+ channel in isolated human atrial myocytes by alpha 1-adrenergic stimulation.* J Membr Biol, 1995. 148(2): p. 185-91.**

**198. Koumi, S., et al., *beta-Adrenergic modulation of the inwardly rectifying potassium channel in isolated human ventricular myocytes. Alteration in channel response to beta-adrenergic stimulation in failing human hearts.* J Clin Invest, 1995. 96(6): p. 2870-81.**

**199. Henry, P., W.L. Pearson, and C.G. Nichols, *Protein kinase C inhibition of cloned inward rectifier (HRK1/KIR2.3) K+ channels expressed in Xenopus oocytes.* J Physiol, 1996. 495 ( Pt 3): p. 681-8.**

**200. Dart, C. and M.L. Leyland, *Targeting of an A kinase-anchoring protein, AKAP79, to an inwardly rectifying potassium channel, Kir2.1.* J Biol Chem, 2001. 276(23): p. 20499-505.**

**201. Zitron, E., et al., *Human cardiac inwardly rectifying current IKir2.2 is upregulated by activation of protein kinase A.* Cardiovasc Res, 2004. 63(3): p. 520-7.**

**202. Harvey, R.D. and R.E. Ten Eick, *On the role of sodium ions in the regulation of the inward-rectifying potassium conductance in cat ventricular myocytes.* J Gen Physiol, 1989. 94(2): p. 329-48.**

**203. Du, X., et al., *Characteristic interactions with phosphatidylinositol 4,5-bisphosphate determine regulation of kir channels by diverse modulators.* J Biol Chem, 2004. 279(36): p. 37271-81.**

**204. Yang, B., et al., *The muscle-specific microRNA miR-1 regulates cardiac arrhythmogenic potential by targeting GJA1 and KCNJ2.* Nat Med, 2007. 13(4): p. 486-91.**

**205. Eder, P. and K. Groschner, *TRPC3/6/7: Topical aspects of biophysics and pathophysiology.* Channels (Austin), 2008. 2(2): p. 94-9.**

**206. Eder, P. and J.D. Molkentin, *TRPC channels as effectors of cardiac hypertrophy.* Circ Res, 2011. 108(2): p. 265-72.**

**207. Venkatachalam, K. and C. Montell, *TRP channels.* Annu Rev Biochem, 2007. 76: p. 387-417.**

**208. Clapham, D.E., L.W. Runnels, and C. Strubing, *The TRP ion channel family.* Nat Rev Neurosci, 2001. 2(6): p. 387-96.**

**209. Eder, P., M. Poteser, and K. Groschner, *TRPC3: a multifunctional, pore-forming signalling molecule.* Handb Exp Pharmacol, 2007(179): p. 77-92.**

**210. Groschner, K. and C. Rosker, *TRPC3: a versatile transducer molecule that serves integration and diversification of cellular signals.* Naunyn Schmiedebergs Arch Pharmacol, 2005. 371(4): p. 251-6.**

**211. Dietrich, A., et al., *Functional characterization and physiological relevance of the TRPC3/6/7 subfamily of cation channels.* Naunyn Schmiedebergs Arch Pharmacol, 2005. 371(4): p. 257-65.**

**212. Kiyonaka, S., et al., *Selective and direct inhibition of TRPC3 channels underlies biological activities of a pyrazole compound.* Proc Natl Acad Sci U S A, 2009. 106(13): p. 5400-5.**

**213. Nilius, B., et al., *Transient receptor potential cation channels in disease.* Physiol Rev, 2007. 87(1): p. 165-217.**

**214. Vannier, B., et al., *The membrane topology of human transient receptor potential 3 as inferred from glycosylation-scanning mutagenesis and epitope immunocytochemistry.* J Biol Chem, 1998. 273(15): p. 8675-9.**

**215. Zhu, X., et al., *trp, a novel mammalian gene family essential for agonist-activated capacitative Ca2+ entry.* Cell, 1996. 85(5): p. 661-71.**

**216. Tano, J.Y., K. Smedlund, and G. Vazquez, *Endothelial TRPC3/6/7 proteins at the edge of cardiovascular disease.* Cardiovasc Hematol Agents Med Chem, 2010. 8(1): p. 76-86.**

**217. Dalrymple, A., et al., *Mechanical stretch regulates TRPC expression and calcium entry in human myometrial smooth muscle cells.* Mol Hum Reprod, 2007. 13(3): p. 171-9.**

**218. Dietrich, A., et al., *Cation channels of the transient receptor potential superfamily: their role in physiological and pathophysiological processes of smooth muscle cells.* Pharmacol Ther, 2006. 112(3): p. 744-60.**

**219. Dietrich, A., et al., *N-linked protein glycosylation is a major determinant for basal TRPC3 and TRPC6 channel activity.* J Biol Chem, 2003. 278(48): p. 47842-52.**

**220. Hurst, R.S., et al., *Ionic currents underlying HTRP3 mediated agonist-dependent Ca2+ influx in stably transfected HEK293 cells.* FEBS Lett, 1998. 422(3): p. 333-8.**

**221. Dietrich, A., et al., *The diacylgylcerol-sensitive TRPC3/6/7 subfamily of cation channels: functional characterization and physiological relevance.* Pflugers Arch, 2005. 451(1): p. 72-80.**

**222. Onohara, N., et al., *TRPC3 and TRPC6 are essential for angiotensin II-induced cardiac hypertrophy.* EMBO J, 2006. 25(22): p. 5305-16.**

**223. Peppiatt-Wildman, C.M., et al., *Endothelin-1 activates a Ca2+-permeable cation channel with TRPC3 and TRPC7 properties in rabbit coronary artery myocytes.* J Physiol, 2007. 580(Pt.3): p. 755-64.**

**224. Hofmann, T., et al., *Direct activation of human TRPC6 and TRPC3 channels by diacylglycerol.* Nature, 1999. 397(6716): p. 259-63.**

**225. Lintschinger, B., et al., *Coassembly of Trp1 and Trp3 proteins generates diacylglycerol- and Ca2+-sensitive cation channels.* J Biol Chem, 2000. 275(36): p. 27799-805.**

**226. McKay, R.R., et al., *Cloning and expression of the human transient receptor potential 4 (TRP4) gene: localization and functional expression of human TRP4 and TRP3.* Biochem J, 2000. 351 Pt 3: p. 735-46.**

**227. Kiselyov, K., et al., *Functional interaction between InsP3 receptors and store-operated Htrp3 channels.* Nature, 1998. 396(6710): p. 478-82.**

**228. Zhang, Z., et al., *Activation of Trp3 by inositol 1,4,5-trisphosphate receptors through displacement of inhibitory calmodulin from a common binding domain.* Proc Natl Acad Sci U S A, 2001. 98(6): p. 3168-73.**

**229. Balzer, M., B. Lintschinger, and K. Groschner, *Evidence for a role of Trp proteins in the oxidative stress-induced membrane conductances of porcine aortic endothelial cells.* Cardiovasc Res, 1999. 42(2): p. 543-9.**

**230. Groschner, K., C. Rosker, and M. Lukas, *Role of TRP channels in oxidative stress.* Novartis Found Symp, 2004. 258: p. 222-30; discussion 231-5, 263-6.**

**231. Poteser, M., et al., *TRPC3 and TRPC4 associate to form a redox-sensitive cation channel. Evidence for expression of native TRPC3-TRPC4 heteromeric channels in endothelial cells.* J Biol Chem, 2006. 281(19): p. 13588-95.**

**232. Graziani, A., et al., *Cellular cholesterol controls TRPC3 function: evidence from a novel dominant-negative knockdown strategy.* Biochem J, 2006. 396(1): p. 147-55.**

**233. Brazer, S.C., et al., *Caveolin-1 contributes to assembly of store-operated Ca2+ influx channels by regulating plasma membrane localization of TRPC1.* J Biol Chem, 2003. 278(29): p. 27208-15.**

**234. Sinkins, W.G., et al., *Association of immunophilins with mammalian TRPC channels.* J Biol Chem, 2004. 279(33): p. 34521-9.**

**235. Goel, M., C.D. Zuo, and W.P. Schilling, *Role of cAMP/PKA signaling cascade in vasopressin-induced trafficking of TRPC3 channels in principal cells of the collecting duct.* Am J Physiol Renal Physiol, 2010. 298(4): p. F988-96.**

**236. Trebak, M., et al., *Negative regulation of TRPC3 channels by protein kinase C-mediated phosphorylation of serine 712.* Mol Pharmacol, 2005. 67(2): p. 558-63.**

**237. Harada, M.L., X.; Qi, Y.; Xiao, J.; Shi, Y.; Tardif, JC., Nattel, S. *MicroRNA26 Regulation of TRPC3 Subunits Underlies Profibrillatory Fibroblast Activation in a Canine Atrial Fibrillation Model*. in *AHA*. 2011. Circulation.**

**238. Wightman, B., I. Ha, and G. Ruvkun, *Posttranscriptional regulation of the heterochronic gene lin-14 by lin-4 mediates temporal pattern formation in C. elegans.* Cell, 1993. 75(5): p. 855-62.**

**239. Lee, R.C., R.L. Feinbaum, and V. Ambros, *The C. elegans heterochronic gene lin-4 encodes small RNAs with antisense complementarity to lin-14.* Cell, 1993. 75(5): p. 843-54.**

**240. Reinhart, B.J., et al., *The 21-nucleotide let-7 RNA regulates developmental timing in Caenorhabditis elegans.* Nature, 2000. 403(6772): p. 901-6.**

**241. Pasquinelli, A.E., et al., *Conservation of the sequence and temporal expression of let-7 heterochronic regulatory RNA.* Nature, 2000. 408(6808): p. 86-9.**

**242. Lagos-Quintana, M., et al., *Identification of novel genes coding for small expressed RNAs.* Science, 2001. 294(5543): p. 853-8.**

**243. Lau, N.C., et al., *An abundant class of tiny RNAs with probable regulatory roles in Caenorhabditis elegans.* Science, 2001. 294(5543): p. 858-62.**

**244. Lee, R.C. and V. Ambros, *An extensive class of small RNAs in Caenorhabditis elegans.* Science, 2001. 294(5543): p. 862-4.**

**245. Calin, G.A., et al., *Frequent deletions and down-regulation of micro- RNA genes miR15 and miR16 at 13q14 in chronic lymphocytic leukemia.* Proc Natl Acad Sci U S A, 2002. 99(24): p. 15524-9.**

**246. Zhao, Y., E. Samal, and D. Srivastava, *Serum response factor regulates a muscle-specific microRNA that targets Hand2 during cardiogenesis.* Nature, 2005. 436(7048): p. 214-20.**

**247. van Rooij, E., *The art of microRNA research.* Circ Res, 2011. 108(2): p. 219-34.**

**248. van Rooij, E., A.L. Purcell, and A.A. Levin, *Developing microRNA therapeutics.* Circ Res, 2012. 110(3): p. 496-507.**

**249. Bushati, N. and S.M. Cohen, *microRNA functions.* Annu Rev Cell Dev Biol, 2007. 23: p. 175-205.**

**250. Bartel, D.P., *MicroRNAs: target recognition and regulatory functions.* Cell, 2009. 136(2): p. 215-33.**

**251. Kim, V.N., *MicroRNA biogenesis: coordinated cropping and dicing.* Nat Rev Mol Cell Biol, 2005. 6(5): p. 376-85.**

**252. Bartel, D.P., *MicroRNAs: genomics, biogenesis, mechanism, and function.* Cell, 2004. 116(2): p. 281-97.**

**253. Berezikov, E., *Evolution of microRNA diversity and regulation in animals.* Nat Rev Genet, 2011. 12(12): p. 846-60.**

**254. Cullen, B.R., *Transcription and processing of human microRNA precursors.* Mol Cell, 2004. 16(6): p. 861-5.**

**255. Denli, A.M., et al., *Processing of primary microRNAs by the Microprocessor complex.* Nature, 2004. 432(7014): p. 231-5.**

**256. Lee, Y., et al., *The nuclear RNase III Drosha initiates microRNA processing.* Nature, 2003. 425(6956): p. 415-9.**

**257. Okamura, K., et al., *The mirtron pathway generates microRNA-class regulatory RNAs in Drosophila.* Cell, 2007. 130(1): p. 89-100.**

**258. Ruby, J.G., C.H. Jan, and D.P. Bartel, *Intronic microRNA precursors that bypass Drosha processing.* Nature, 2007. 448(7149): p. 83-6.**

**259. Lund, E., et al., *Nuclear export of microRNA precursors.* Science, 2004. 303(5654): p. 95-8.**

**260. Bohnsack, M.T., K. Czaplinski, and D. Gorlich, *Exportin 5 is a RanGTP-dependent dsRNA-binding protein that mediates nuclear export of pre-miRNAs.* RNA, 2004. 10(2): p. 185-91.**

**261. Yi, R., et al., *Exportin-5 mediates the nuclear export of pre-microRNAs and short hairpin RNAs.* Genes Dev, 2003. 17(24): p. 3011-6.**

**262. Chendrimada, T.P., et al., *TRBP recruits the Dicer complex to Ago2 for microRNA processing and gene silencing.* Nature, 2005. 436(7051): p. 740-4.**

**263. Wang, Z. and X. Luo, *MicroRNA Interference: Concept and Technologies*, in *RNAi Technology*, R.K. Gaur, et al., Editors. 2011, CRC Press.**

**264. Chendrimada, T.P., et al., *MicroRNA silencing through RISC recruitment of eIF6.* Nature, 2007. 447(7146): p. 823-8.**

**265. Gregory, R.I., et al., *Human RISC couples microRNA biogenesis and posttranscriptional gene silencing.* Cell, 2005. 123(4): p. 631-40.**

**266. Lewis, B.P., et al., *Prediction of mammalian microRNA targets.* Cell, 2003. 115(7): p. 787-98.**

**267. Lewis, B.P., C.B. Burge, and D.P. Bartel, *Conserved seed pairing, often flanked by adenosines, indicates that thousands of human genes are microRNA targets.* Cell, 2005. 120(1): p. 15-20.**

**268. Khvorova, A., A. Reynolds, and S.D. Jayasena, *Functional siRNAs and miRNAs exhibit strand bias.* Cell, 2003. 115(2): p. 209-16.**

**269. Carthew, R.W. and E.J. Sontheimer, *Origins and Mechanisms of miRNAs and siRNAs.* Cell, 2009. 136(4): p. 642-55.**

**270. Filipowicz, W., S.N. Bhattacharyya, and N. Sonenberg, *Mechanisms of post-transcriptional regulation by microRNAs: are the answers in sight?* Nat Rev Genet, 2008. 9(2): p. 102-14.**

**271. Kantharidis, P., et al., *Diabetes complications: the microRNA perspective.* Diabetes, 2011. 60(7): p. 1832-7.**

**272. Croce, C.M., *Causes and consequences of microRNA dysregulation in cancer.* Nat Rev Genet, 2009. 10(10): p. 704-14.**

**273. Christensen, M. and G.M. Schratt, *microRNA involvement in developmental and functional aspects of the nervous system and in neurological diseases.* Neurosci Lett, 2009. 466(2): p. 55-62.**

**274. Griffiths-Jones, S., *The microRNA Registry.* Nucleic Acids Res, 2004. 32(Database issue): p. D109-11.**

**275. Small, E.M., R.J. Frost, and E.N. Olson, *MicroRNAs add a new dimension to cardiovascular disease.* Circulation, 2010. 121(8): p. 1022-32.**

**276. Berezikov, E., et al., *Phylogenetic shadowing and computational identification of human microRNA genes.* Cell, 2005. 120(1): p. 21-4.**

**277. Krek, A., et al., *Combinatorial microRNA target predictions.* Nat Genet, 2005. 37(5): p. 495-500.**

**278. John, B., et al., *Human MicroRNA targets.* PLoS Biol, 2004. 2(11): p. e363.**

**279. Thomson, D.W., C.P. Bracken, and G.J. Goodall, *Experimental strategies for microRNA target identification.* Nucleic Acids Res, 2011. 39(16): p. 6845-53.**

**280. Wang, Z., *The guideline of the design and validation of MiRNA mimics.* Methods Mol Biol, 2011. 676: p. 211-23.**

**281. Liang, Y., et al., *Characterization of microRNA expression profiles in normal human tissues.* BMC Genomics, 2007. 8: p. 166.**

**282. Chen, J.F., et al., *The role of microRNA-1 and microRNA-133 in skeletal muscle proliferation and differentiation.* Nat Genet, 2006. 38(2): p. 228-33.**

**283. van Rooij, E., et al., *Control of stress-dependent cardiac growth and gene expression by a microRNA.* Science, 2007. 316(5824): p. 575-9.**

**284. Thum, T., et al., *MicroRNA-21 contributes to myocardial disease by stimulating MAP kinase signalling in fibroblasts.* Nature, 2008. 456(7224): p. 980-4.**

**285. van Rooij, E., et al., *Dysregulation of microRNAs after myocardial infarction reveals a role of miR-29 in cardiac fibrosis.* Proc Natl Acad Sci U S A, 2008. 105(35): p. 13027-32.**

**286. Wang, S., et al., *The endothelial-specific microRNA miR-126 governs vascular integrity and angiogenesis.* Dev Cell, 2008. 15(2): p. 261-71.**

**287. Cordes, K.R., et al., *miR-145 and miR-143 regulate smooth muscle cell fate and plasticity.* Nature, 2009. 460(7256): p. 705-10.**

**288. Pradervand, S., et al., *Impact of normalization on miRNA microarray expression profiling.* RNA, 2009. 15(3): p. 493-501.**

**289. Thomson, J.M., J.S. Parker, and S.M. Hammond, *Microarray analysis of miRNA gene expression.* Methods Enzymol, 2007. 427: p. 107-22.**

**290. Aldridge, S. and J. Hadfield, *Introduction to miRNA profiling technologies and cross-platform comparison.* Methods Mol Biol, 2012. 822: p. 19-31.**

**291. Sarver, A.L., *Toward understanding the informatics and statistical aspects of micro-RNA profiling.* J Cardiovasc Transl Res, 2010. 3(3): p. 204-11.**

**292. Creighton, C.J., J.G. Reid, and P.H. Gunaratne, *Expression profiling of microRNAs by deep sequencing.* Brief Bioinform, 2009. 10(5): p. 490-7.**

**293. Davison, T.S., C.D. Johnson, and B.F. Andruss, *Analyzing micro-RNA expression using microarrays.* Methods Enzymol, 2006. 411: p. 14-34.**

**294. Friedlander, M.R., et al., *Discovering microRNAs from deep sequencing data using miRDeep.* Nat Biotechnol, 2008. 26(4): p. 407-15.**

**295. Chellappan, P. and H. Jin, *Discovery of plant microRNAs and short-interfering RNAs by deep parallel sequencing.* Methods Mol Biol, 2009. 495: p. 121-32.**

**296. Bar, M., et al., *MicroRNA discovery and profiling in human embryonic stem cells by deep sequencing of small RNA libraries.* Stem Cells, 2008. 26(10): p. 2496-505.**

**297. Camarillo, C., M. Swerdel, and R.P. Hart, *Comparison of microarray and quantitative real-time PCR methods for measuring MicroRNA levels in MSC cultures.* Methods Mol Biol, 2011. 698: p. 419-29.**

**298. Wang, B., et al., *Systematic evaluation of three microRNA profiling platforms: microarray, beads array, and quantitative real-time PCR array.* PLoS One, 2011. 6(2): p. e17167.**

**299. Swartzman, E., et al., *Expanding applications of protein analysis using proximity ligation and qPCR.* Methods, 2010. 50(4): p. S23-6.**

**300. Benes, V. and M. Castoldi, *Expression profiling of microRNA using real-time quantitative PCR, how to use it and what is available.* Methods, 2010. 50(4): p. 244-9.**

**301. Schmittgen, T.D., et al., *Real-time PCR quantification of precursor and mature microRNA.* Methods, 2008. 44(1): p. 31-8.**

**302. Chen, C., et al., *Real-time quantification of microRNAs by stem-loop RT-PCR.* Nucleic Acids Res, 2005. 33(20): p. e179.**

**303. McClure, L.V., Y.T. Lin, and C.S. Sullivan, *Detection of viral microRNAs by Northern blot analysis.* Methods Mol Biol, 2011. 721: p. 153-71.**

**304. Varallyay, E., J. Burgyan, and Z. Havelda, *MicroRNA detection by northern blotting using locked nucleic acid probes.* Nat Protoc, 2008. 3(2): p. 190-6.**

**305. Valoczi, A., et al., *Sensitive and specific detection of microRNAs by northern blot analysis using LNA-modified oligonucleotide probes.* Nucleic Acids Res, 2004. 32(22): p. e175.**

**306. Davis-Dusenbery, B.N. and A. Hata, *Mechanisms of control of microRNA biogenesis.* J Biochem, 2010. 148(4): p. 381-92.**

**307. Wang, Z., Y. Lu, and B. Yang, *MicroRNAs and atrial fibrillation: new fundamentals.* Cardiovasc Res, 2011. 89(4): p. 710-21.**

**308. Zhou, X., et al., *Characterization and identification of microRNA core promoters in four model species.* PLoS Comput Biol, 2007. 3(3): p. e37.**

**309. O'Donnell, K.A., et al., *c-Myc-regulated microRNAs modulate E2F1 expression.* Nature, 2005. 435(7043): p. 839-43.**

**310. He, L., et al., *A microRNA component of the p53 tumour suppressor network.* Nature, 2007. 447(7148): p. 1130-4.**

**311. Liu, N., et al., *An intragenic MEF2-dependent enhancer directs muscle-specific expression of microRNAs 1 and 133.* Proc Natl Acad Sci U S A, 2007. 104(52): p. 20844-9.**

**312. Zhang, X., et al., *Synergistic effects of the GATA-4-mediated miR-144/451 cluster in protection against simulated ischemia/reperfusion-induced cardiomyocyte death.* J Mol Cell Cardiol, 2010. 49(5): p. 841-50.**

**313. Lin, Z., et al., *miR-23a functions downstream of NFATc3 to regulate cardiac hypertrophy.* Proc Natl Acad Sci U S A, 2009. 106(29): p. 12103-8.**

**314. da Costa Martins, P.A., et al., *MicroRNA-199b targets the nuclear kinase Dyrk1a in an auto-amplification loop promoting calcineurin/NFAT signalling.* Nat Cell Biol, 2010. 12(12): p. 1220-7.**

**315. Krutzfeldt, J., M.N. Poy, and M. Stoffel, *Strategies to determine the biological function of microRNAs.* Nat Genet, 2006. 38 Suppl: p. S14-9.**

**316. Ford, L.P. and A. Cheng, *Using synthetic precursor and inhibitor miRNAs to understand miRNA function.* Methods Mol Biol, 2008. 419: p. 289-301.**

**317. Jin, H., et al., *Strategies to identify microRNA targets: new advances.* N Biotechnol, 2010. 27(6): p. 734-8.**

**318. Sayed, D., et al., *MicroRNA-21 targets Sprouty2 and promotes cellular outgrowths.* Mol Biol Cell, 2008. 19(8): p. 3272-82.**

**319. Ebert, M.S., J.R. Neilson, and P.A. Sharp, *MicroRNA sponges: competitive inhibitors of small RNAs in mammalian cells.* Nat Methods, 2007. 4(9): p. 721-6.**

**320. Care, A., et al., *MicroRNA-133 controls cardiac hypertrophy.* Nat Med, 2007. 13(5): p. 613-8.**

**321. Thum, T., *MicroRNA therapeutics in cardiovascular medicine.* EMBO Mol Med, 2012. 4(1): p. 3-14.**

**322. Small, E.M. and E.N. Olson, *Pervasive roles of microRNAs in cardiovascular biology.* Nature, 2011. 469(7330): p. 336-42.**

**323. Weiler, J., J. Hunziker, and J. Hall, *Anti-miRNA oligonucleotides (AMOs): ammunition to target miRNAs implicated in human disease?* Gene Ther, 2006. 13(6): p. 496-502.**

**324. Petersen, M. and J. Wengel, *LNA: a versatile tool for therapeutics and genomics.* Trends Biotechnol, 2003. 21(2): p. 74-81.**

**325. Faria, M. and H. Ulrich, *Sugar boost: when ribose modifications improve oligonucleotide performance.* Curr Opin Mol Ther, 2008. 10(2): p. 168-75.**

**326. Krutzfeldt, J., et al., *Silencing of microRNAs in vivo with 'antagomirs'.* Nature, 2005. 438(7068): p. 685-9.**

**327. Ruberti, F., C. Barbato, and C. Cogoni, *Targeting microRNAs in neurons: tools and perspectives.* Exp Neurol, 2012. 235(2): p. 419-26.**

**328. Hill, J.A. and E.N. Olson, *Cardiac plasticity.* N Engl J Med, 2008. 358(13): p. 1370-80.**

**329. Boettger, T. and T. Braun, *A new level of complexity: the role of microRNAs in cardiovascular development.* Circ Res, 2012. 110(7): p. 1000-13.**

**330. Albinsson, S., et al., *MicroRNAs are necessary for vascular smooth muscle growth, differentiation, and function.* Arterioscler Thromb Vasc Biol, 2010. 30(6): p. 1118-26.**

**331. Chen, J.F., et al., *Targeted deletion of Dicer in the heart leads to dilated cardiomyopathy and heart failure.* Proc Natl Acad Sci U S A, 2008. 105(6): p. 2111-6.**

**332. da Costa Martins, P.A., et al., *Conditional dicer gene deletion in the postnatal myocardium provokes spontaneous cardiac remodeling.* Circulation, 2008. 118(15): p. 1567-76.**

**333. Ivey, K.N., et al., *MicroRNA regulation of cell lineages in mouse and human embryonic stem cells.* Cell Stem Cell, 2008. 2(3): p. 219-29.**

**334. Liu, N., et al., *microRNA-133a regulates cardiomyocyte proliferation and suppresses smooth muscle gene expression in the heart.* Genes Dev, 2008. 22(23): p. 3242-54.**

**335. Zhao, Y., et al., *Dysregulation of cardiogenesis, cardiac conduction, and cell cycle in mice lacking miRNA-1-2.* Cell, 2007. 129(2): p. 303-17.**

**336. Wang, J., et al., *Bmp signaling regulates myocardial differentiation from cardiac progenitors through a MicroRNA-mediated mechanism.* Dev Cell, 2010. 19(6): p. 903-12.**

**337. Ventura, A., et al., *Targeted deletion reveals essential and overlapping functions of the miR-17 through 92 family of miRNA clusters.* Cell, 2008. 132(5): p. 875-86.**

**338. Harris, T.A., et al., *MicroRNA-126 regulates endothelial expression of vascular cell adhesion molecule 1.* Proc Natl Acad Sci U S A, 2008. 105(5): p. 1516-21.**

**339. Kuhnert, F., et al., *Attribution of vascular phenotypes of the murine Egfl7 locus to the microRNA miR-126.* Development, 2008. 135(24): p. 3989-93.**

**340. Elia, L., et al., *The knockout of miR-143 and -145 alters smooth muscle cell maintenance and vascular homeostasis in mice: correlates with human disease.* Cell Death Differ, 2009. 16(12): p. 1590-8.**

**341. Boettger, T., et al., *Acquisition of the contractile phenotype by murine arterial smooth muscle cells depends on the Mir143/145 gene cluster.* J Clin Invest, 2009. 119(9): p. 2634-47.**

**342. Morton, S.U., et al., *microRNA-138 modulates cardiac patterning during embryonic development.* Proc Natl Acad Sci U S A, 2008. 105(46): p. 17830-5.**

**343. Latronico, M.V. and G. Condorelli, *MicroRNAs and cardiac pathology.* Nat Rev Cardiol, 2009. 6(6): p. 419-29.**

**344. Catalucci, D., P. Gallo, and G. Condorelli, *MicroRNAs in cardiovascular biology and heart disease.* Circ Cardiovasc Genet, 2009. 2(4): p. 402-8.**

**345. Divakaran, V. and D.L. Mann, *The emerging role of microRNAs in cardiac remodeling and heart failure.* Circ Res, 2008. 103(10): p. 1072-83.**

**346. Ordovas, J.M. and C.E. Smith, *Epigenetics and cardiovascular disease.* Nat Rev Cardiol, 2010. 7(9): p. 510-9.**

**347. van Rooij, E., et al., *A signature pattern of stress-responsive microRNAs that can evoke cardiac hypertrophy and heart failure.* Proc Natl Acad Sci U S A, 2006. 103(48): p. 18255-60.**

**348. Callis, T.E., et al., *MicroRNA-208a is a regulator of cardiac hypertrophy and conduction in mice.* J Clin Invest, 2009. 119(9): p. 2772-86.**

**349. Ikeda, S., et al., *MicroRNA-1 negatively regulates expression of the hypertrophy-associated calmodulin and Mef2a genes.* Mol Cell Biol, 2009. 29(8): p. 2193-204.**

**350. Sayed, D., et al., *MicroRNAs play an essential role in the development of cardiac hypertrophy.* Circ Res, 2007. 100(3): p. 416-24.**

**351. Hua, Y., Y. Zhang, and J. Ren, *IGF-1 deficiency resists cardiac hypertrophy and myocardial contractile dysfunction: role of microRNA-1 and microRNA-133a.* J Cell Mol Med, 2012. 16(1): p. 83-95.**

**352. Elia, L., et al., *Reciprocal regulation of microRNA-1 and insulin-like growth factor-1 signal transduction cascade in cardiac and skeletal muscle in physiological and pathological conditions.* Circulation, 2009. 120(23): p. 2377-85.**

**353. Cheng, Y., et al., *MicroRNAs are aberrantly expressed in hypertrophic heart: do they play a role in cardiac hypertrophy?* Am J Pathol, 2007. 170(6): p. 1831-40.**

**354. Patrick, D.M., et al., *Stress-dependent cardiac remodeling occurs in the absence of microRNA-21 in mice.* J Clin Invest, 2010. 120(11): p. 3912-6.**

**355. Duisters, R.F., et al., *miR-133 and miR-30 regulate connective tissue growth factor: implications for a role of microRNAs in myocardial matrix remodeling.* Circ Res, 2009. 104(2): p. 170-8, 6p following 178.**

**356. Matkovich, S.J., et al., *MicroRNA-133a protects against myocardial fibrosis and modulates electrical repolarization without affecting hypertrophy in pressure-overloaded adult hearts.* Circ Res, 2010. 106(1): p. 166-75.**

**357. Castoldi, G., et al., *MiR-133a regulates collagen 1A1: potential role of miR-133a in myocardial fibrosis in angiotensin II-dependent hypertension.* J Cell Physiol, 2012. 227(2): p. 850-6.**

**358. Rane, S., et al., *Downregulation of miR-199a derepresses hypoxia-inducible factor-1alpha and Sirtuin 1 and recapitulates hypoxia preconditioning in cardiac myocytes.* Circ Res, 2009. 104(7): p. 879-86.**

**359. Ren, X.P., et al., *MicroRNA-320 is involved in the regulation of cardiac ischemia/reperfusion injury by targeting heat-shock protein 20.* Circulation, 2009. 119(17): p. 2357-66.**

**360. Dong, S., et al., *MicroRNA expression signature and the role of microRNA-21 in the early phase of acute myocardial infarction.* J Biol Chem, 2009. 284(43): p. 29514-25.**

**361. Sayed, D., et al., *MicroRNA-21 is a downstream effector of AKT that mediates its antiapoptotic effects via suppression of Fas ligand.* J Biol Chem, 2010. 285(26): p. 20281-90.**

**362. Wang, X., et al., *MicroRNA-494 targeting both proapoptotic and antiapoptotic proteins protects against ischemia/reperfusion-induced cardiac injury.* Circulation, 2010. 122(13): p. 1308-18.**

**363. Fiedler, J., et al., *MicroRNA-24 regulates vascularity after myocardial infarction.* Circulation, 2011. 124(6): p. 720-30.**

**364. Hu, S., et al., *Novel microRNA prosurvival cocktail for improving engraftment and function of cardiac progenitor cell transplantation.* Circulation, 2011. 124(11 Suppl): p. S27-34.**

**365. Hullinger, T.G., et al., *Inhibition of miR-15 protects against cardiac ischemic injury.* Circ Res, 2012. 110(1): p. 71-81.**

**366. Cimmino, A., et al., *miR-15 and miR-16 induce apoptosis by targeting BCL2.* Proc Natl Acad Sci U S A, 2005. 102(39): p. 13944-9.**

**367. Nishi, H., et al., *MicroRNA-15b modulates cellular ATP levels and degenerates mitochondria via Arl2 in neonatal rat cardiac myocytes.* J Biol Chem, 2010. 285(7): p. 4920-30.**

**368. van Solingen, C., et al., *Antagomir-mediated silencing of endothelial cell specific microRNA-126 impairs ischemia-induced angiogenesis.* J Cell Mol Med, 2009. 13(8A): p. 1577-85.**

**369. Bonauer, A., et al., *MicroRNA-92a controls angiogenesis and functional recovery of ischemic tissues in mice.* Science, 2009. 324(5935): p. 1710-3.**

**370. Roy, S., et al., *MicroRNA expression in response to murine myocardial infarction: miR-21 regulates fibroblast metalloprotease-2 via phosphatase and tensin homologue.* Cardiovasc Res, 2009. 82(1): p. 21-9.**

**371. Lerner, D.L., et al., *Accelerated onset and increased incidence of ventricular arrhythmias induced by ischemia in Cx43-deficient mice.* Circulation, 2000. 101(5): p. 547-52.**

**372. Plaster, N.M., et al., *Mutations in Kir2.1 cause the developmental and episodic electrical phenotypes of Andersen's syndrome.* Cell, 2001. 105(4): p. 511-9.**

**373. Belevych, A.E., et al., *MicroRNA-1 and -133 increase arrhythmogenesis in heart failure by dissociating phosphatase activity from RyR2 complex.* PLoS One, 2011. 6(12): p. e28324.**

**374. Terentyev, D., et al., *miR-1 overexpression enhances Ca(2+) release and promotes cardiac arrhythmogenesis by targeting PP2A regulatory subunit B56alpha and causing CaMKII-dependent hyperphosphorylation of RyR2.* Circ Res, 2009. 104(4): p. 514-21.**

**375. Shan, H., et al., *Downregulation of miR-133 and miR-590 contributes to nicotine-induced atrial remodelling in canines.* Cardiovasc Res, 2009. 83(3): p. 465-72.**

**376. Pandit, S.V., et al., *Ionic determinants of functional reentry in a 2-D model of human atrial cells during simulated chronic atrial fibrillation.* Biophys J, 2005. 88(6): p. 3806-21.**

**377. Priori, S.G., et al., *A novel form of short QT syndrome (SQT3) is caused by a mutation in the KCNJ2 gene.* Circ Res, 2005. 96(7): p. 800-7.**

**378. Han, M., et al., *GATA4 expression is primarily regulated via a miR-26b-dependent post-transcriptional mechanism during cardiac hypertrophy.* Cardiovasc Res, 2012. 93(4): p. 645-54.**

**379. Wu, X., et al., *TRPC channels are necessary mediators of pathologic cardiac hypertrophy.* Proc Natl Acad Sci U S A, 2010. 107(15): p. 7000-5.**

**380. Lin, C.C., et al., *Activation of the calcineurin-nuclear factor of activated T-cell signal transduction pathway in atrial fibrillation.* Chest, 2004. 126(6): p. 1926-32.**

**381. Tavi, P., et al., *Pacing-induced calcineurin activation controls cardiac Ca2+ signalling and gene expression.* J Physiol, 2004. 554(Pt 2): p. 309-20.**

**382. Crabtree, G.R. and E.N. Olson, *NFAT signaling: choreographing the social lives of cells.* Cell, 2002. 109 Suppl: p. S67-79.**

**383. Crabtree, G.R., *Generic signals and specific outcomes: signaling through Ca2+, calcineurin, and NF-AT.* Cell, 1999. 96(5): p. 611-4.**

**384. Rossow, C.F., K.W. Dilly, and L.F. Santana, *Differential calcineurin/NFATc3 activity contributes to the Ito transmural gradient in the mouse heart.* Circ Res, 2006. 98(10): p. 1306-13.**

**385. Rossow, C.F., et al., *NFATc3-induced reductions in voltage-gated K+ currents after myocardial infarction.* Circ Res, 2004. 94(10): p. 1340-50.**

**386. Xiao, L., et al., *Mechanisms underlying rate-dependent remodeling of transient outward potassium current in canine ventricular myocytes.* Circ Res, 2008. 103(7): p. 733-42.**

**387. Layne, J.J., et al., *NFATc3 regulates BK channel function in murine urinary bladder smooth muscle.* Am J Physiol Cell Physiol, 2008. 295(3): p. C611-23.**

**388. LeWitt, P.A., et al., *AAV2-GAD gene therapy for advanced Parkinson's disease: a double-blind, sham-surgery controlled, randomised trial.* Lancet Neurol, 2011. 10(4): p. 309-19.**

**389. Cideciyan, A.V., et al., *Vision 1 year after gene therapy for Leber's congenital amaurosis.* N Engl J Med, 2009. 361(7): p. 725-7.**

**390. Maguire, A.M., et al., *Safety and efficacy of gene transfer for Leber's congenital amaurosis.* N Engl J Med, 2008. 358(21): p. 2240-8.**

**391. Pages, G., et al., *Mitogen-activated protein kinases p42mapk and p44mapk are required for fibroblast proliferation.* Proc Natl Acad Sci U S A, 1993. 90(18): p. 8319-23.**

**392. Dudley, D.T., et al., *A synthetic inhibitor of the mitogen-activated protein kinase cascade.* Proc Natl Acad Sci U S A, 1995. 92(17): p. 7686-9.**